

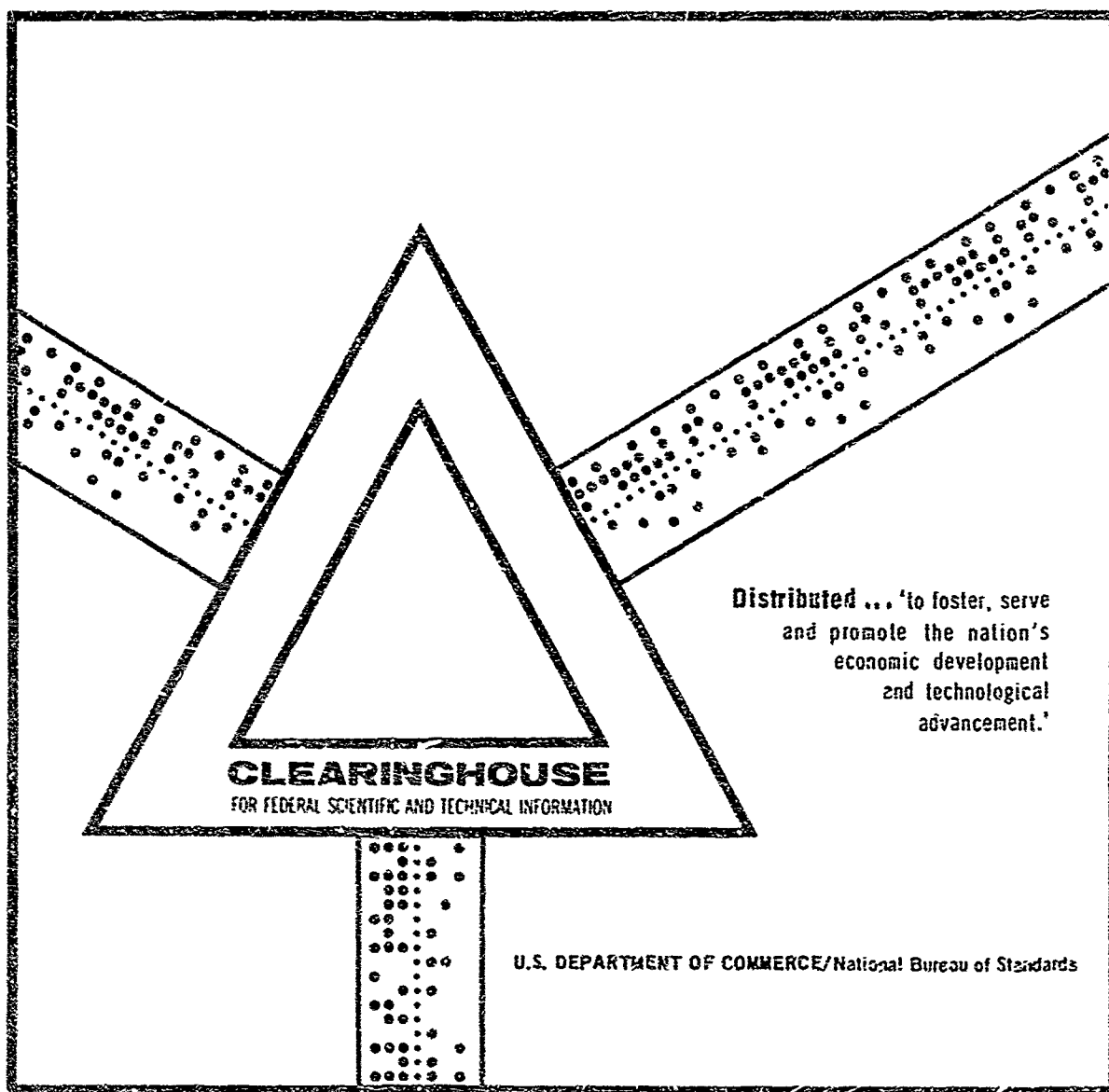
AD 701 004

PROTOTYPE CLUSTER-PARACHUTE RECOVERY SYSTEM
FOR A 50,000-POUND UNIT LOAD. VOLUME I. DESIGN
STUDY

Royce A. Toni, et al

Pioneer Parachute Company, Incorporated
Manchester, Connecticut

January 1969



This document has been approved for public release and sale.

This document has been approved
for public release and sale; its
distribution is unlimited.

AD _____

TECHNICAL REPORT
69-82-AD

PROTOTYPE CLUSTER-PARACHUTE RECOVERY SYSTEM
FOR A 50,000-lb UNIT LOAD
VOLUME I - DESIGN STUDY

by

Royce A. Tcni, Wolfgang R. Mueller,
Milan M. Knor, Marcia G. Wood

Pioneer Parachute Company, Inc.
Pioneer Industrial Park
Manchester, Connecticut 06040

Contract No. DAAG17-68-0142

Project Reference:
1F162203D195

January 1969

Airdrop Engineering Laboratory
U. S. ARMY NATICK LABORATORIES
Natick, Massachusetts 01760

FOREWORD

This work was initiated in an effort toward the design and fabrication of a prototype recovery parachute assembly to enable the airdrop, by use of parachutes in a cluster, of a 50,000-lb unit load. The first phase of this study was concerned solely with the design aspects; the second phase dealt with fabrication.

Volume I contains the results of a study to determine the most suitable parachute assembly design. This study, i.e. Volume II, establishes the basis for the direct design effort.

This work was conducted under U.S. Army Project 1F162203D-195, Exploratory Development of Airdrop Systems, by Pioneer Parachute Company, Manchester, Connecticut, under contract No. DAAG17-68-0142.

The project engineer was Mr. Royce A. Toni of the contracting agency. The work was performed under the direction of Mr. Arthur W. Cluridge, the project engineer for the U.S. Army Natick Laboratories.

TABLE OF CONTENTS

<u>Section</u>	<u>Page</u>
Foreword	iii
Abstract	vi
1. INTRODUCTION	1
2. SYMBOLS	1
3. SYSTEM REQUIREMENTS	3
4. DESIGN-STUDY OBJECTIVES	4
5. STEADY-STATE DRAG	5
a. El Centro, Calif., Full-scale Drop Tests	5
b. Wind-tunnel Tests	35
6. DEPLOYMENT	37
7. INFLATION	41
8. WEIGHT, STRENGTH, AND COST OF CANDIDATE MATERIALS FOR PARACHUTE ASSEMBLY	41
9. SIZING THE PARACHUTE ASSEMBLY	90
10. PERFORMANCE	105
a. Effective Drag History	105
b. Maximum Cluster Loads	145
c. Maximum Load Experienced by Any Single Parachute	149
d. Reliability with Regard to Maximum Rate of Descent	154
11. PRELIMINARY DESIGN	154
a. Maximum Canopy Stress for a Vent-pulldown Parachute	155
(1) G-11A Cargo Parachute	155
(2) Prototype Parachute Assembly ($D_0 = 135$ ft)	159

<u>Section</u>	<u>Page</u>
b. Selection of Material for the Prototype Parachute Assembly ($D_0 = 135$ ft)	160
(1) Canopy	160
(2) Suspension Lines	160
(3) Riser, Riser Extension, and Center Line	161
c. Consideration of Center Line as Primary Load-carrying Member	162
12. CONCLUSIONS AND RECOMMENDATIONS	163
13. ACKNOWLEDGMENTS	167
14. REFERENCES	167

APPENDIX

DRAG COEFFICIENT, INFLATION CHARACTERISTICS AND CLUSTER PERFORMANCE OF MODIFIED G-11A PARACHUTE MODELS

ABSTRACT

This report covers a two-phase, 7-month research and development program to design and fabricate a prototype cargo-recovery parachute assembly for airdropping heavy unit loads in the order of 50,000-lb. The design study covers the trade-off analysis and cost effectiveness aspects for a complete parachute assembly. From these studies, a design analysis and a complete detailed design were made based on the specified performance and design requirements.

Use of data reduction on full-scale cargo drops with G-11A parachutes with vent-pull down configuration, scale model wind tunnel tests and parametric studies determined that it is feasible to use a cargo parachute of 135 ft. diam. with a vent-pull down in a cluster of six to recover a load unit of 50,000-lb.

1. INTRODUCTION

With the advent of super-cargo aircraft, such as the Air Force's C-5A, there is a need for developing an operational 50,000-lb-capacity airdrop system. Owing to the relatively high payload weight, it is obvious that such a system must be comprised of a group of parachutes forming a cluster.

The problems associated with clustered-parachute operation are reviewed extensively (2, 3, 4). The primary problem of cluster-parachute operation can be attributed to the fact that they do not follow a synchronous and repeatable inflation pattern. As a result, one or more parachutes carry excessive loads and, therefore, all must be designed stronger and heavier. In addition, the possibility exists that the lagging parachutes may be blanketed so severely that one or more either fail to inflate at all, or are so tardy in inflating that steady-state descent is attained only after an excessive loss in altitude.

In general, the problems in the heavy-supply drop of a 50,000-lb payload are those common to the performance of clusters of large parachutes, except that in this particular case they are accentuated by the extremely high payload weight which directly affects the size and number of parachutes.

The intent here is to optimize state-of-the-art techniques to enhance the cluster-parachute performance, thereby enabling its design to be as efficient as possible in terms of weight, volume, and cost. The purpose of this report is to present the results of a study conducted to determine the most suitable design for a prototype recovery parachute assembly to enable the airdrop, by use of parachutes in a cluster, of a 50,000-lb unit load.

2. SYMBOLS

- | | |
|-------|--|
| c | Factor related to suspension-line convergence angle, dimensionless |
| C_D | Drag coefficient, dimensionless |
| D | Diameter, ft |
| e | Factor related to strength loss by abrasion, dimensionless |

F Force, lb
 H Altitude above terrain, ft
 h Bag-strip distance, ft
 j Safety factor, dimensionless
 k Factor related to strength loss by fatigue, dimensionless
 L Length, ft
 M Mass, slugs
 N Number of gores, dimensionless
 o Factor related to strength loss in material from water and water-vapor absorption, dimensionless
 q Aerodynamic pressure, lb/ft²
 R Radius, ft
 r Range, ft
 R/D Rate of descent associated with El Centro drop data, ft/sec
 S_o Total cloth area of canopy, ft²
 t Time, sec
 u Factor involving strength loss at connection of the suspension line and the drag-producing surface of riser, dimensionless
 V Velocity, ft/sec
 W Payload weight, lb
 γ Path angle, deg
 ρ Atmospheric density, slugs/ft³

Subscripts

A/C Aircraft
 b Bag containing folded parachute

C Center line
 c Conveying body or payload
 CL Cluster
 ext Extraction system
 g Gore
 i-n ith chute of cluster comprised of n chutes
 o At $t = 0$
 R Reefed state
 S Suspension line
 s Stripped material from containing bag
 ST Standard or unmodified

3. SYSTEM REQUIREMENTS

A program was initiated to design a complete parachute recovery assembly consisting of parachute canopy, reefing system, risers, riser extensions, deployment system, and other necessary components and related hardware to enable the airdrop, by use of parachutes in a cluster, of a 50,000-lb unit load. Since the purpose is to determine the most suitable design for the parachute recovery system, it is important that the final design meet the following requirements:

(a) Performance

- (1) Gross rigged weight: 50,000 lb.
- (2) Deployment speed: 130 to 150 KEAS.
- (3) Vertical impact velocity: not to exceed 28.5 ft/sec from sea level to 5000 ft for temperatures between -65 and +100°F.
- (4) Drop altitude: minimum attainable, but not to exceed 1500 ft above the drop-zone terrain.
- (5) Maximum force applied to cargo-parachute release assembly: not to exceed 2.5 times gross rigged weight.

(b) Physical

- (1) Type of canopy: solid-flat circular.
- (2) Cluster: comprised of not fewer than four nor more than eight parachute recovery systems.

(3) Reefing: skirt reefing to control parachute forces within acceptable limits.

(4) Opening and performance aids: a permanent vent-control center line to be attached between the apex of the canopy and the confluence point of the canopy-suspension system to effect a permanent pulldown of the vent of the canopy to the vicinity of the canopy skirt.

(5) Deployment system: a full deployment bag similar to that employed with the G-11A cargo parachute.

(6) Risers and riser extensions: appropriate length so as to attain optimum parachute-cluster performance.

(7) Canopy color: olive green, shade no. 106.

(8) Safety factors: 2.0 for the textile components of the parachute recovery system; 1.75 for its metal components.

4. DESIGN-STUDY OBJECTIVES

The primary objectives of this design study, in pursuit of the most suitable design for the parachute recovery system, are listed as follows.

(a) To determine the size of the parachute assembly.

(b) To determine the number of parachute assemblies in the cluster.

(c) To determine the lengths and strength requirements of

- (1) the suspension lines,
- (2) the risers,
- (3) the riser extensions, and
- (4) the center line.

(d) To determine opening characteristics associated with the cluster.

(e) To determine the maximum load imposed upon a parachute assembly.

(f) To determine allowable reefing-cutter tolerances.

(g) To determine the strength requirements of the main seam.

The attainment of these objectives was aided considerably by data from the U.S. Army Natick Laboratories concerning full-scale drop test of 100-ft-diam. G-11A cargo parachutes. These drops ranged from single parachutes to clusters of five, and all the cluster drops utilized the vent-pulldown technique. The data from these drops proved most beneficial.

since the drops were conducted in the operational environment nearly identical to that expected of the system under study; the parachutes used in these drops were of a size on the order of those under study; and finally, since the parachutes were a solid-flat circular type with vent pull-down as are those expected in this system.

To better achieve the previously cited objectives, a limited wind tunnel program was conducted by Dr. H. G. Heinrich of the University of Minnesota. The primary purpose of this tunnel effort was to determine the effect of certain parameters (such as suspension-line lengths, center-line lengths, and number of chutes in clusters) on the aerodynamic characteristics of clustered, vent-pulldown parachutes.

5. STEADY-STATE DRAG

a. El Centro, Calif., Full-scale Drop Tests

Preliminary indications of extensive full-scale drop tests conducted at El Centro, Calif., point toward an increase in drag efficiency obtainable by modifying the parachute to use a vent pulldown. Table 1 lists a few of these drops which produced the available data. Figures 1 through 25 present the reduced data from which an average steady-state vertical rate of descent can be derived. Use of this vertical rate of descent enables the calculation of the drag coefficient of a parachute cluster during its steady-state mode of operation.

Scrutiny of Figs. 1 through 25 discloses certain relationships, primarily the effect of vent pulldown on drag and the effect of the number of parachutes in a cluster on the cluster drag. These relationships are clearly illustrated in Figs. 26 and 27.

Figure 26 reveals the ratio of the steady-state drag coefficient of a modified (vent pulldown or use of a center line) single G-11A cargo parachute to the drag coefficient of a standard configuration as a function of the ratio of center-line length to parachute diameter. Although this figure is limited to only one suspension-line length (that is, $0.95D$), it does show that the drag increase of the modified configuration is of the order of 20% over that of standard, and that this 20% increase occurs when the vent is pulled down at or immediately above the vicinity of the skirt.

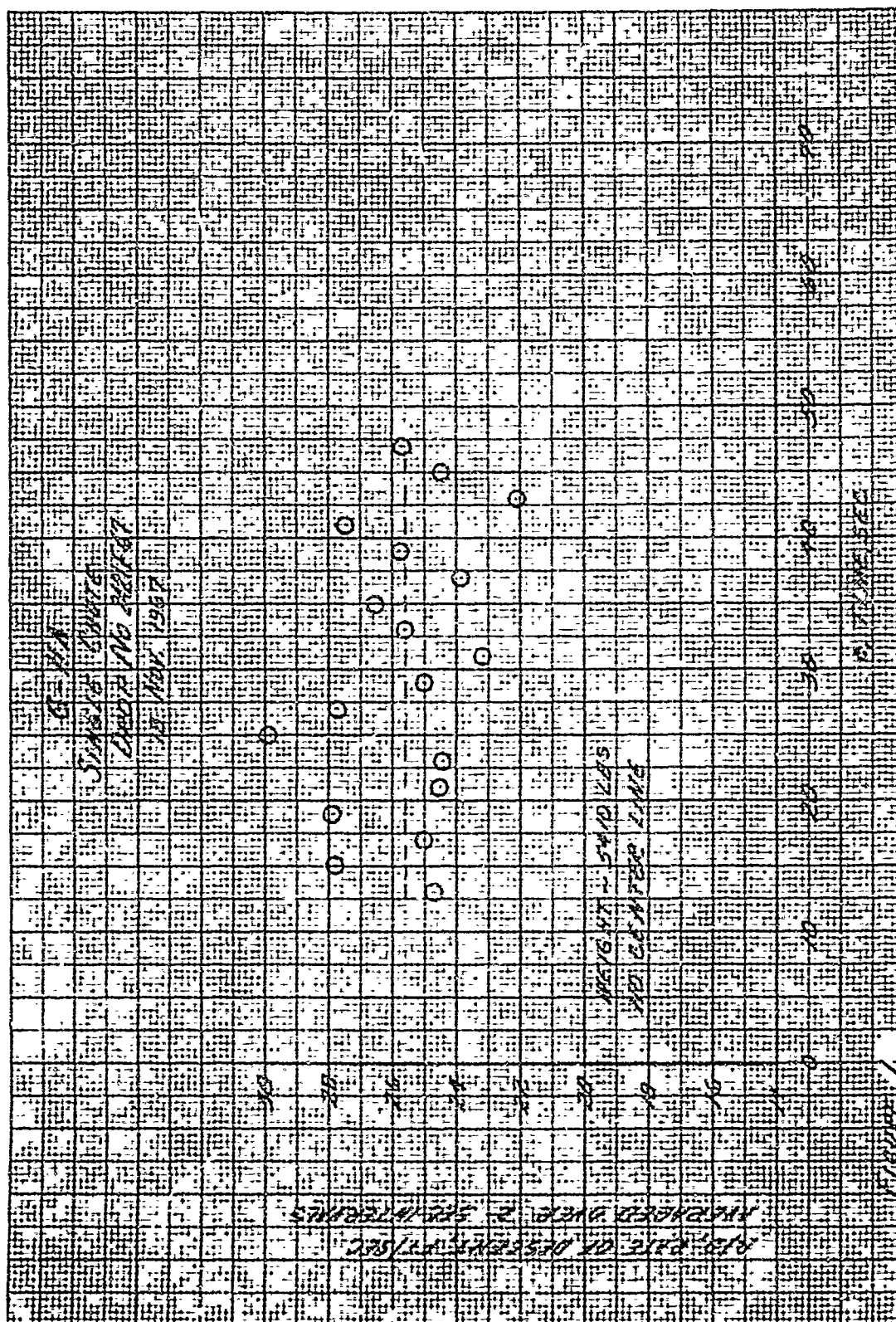
TABLE 1
EL CENTRO DROP TESTS OF VARIOUS G-11A CONFIGURATIONS

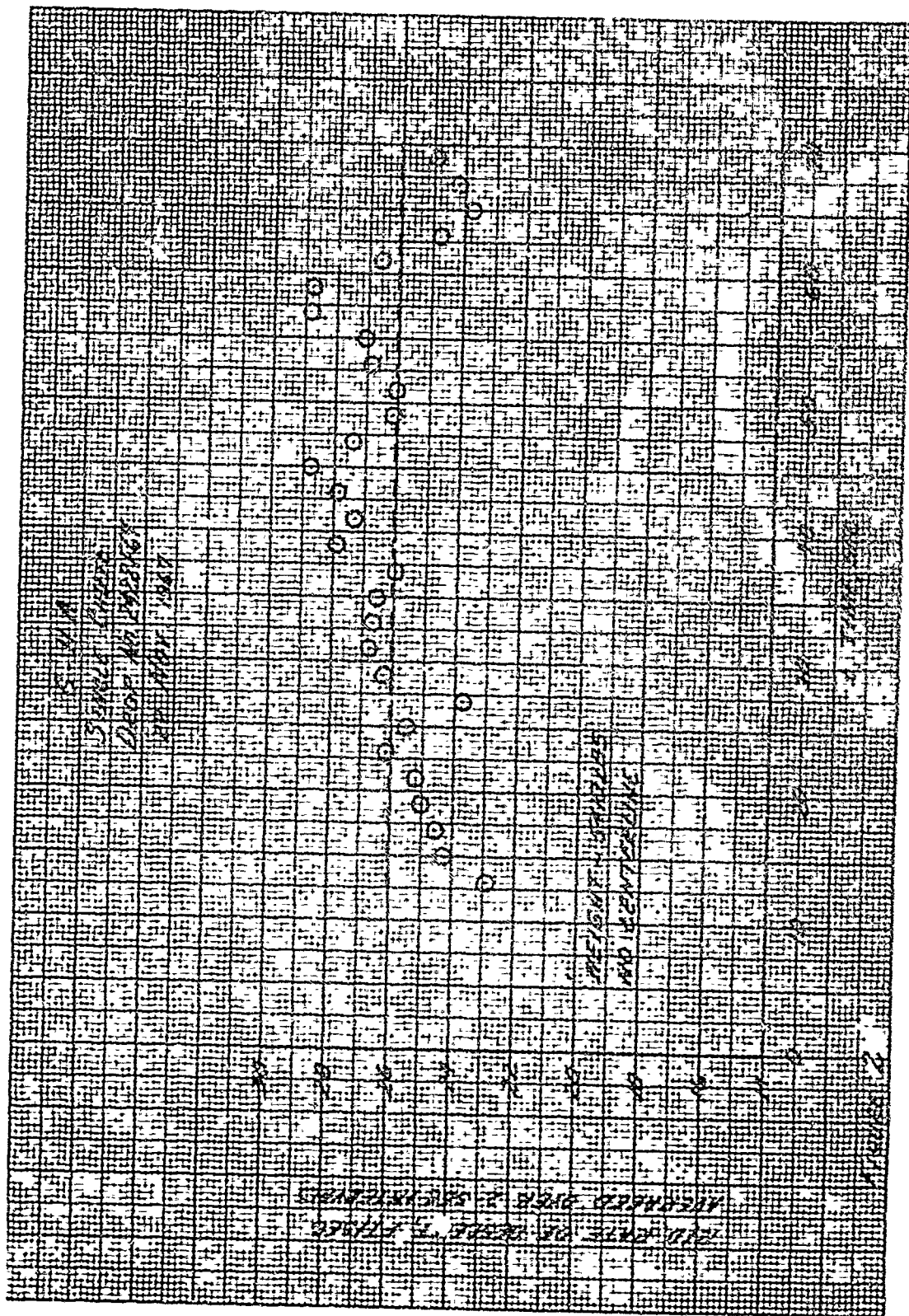
Drop no. & date	L_c , ft	n	W, lb	V, ft/sec	$(C_{D_o})_{CL}$	Comments
2421F67 18 Nov 67	None	1	5,410	25.6	0.91	Standard
2422F67 22 Nov 67	None	1	5,410	26.1	0.88	Standard
2181F67 30 Nov 67	None	1	5,410	23.9	1.05	Standard High $(C_{D_o})_{CL}$
0622F67 6 Apr 67	76	1	5,000	21.9	1.15	L_c not known
0051F67 20 Jan 67	90	1	4,580	20.8	1.17	L_c not known
1208F67 3 Jul 67	96	1	4,980	19.7	1.42	High
1619F67 12 Sep 67	95	1	5,410	23.5	1.08	Good data
0404F67 7 Mar 67	94	1	4,580	20.4	1.22	L_c not known
0405F67 9 Mar 67	96	1	4,580	22.0	1.05	Good data
0520F67 30 Mar 67	94	1	6,000	16.5	2.44	L_c not known High $(C_{D_o})_{CL}$
2431F66 18 Oct 66	102	1	4,580	25.5	0.78	L_c not known
2464F66 24 Oct 66	102	1	4,580	24.1	0.87	L_c not known
1781F67 4 Oct 67	95	2	10,650	24.6	0.97	
1783F67 6 Oct 67	95	2	10,650	21.9	1.23	High
1782F67 9 Oct 67	95	2	10,650	24.7	0.97	
1990F67 11 Oct 67	95	2	10,650	24.9	0.95	

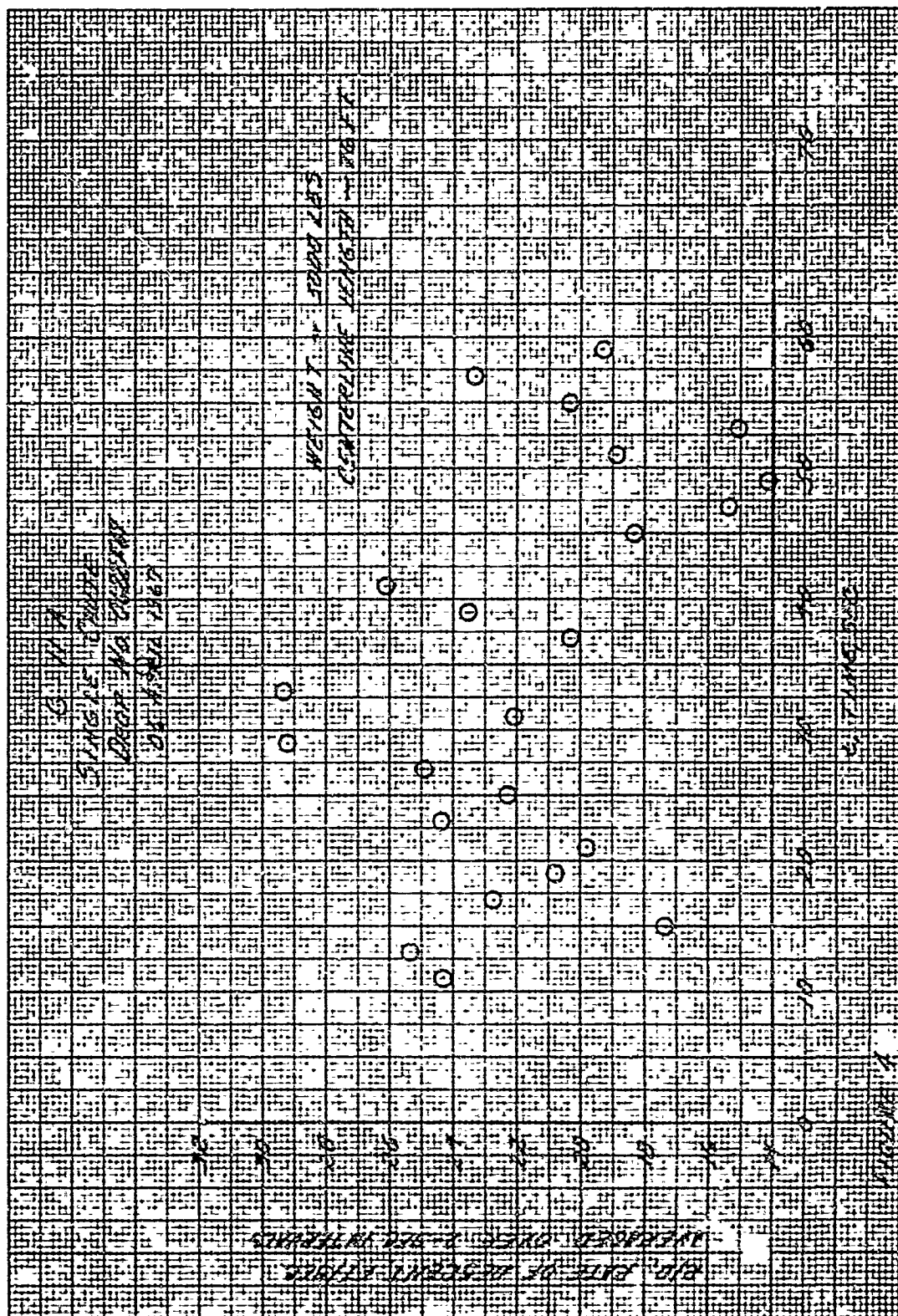
(continued)

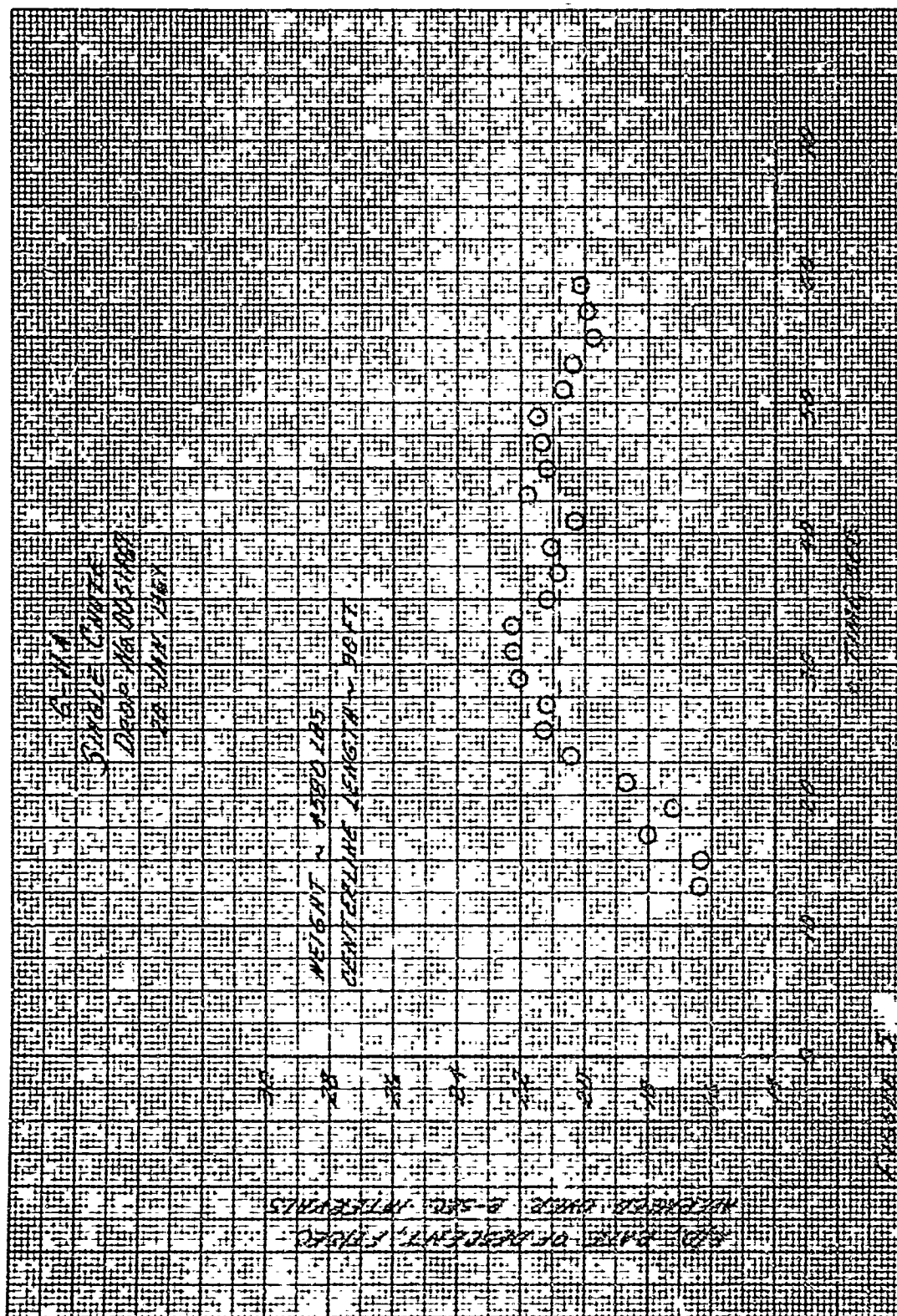
TABLE 1 (cont'd)

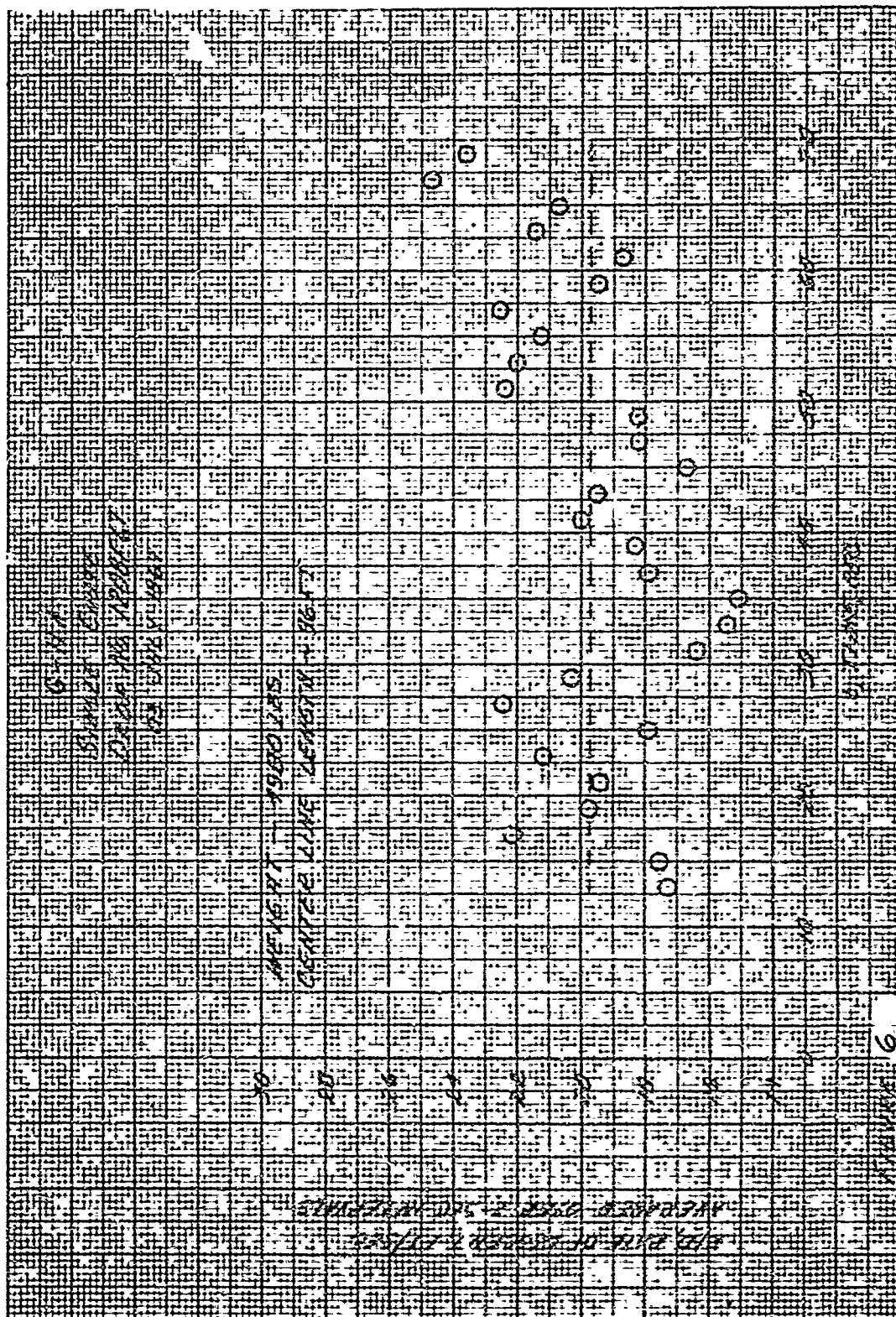
Drop no. & date	L_c , ft	n	W, lb	V , ft/sec	$(C_{D_o})_{CL}$	Comments
2005F67 13 Oct 67	95	2	10,650	24.5	0.98	
2014F67 23 Oct 67	95	3	16,000	24.2	1.01	
2015F67 27 Oct 67	95	3	16,000	21.3	1.30	High
2139F67 1 Nov 67	95	3	16,000	22.3	1.19	High
2013F67 16 Nov 67	95	3	16,000	24.2	1.01	
2140F67 20 Nov 67	95	3	16,000	24.6	0.98	
2401F67 5 Jan 68	95	5	26,400	25.9	0.87	
2490F67 10 Jan 68	95	5	26,400	25.2	0.92	
0078F68 19 Jan 68	95	5	26,400	27.1	0.80	Low

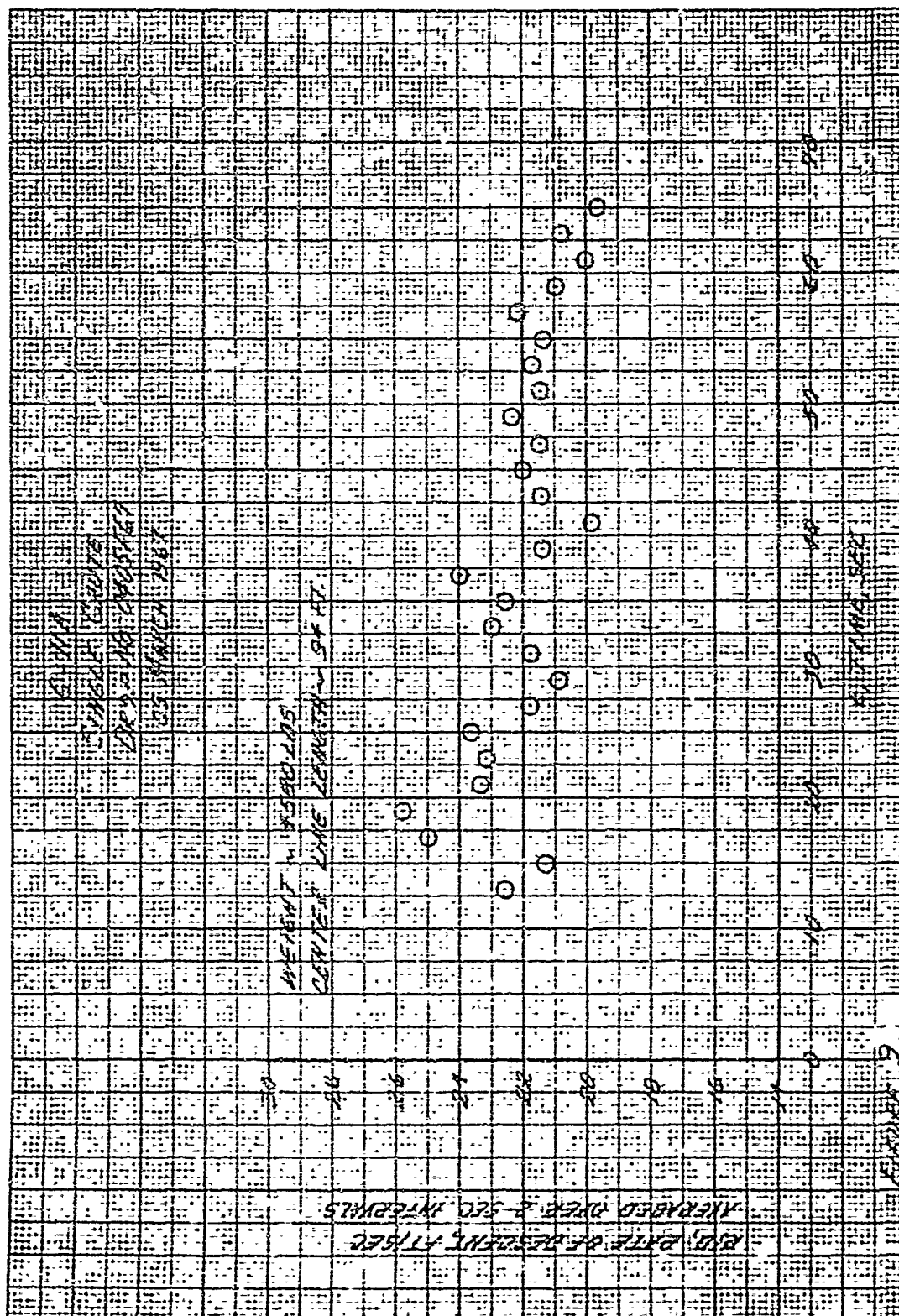


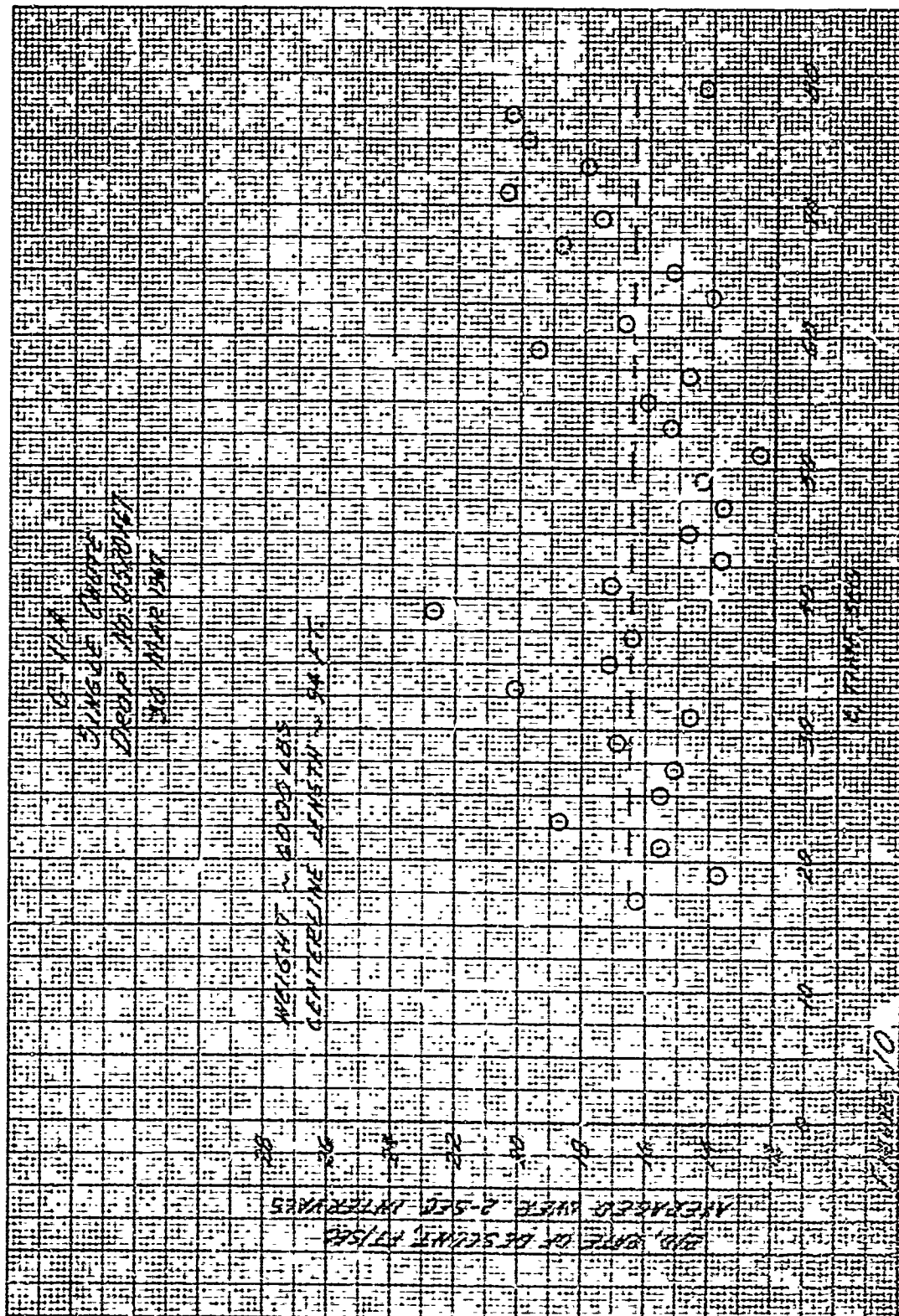


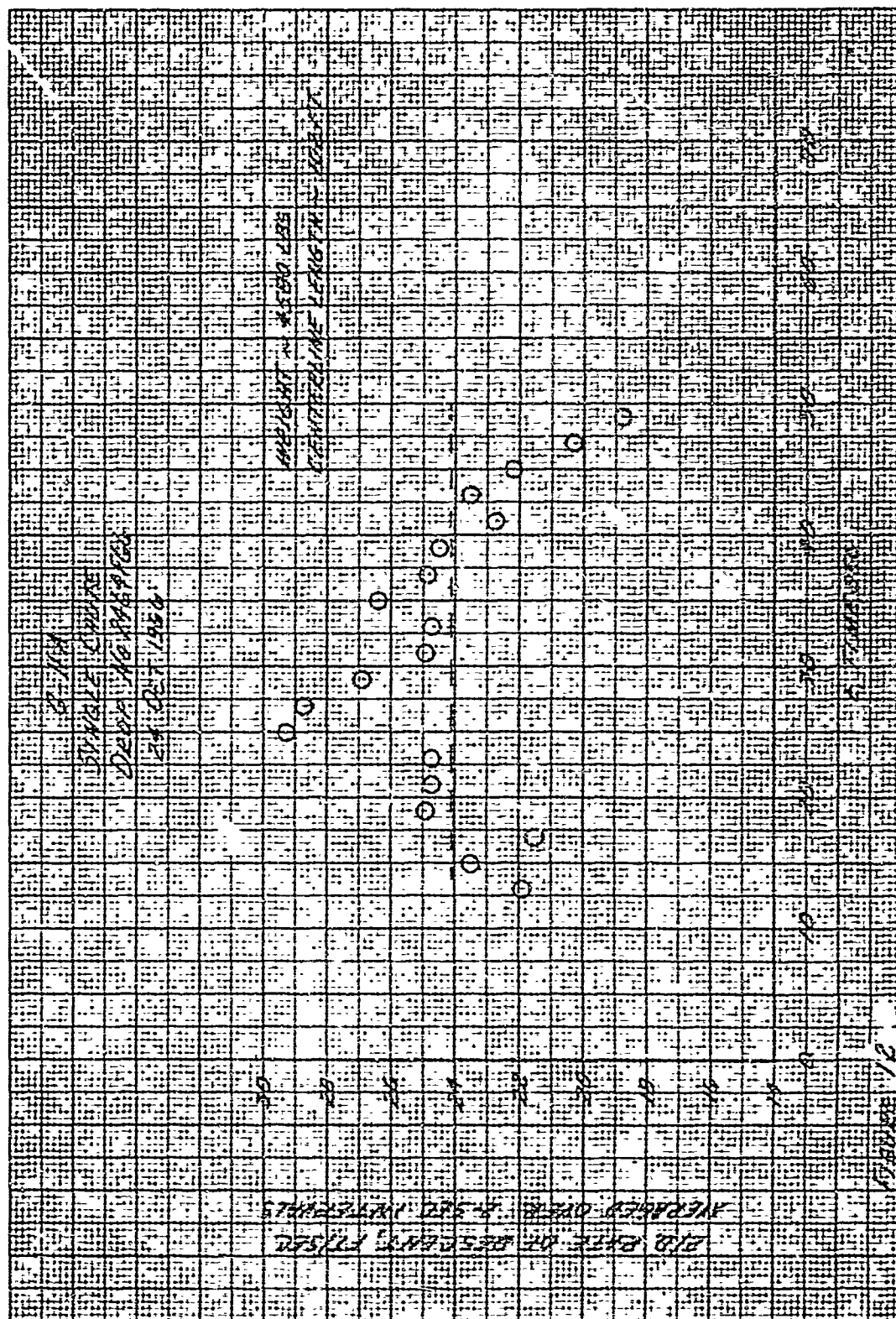


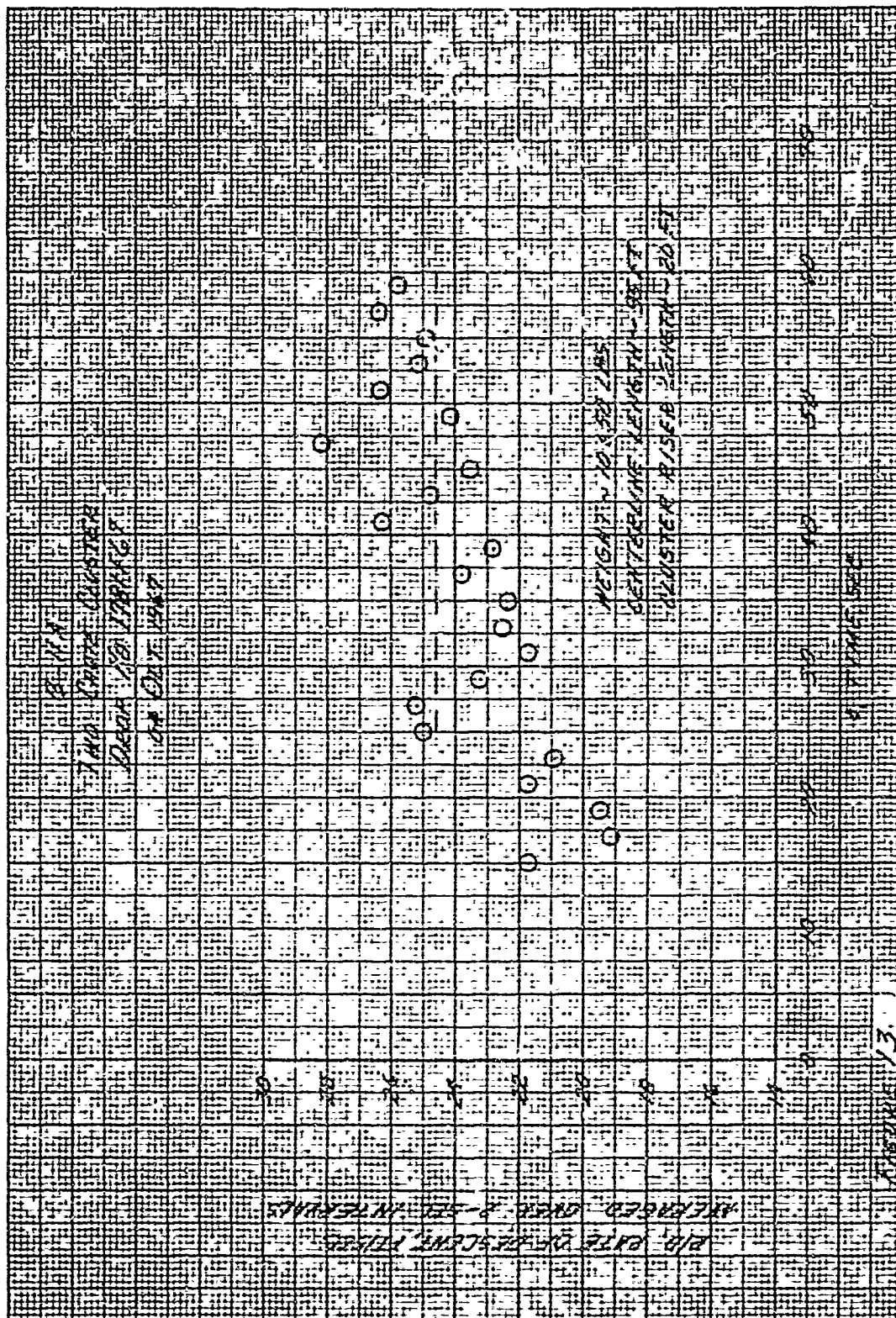


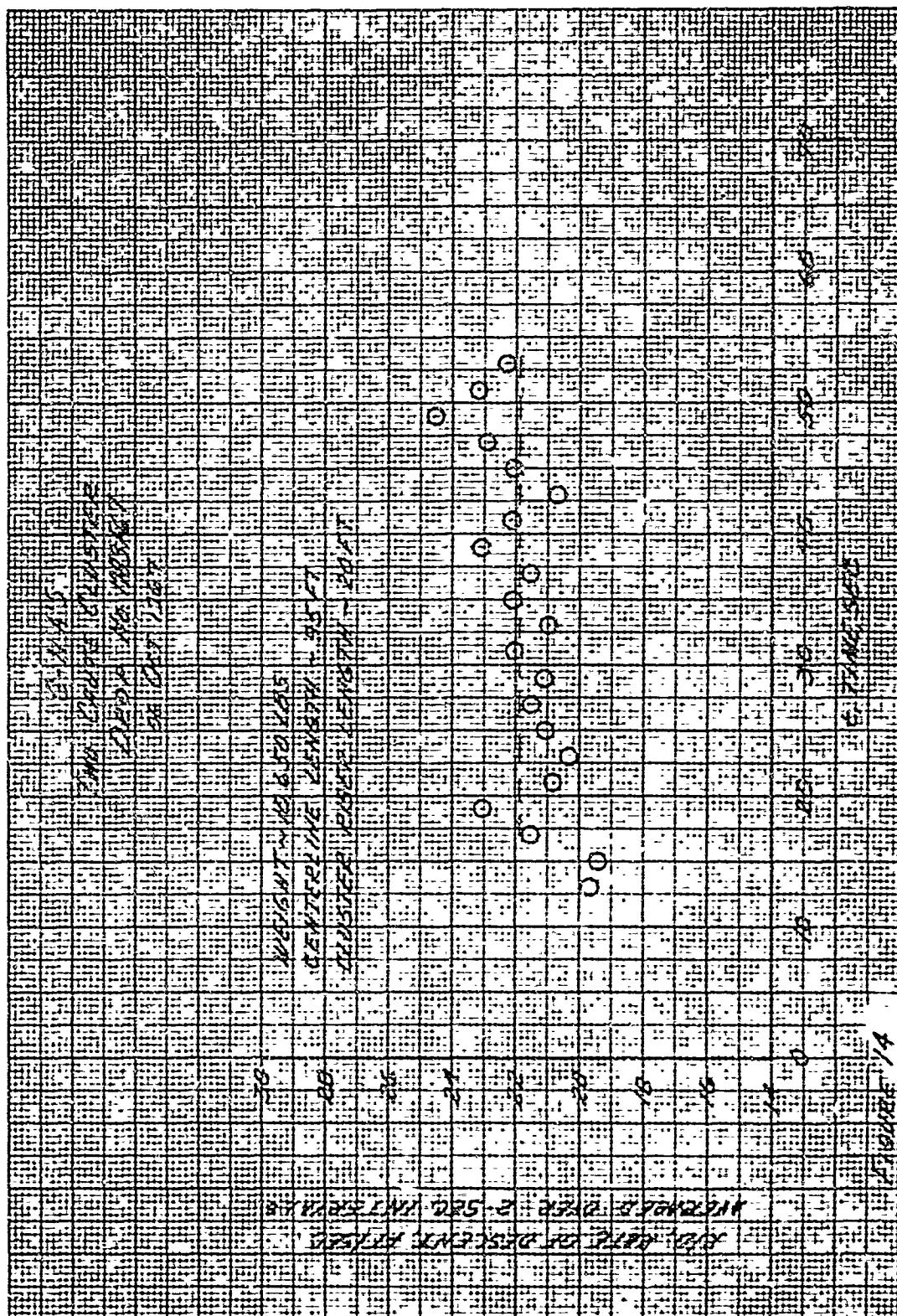


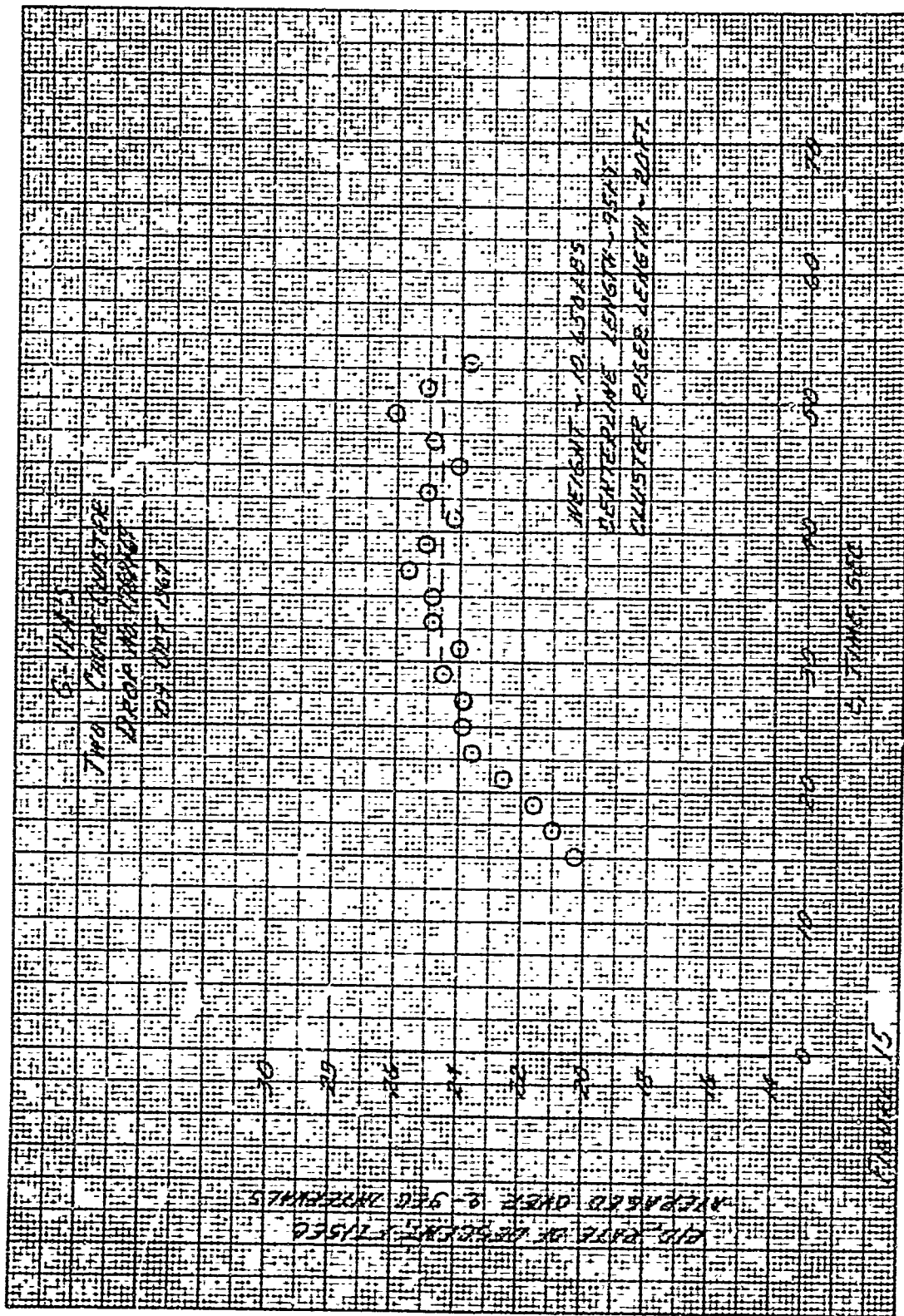


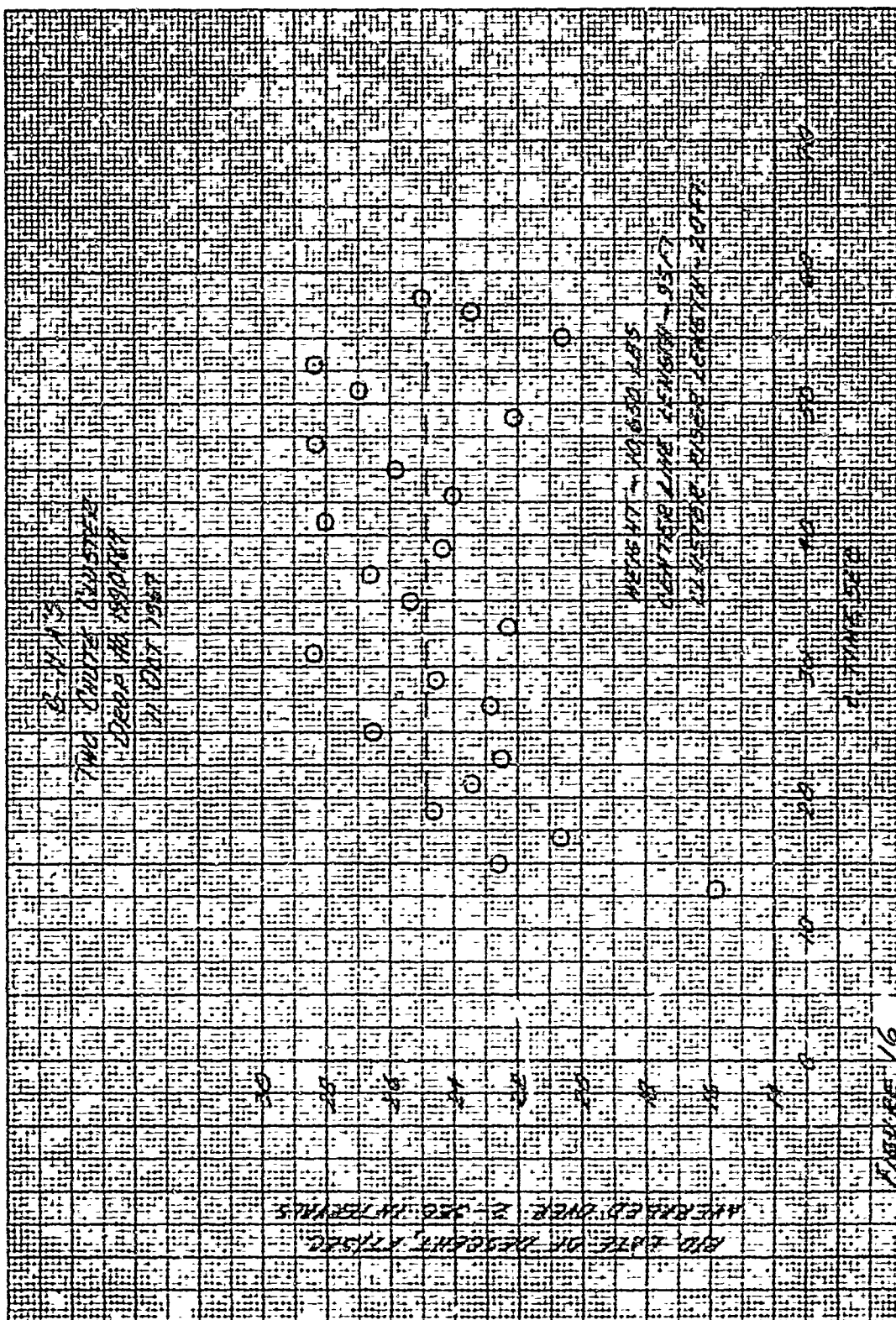


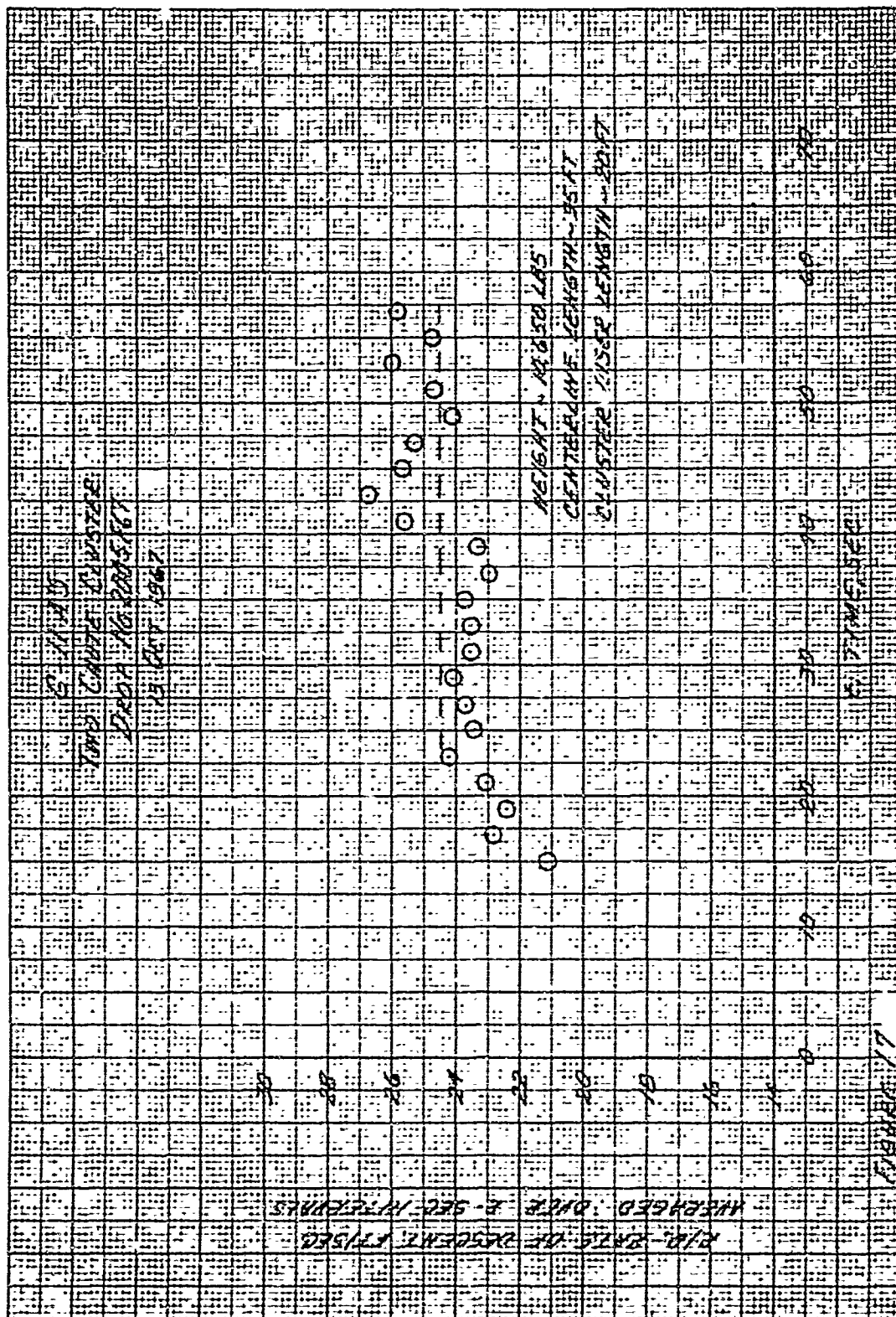


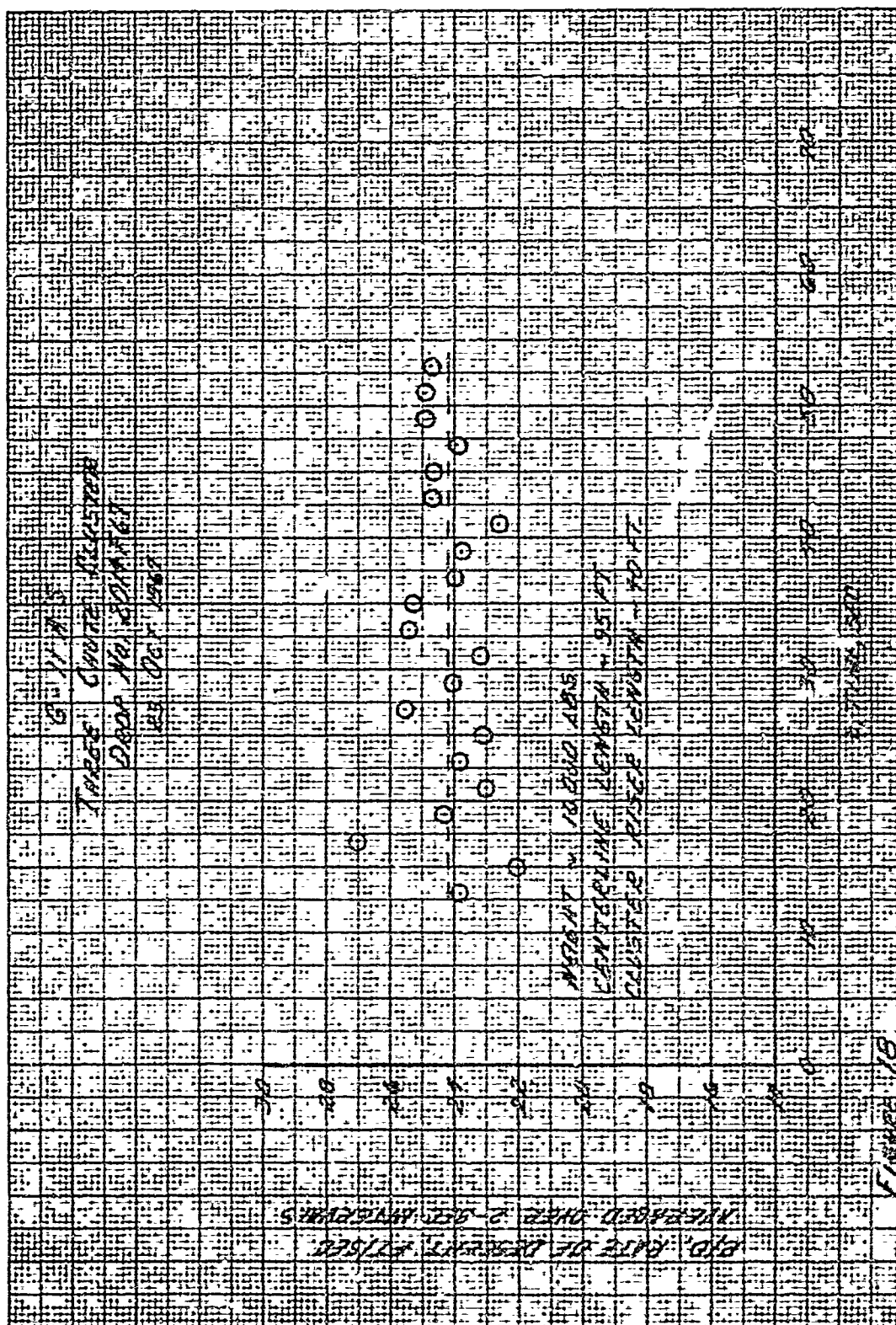


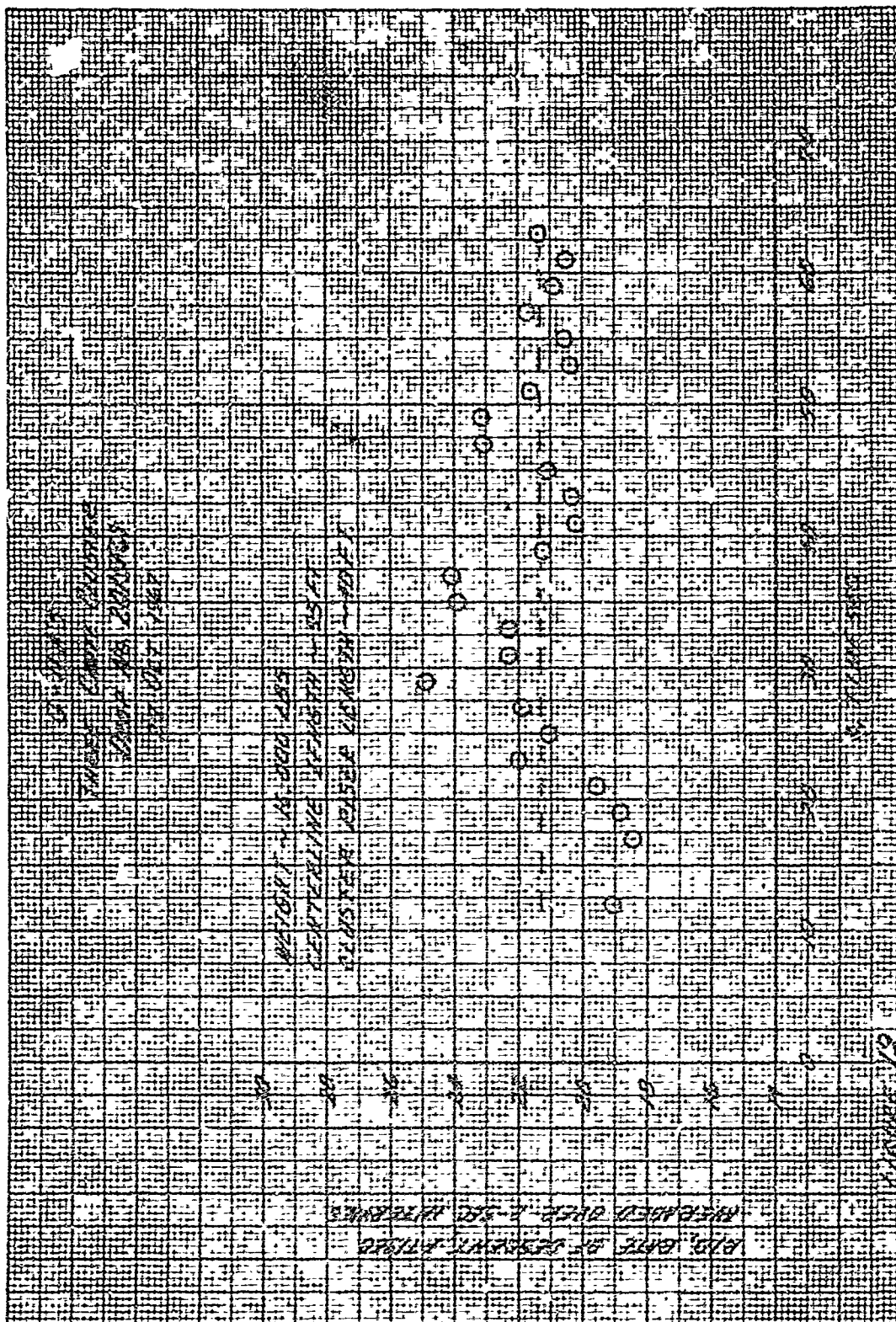


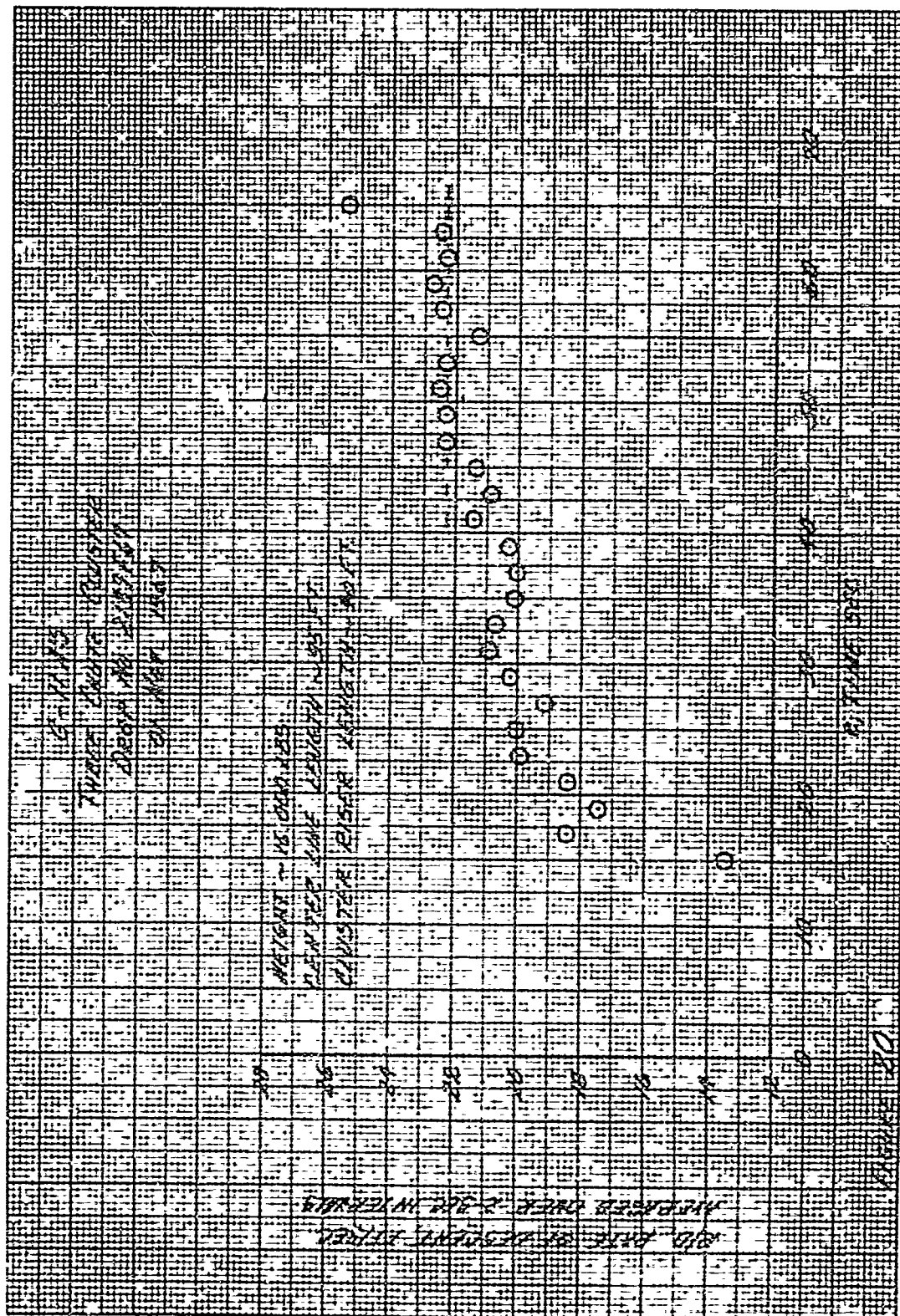






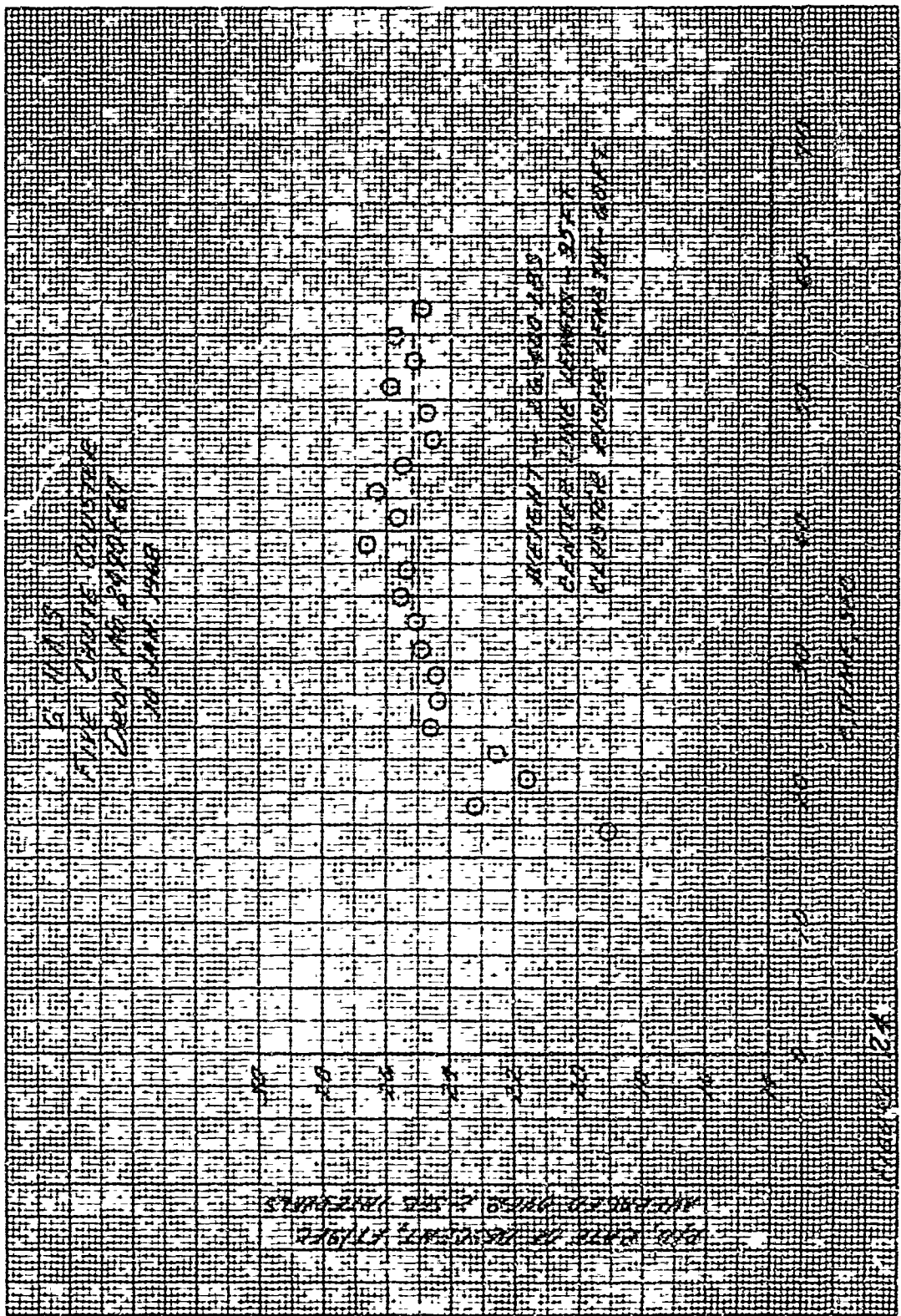


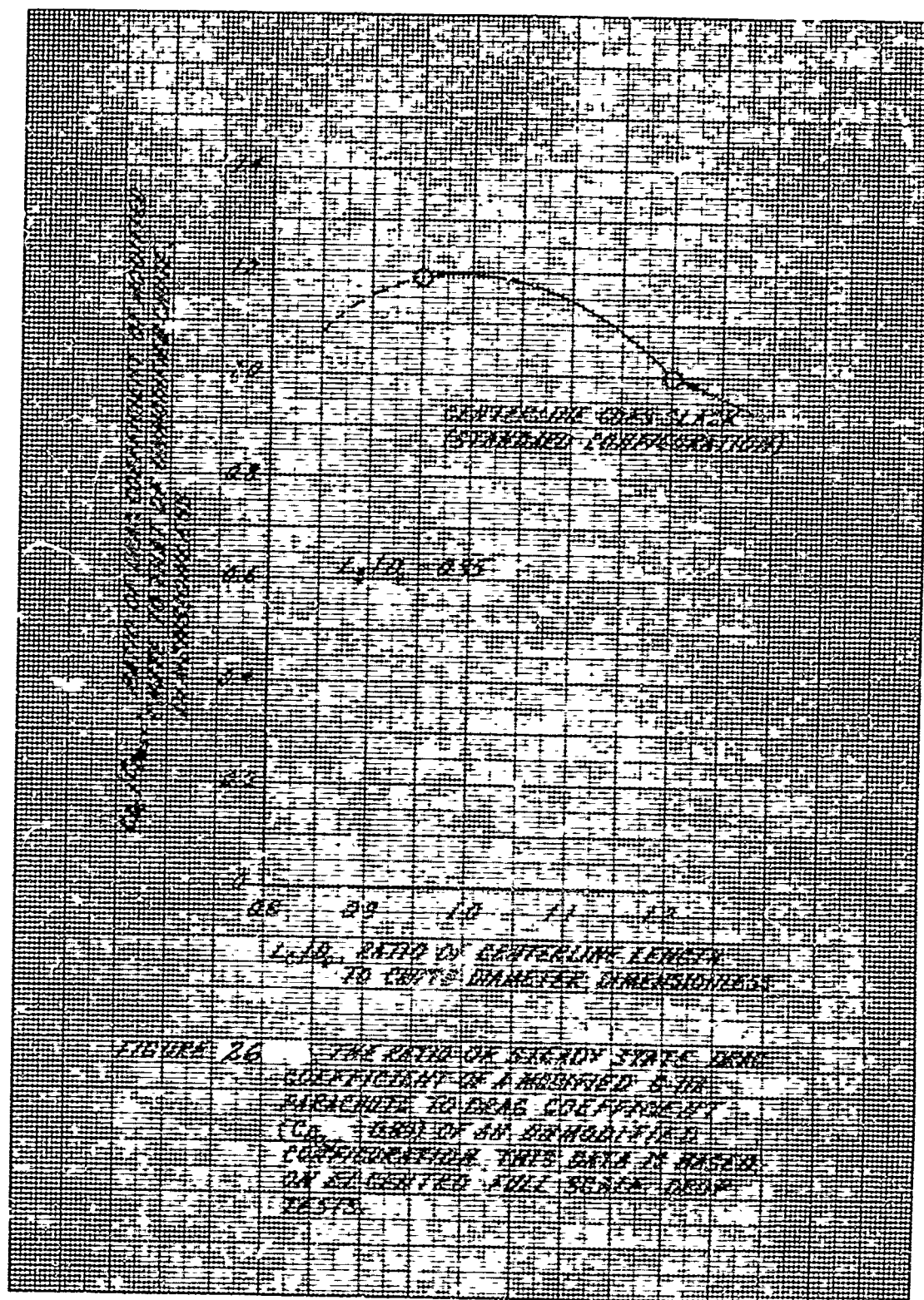












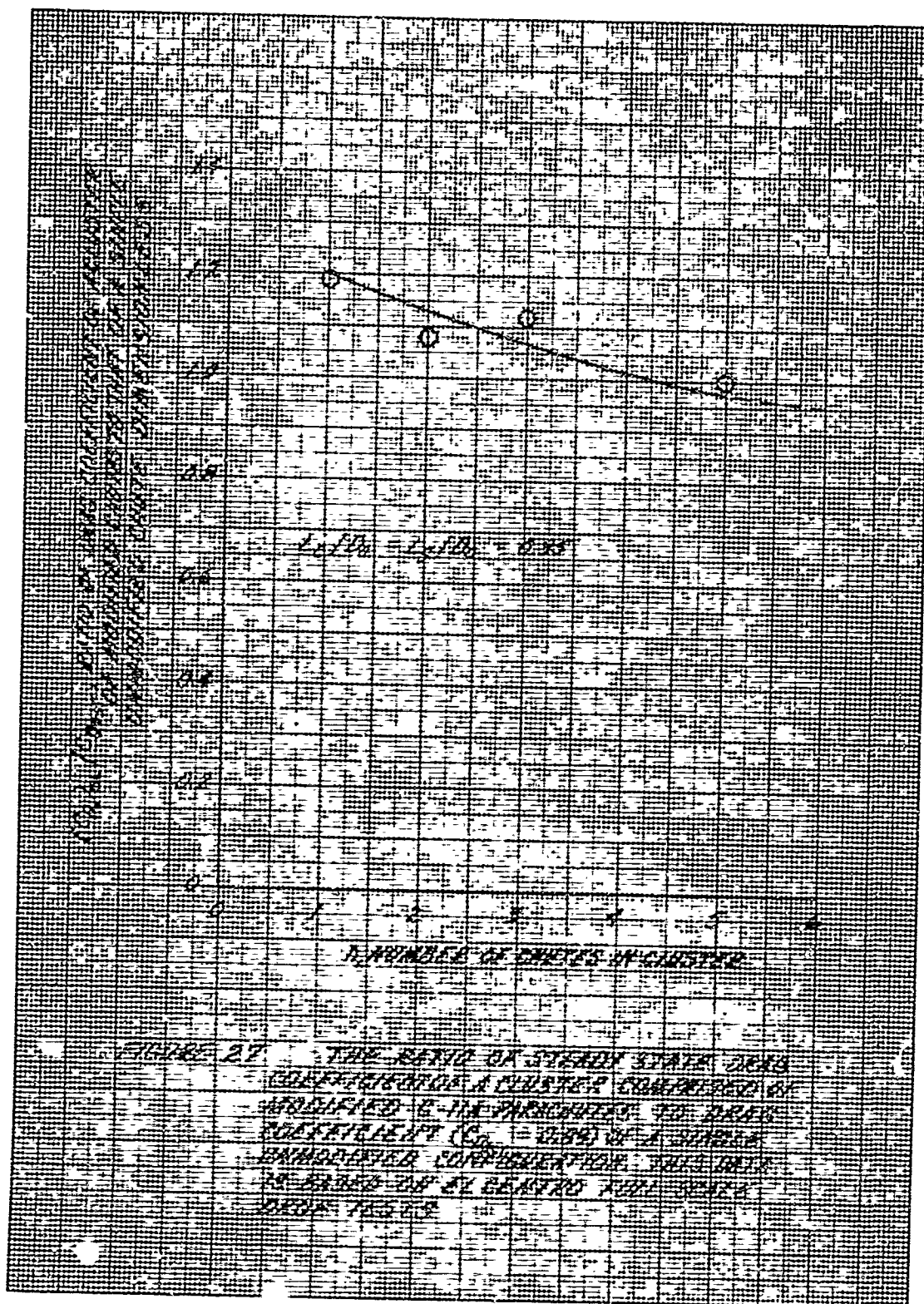


Figure 27 reveals the ratio of the steady-state drag coefficient of a cluster comprised of modified G-11A cargo parachutes to the drag coefficient of a single, standard configuration as a function of the number of chutes in the cluster. Again, this figure is limited to only one suspension-line length, namely $0.95D_0$; however, it does show that, for a cluster of six chutes employing a vent pulldown at the skirt, the parachute-cluster steady-state drag becomes of the order of 95% of that of a single, standard configuration. Hence, the loss in drag for a parachute cluster comprised of vent-pulldown parachutes is limited when compared with the drag of the same parachute used in its standard configuration in a single mode of operation.

Normally it becomes extremely difficult to analyze the deviations (from drop to drop) in the vertical rates of descent that are associated with a parachute recovery system. It is felt that, with a cluster-parachute system, the deviations are somewhat reduced because, primarily, the system's motion is relatively more perpendicular to the horizon than that of a single chute. Figure 28 expresses (for a series of drops) the approximate ratio of the deviation in the steady-state vertical rates of descent (from drop to drop) to the deviation of a single, standard configuration as a function of the number of chutes in a cluster. From this curve, it can be seen that the deviation in rates of descent of the single modified chute is double that of the single standard chute. For a cluster of six modified chutes (vent pulled down to skirt), the curve reveals that the deviation in vertical rates of descent is reduced to about 35% greater than that of a single standard chute.

b. Wind-tunnel Tests

Figures 29 and 30 are part of the wind-tunnel testing whose purpose was to establish the effect of suspension-line and center-line lengths on the steady-state drag of a vent-pulldown parachute. This information is based on wind-tunnel studies of single-canopy-configuration model parachutes representative of the G-11A cargo parachute.

Figure 29 shows that, for a parachute with the vent pulled down to the skirt, the drag increases as the suspension-line length increases. This figure indicates a maximum 20% increase in drag for the modified parachute over that of the standard parachute.

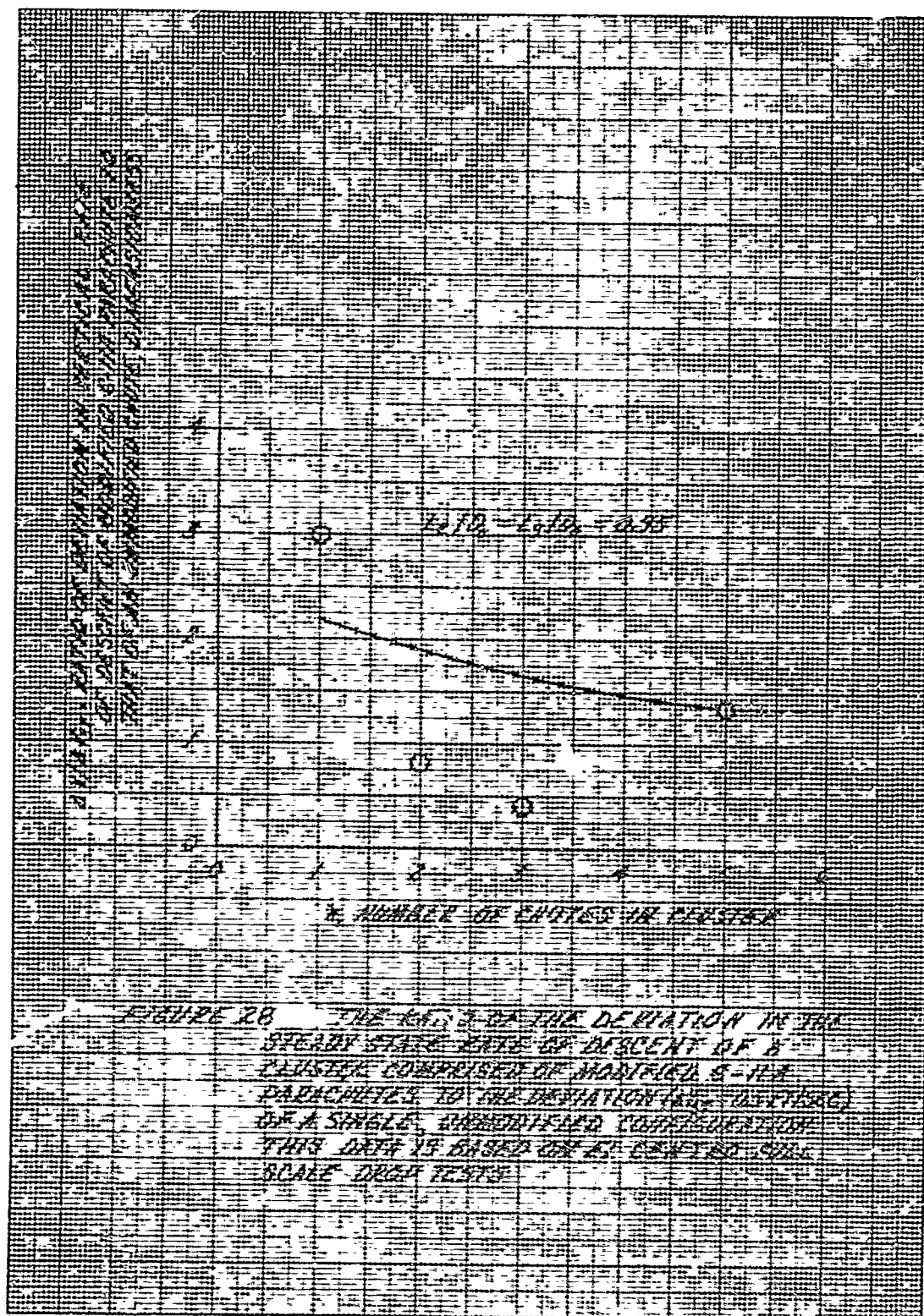


Figure 30 reveals the effect of center-line length (location of the vent with respect to the skirt) on drag for three parachute configurations each having different suspension-line lengths. This figure shows that, for each suspension-line length, the maximum increase in drag occurred when the vent was pulled down to a point immediately above the skirt.

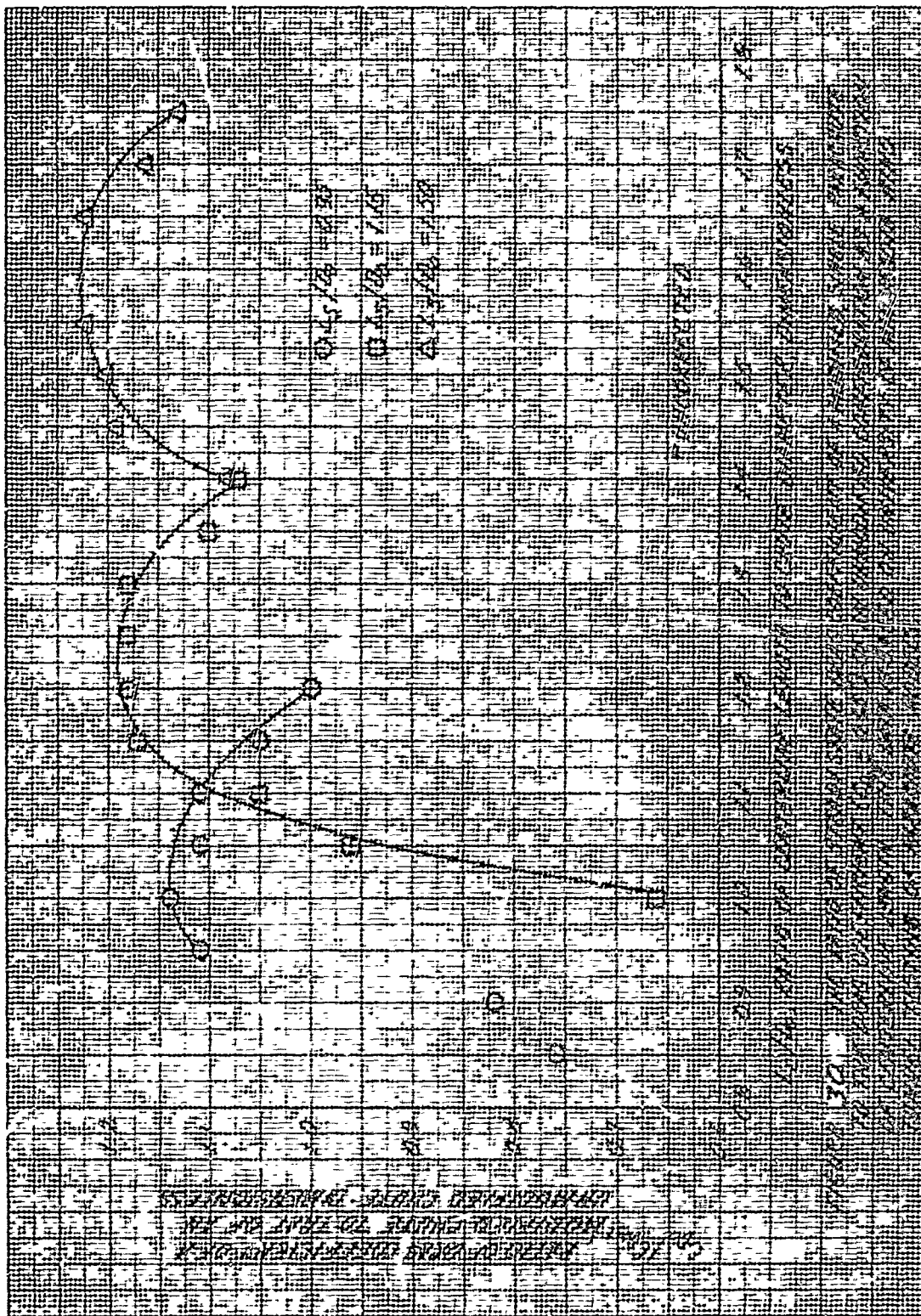
It can be concluded from Fig. 30 that for a suspension-line length of $1.5D_0$ and a center-line length of $1.6D_0$, the increase in drag is some 25% over that of the same parachute in a standard configuration. For a suspension-line length of $1.15D_0$ and a center-line length of $1.25D_0$, this increase in drag is reduced to about 14%. It should be noted that, for the latter case, the reduction of the E1 Centro data indicates a 19% increase in drag (Fig. 26). Hence, the indications resulting from full-scale drop tests and wind-tunnel model tests are consistent.

Wind-tunnel tests are currently being carried out on cluster groupings to determine the variation in steady-state cluster drag with riser-extension length (riser-extension length being defined as the length of the portion of the riser between the individual parachute confluence and the confluence of the cluster). The models being used are representative of the G-11A. As of this writing, no data are available. However, indications are that the drag is maximized for a riser-length-to-parachute-diameter ratio of approximately 1.0.

6. DEPLOYMENT

Although this study is not responsible for the extraction system, it was believed important to have an idea as to the dynamics of the parachute recovery system from the time it left the aircraft (on board the payload) to the time of line stretch. This period of time is referred to as "bag strip," and the entire operation of bag strip is a direct function of the size of the extraction-parachute system.

Figure 31 illustrates the assumed dynamic behavior of the bag-stripping process at some time, t . The following occurs, leading up to t . The extraction system (cluster comprised of three 28- or 35-ft-diam. ringslots) pulls the 50,000-lb-gross rigged weight from the aircraft. Once this payload leaves the aircraft, the force of the extraction system is transferred to the bags containing the main recovery system. This force causes the bags to separate from the payload, whence the bag-stripping process gets under way.



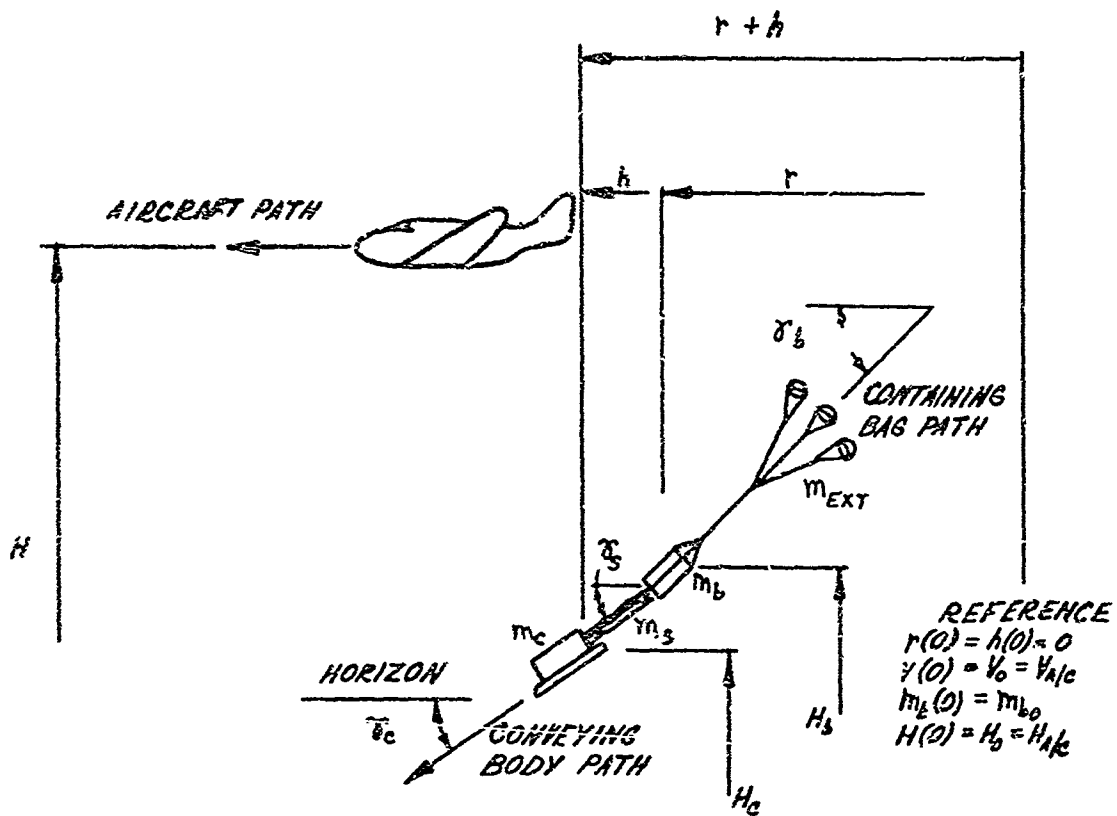


FIGURE 31 - ASSUMED DYNAMIC BEHAVIOR FOR BAG STRIP AT SOME TIME t .

Figures 32 through 55 and Figs. 56 through 79 are the results of a parametric computer study of the system's trajectory during the bag-strip process. The first group of figures is for an extraction system comprised of three 28-ft-diam. ringslot parachutes; the second group is for an extraction system of three 35-ft-diam. ringslot chutes. In each case, it can be seen that the primary parameters are the mass of the main recovery system and the velocity at which the aircraft is moving at the time the payload leaves it.

For illustrative purposes, assume that the extraction system is comprised of three 28-ft-diam. ringslots. Also assume that the speed of the aircraft is 150 knots upon release of the 50,000-lb-gross rigged payload weight at an altitude of 1500 ft above the terrain. Conclude that the main recovery system, when stretched out but not inflated, measures some 314 ft from the payload to the top of the canopies. In addition, the weight of the main recovery system plus the weight of the bags is approximately 1850 lb. Reference to Fig. 34 reveals that the time for complete bag strip is approximately 1.65 sec after the payload leaves the aircraft. This is also shown in Fig. 42. Reference to Fig. 48 reveals that, at 1.65 sec, the bags (which have just emptied themselves completely of their contents) are at an altitude of 1477 ft. At the same time, the payload is at an altitude of 1457 ft. This means that, during the bag-stripping process, the bags lost some 23 ft in altitude and the payload lost some 43 ft in altitude. This information is now taken to describe initial conditions for computing trajectories for the main recovery system.

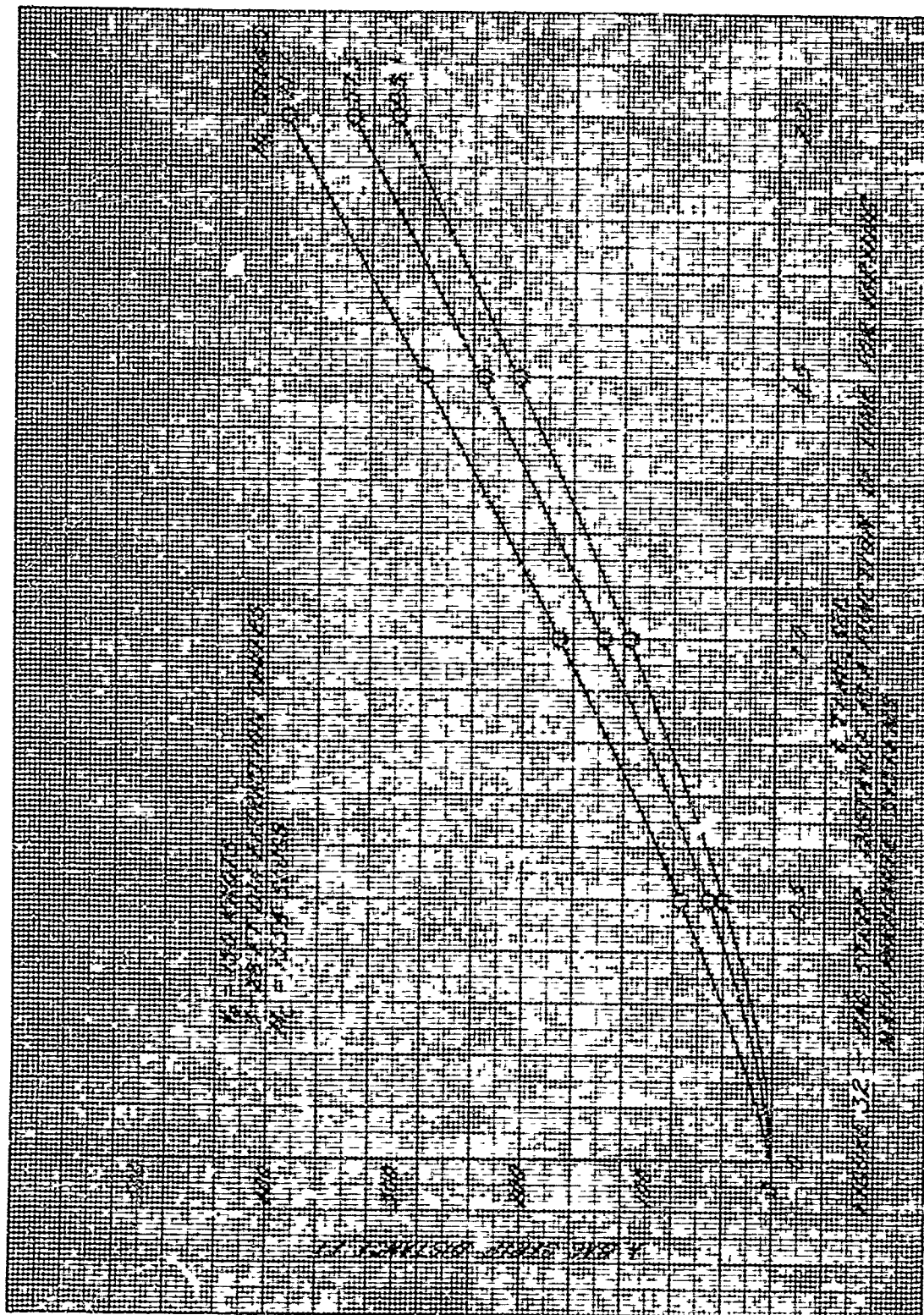
The deployment or "bag-strip" dynamic study, then, should provide some basis for an indication of the system's altitude loss between the time it exists the aircraft and the time it inflates.

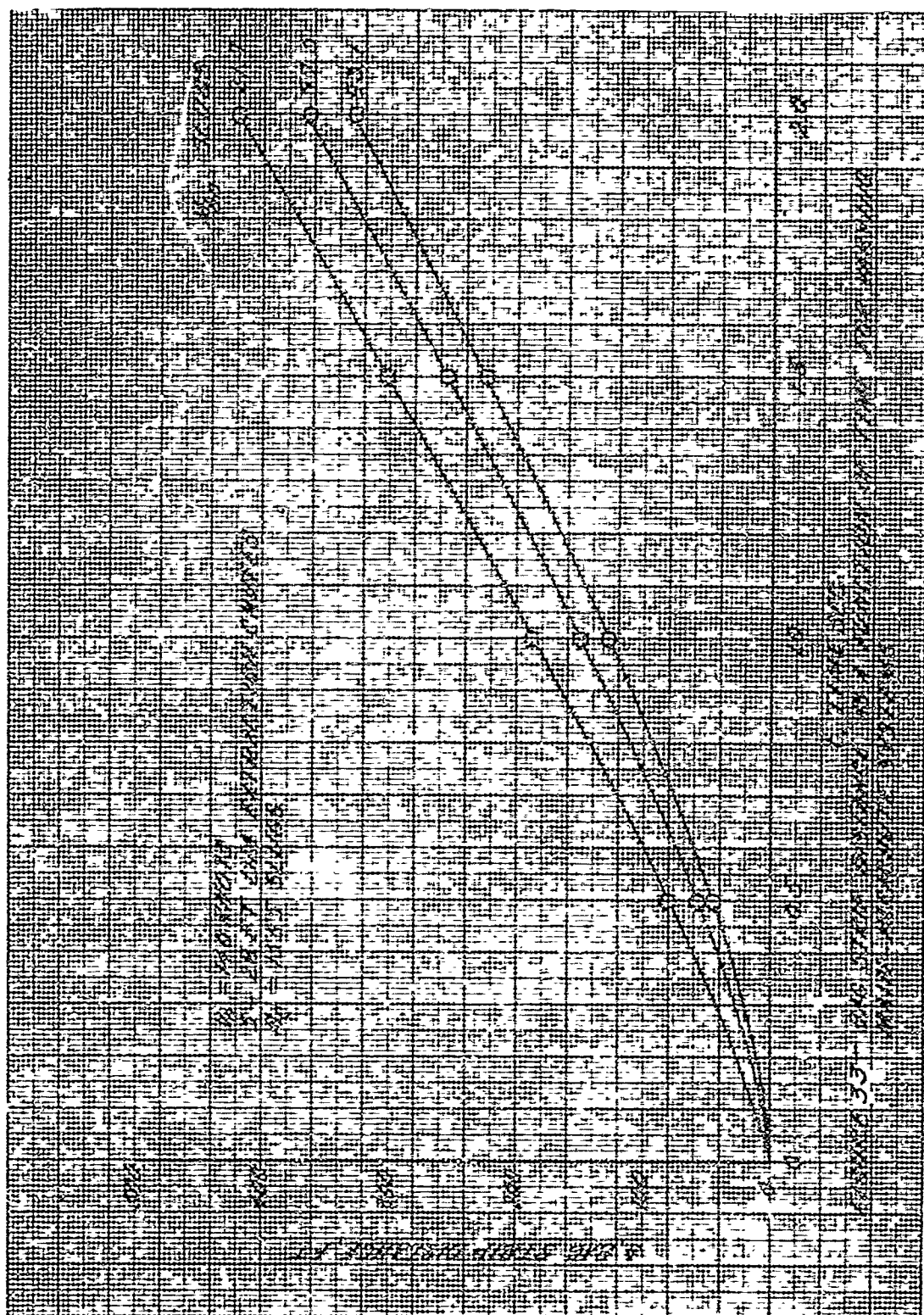
7. INFLATION

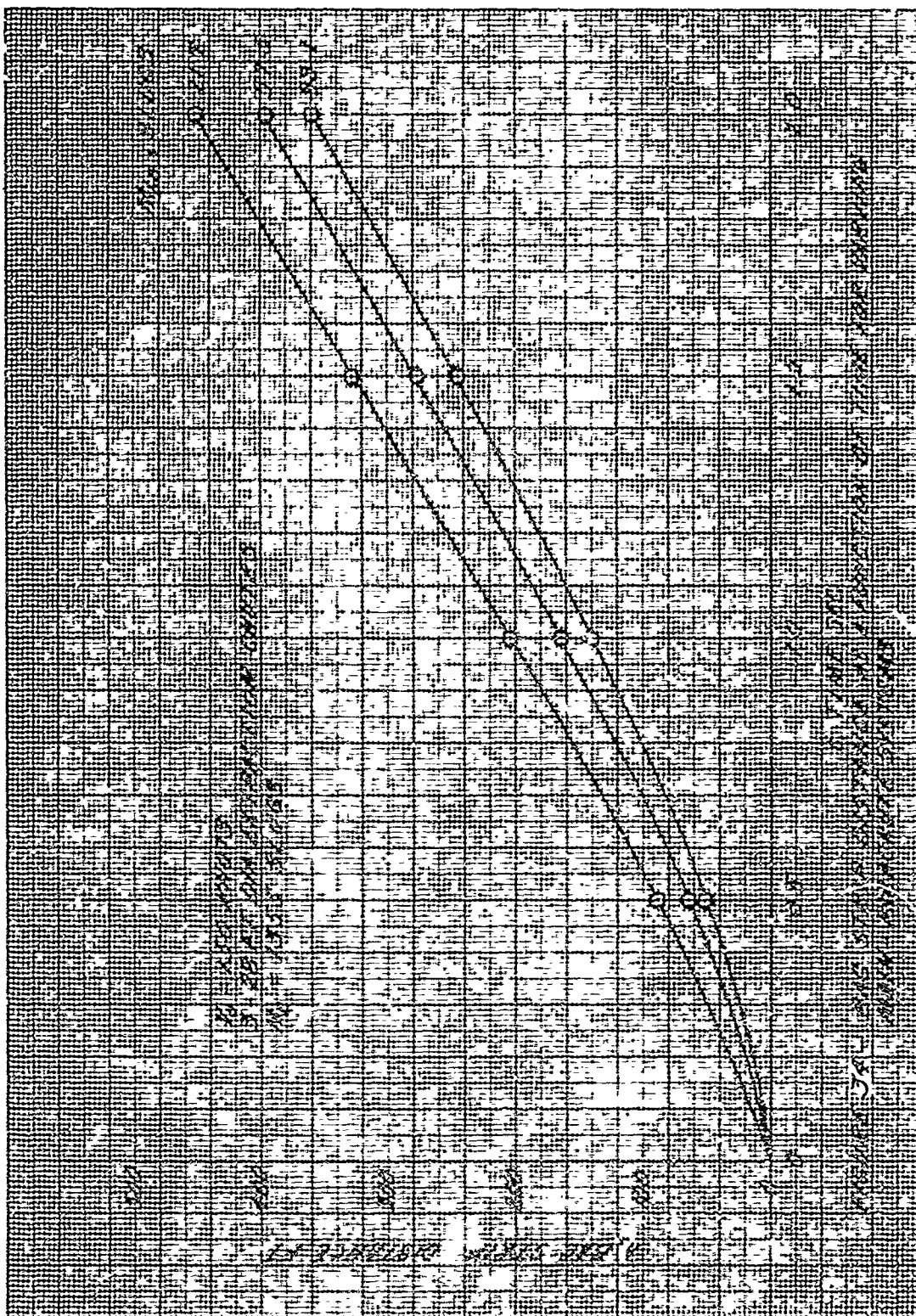
Wind-tunnel tests were conducted on the vent-pulldown parachute (using small models representative of the G-11A parachute) to determine whether an internal parachute assists inflation. The data indicate that the internal parachute is of no help.

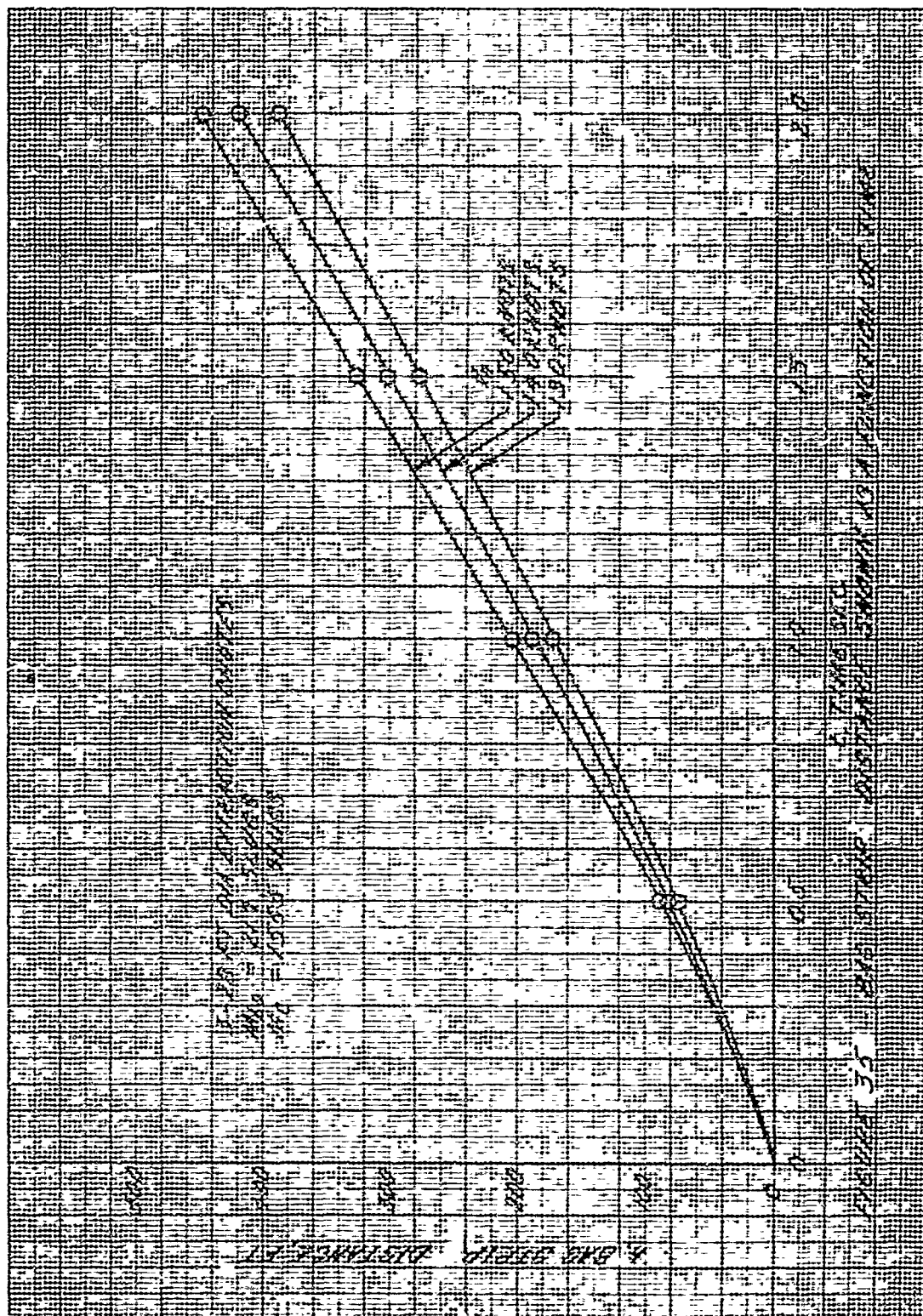
8. WEIGHT, STRENGTH, AND COST OF CANDIDATE MATERIALS FOR PARACHUTE ASSEMBLY

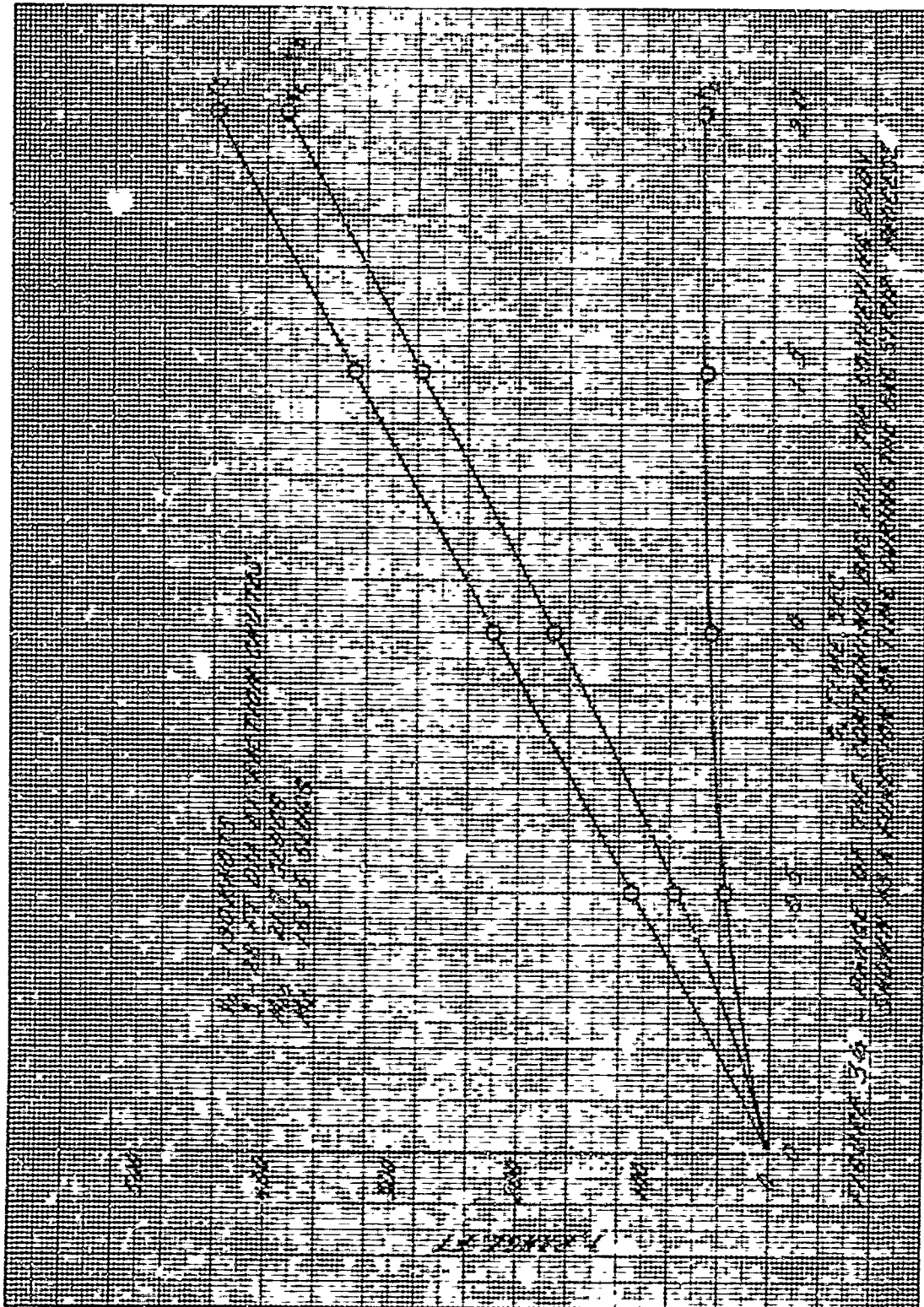
This section presents the weight, strength, and relative cost of various candidate materials for use in the parachute

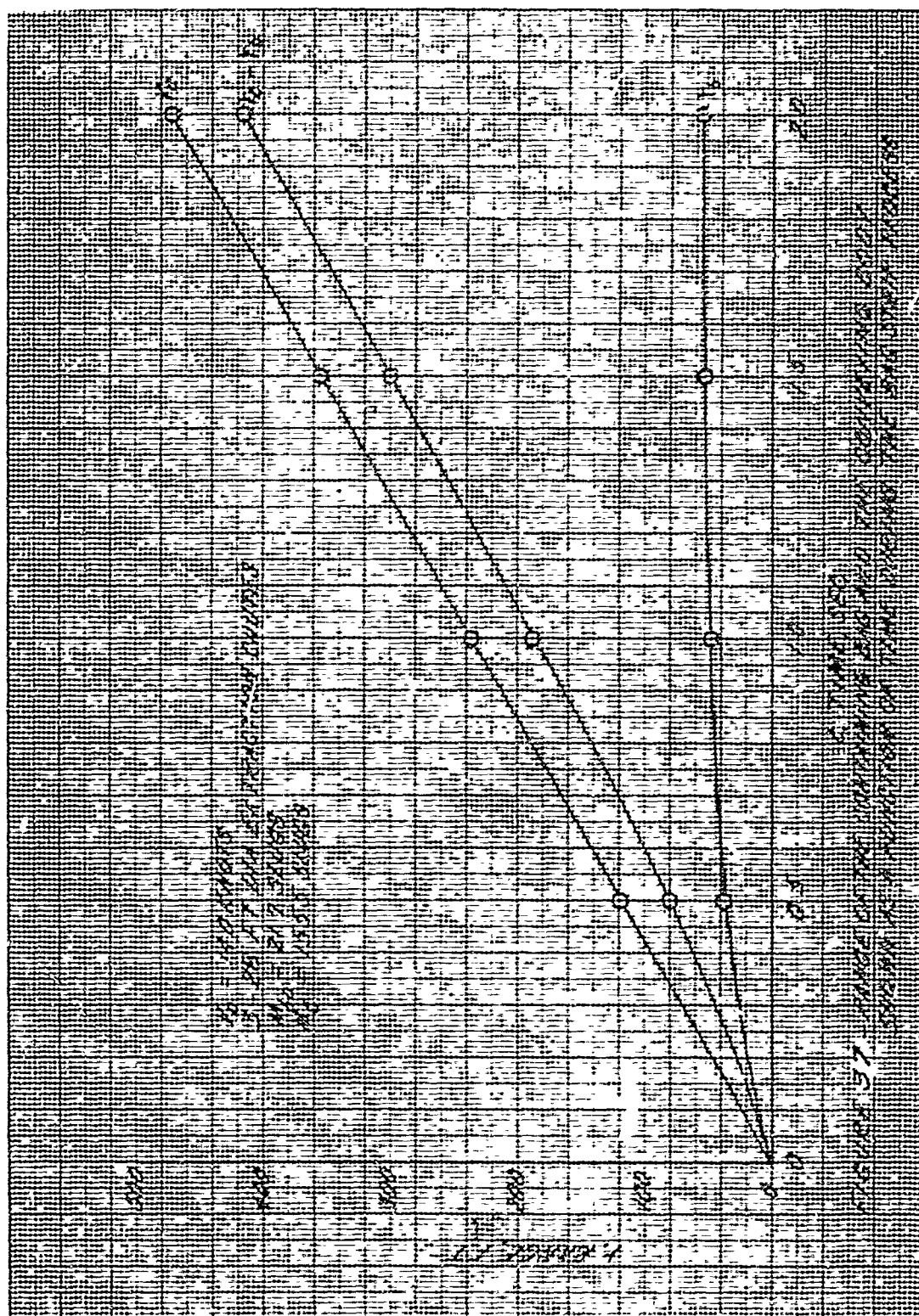


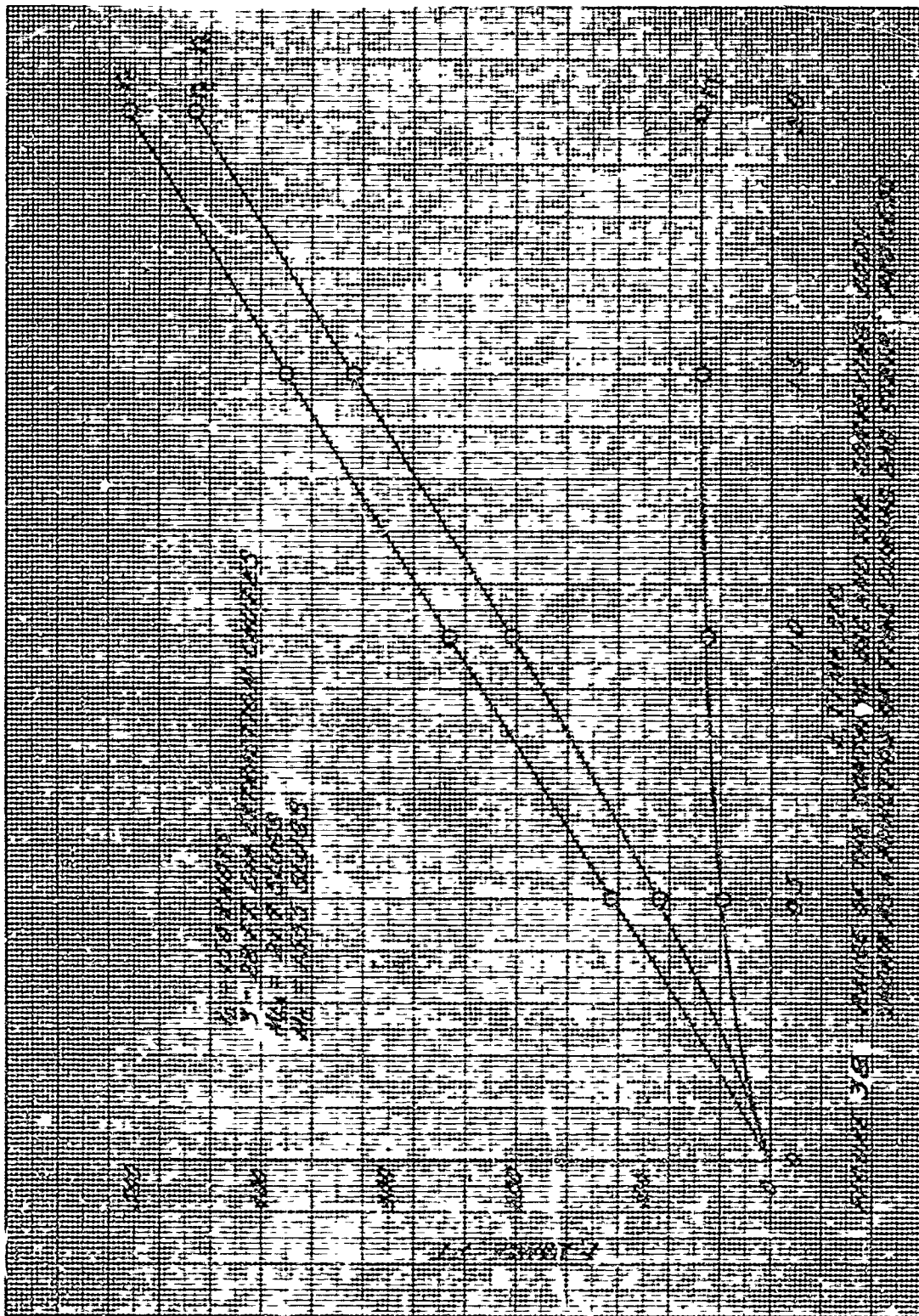


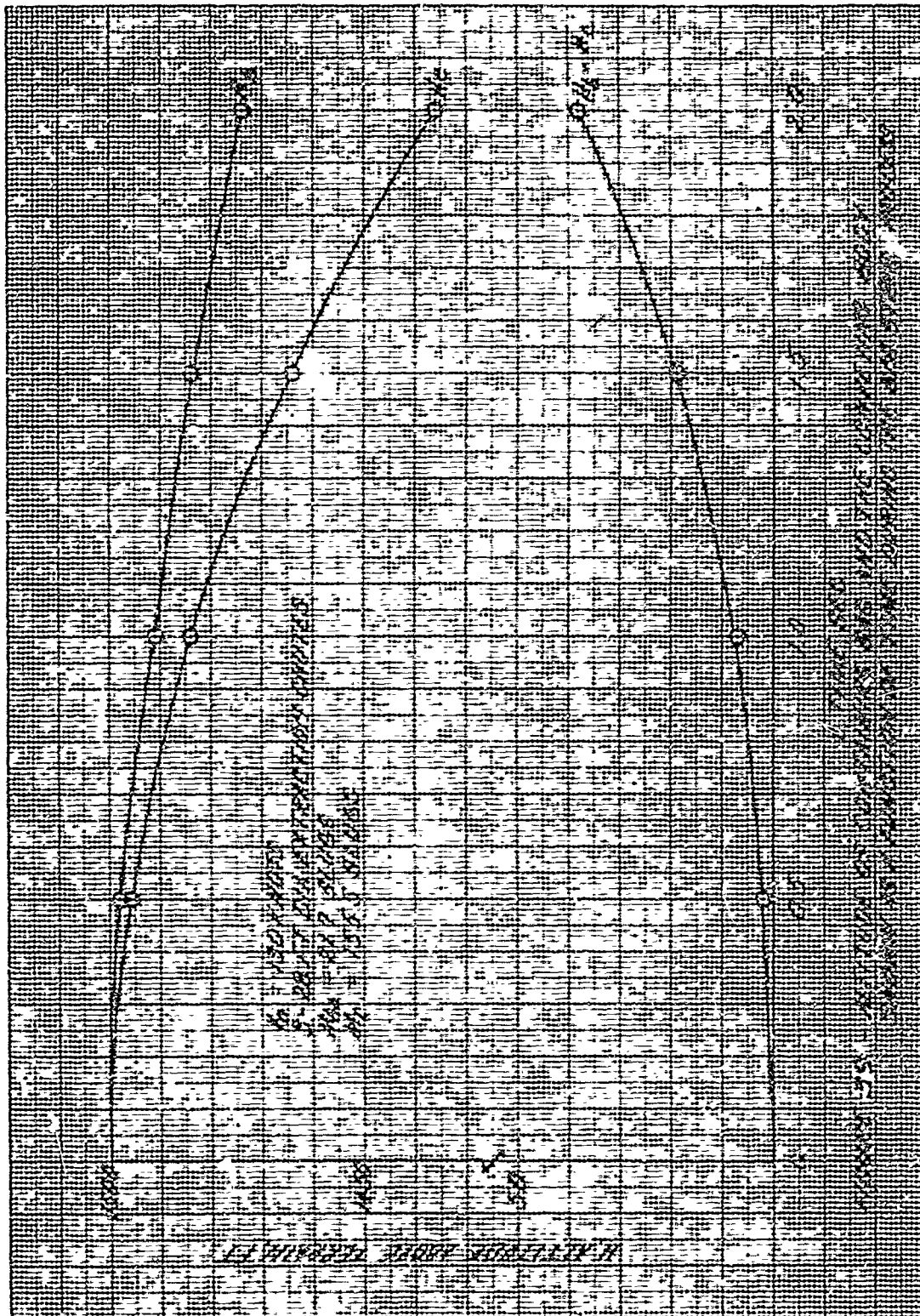


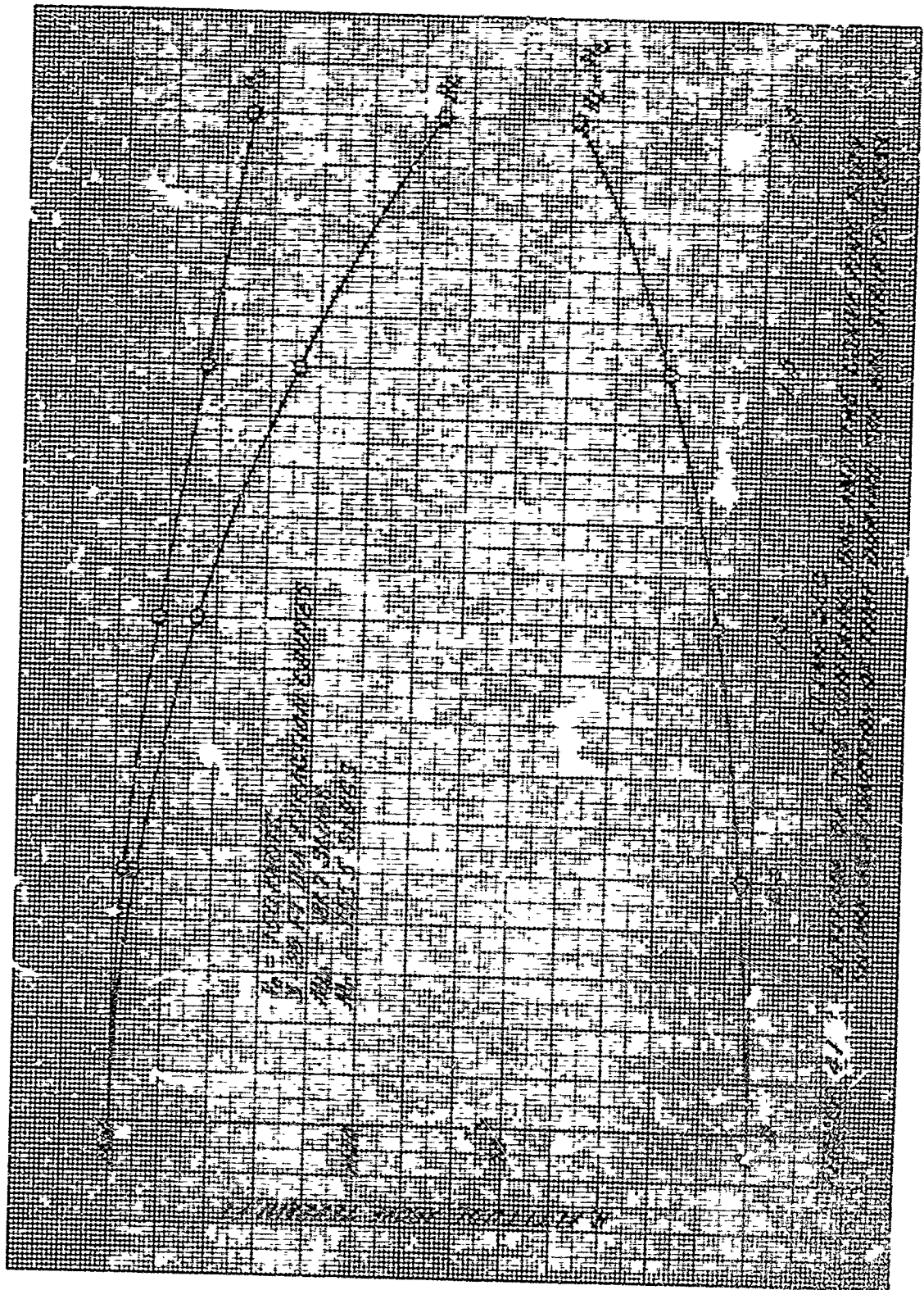


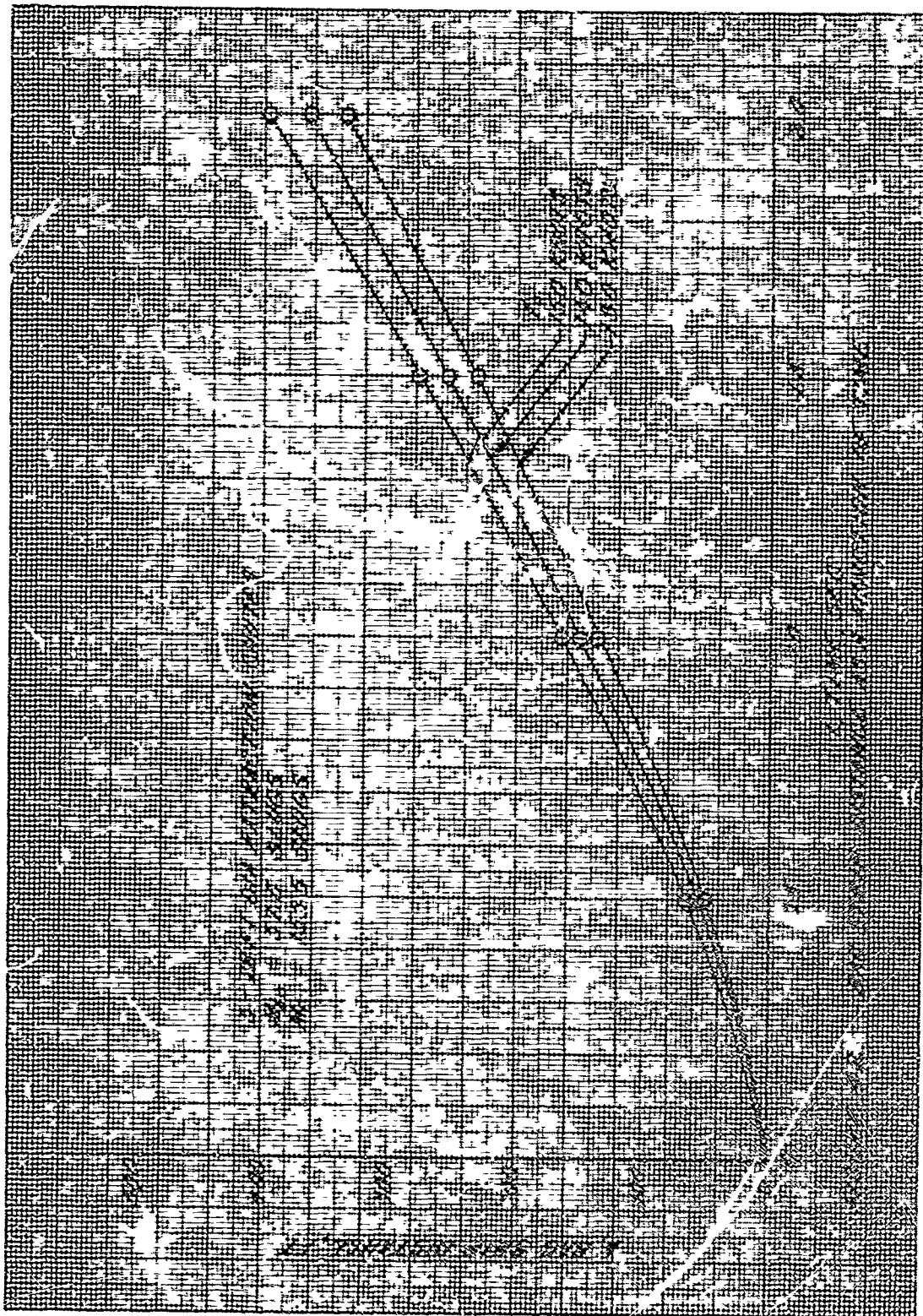


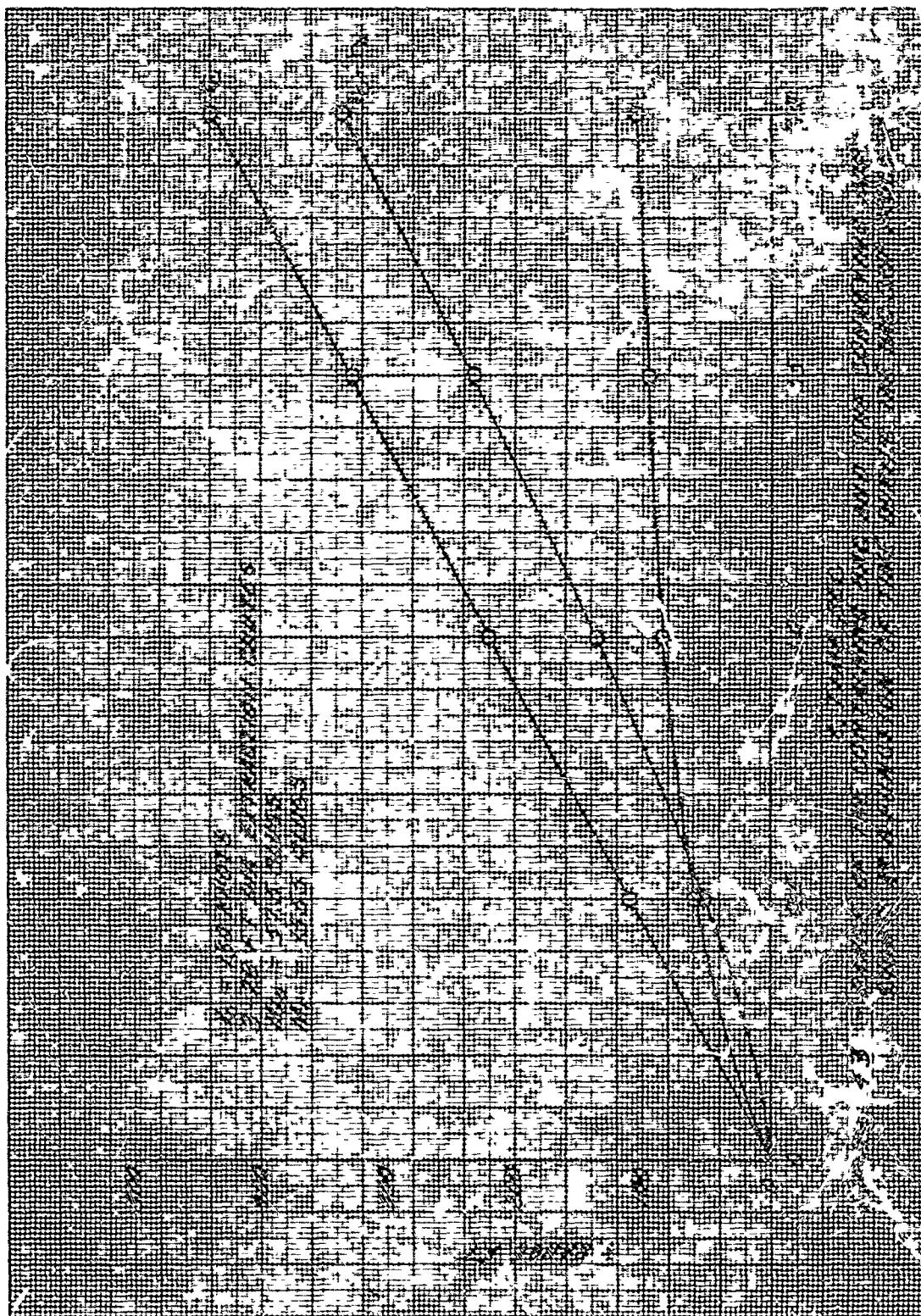


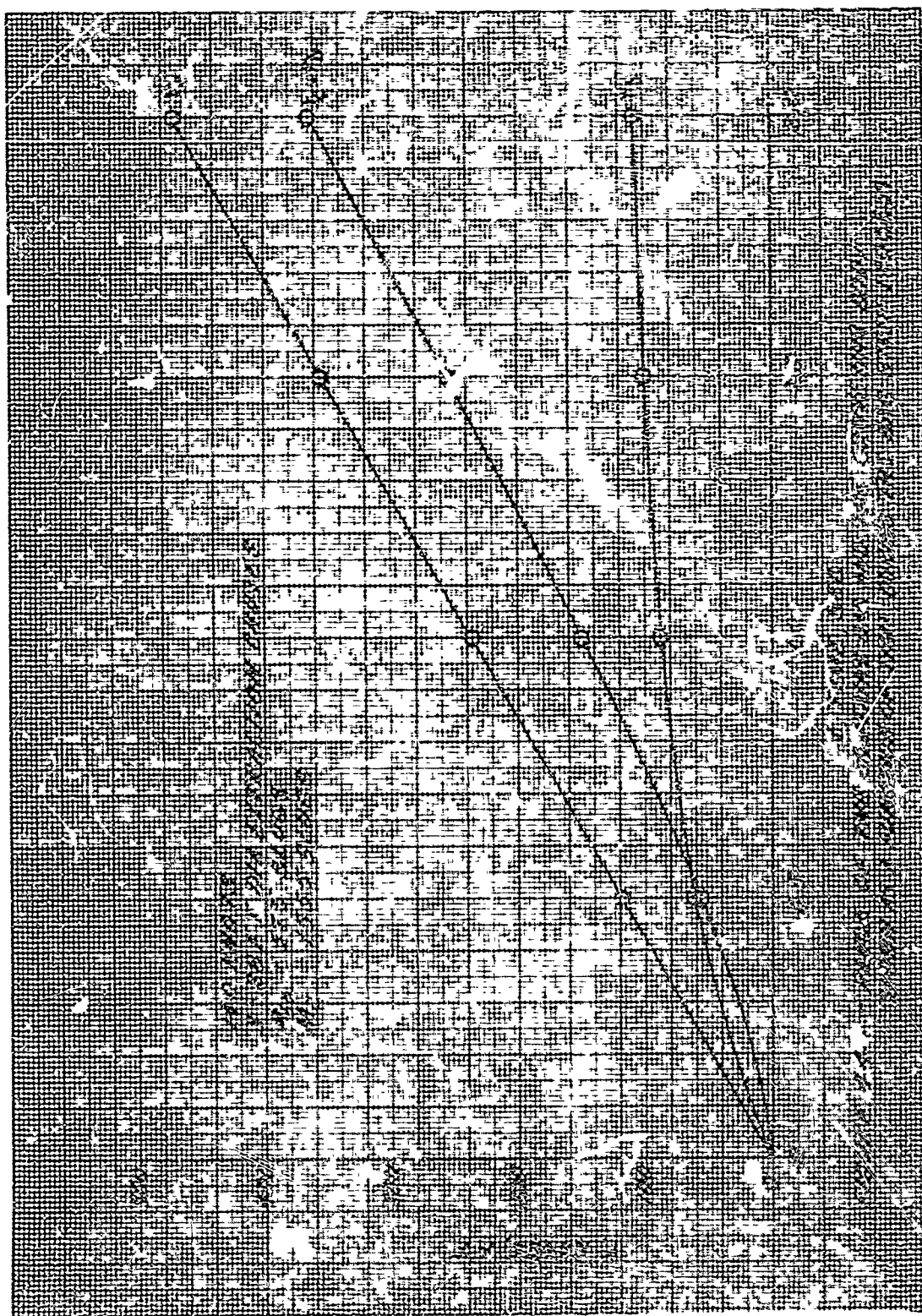


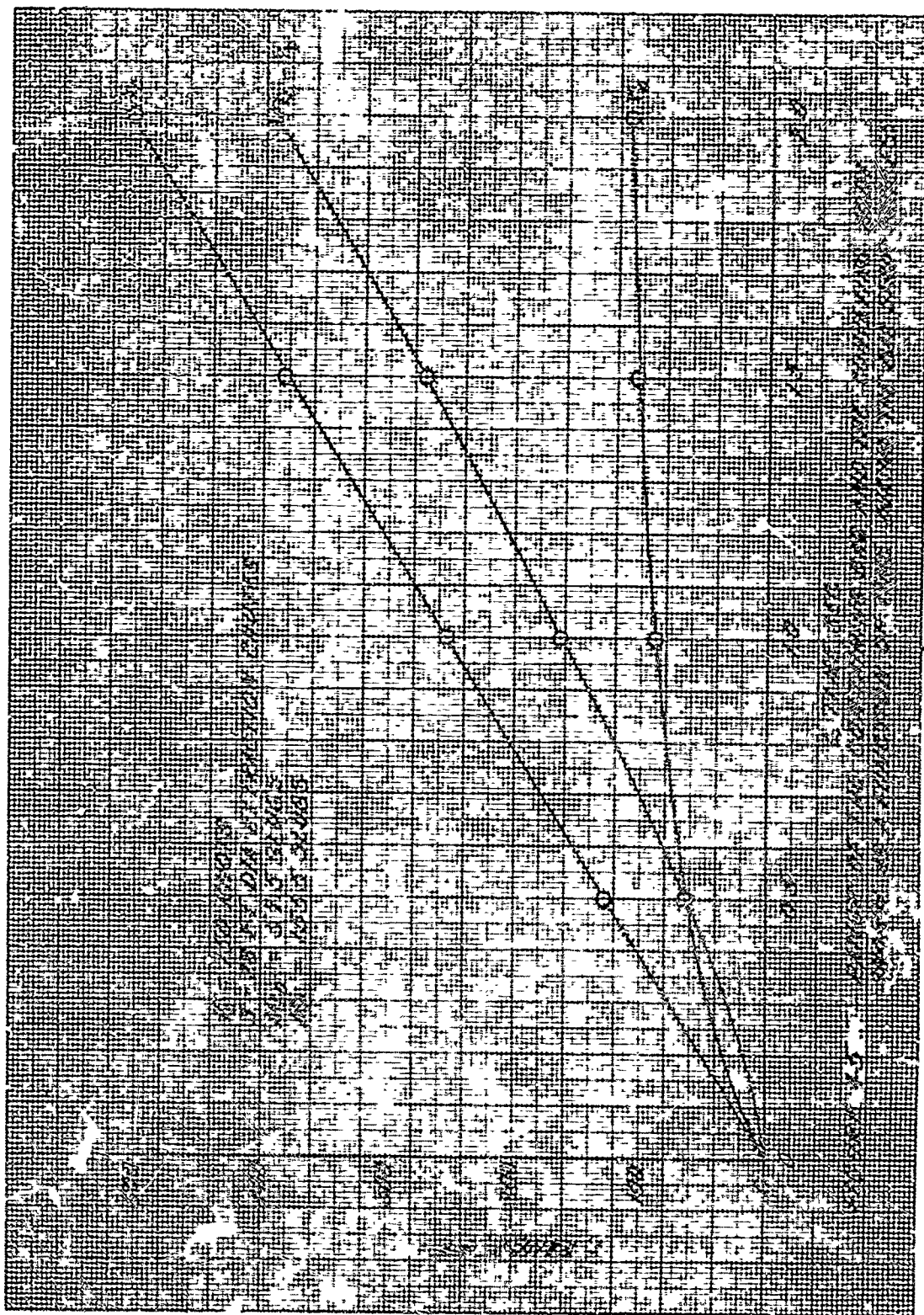


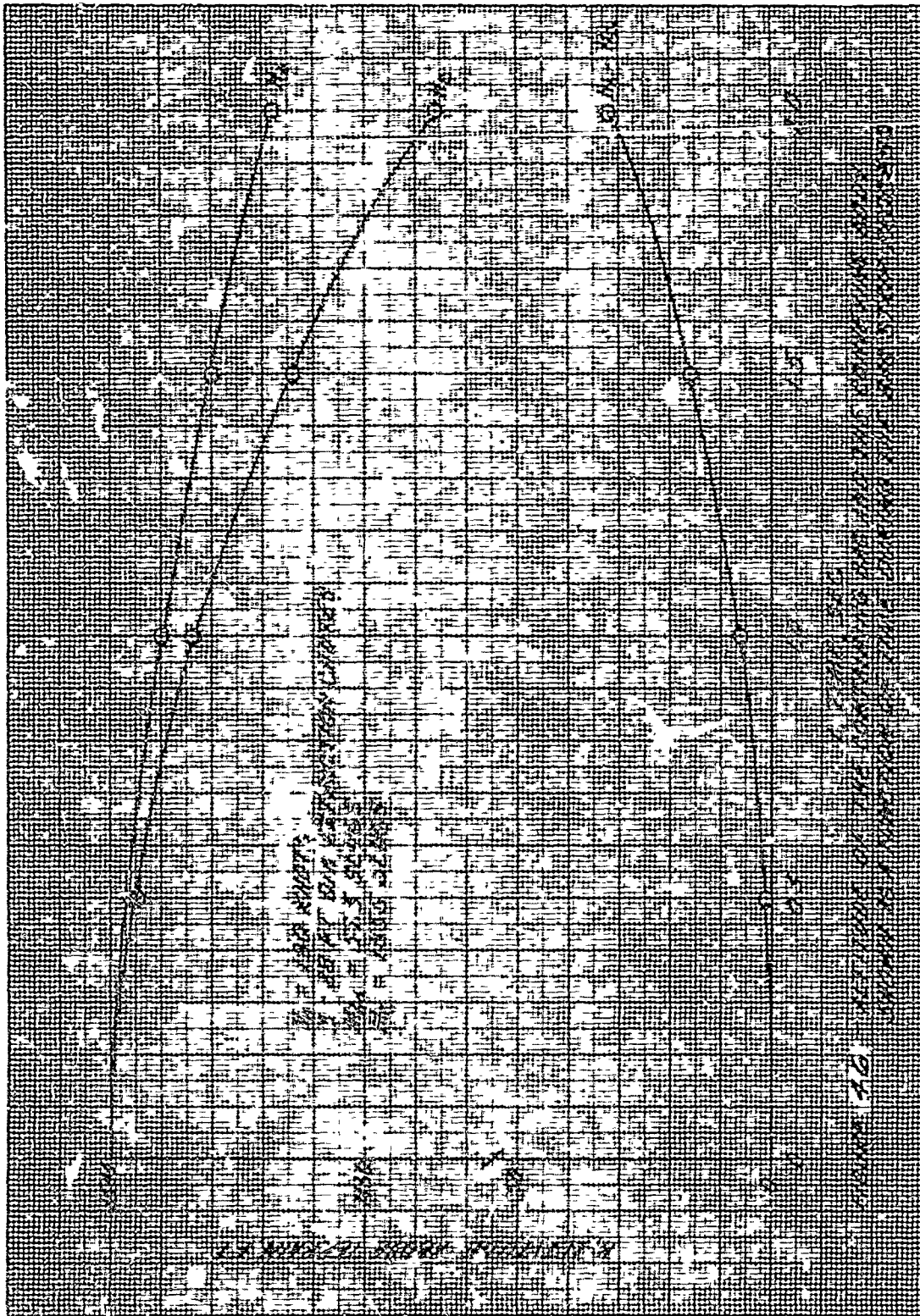




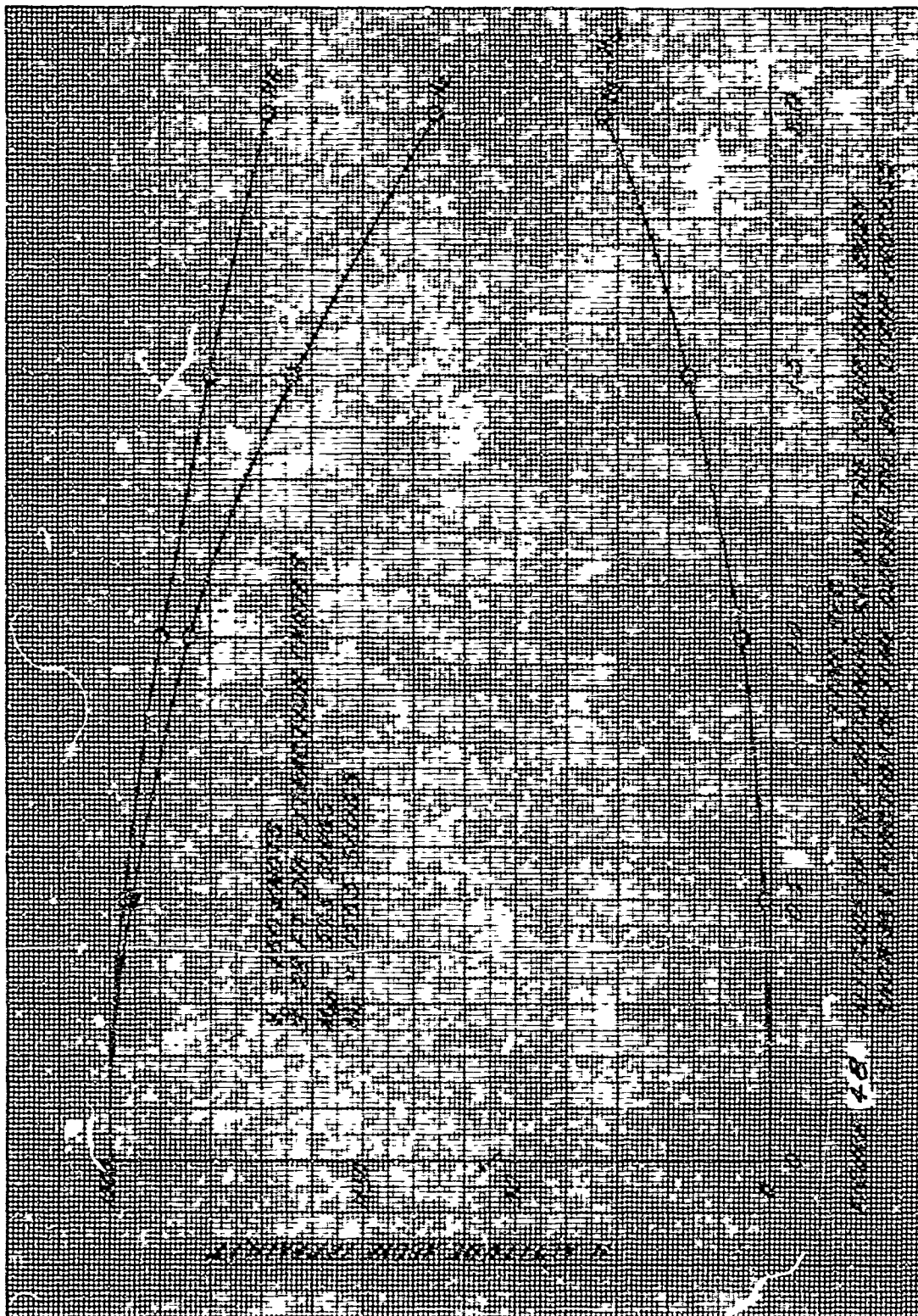


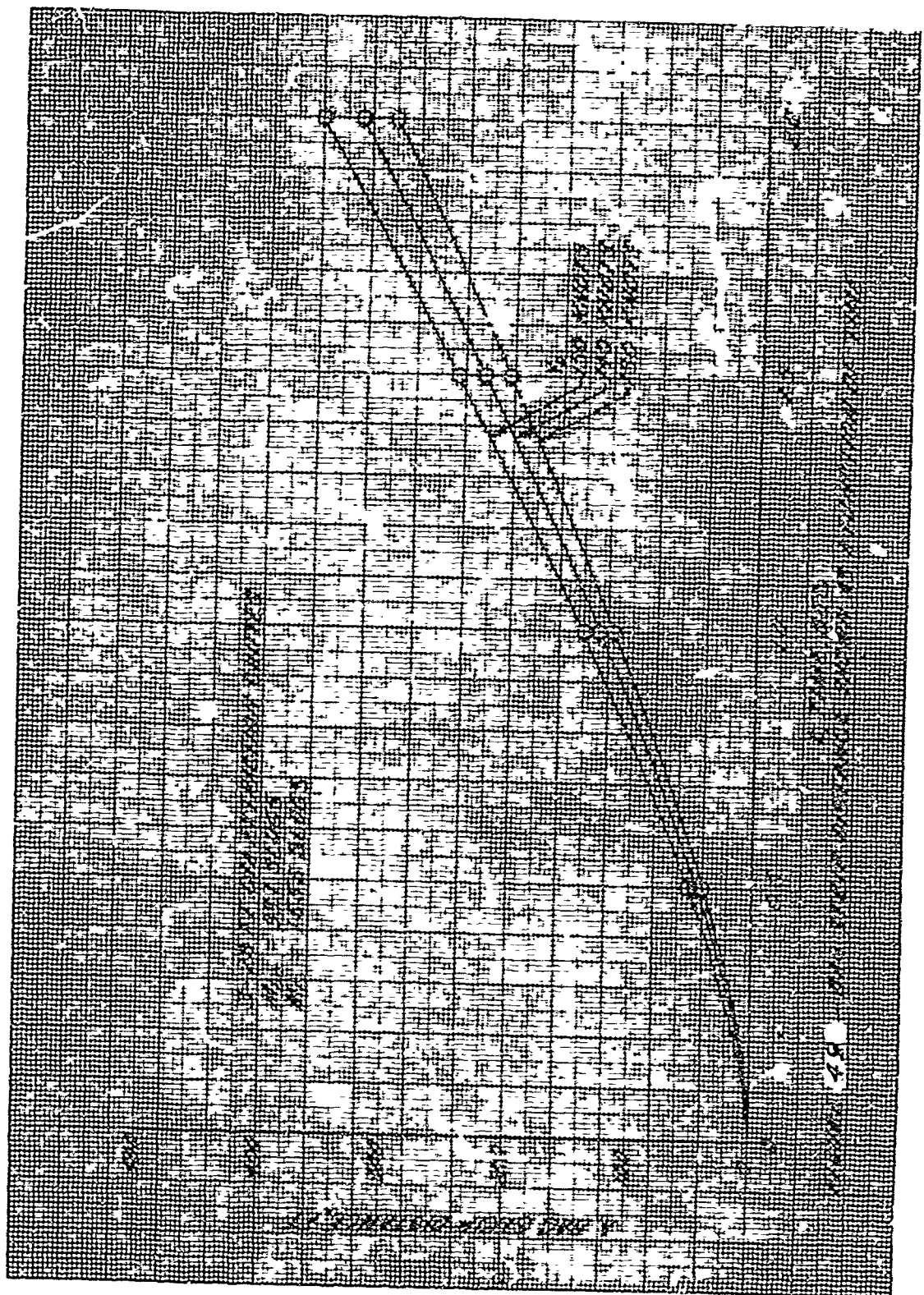


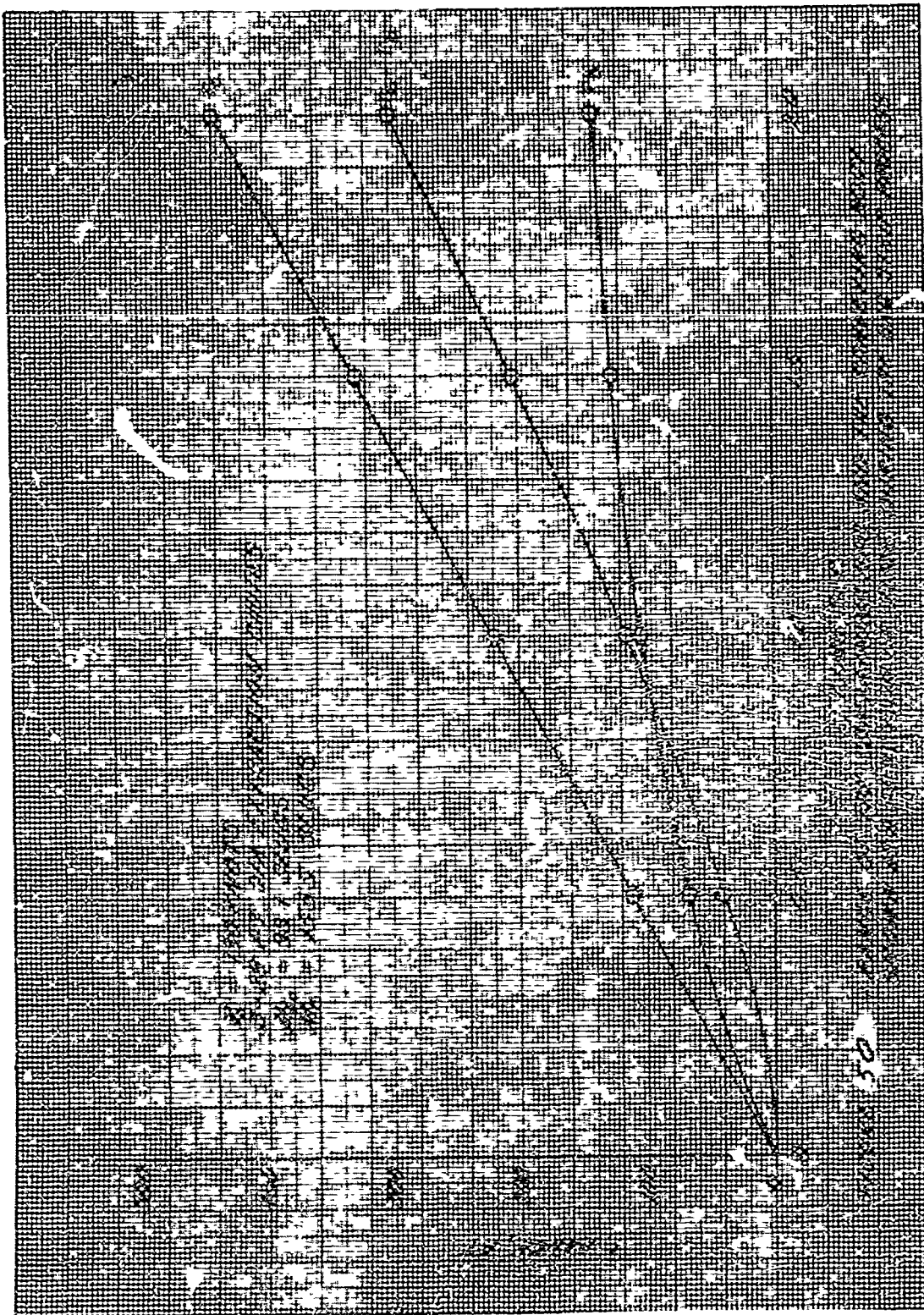


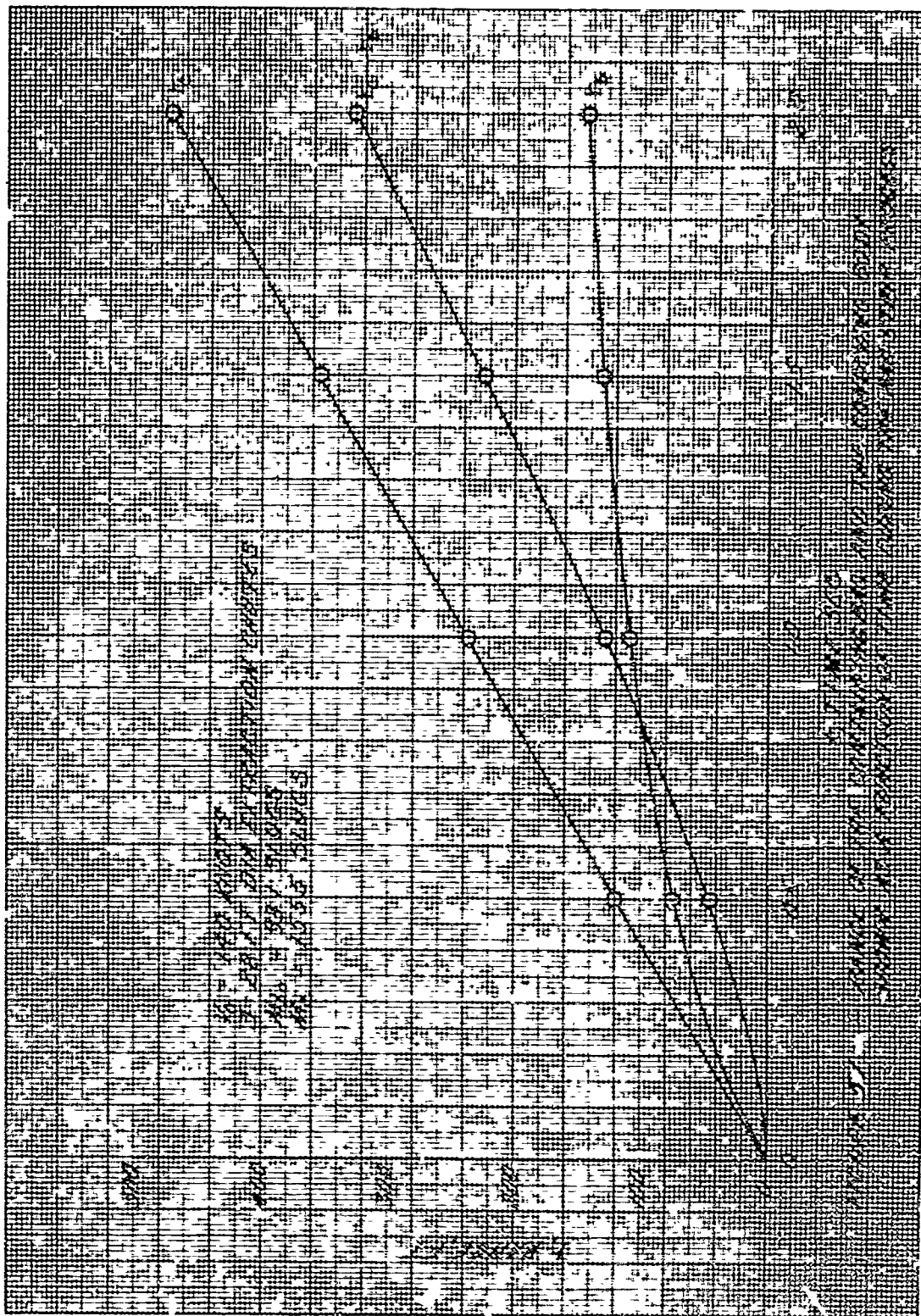


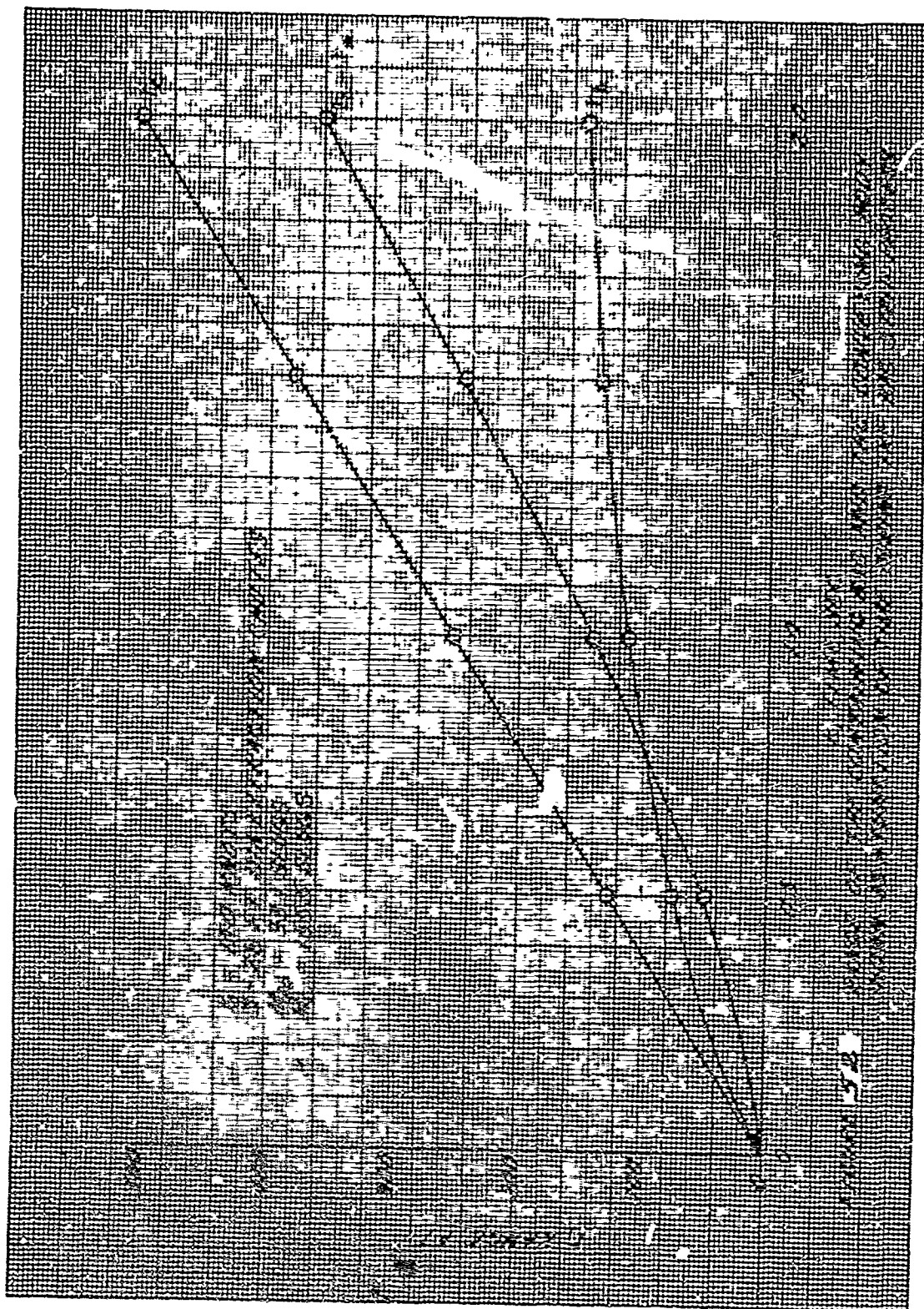


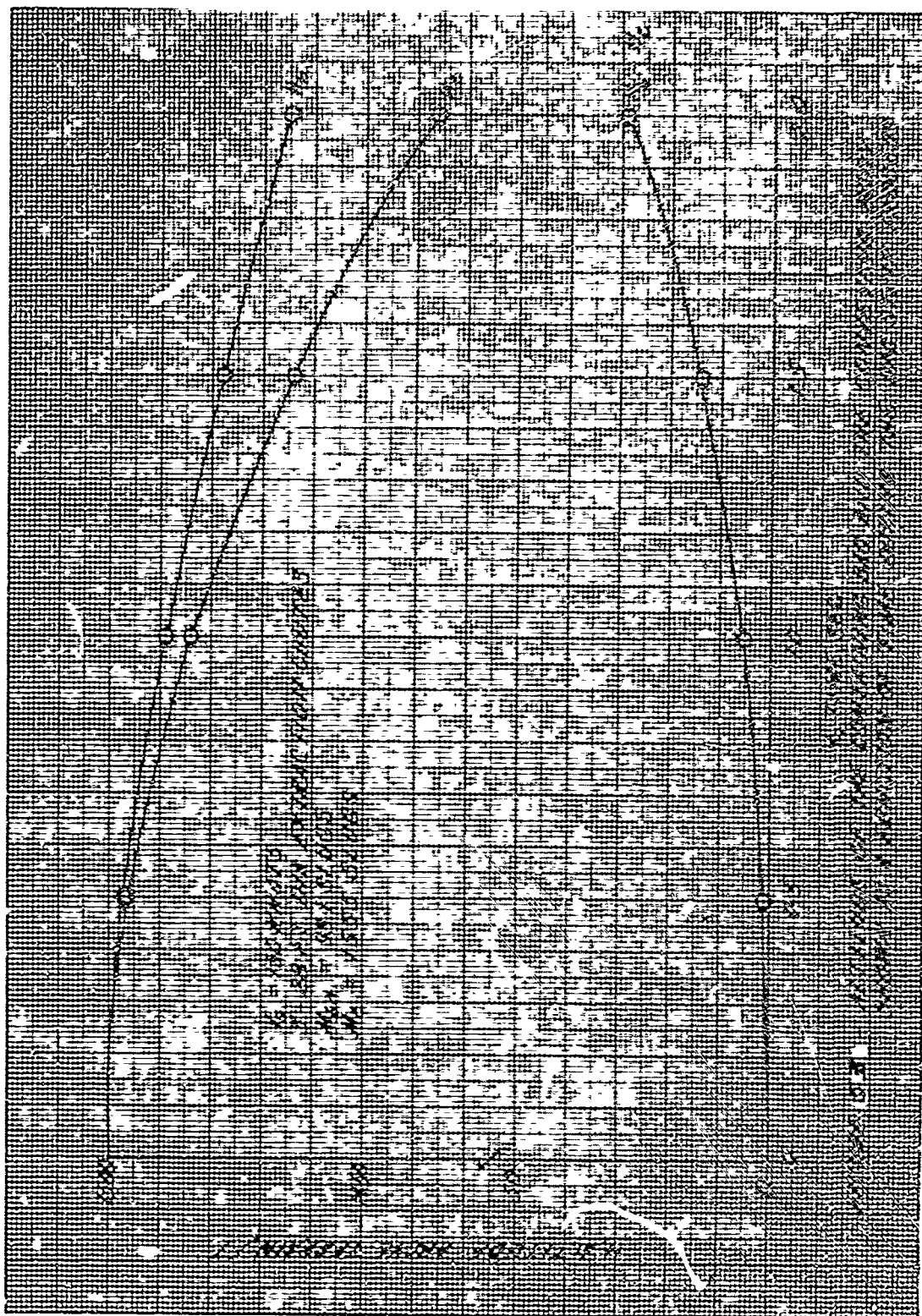


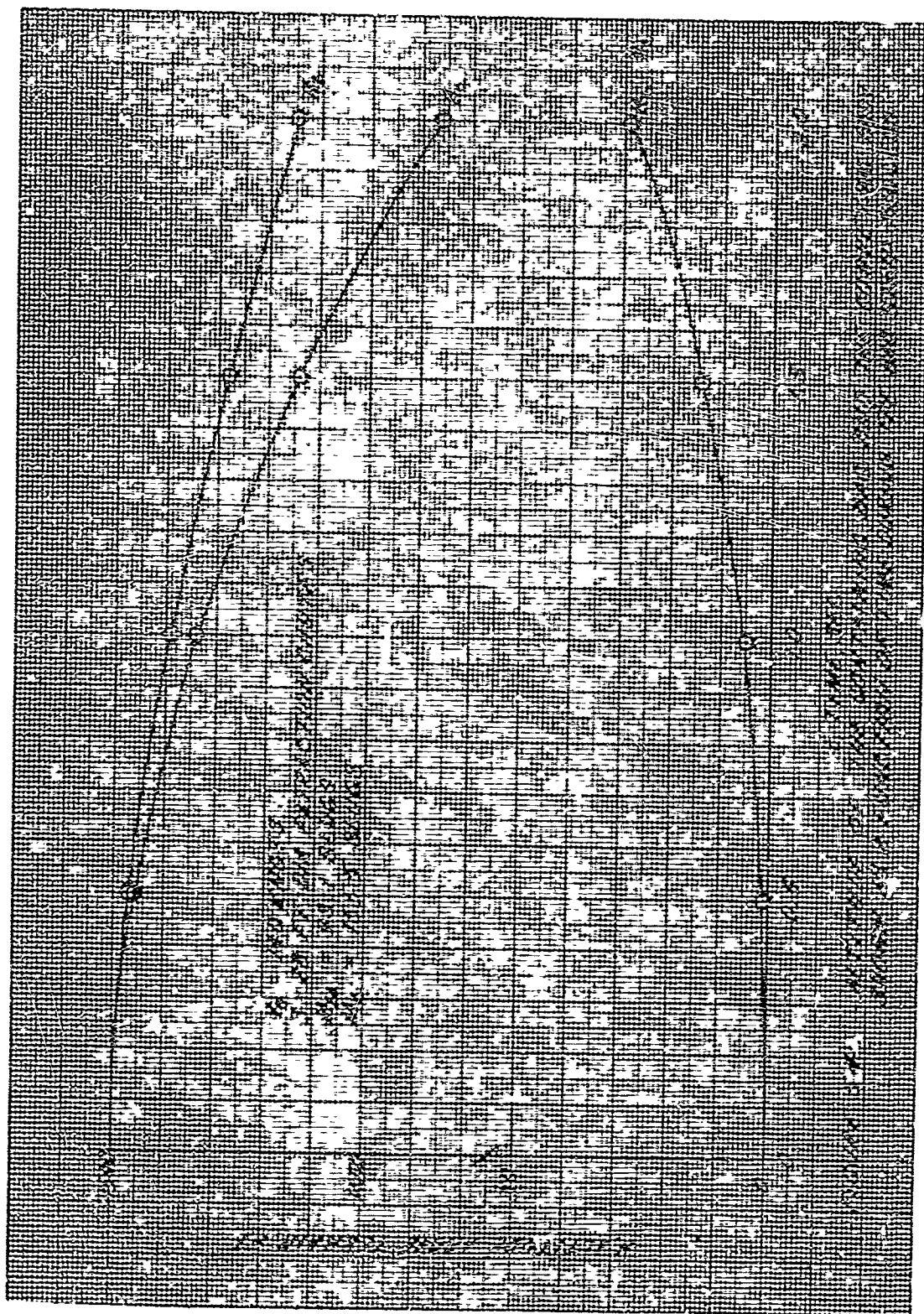


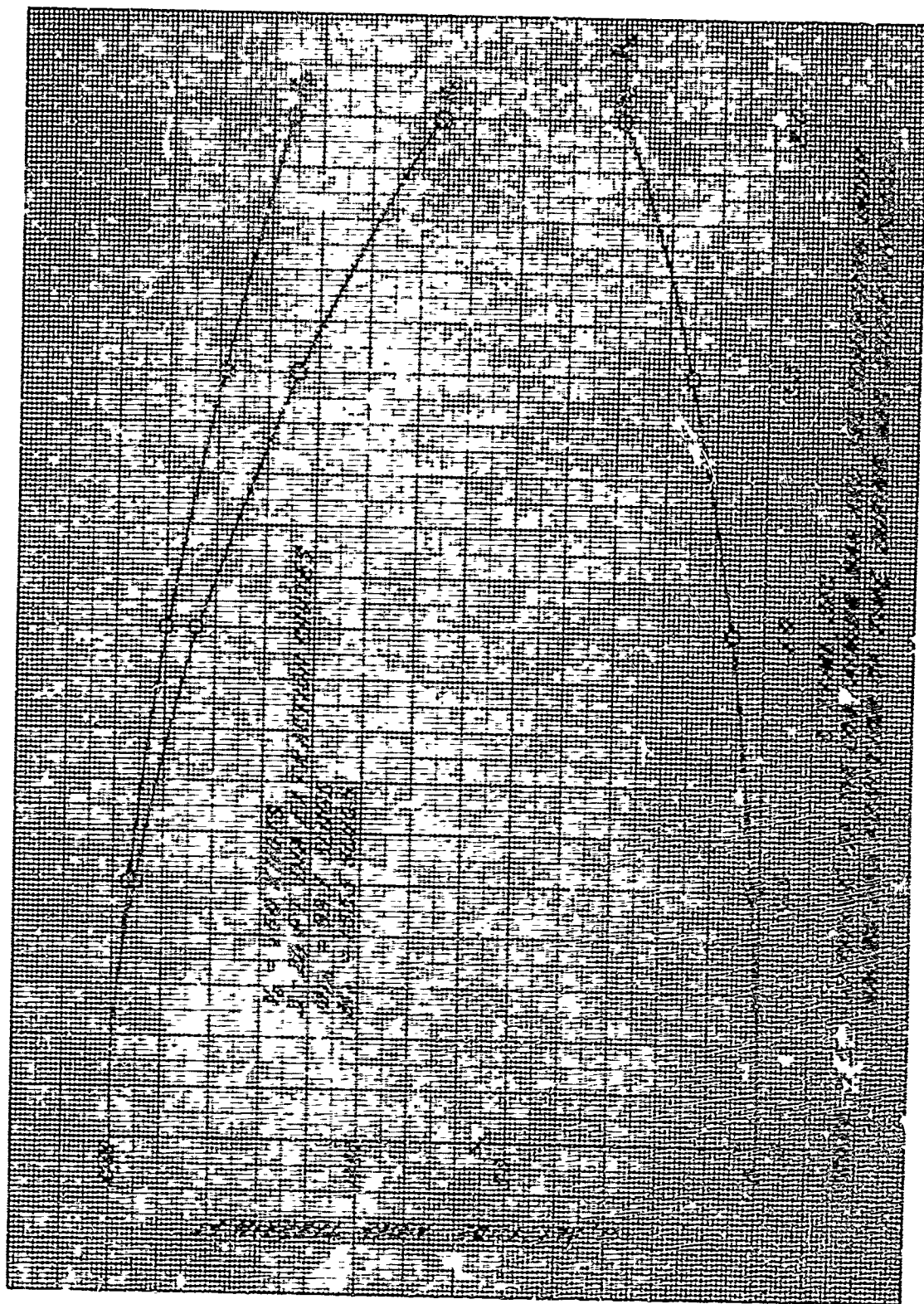


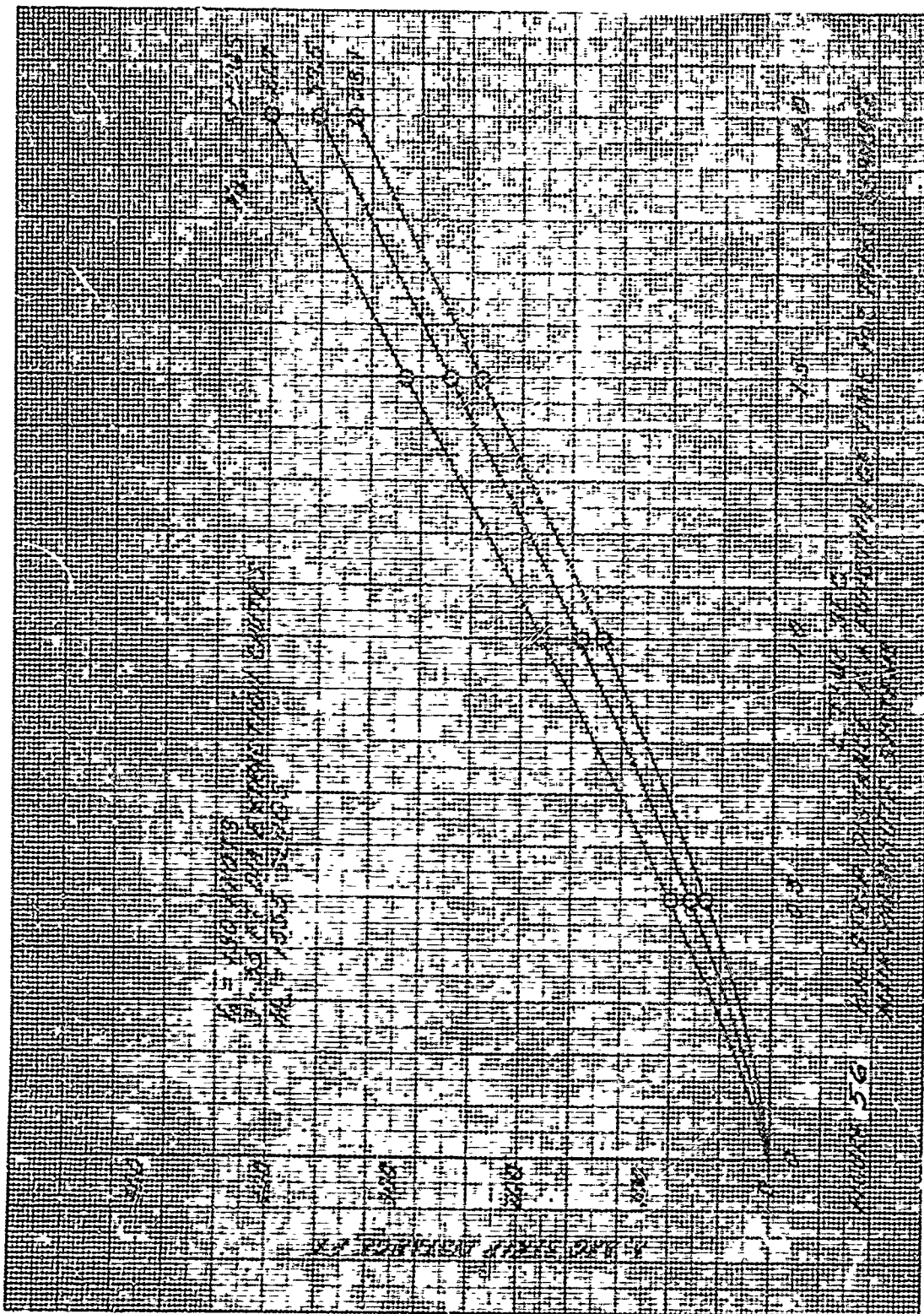


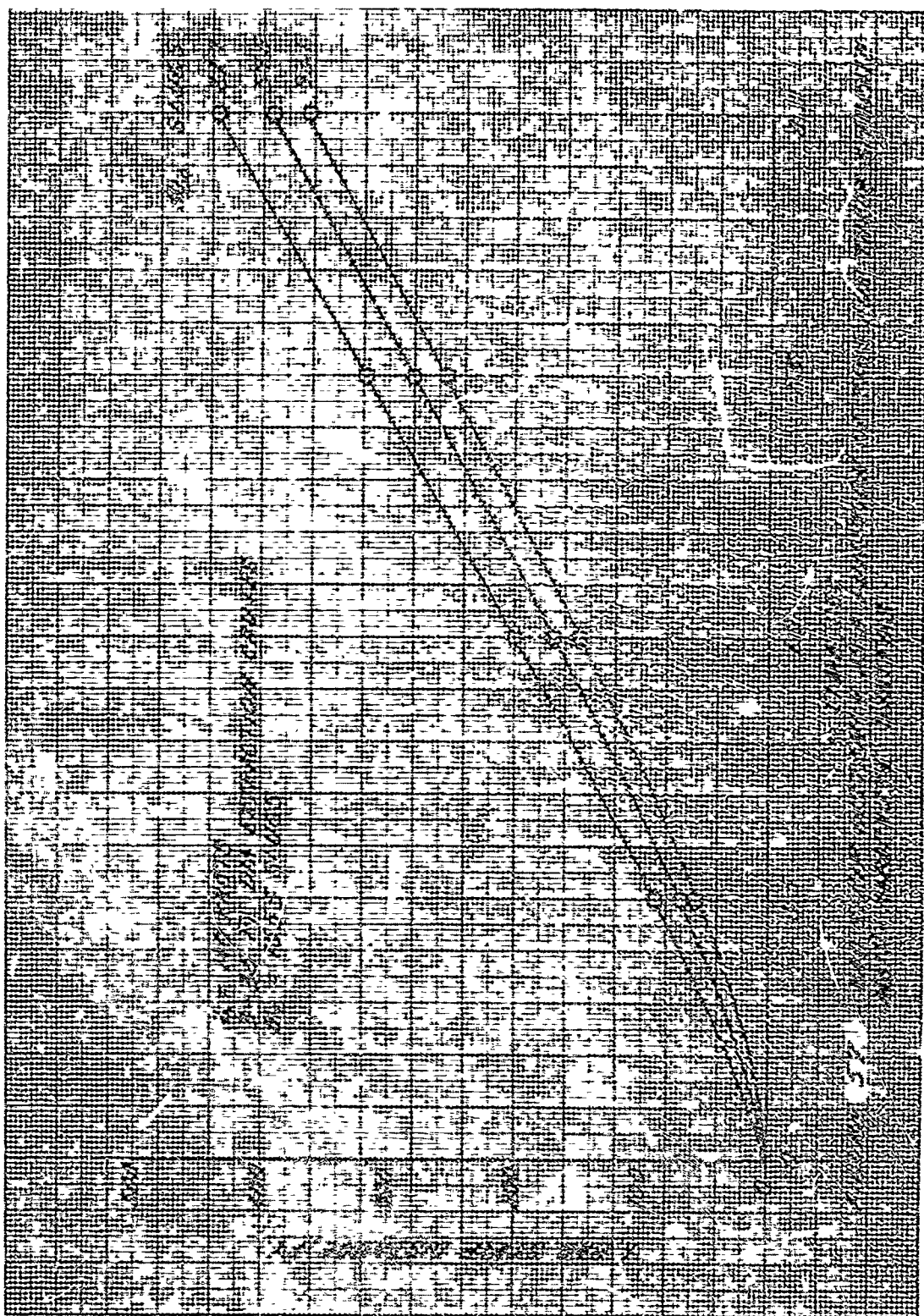


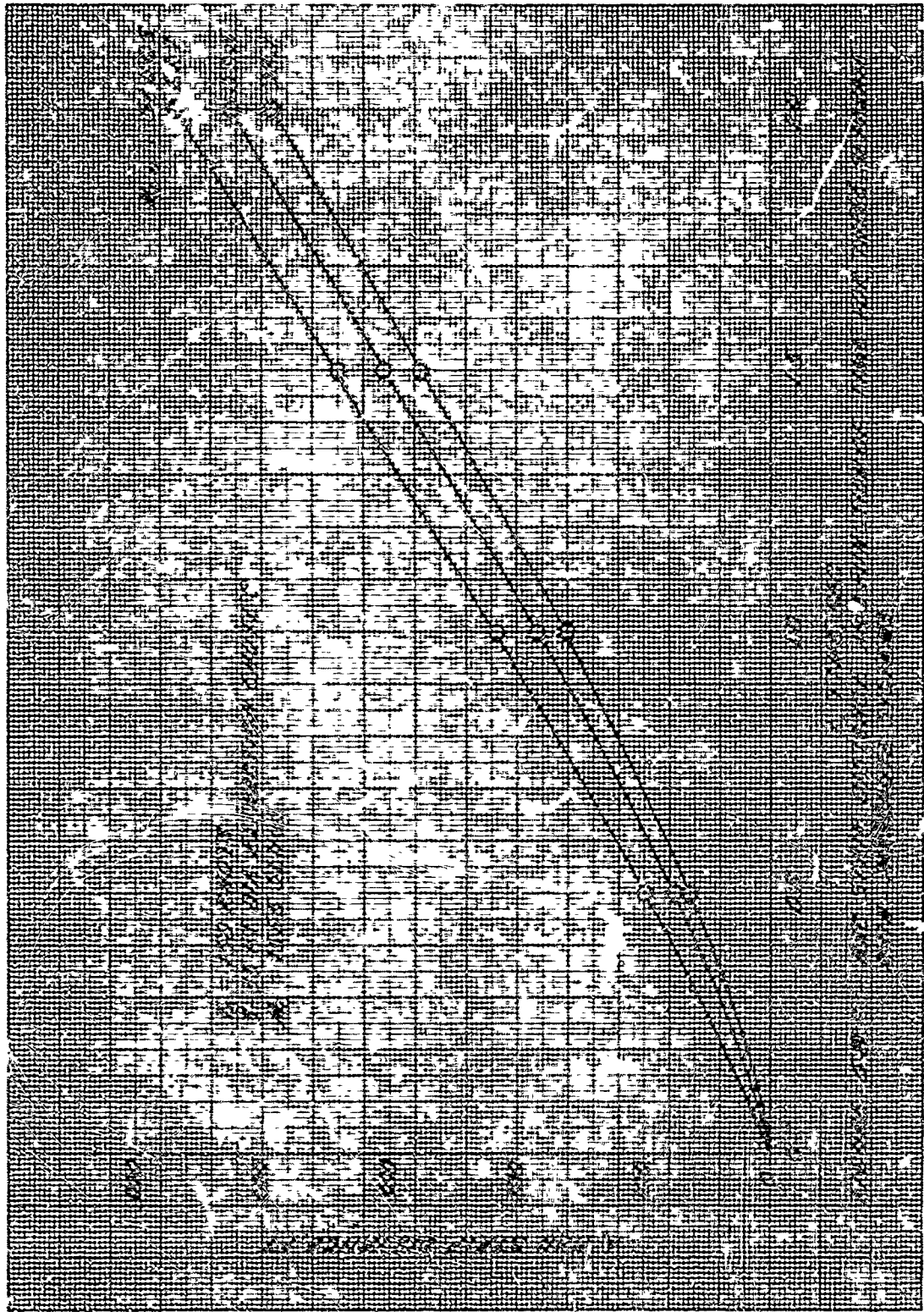


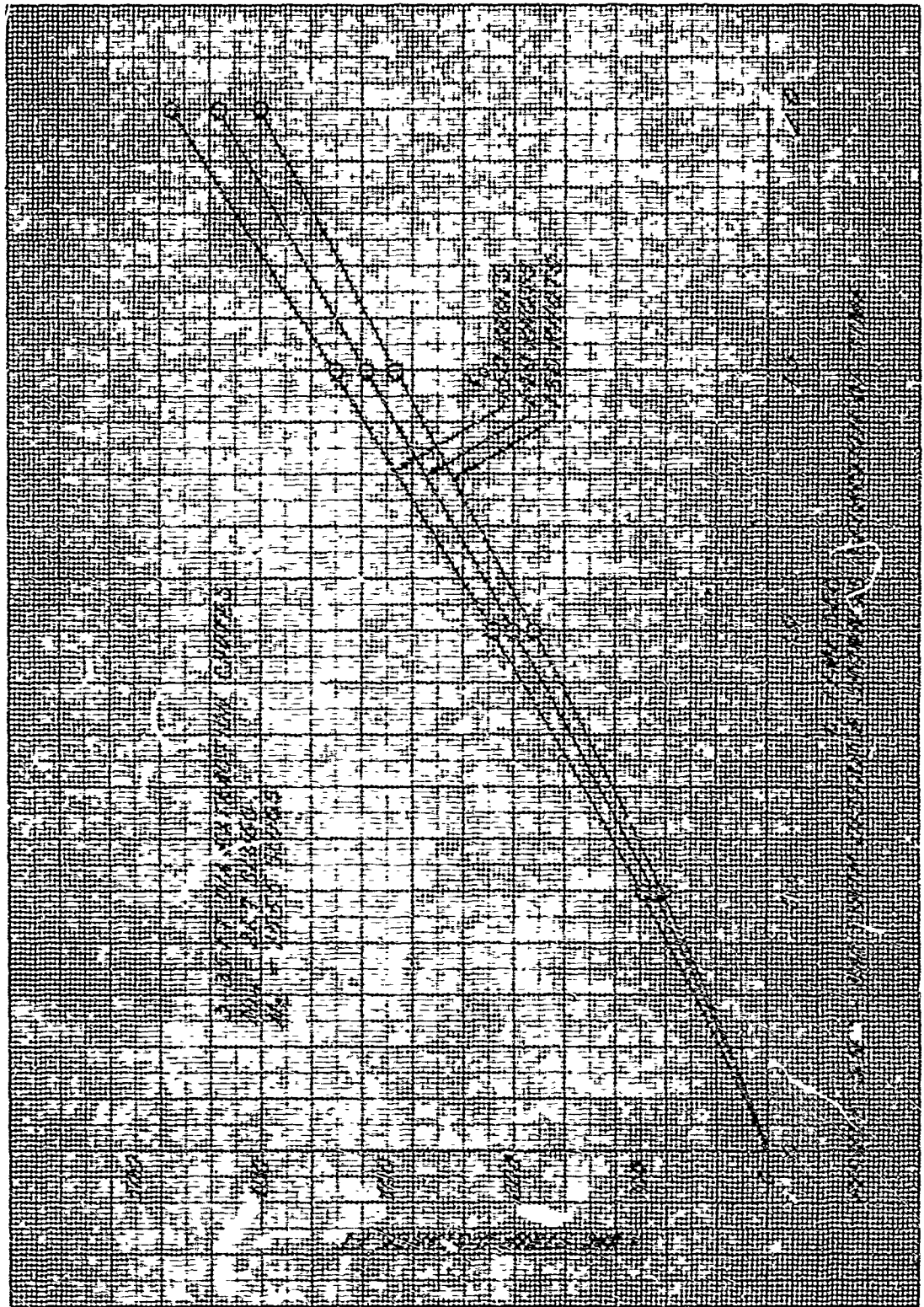


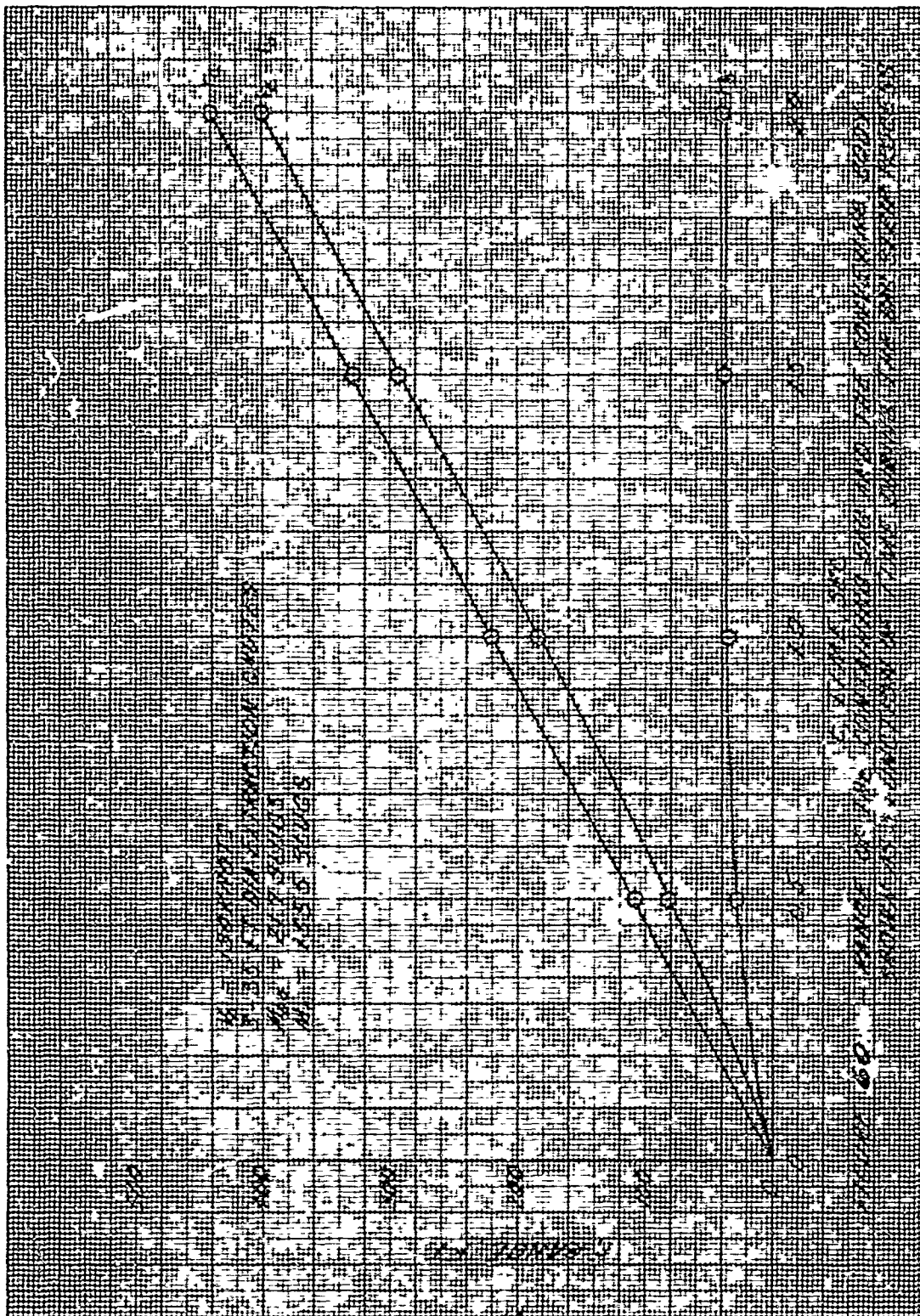


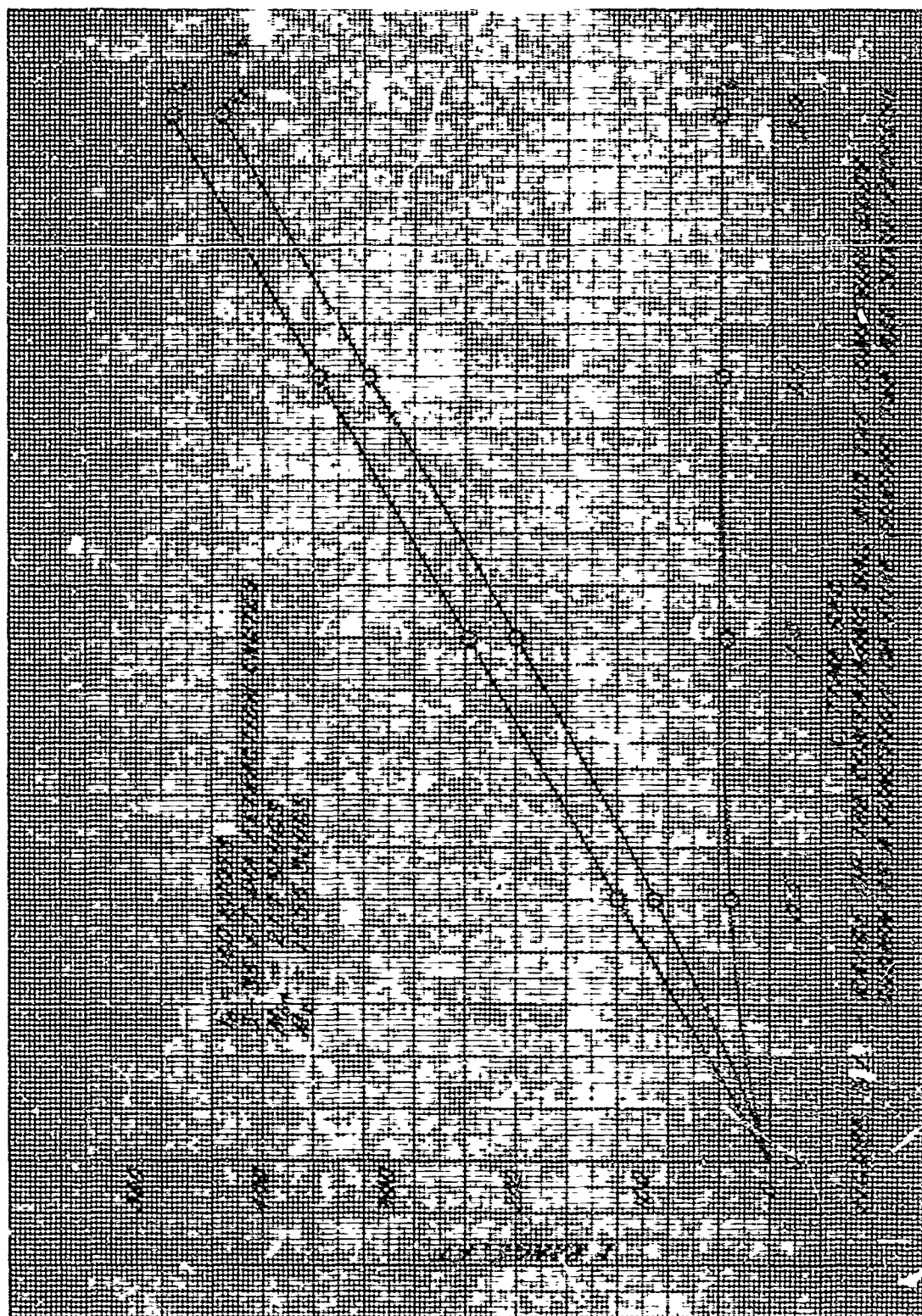


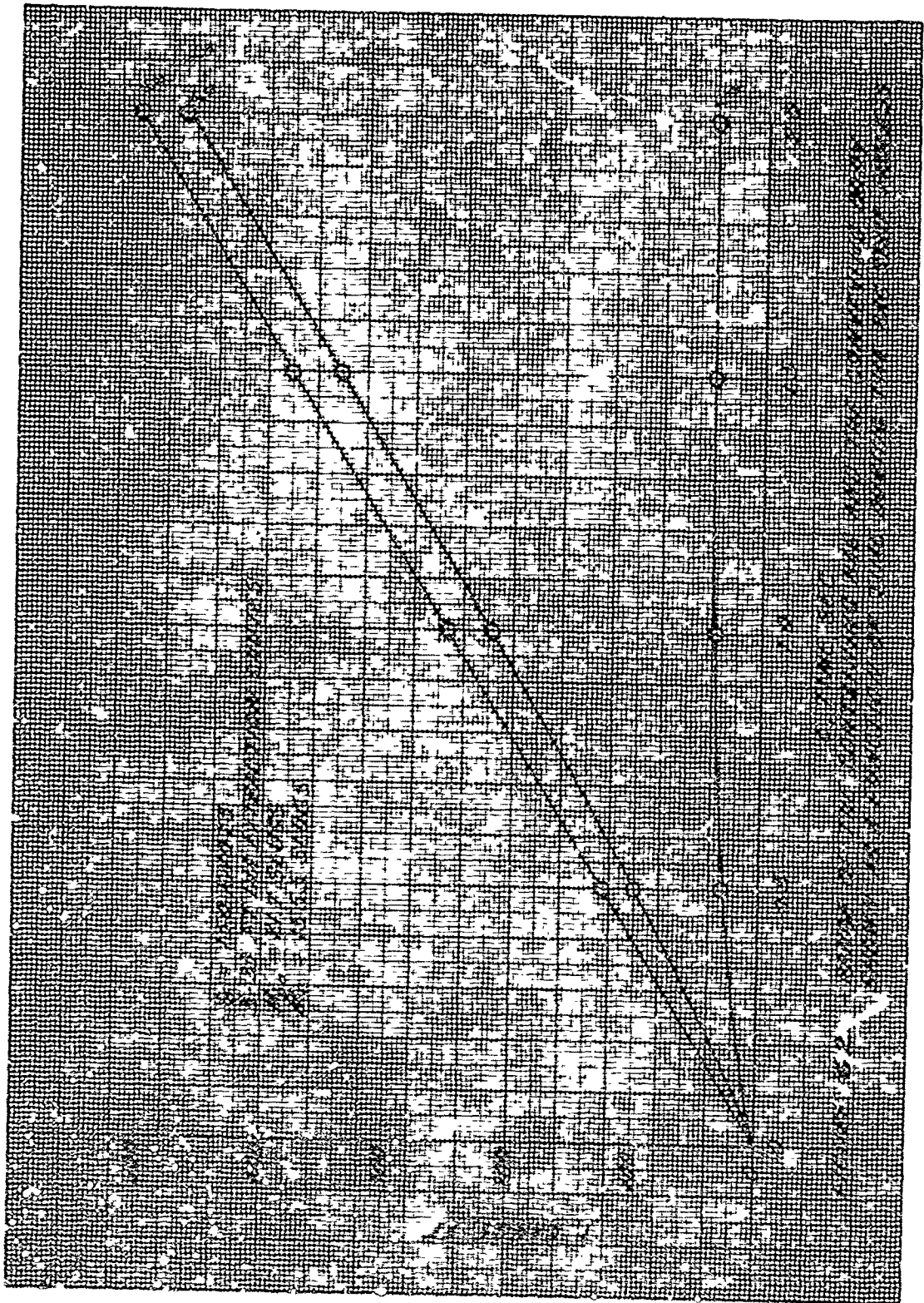


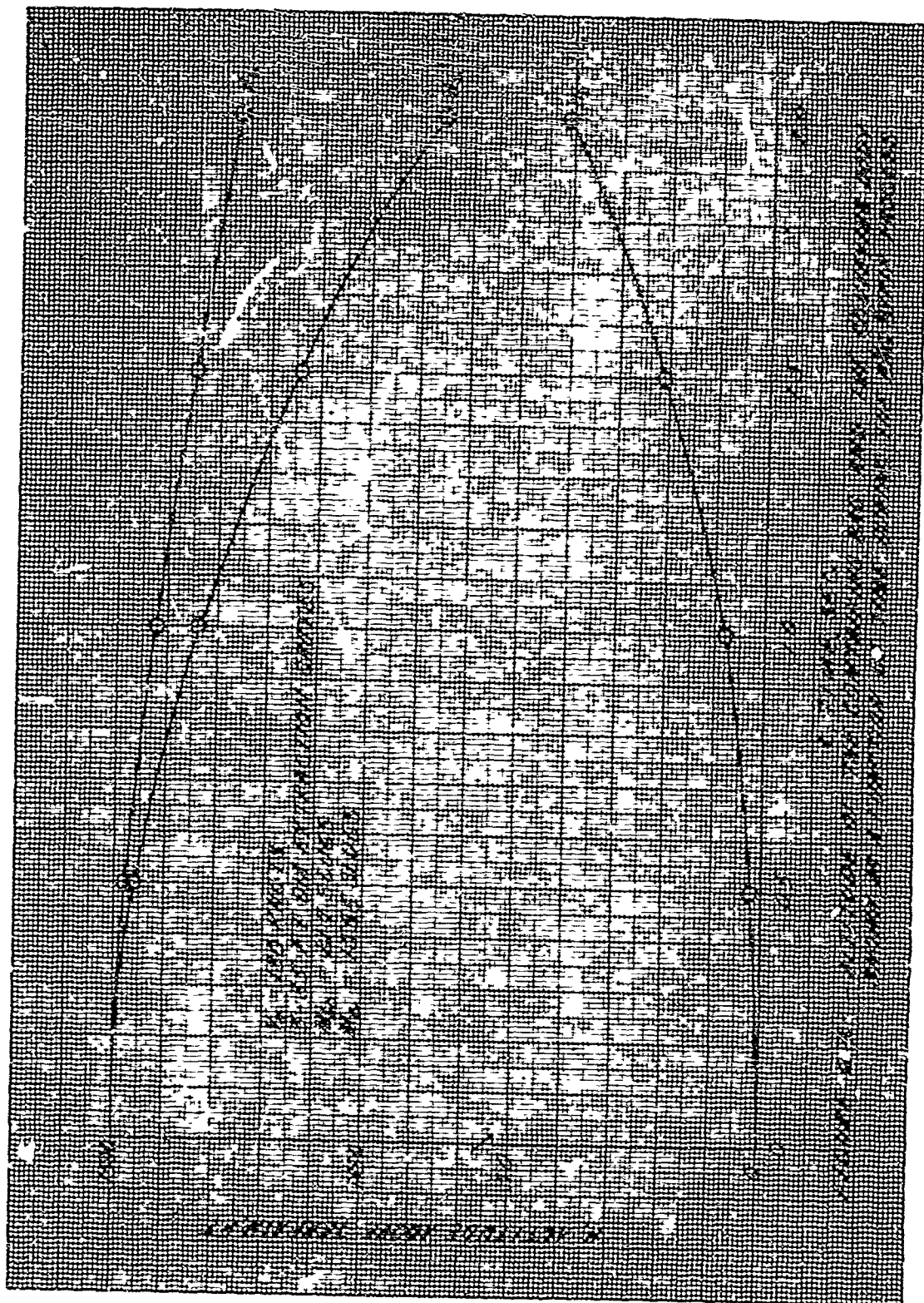


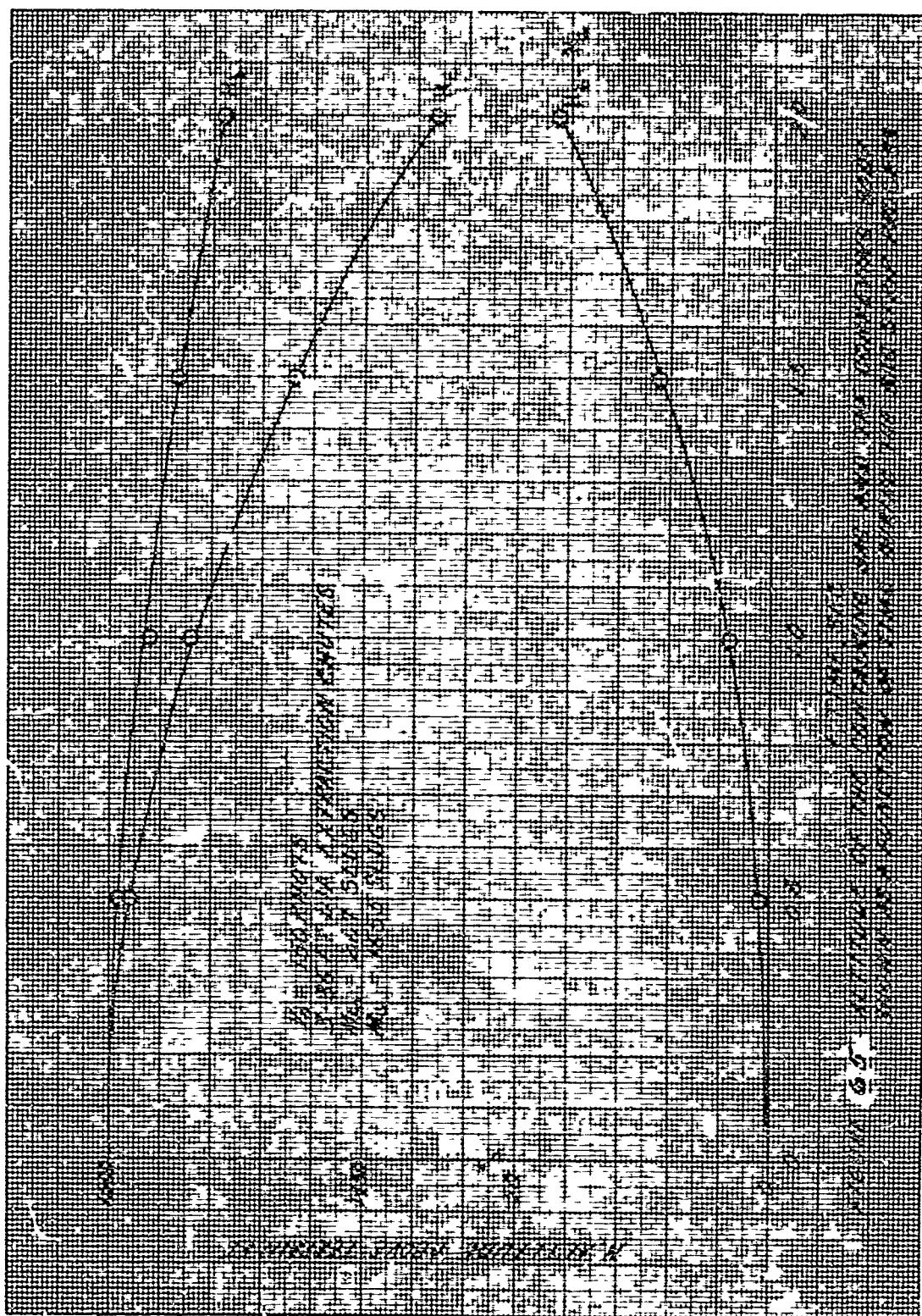


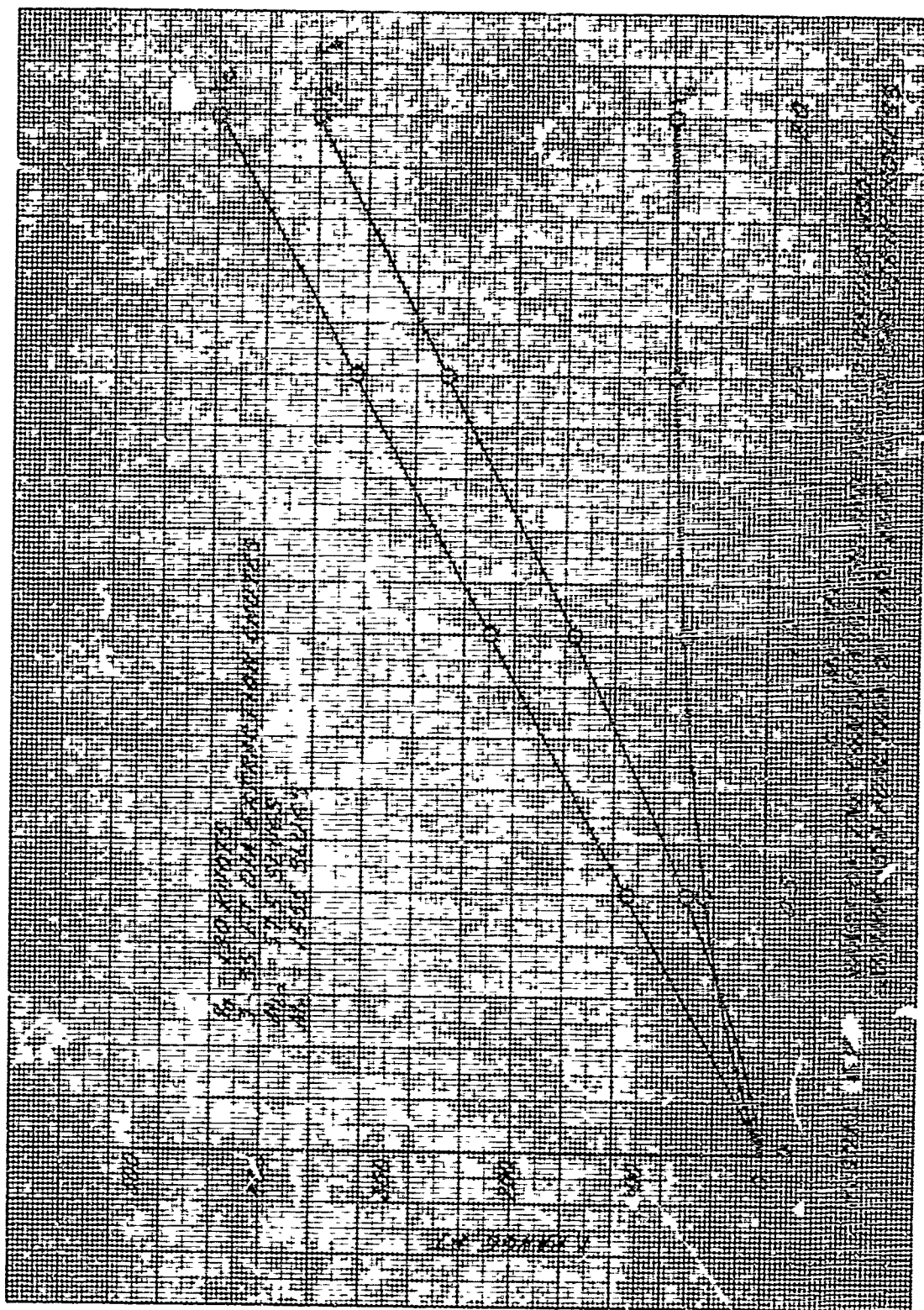


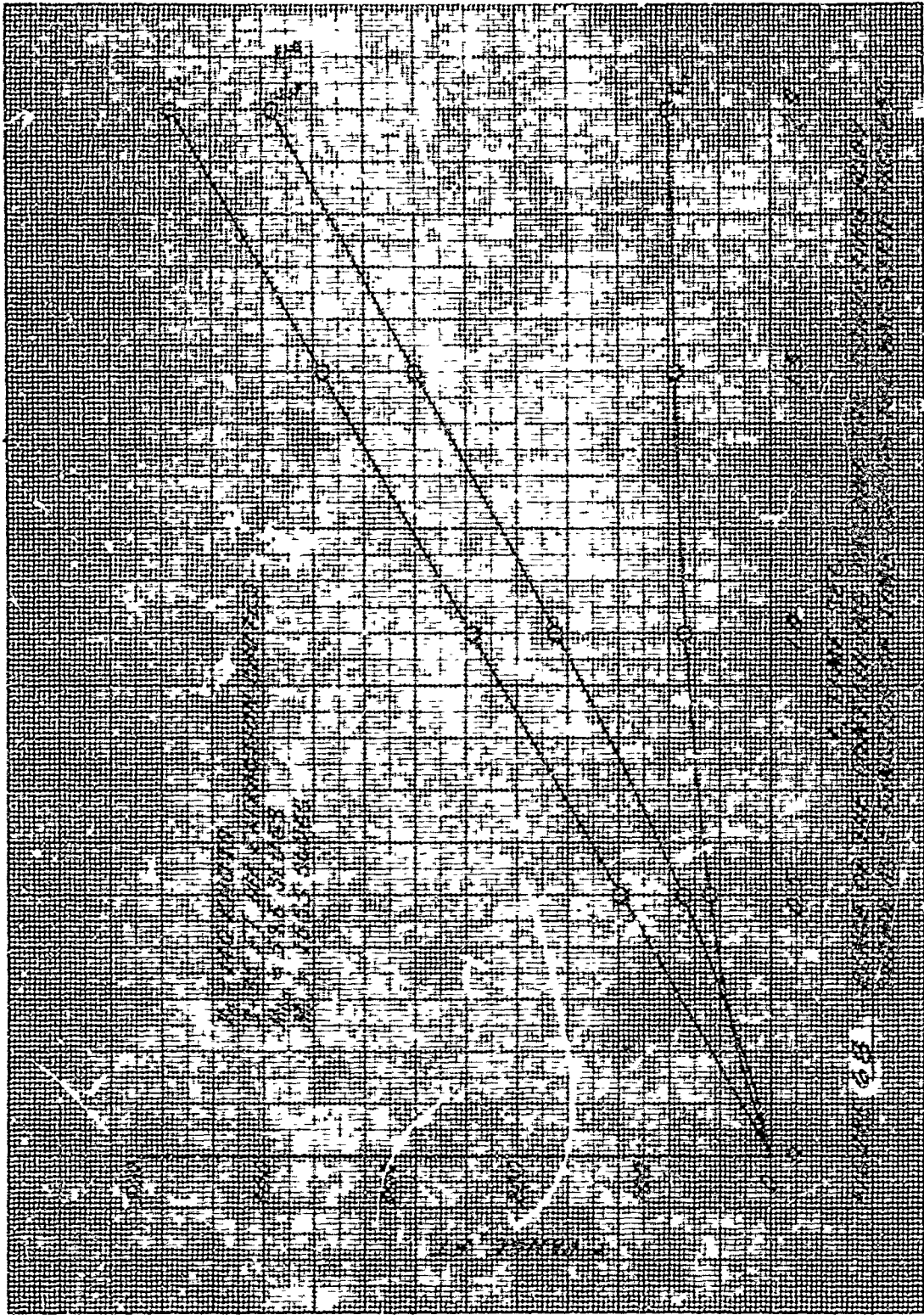


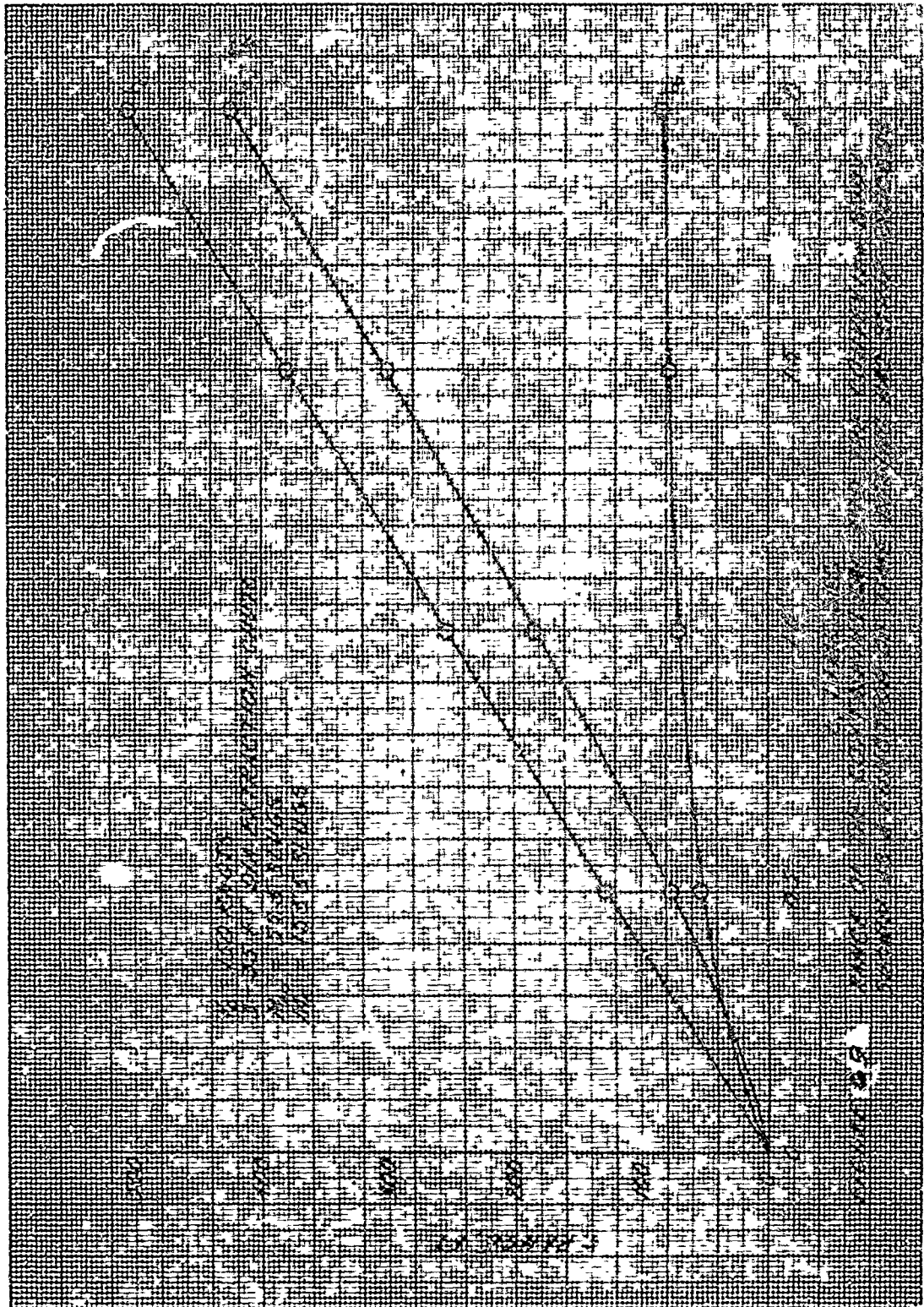


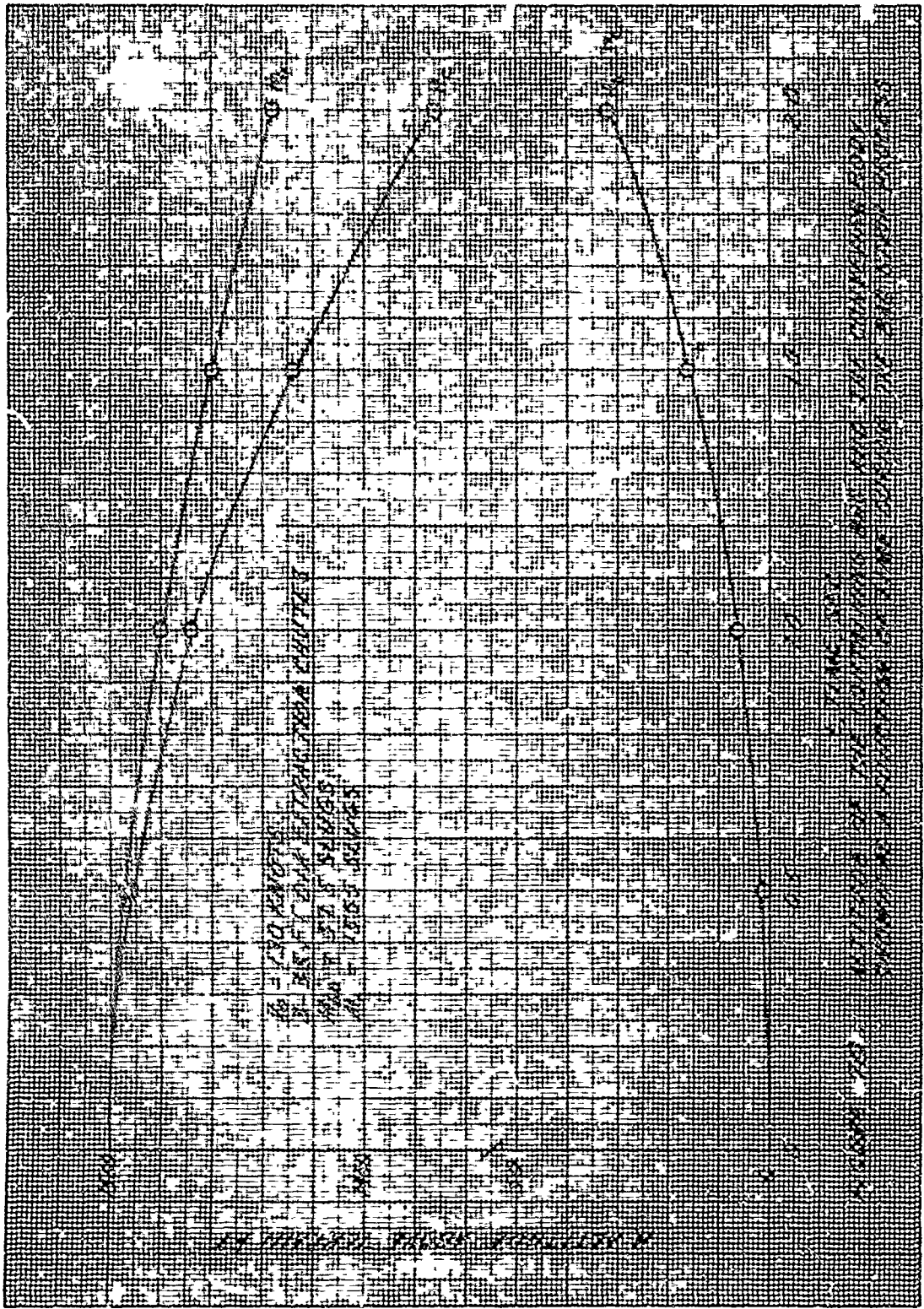






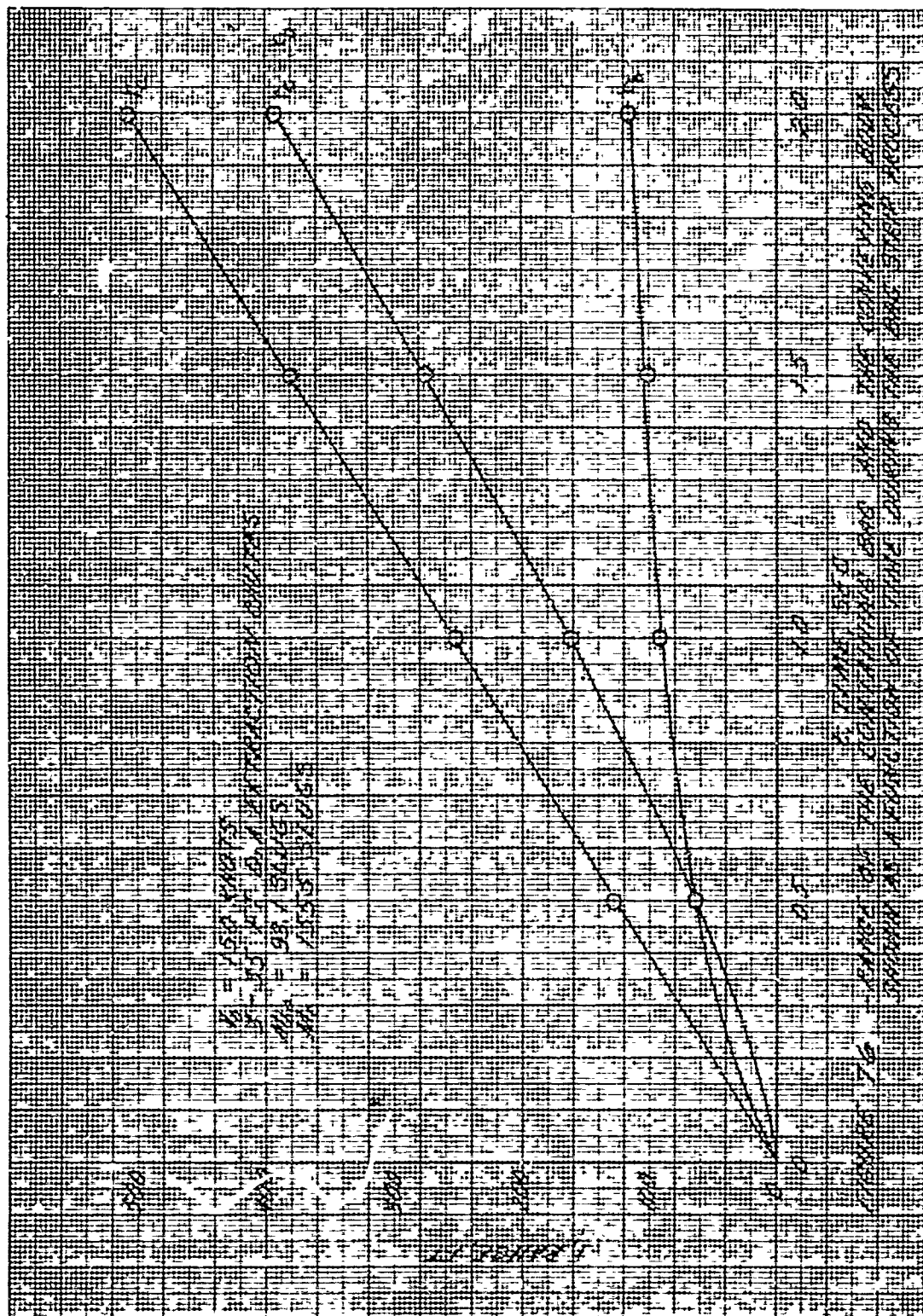




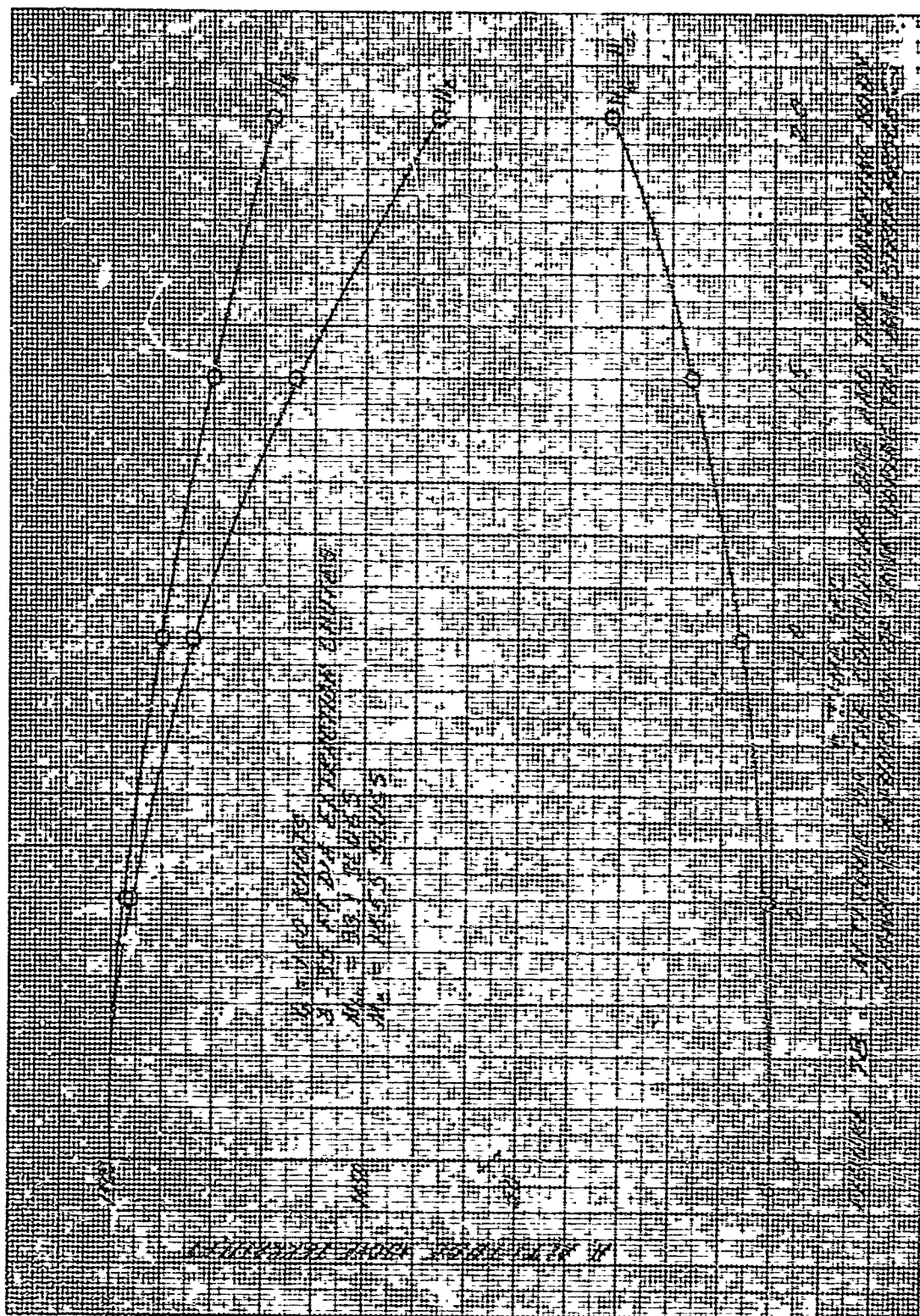












assembly. This information becomes extremely important when, in the next section, the parachute assembly must be sized and, in Section 11, the materials selected. Naturally, the selection of materials will be based on the required material strength, its weight, and its cost. Since a number of choices are available, optimization of selection becomes critical.

At the outset of this study, it was decided that so far as the canopy material was concerned, the choice would be limited to 1.6-oz/yd² MIL-C-7020, Ty. II, or 1.1-oz/yd² MIL-C-7020, Ty. I. The differences in these two canopy materials can be seen in Figs. 80 and 81. Reference to the former shows that, for any given condition, the weight saving in using 1.1-oz/yd² cloth is substantial. However, Fig. 81 reveals that the strength of 1.1-oz/yd² cloth is only 66% that of the 1.6-oz/yd². The same figure shows that the strength-to-weight ratios of both materials are approximately equal, as are the costs. Hence, on the basis of what is depicted in Figs. 80 and 81, it appears that the 1.1-oz/yd² material is the better choice of the two.

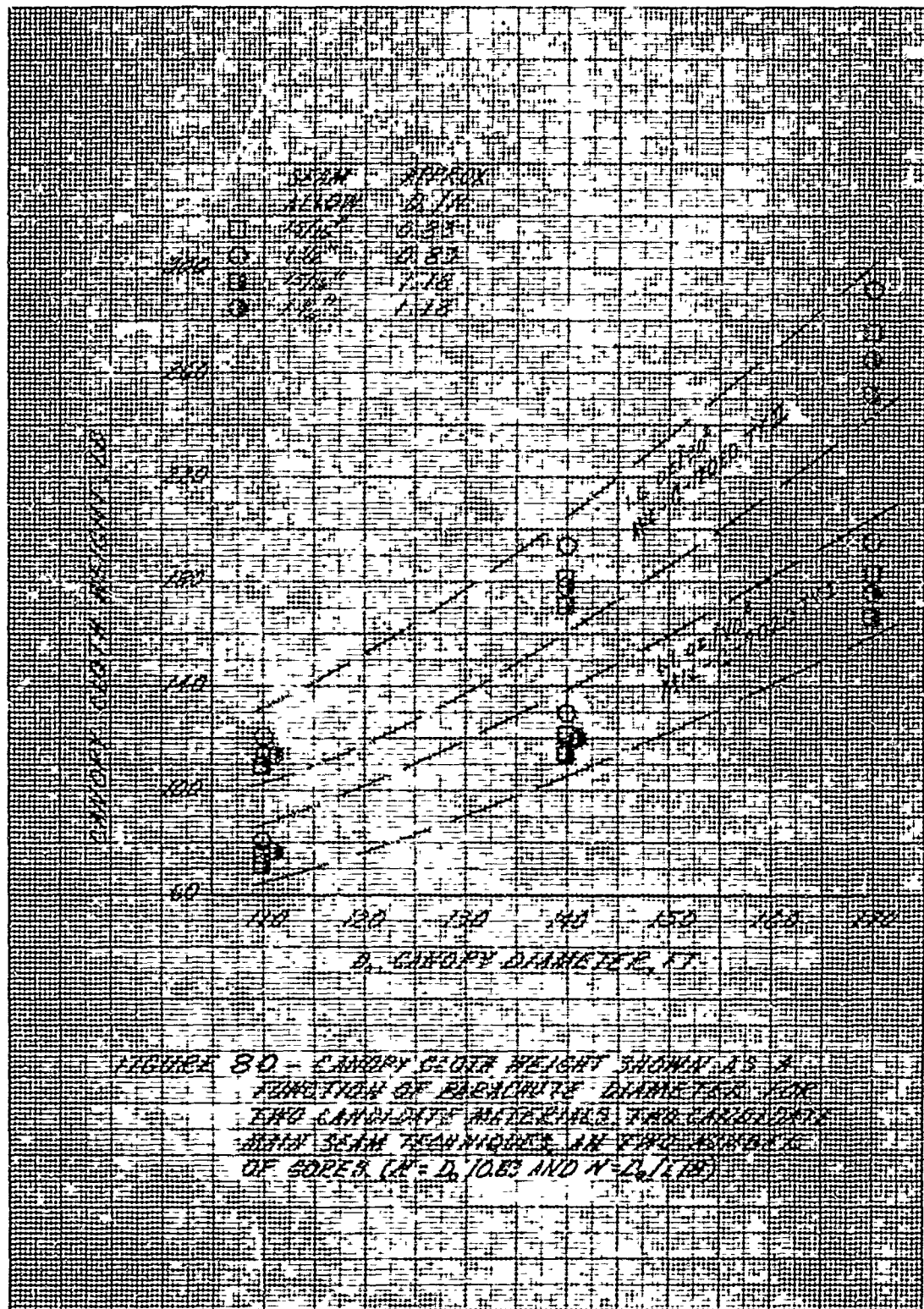
Figures 82 through 86 depict various candidate materials that may be used for suspension lines for the parachute assembly. Reference to Fig. 82 shows the two most efficient, in terms of strength to weight, to be Pioneer Specs. EI-4142 and EI-4151. Reference to Fig. 83 shows that, for any given suspension-line length, these materials weigh considerably less than the others. Finally, Fig. 84 reveals that these same two materials cost considerably less than any of the other candidate suspension-line materials. From Figs. 82 through 84, it can be concluded that Pioneer Spec. EI-4151 competes most favorably with either MIL-C-5040, Ty. II, or MIL-C-7515, Ty. I.

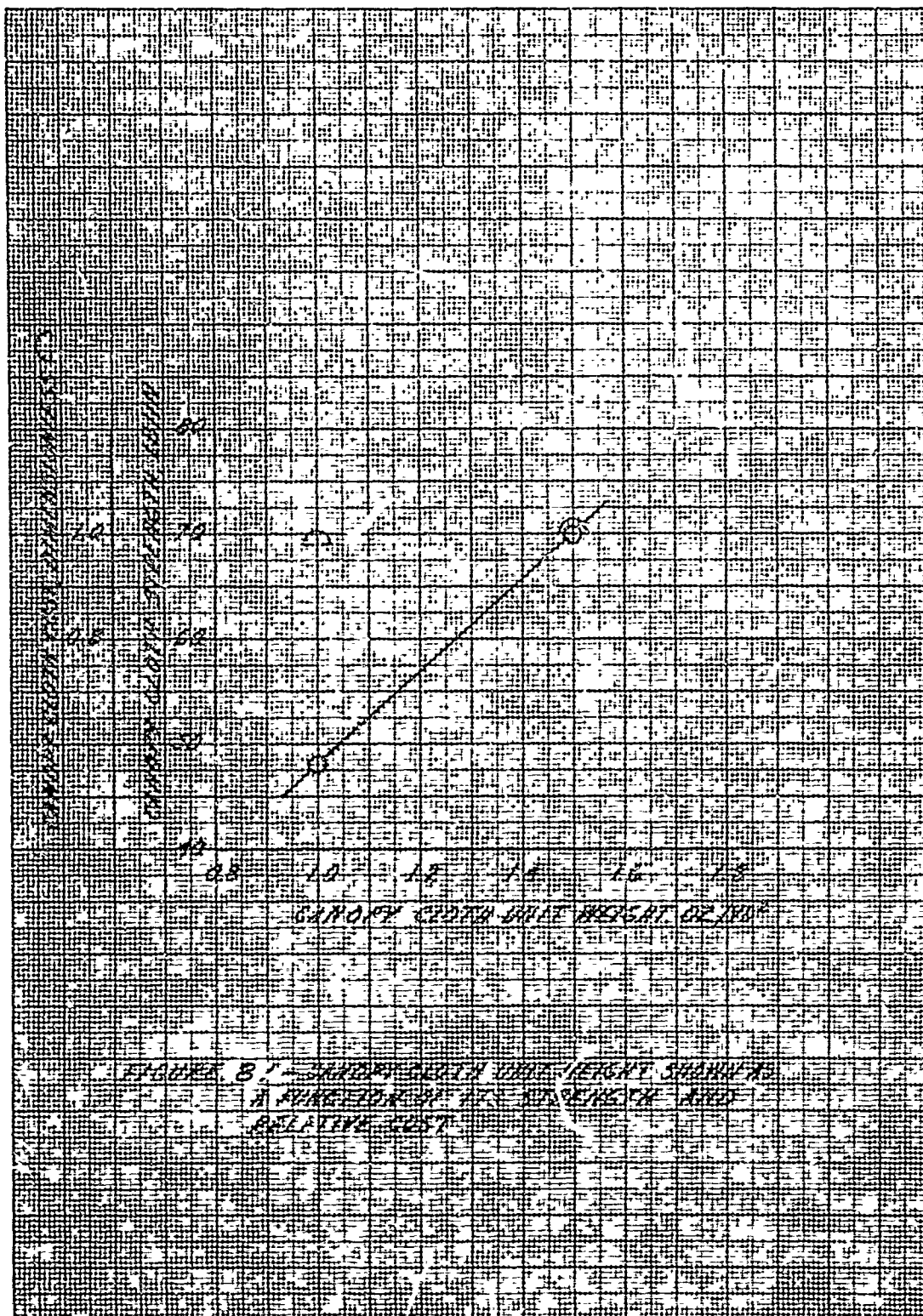
Figures 85 through 87 illustrate various candidate webbing materials that may be used as the riser for the parachute assembly. Finally, Figs. 88 through 90 and Figs. 91 and 92 respectively illustrate various candidate single- and multi-ply webbing materials that may be used for the center line and riser extension for the parachute assembly.

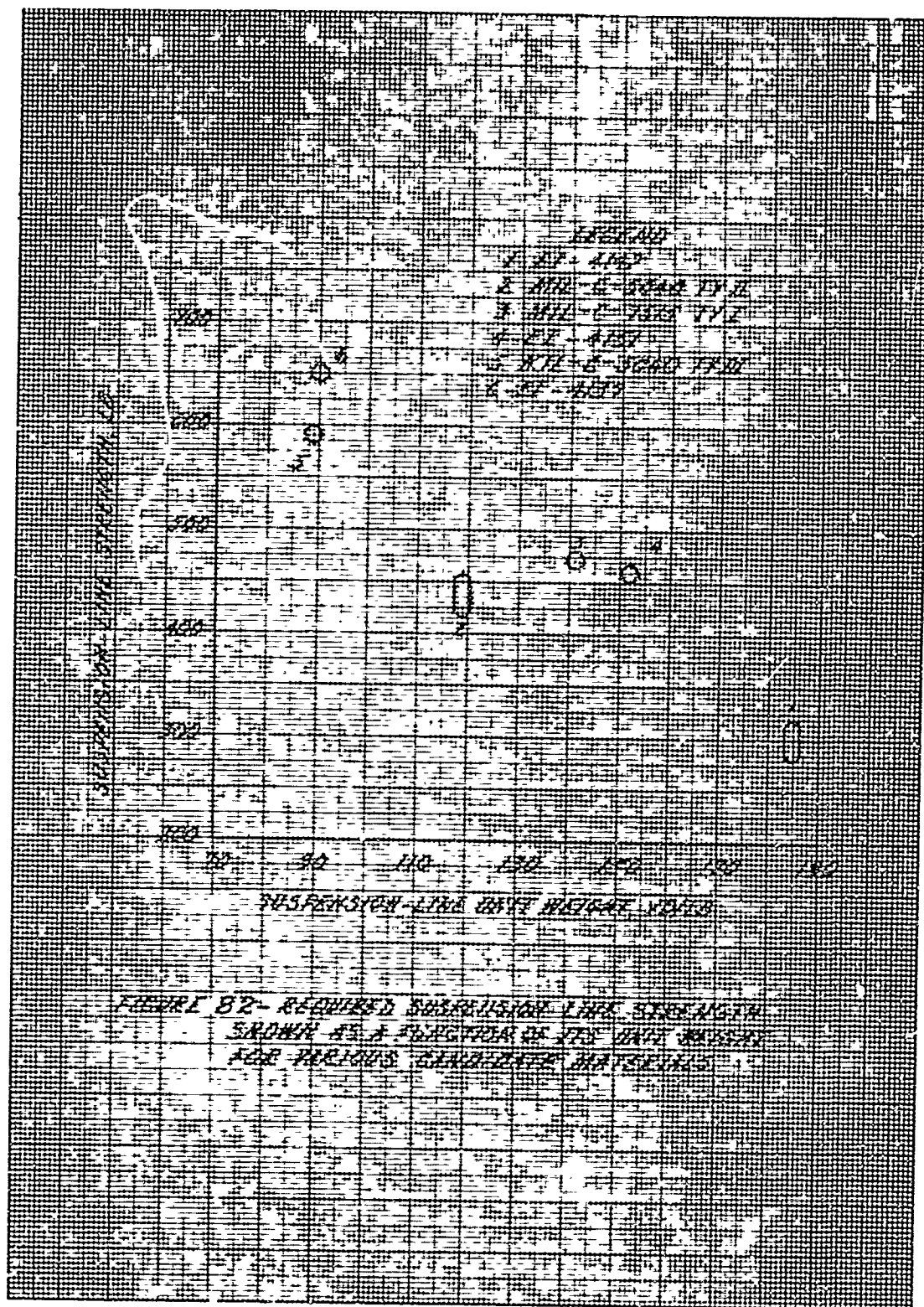
9. SIZING THE PARACHUTE ASSEMBLY

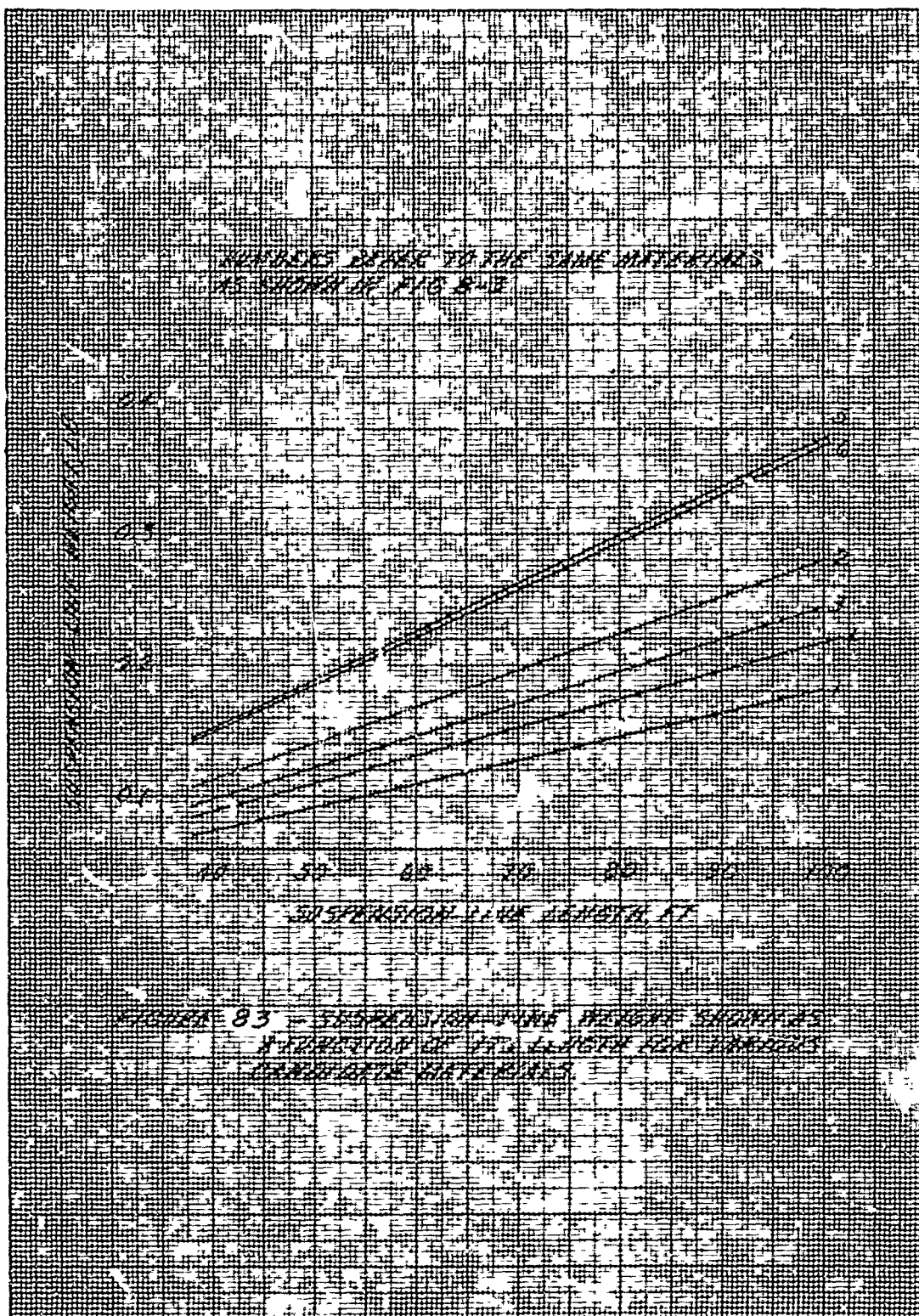
Figure 93 depicts the total canopy area needed (calculated from eq. 9-1) to touch down a 50,000-lb gross rigged weight at 24 ft/sec STP:

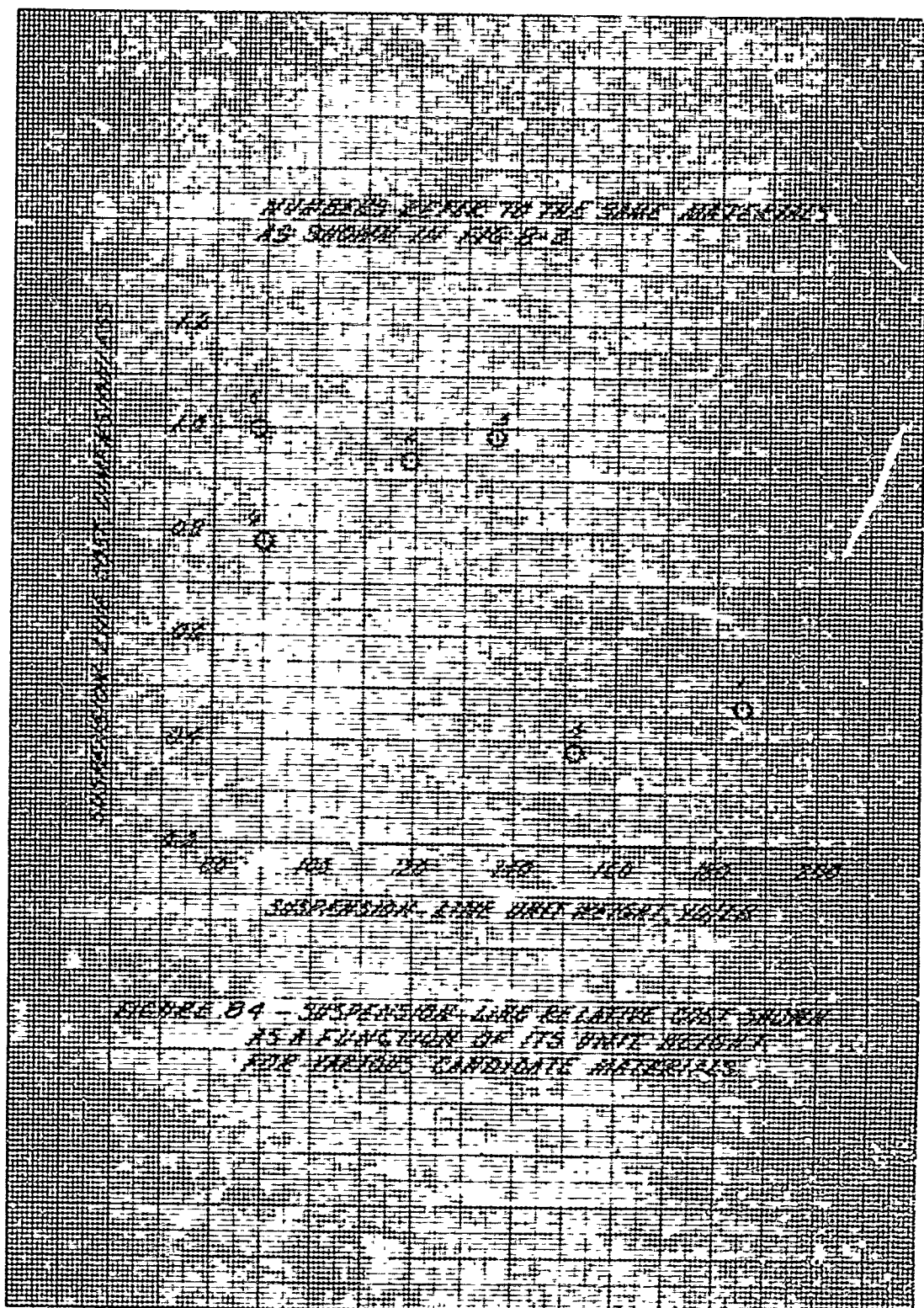
$$(S_o)_{CL} = \frac{2W}{(C_{D_o})_{CL} \rho V^2}, \quad (9-1)$$



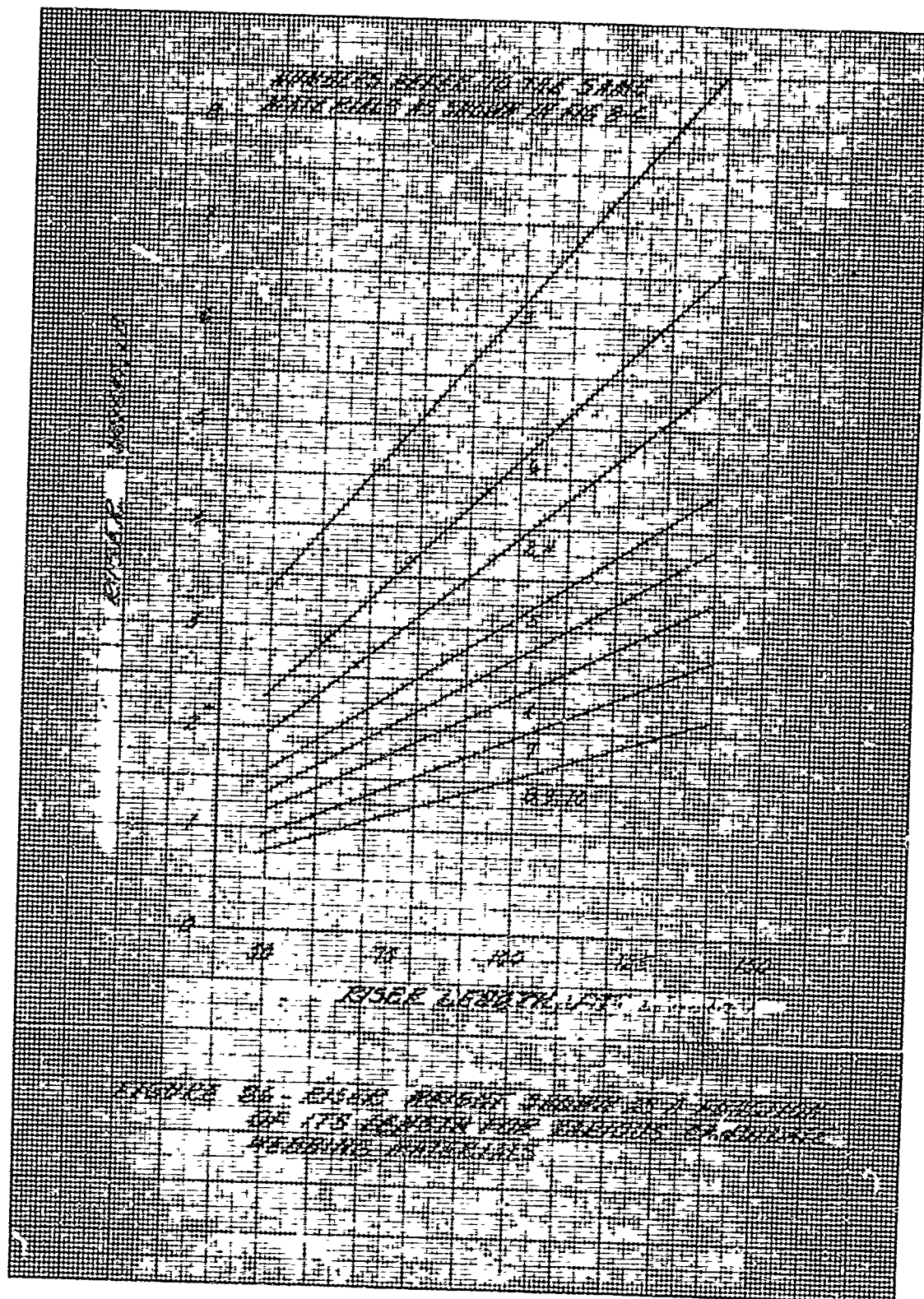


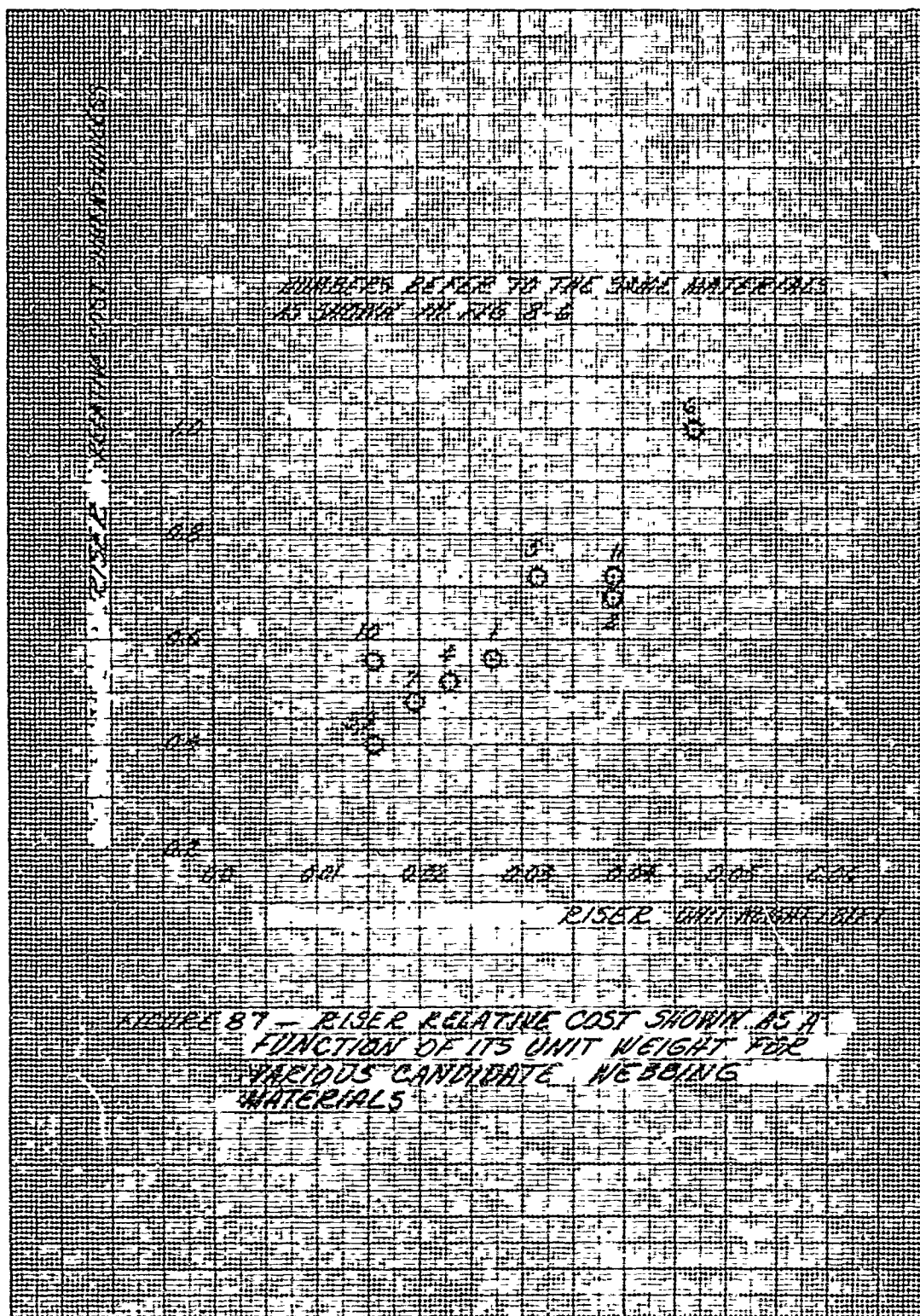


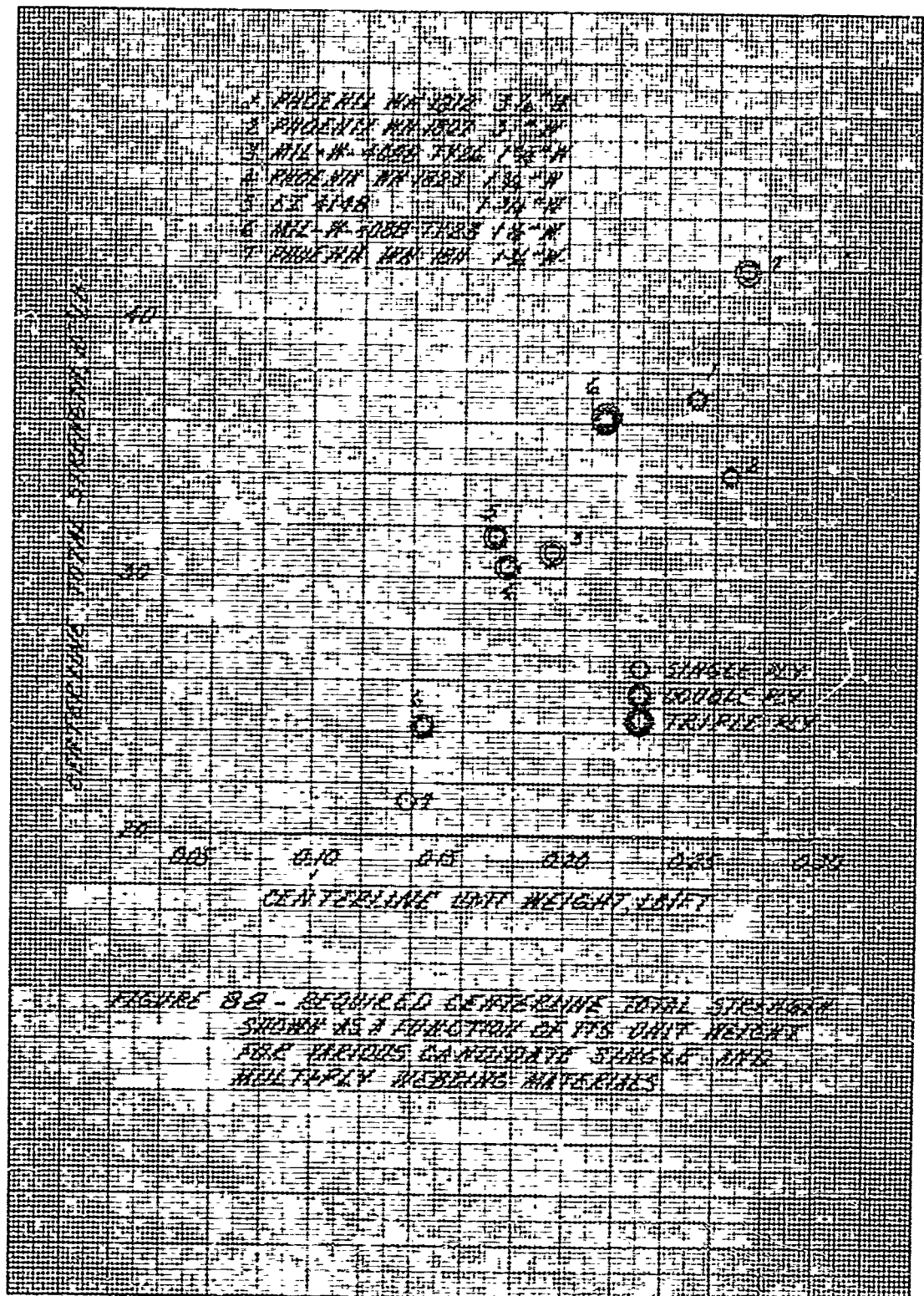


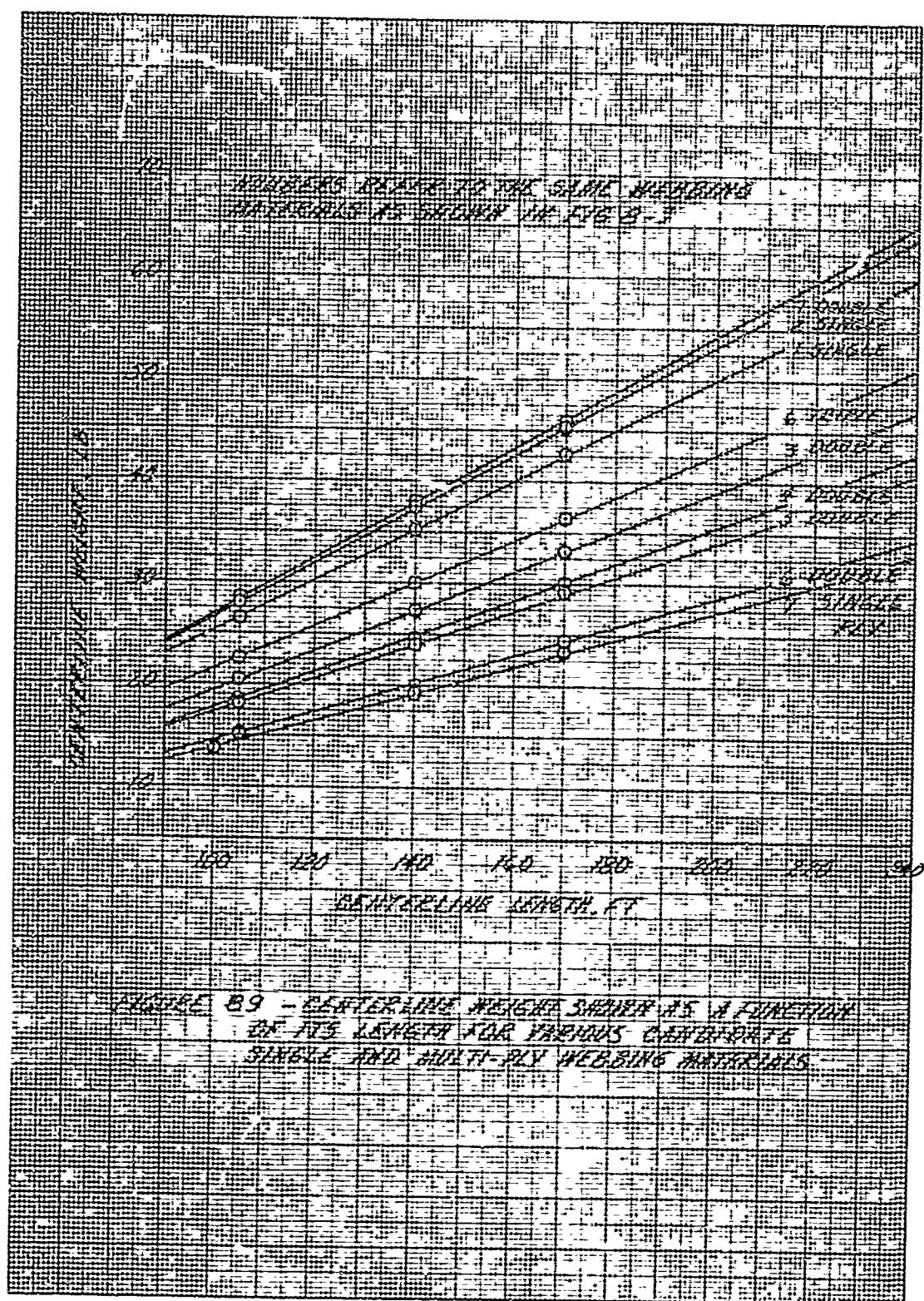


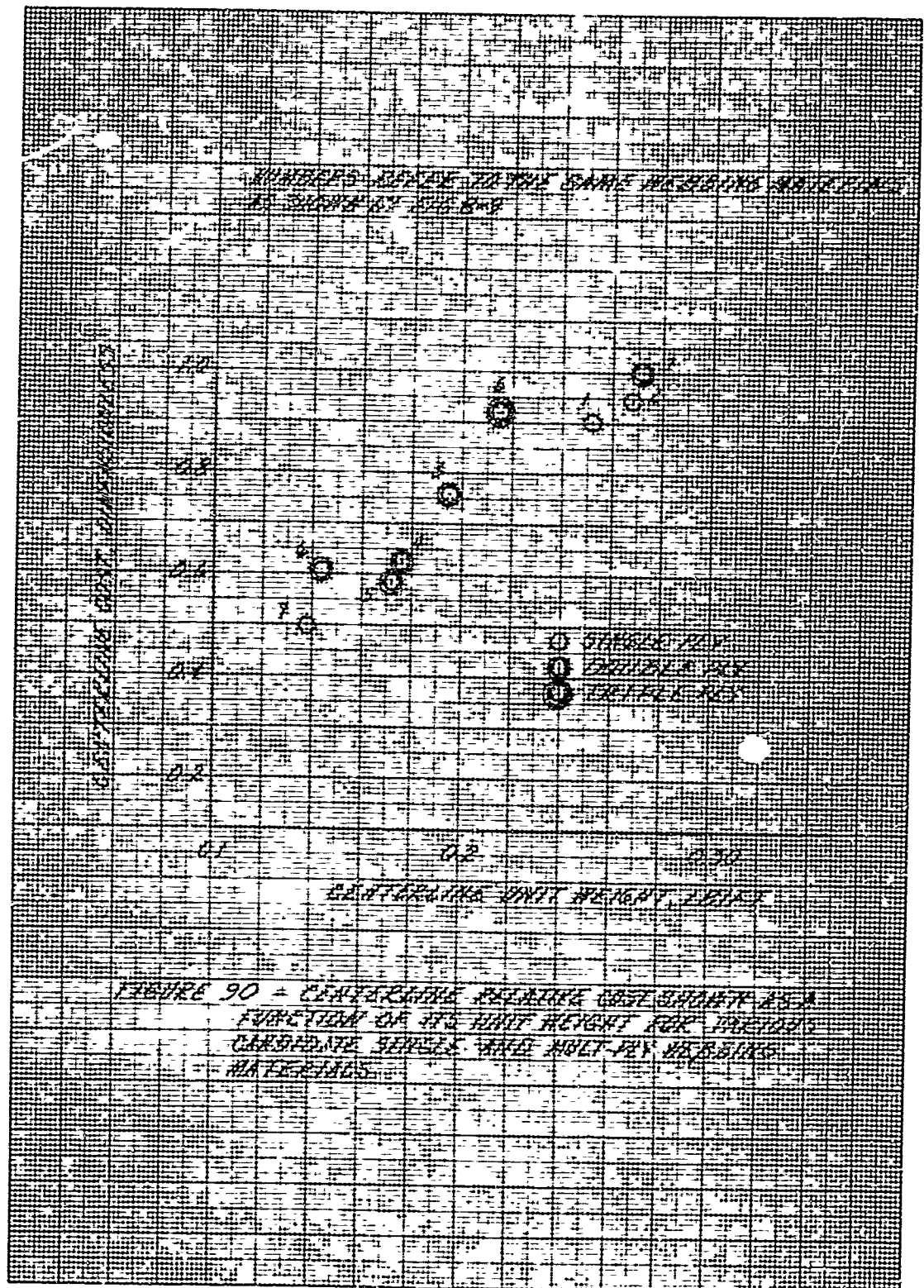


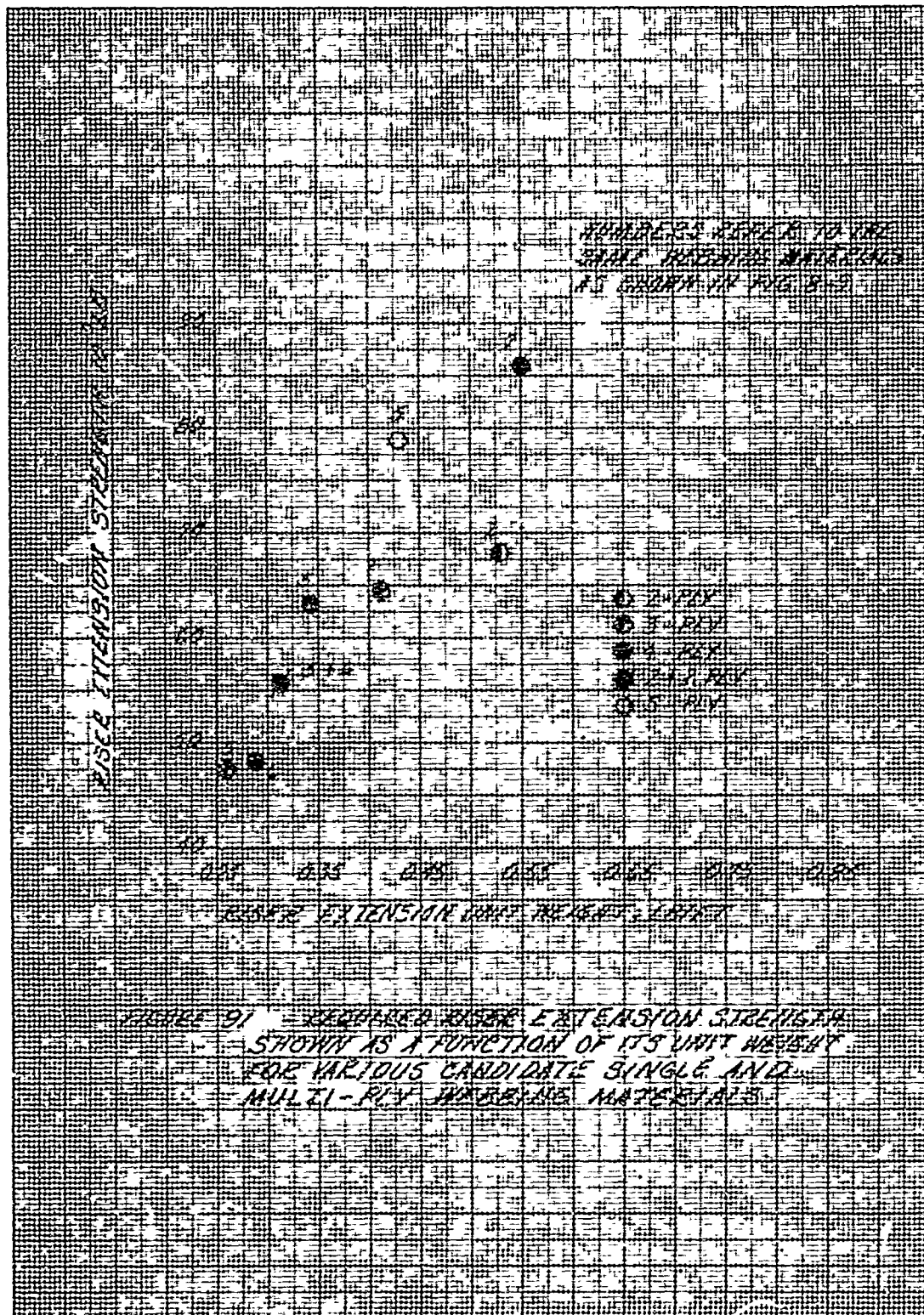


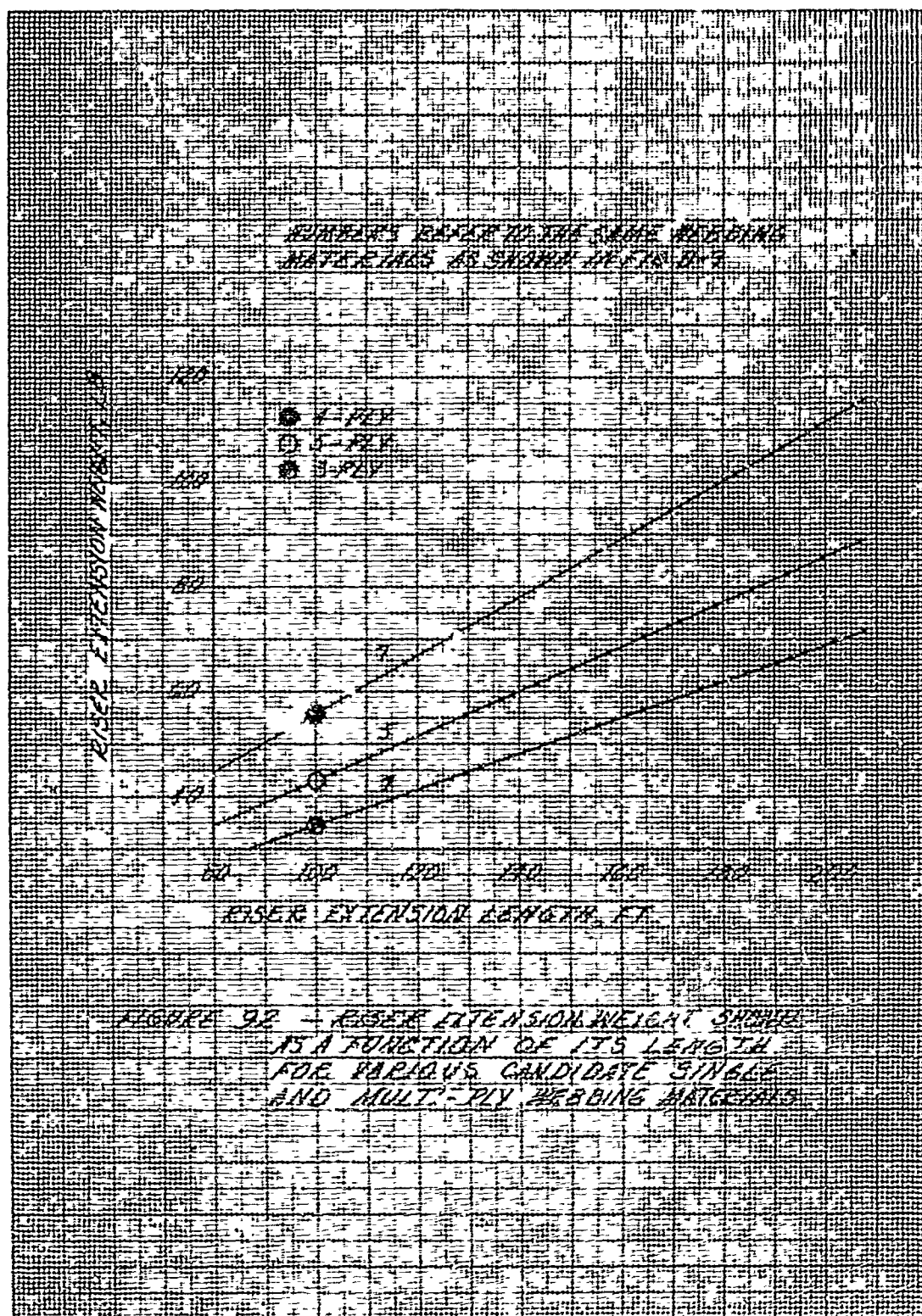


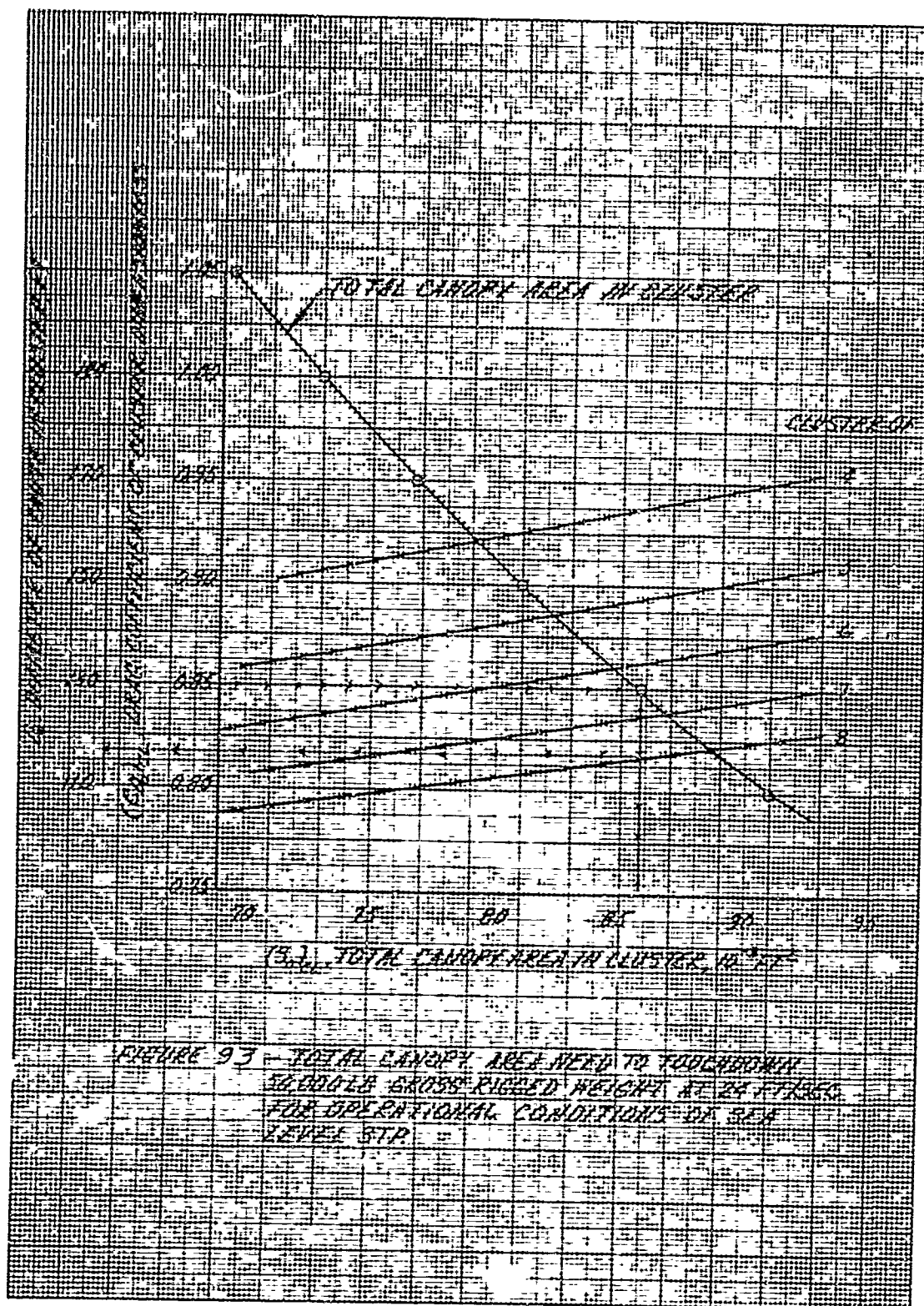












where the cluster steady-state drag coefficient, $(C_{D_0})_{CL}$, is a parameter of considerable significance. Section 5 presents the results of an appreciable effort to determine within a fair degree of accuracy the magnitude of this parameter.

With regard to the number of parachutes selected to comprise the cluster, it was felt that six is the maximum. This is based primarily on the premise that a smaller number of parachutes would require assemblies of larger diameter, making them extremely unwieldy, therefore most undesirable. Using more than six parachutes to comprise the cluster would lead to a condition conducive to a high degree of cluster interference. In addition, using more than six parachutes would mean that the individual assemblies were relatively smaller in diameter, which would limit their overall efficiency.

For a cluster of six parachutes and a cluster steady-state drag coefficient of 0.85 (see Fig. 27), Fig. 93 shows the total canopy area of the cluster to be 85,000 ft². Figure 93 also shows the diameter of each individual parachute to be 135 ft.

10. PERFORMANCE

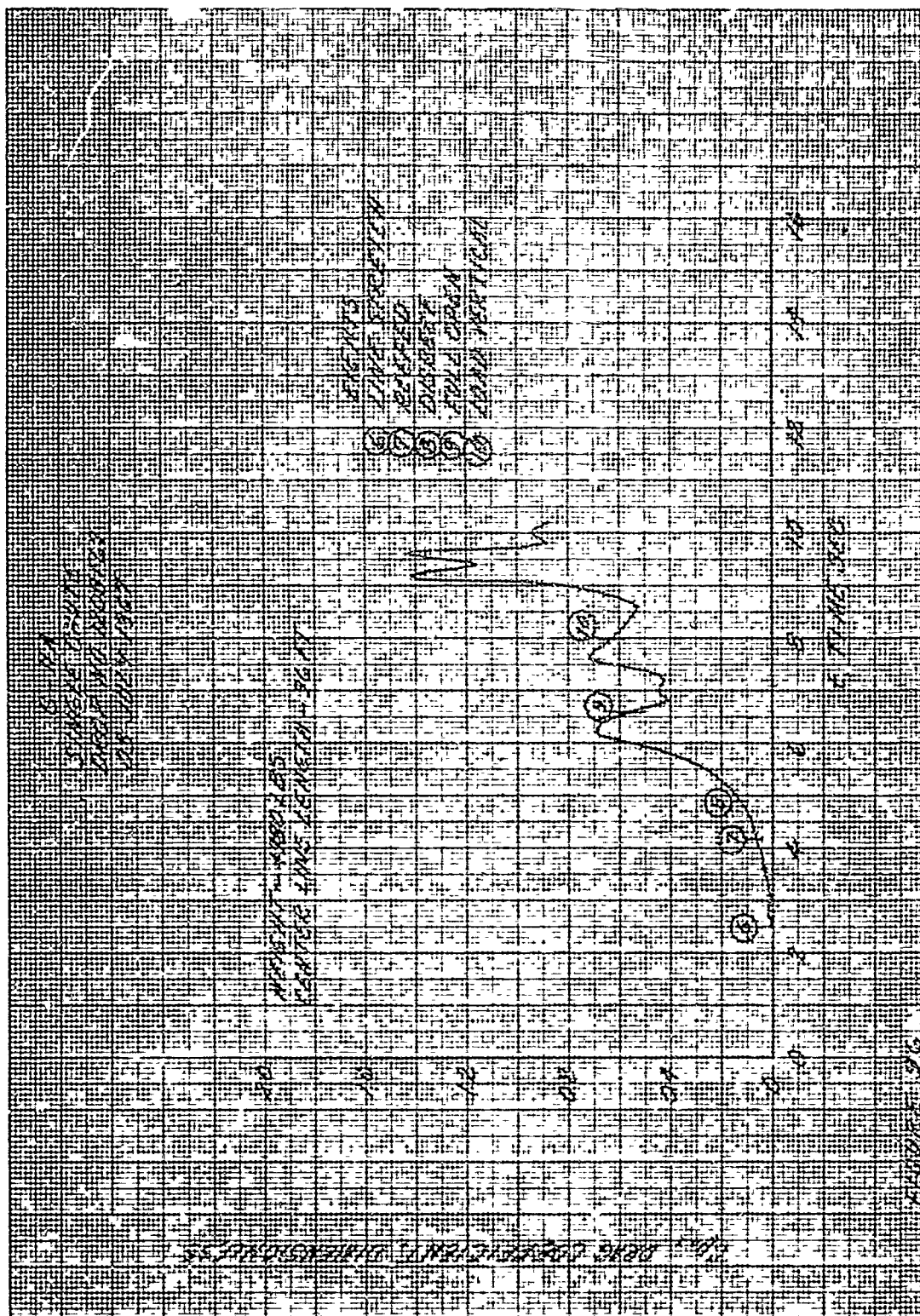
In Section 9, it was shown that a cluster of six 135-ft-diam. parachutes is required. This section will now attempt to establish the maximum load that any one of these parachutes experiences while in its operational mode.

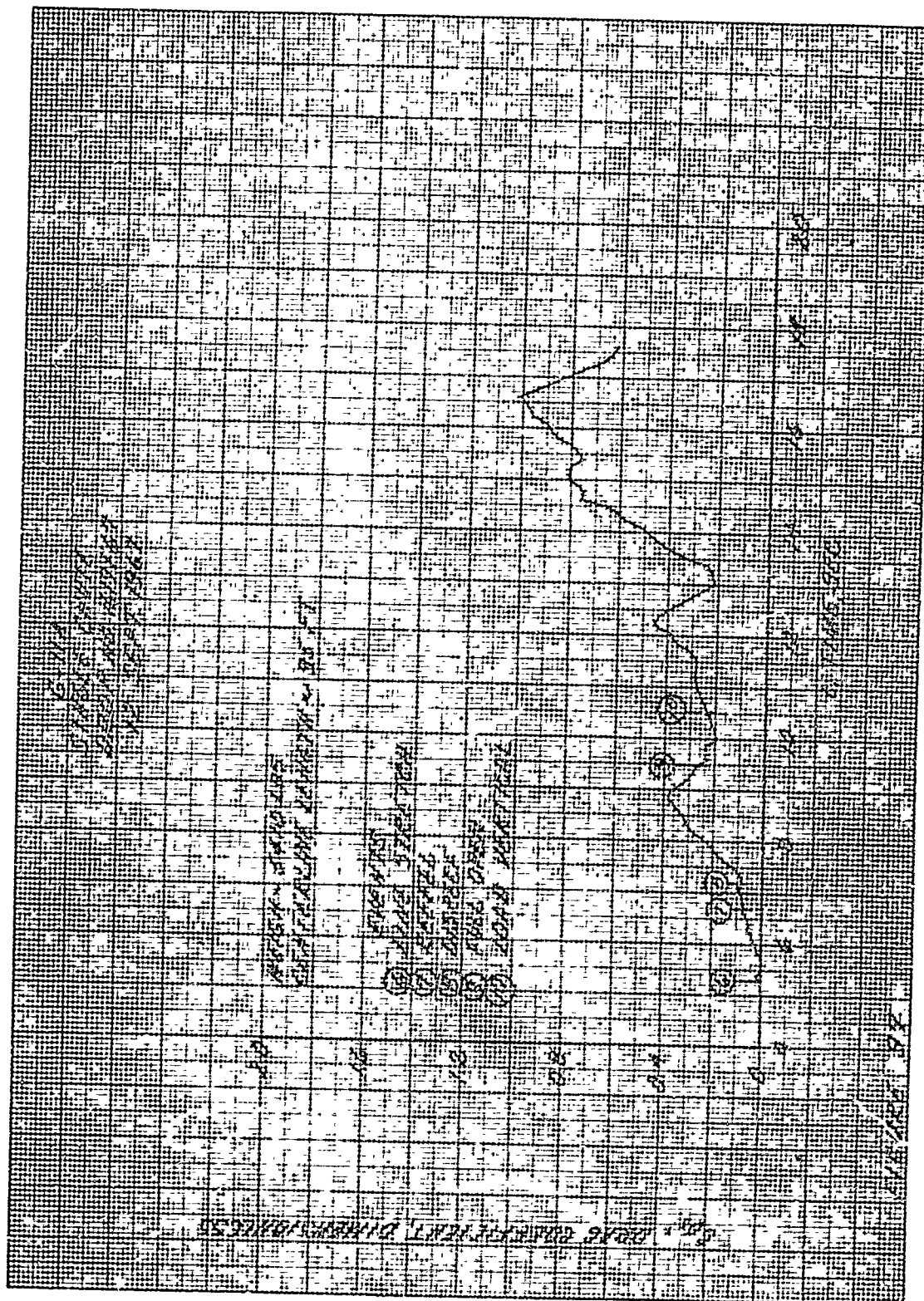
a. Effective Drag History

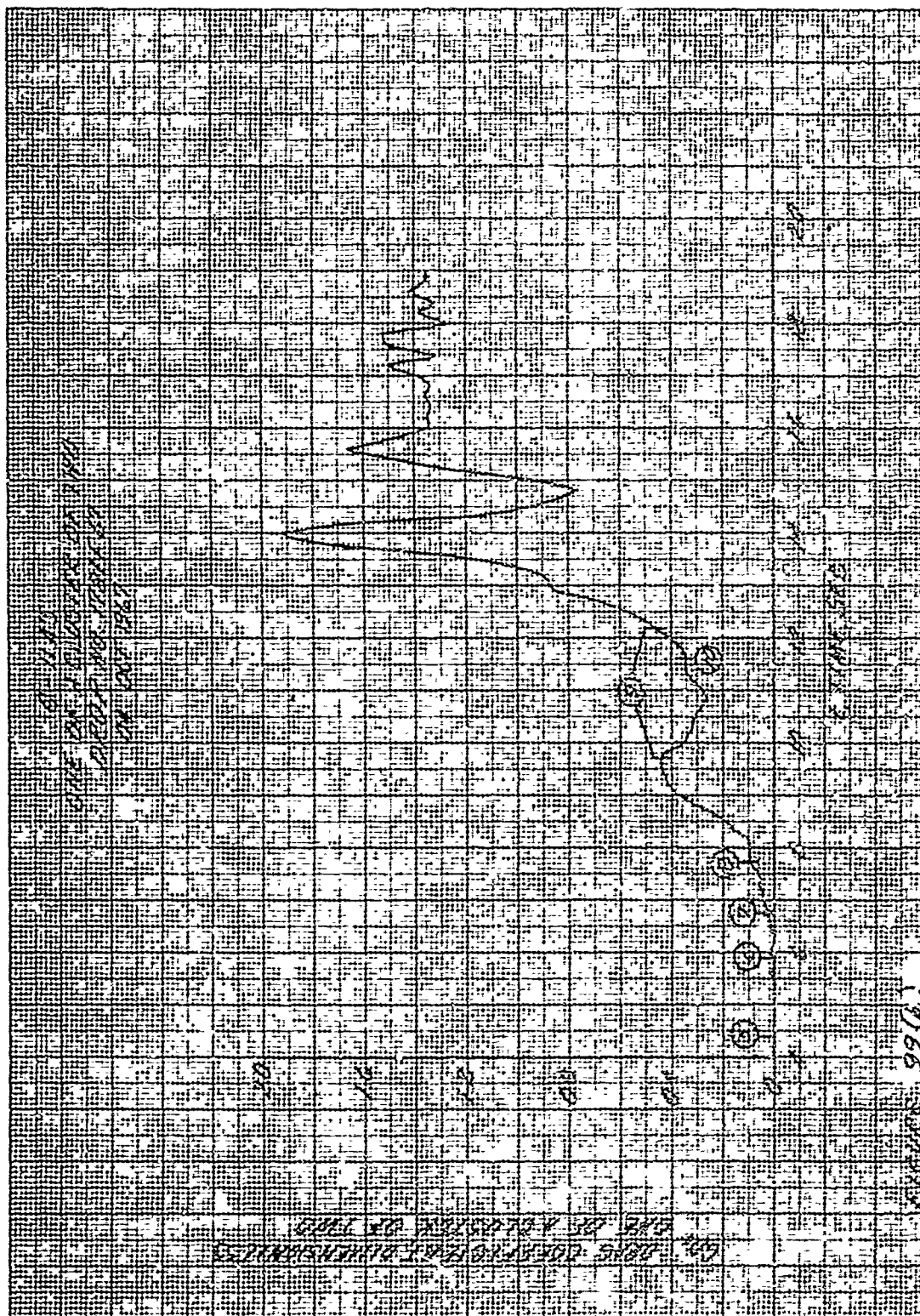
All the numerous views concerning the drag history of a parachute system during its inflation process are premised on empirical studies; none is founded on established theory. The problem of inflation dynamics becomes even more acutely complex for clustered parachutes. Hence, it is felt that a study of the drag histories (Figs. 94 through 108) associated with the drops listed in Table 1 will lead to an envelope from which a drag history can be selected for the 135-ft-diam. parachute. Hence, it is with regard to Figs. 94 through 108 that the drag coefficient for a single chute and for a cluster of chutes can be calculated by the following formulae, respectively:

$$C_{D_0}(t) = \frac{F}{qS_0} \quad (10-1)$$

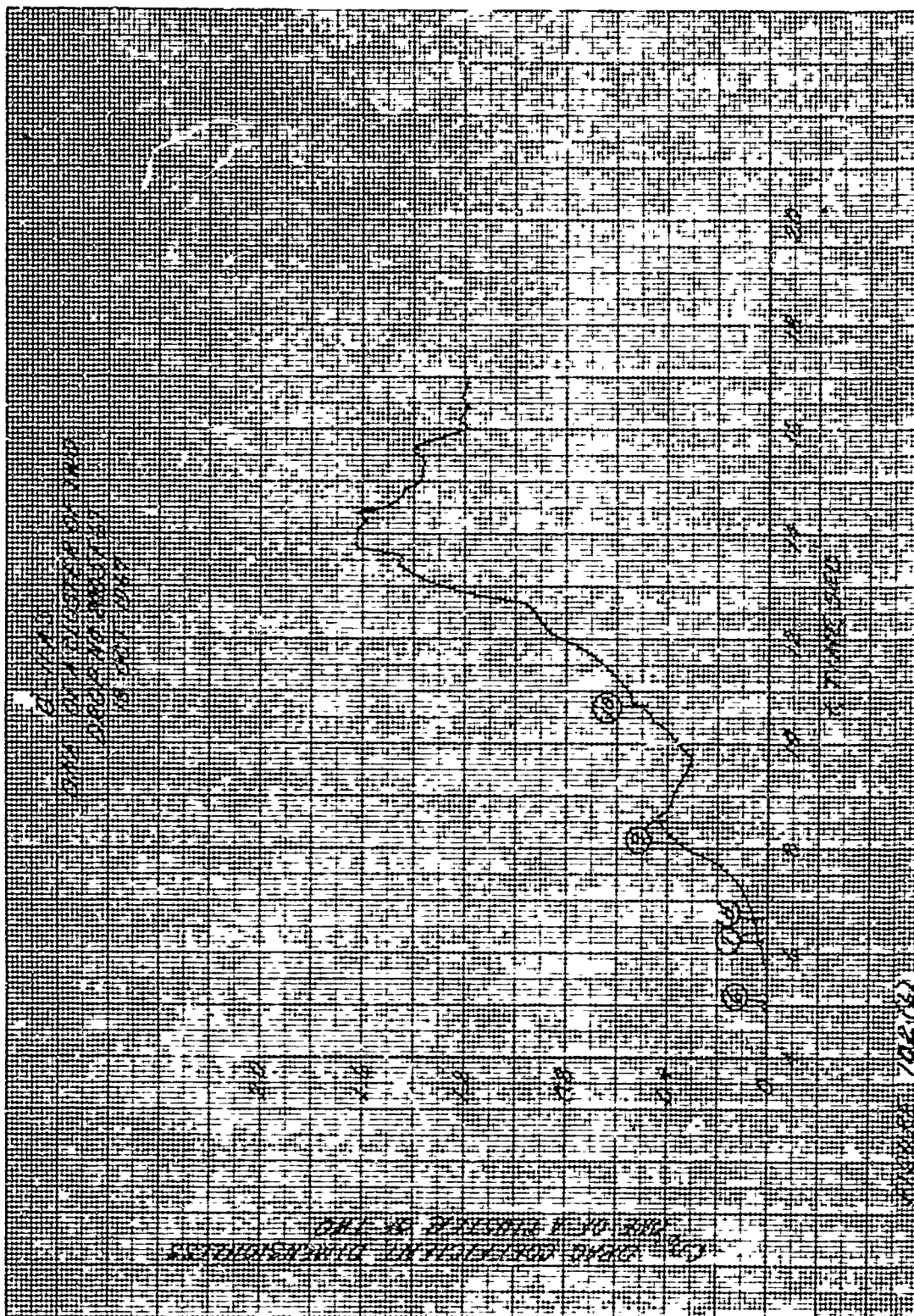
and

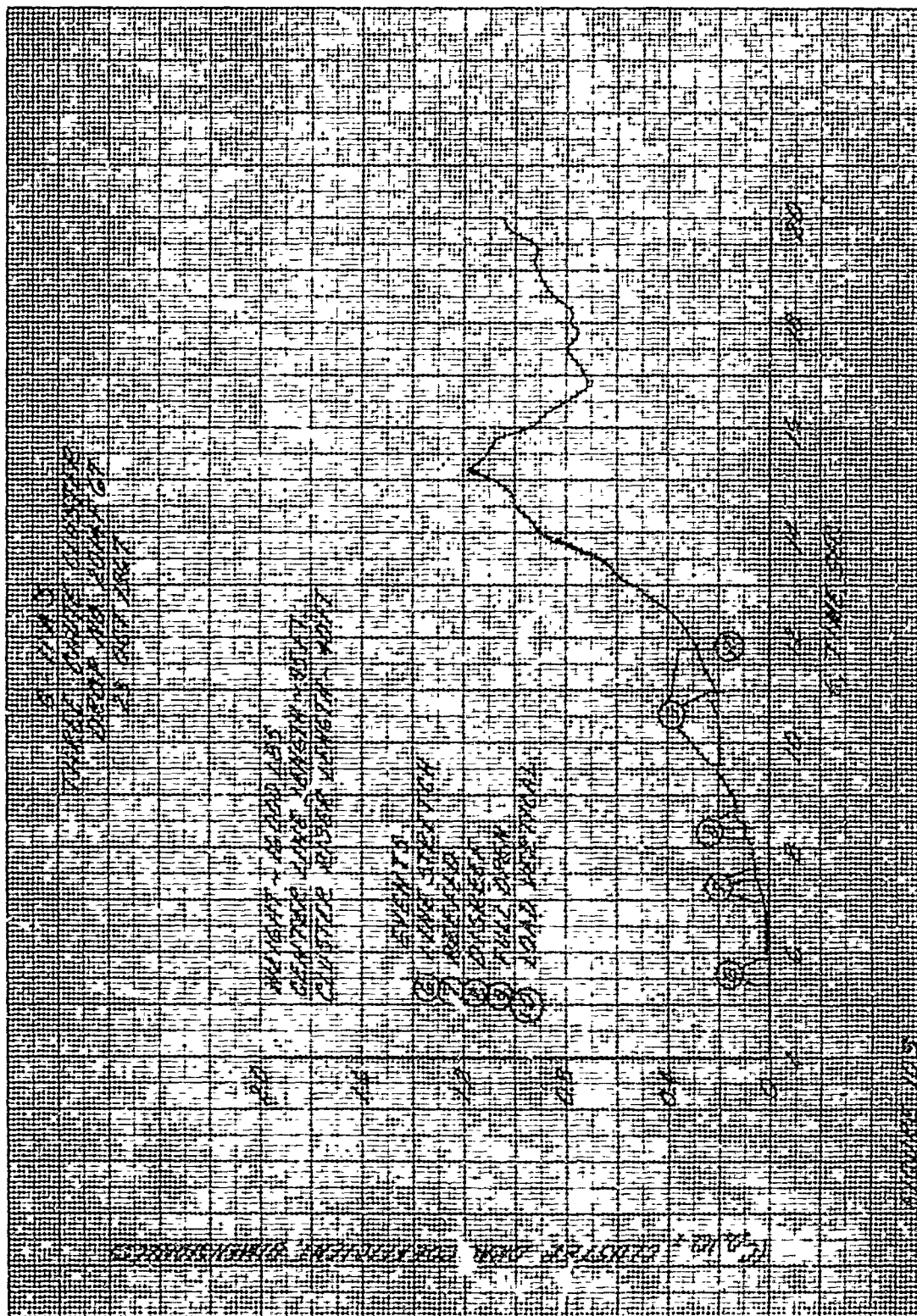


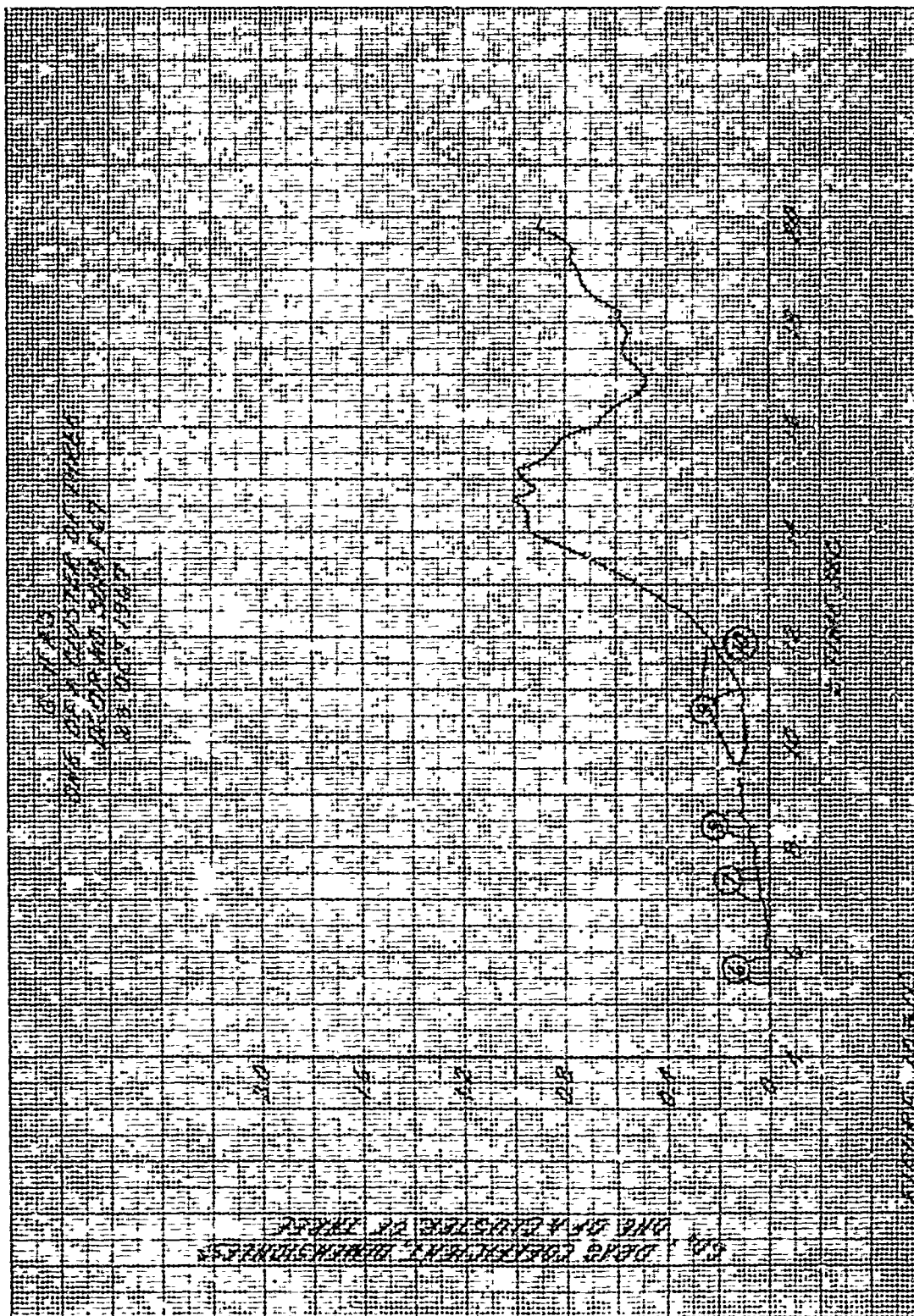


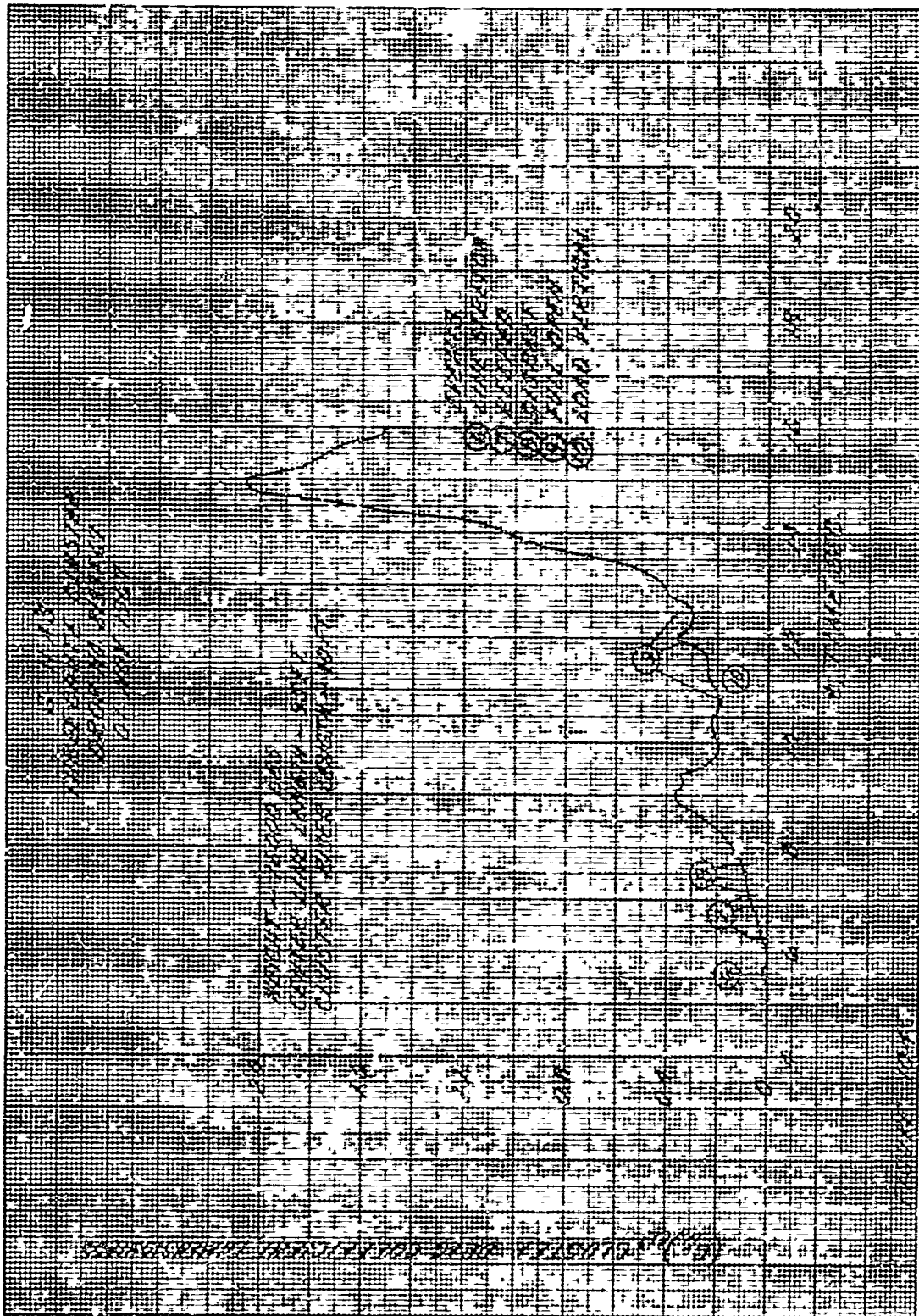


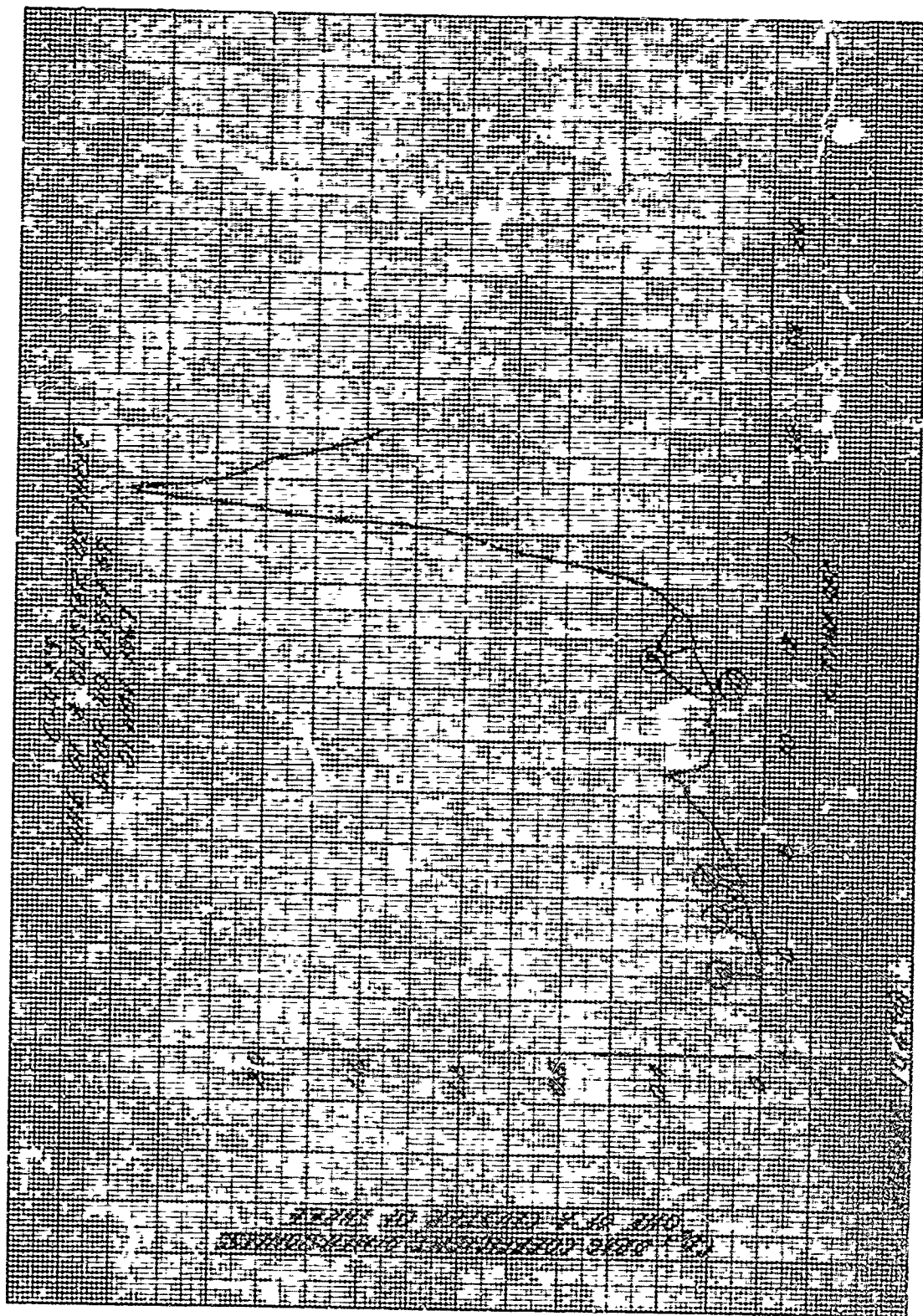


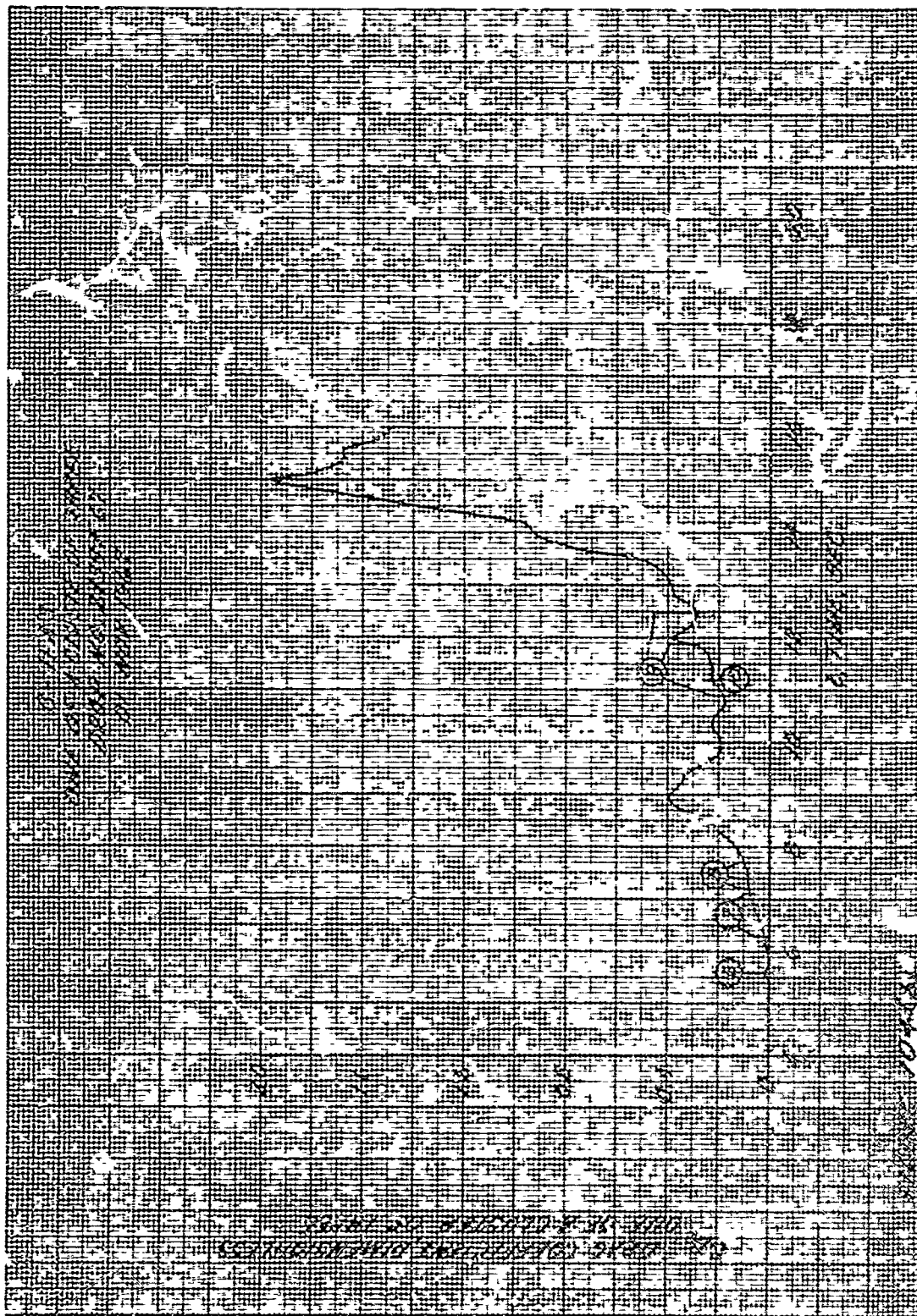


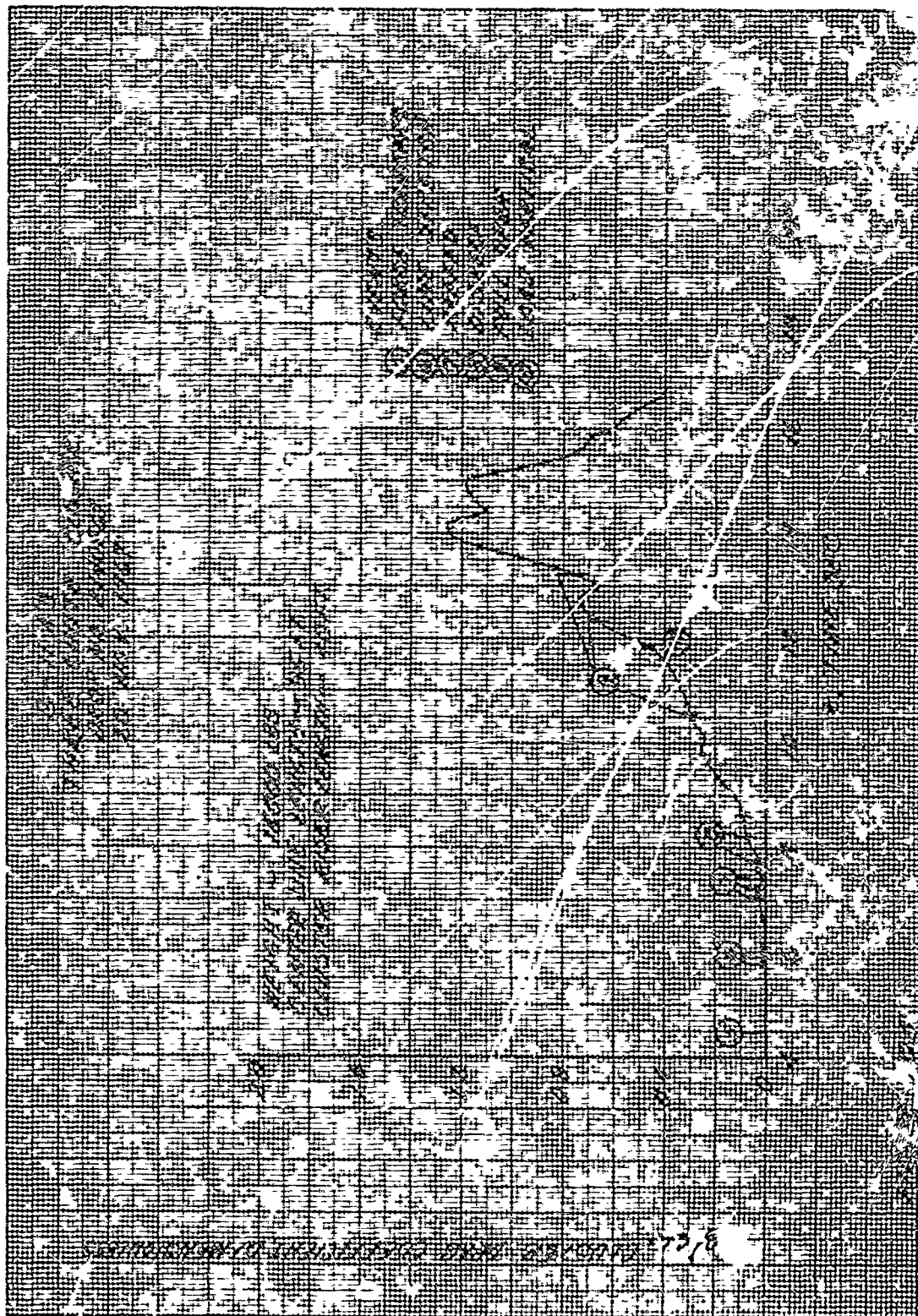


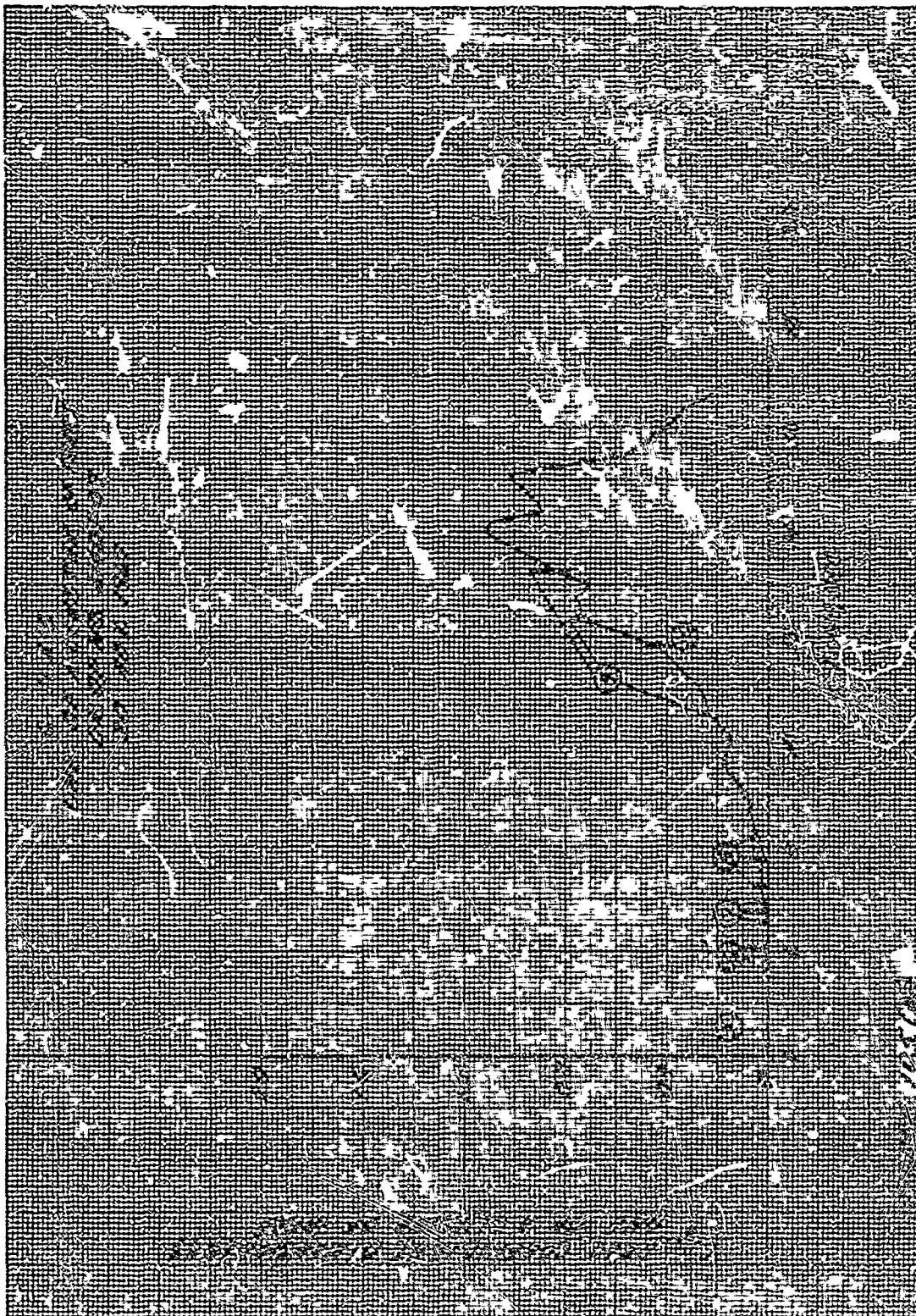


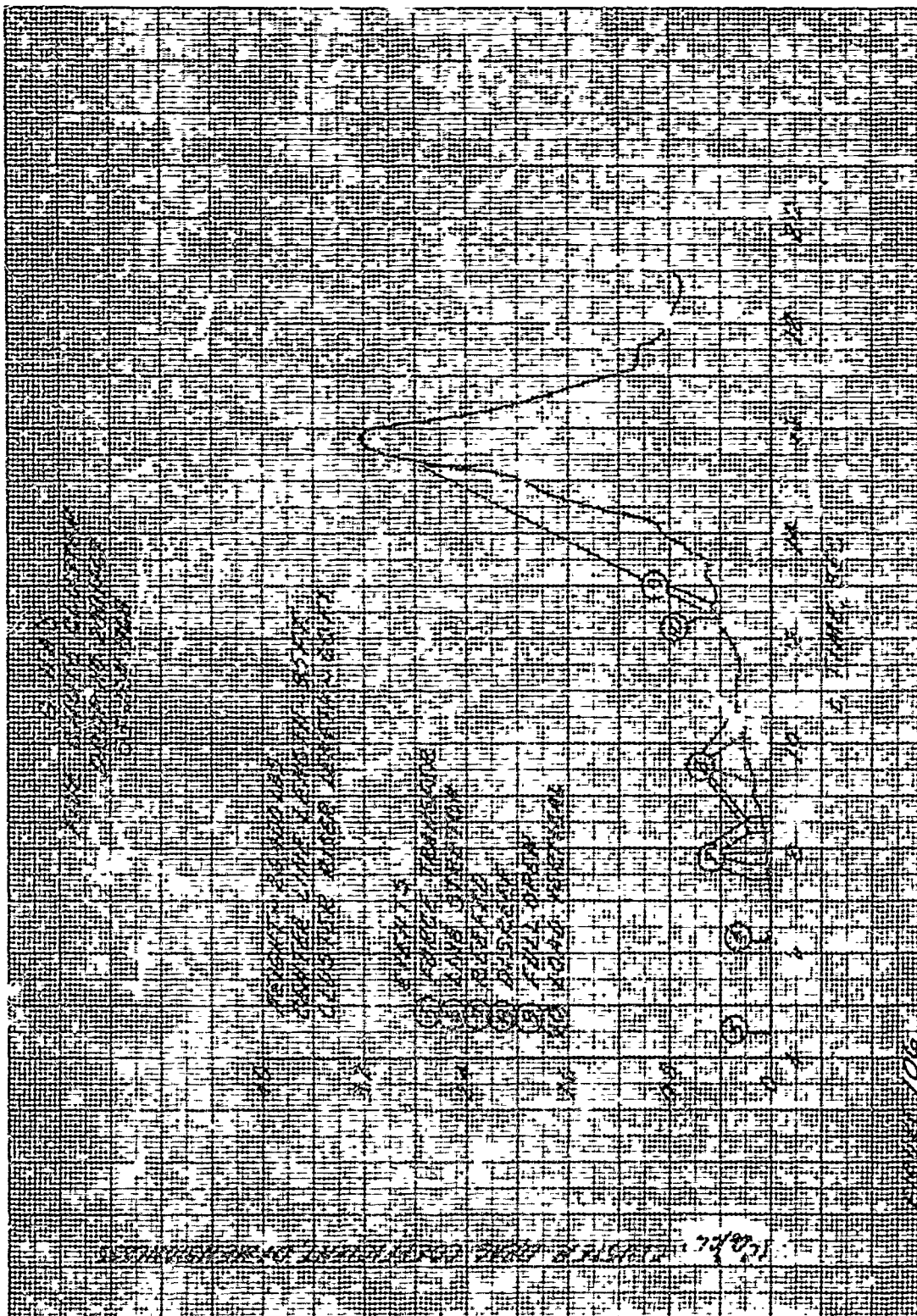


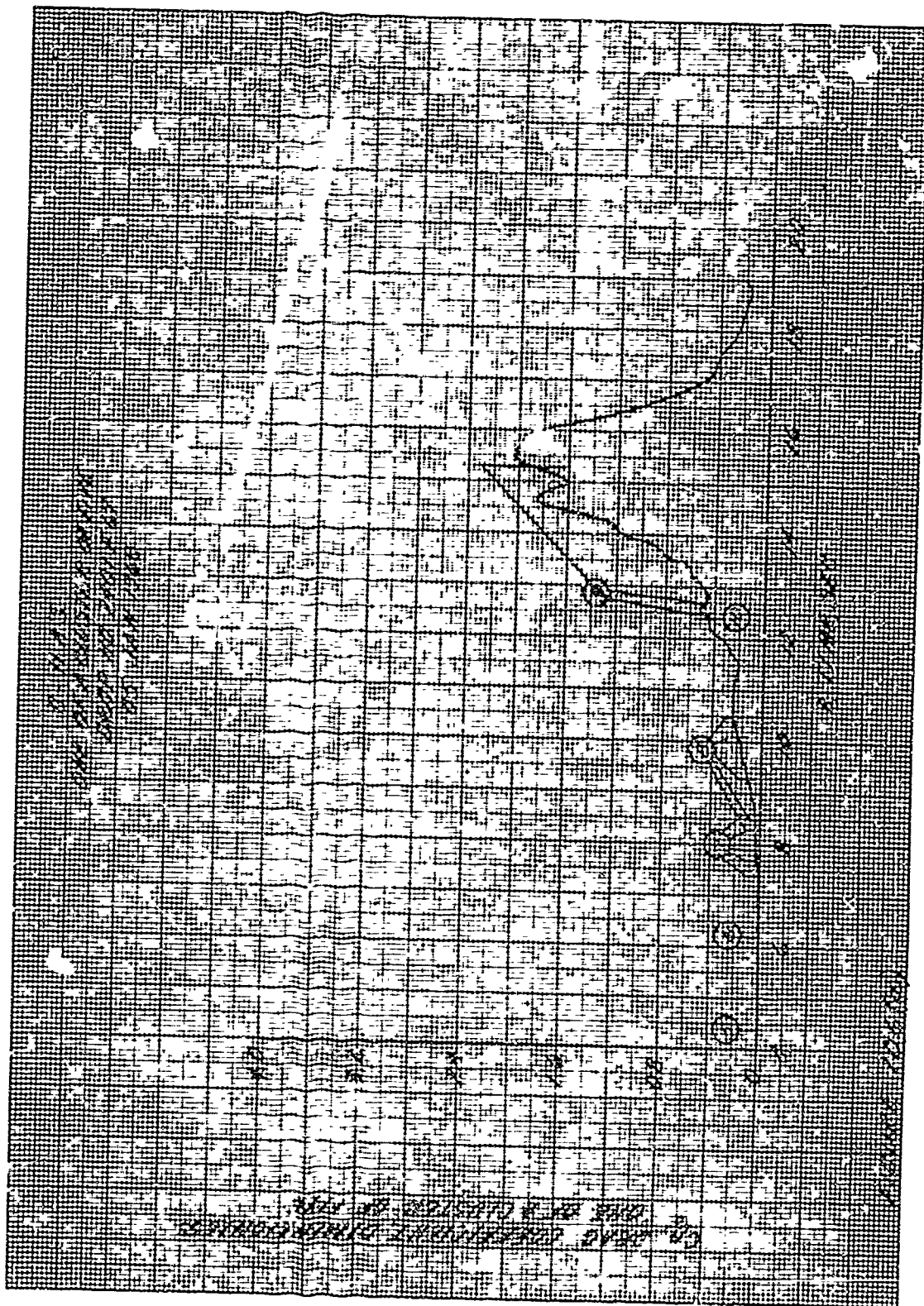


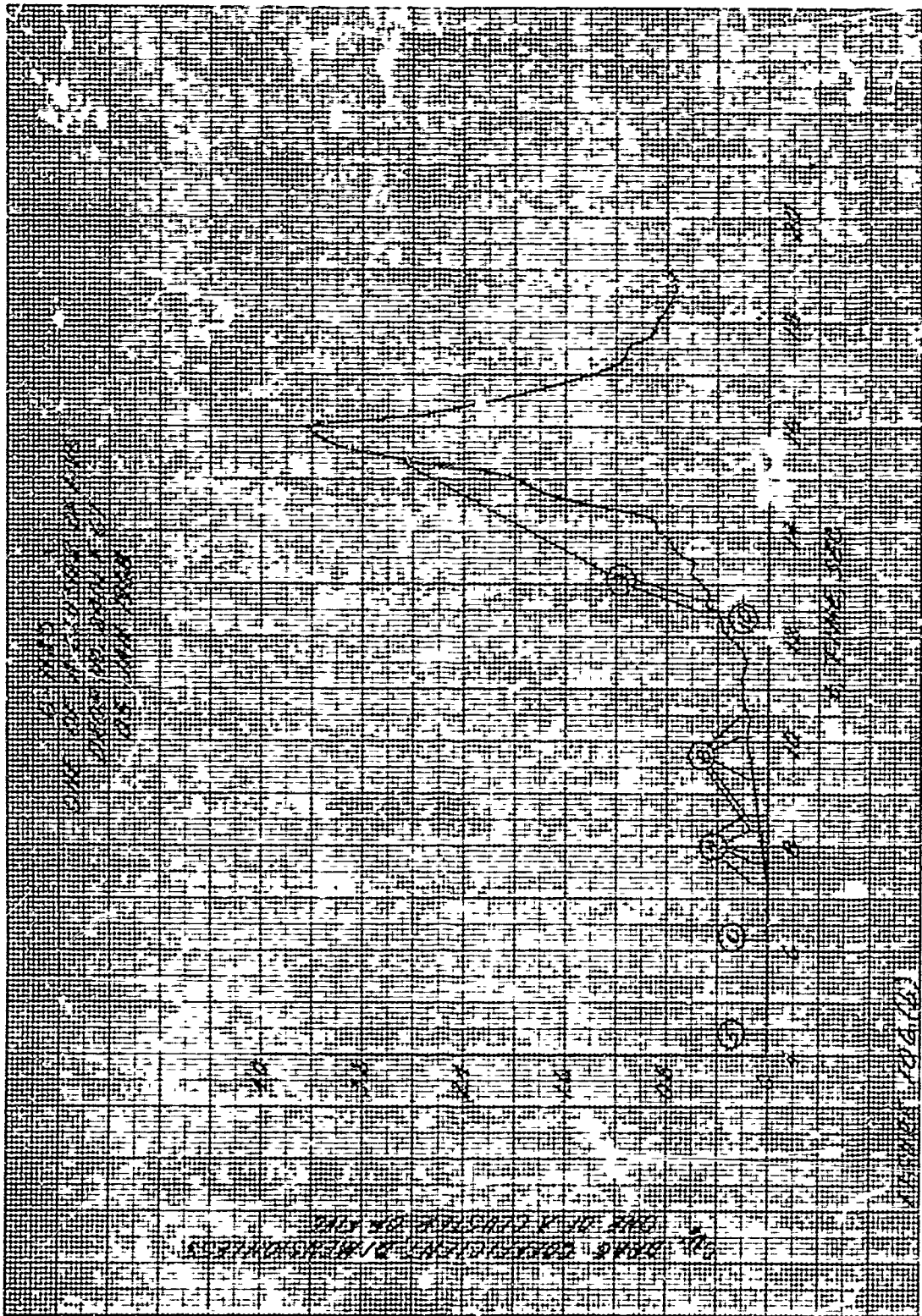


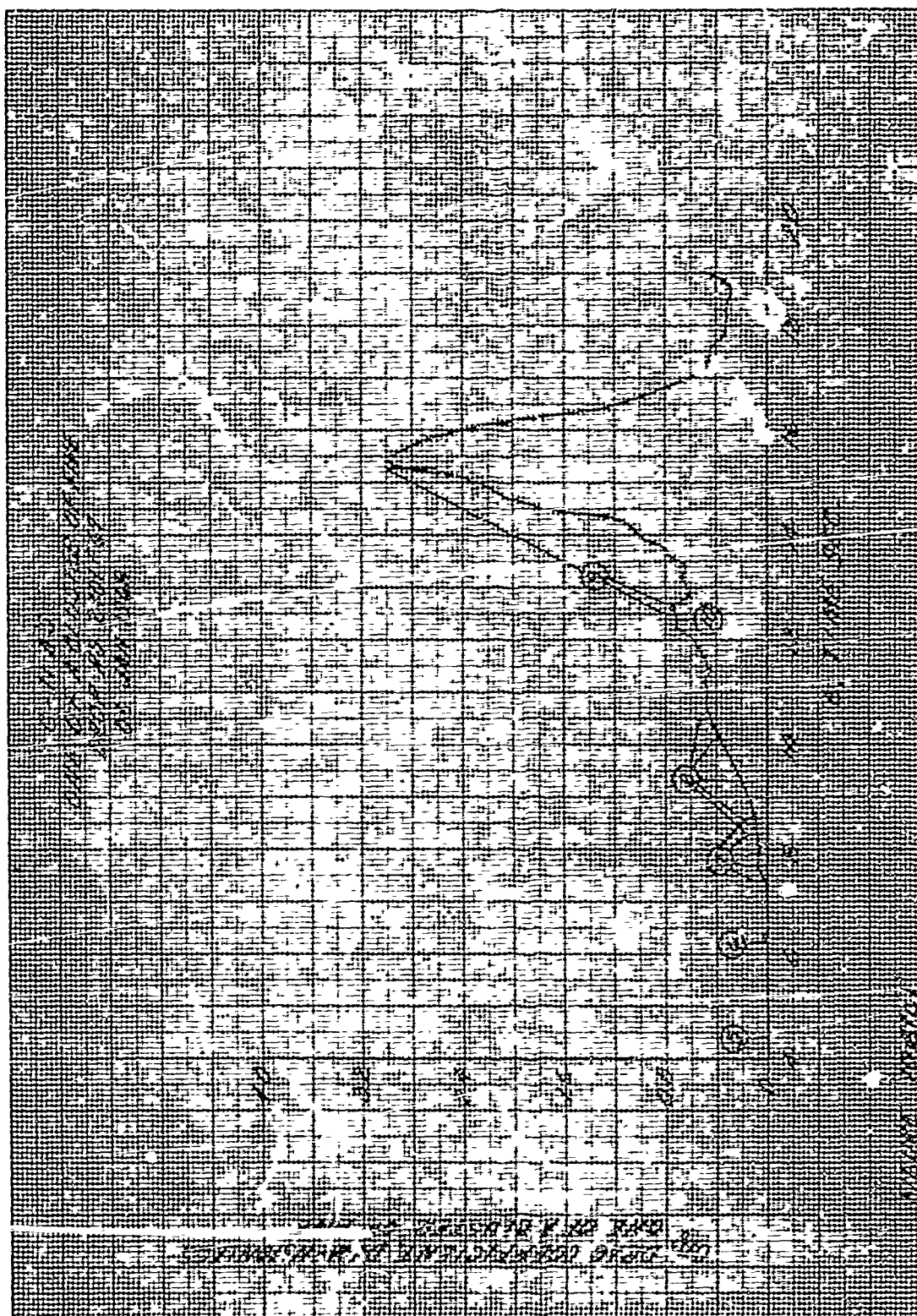


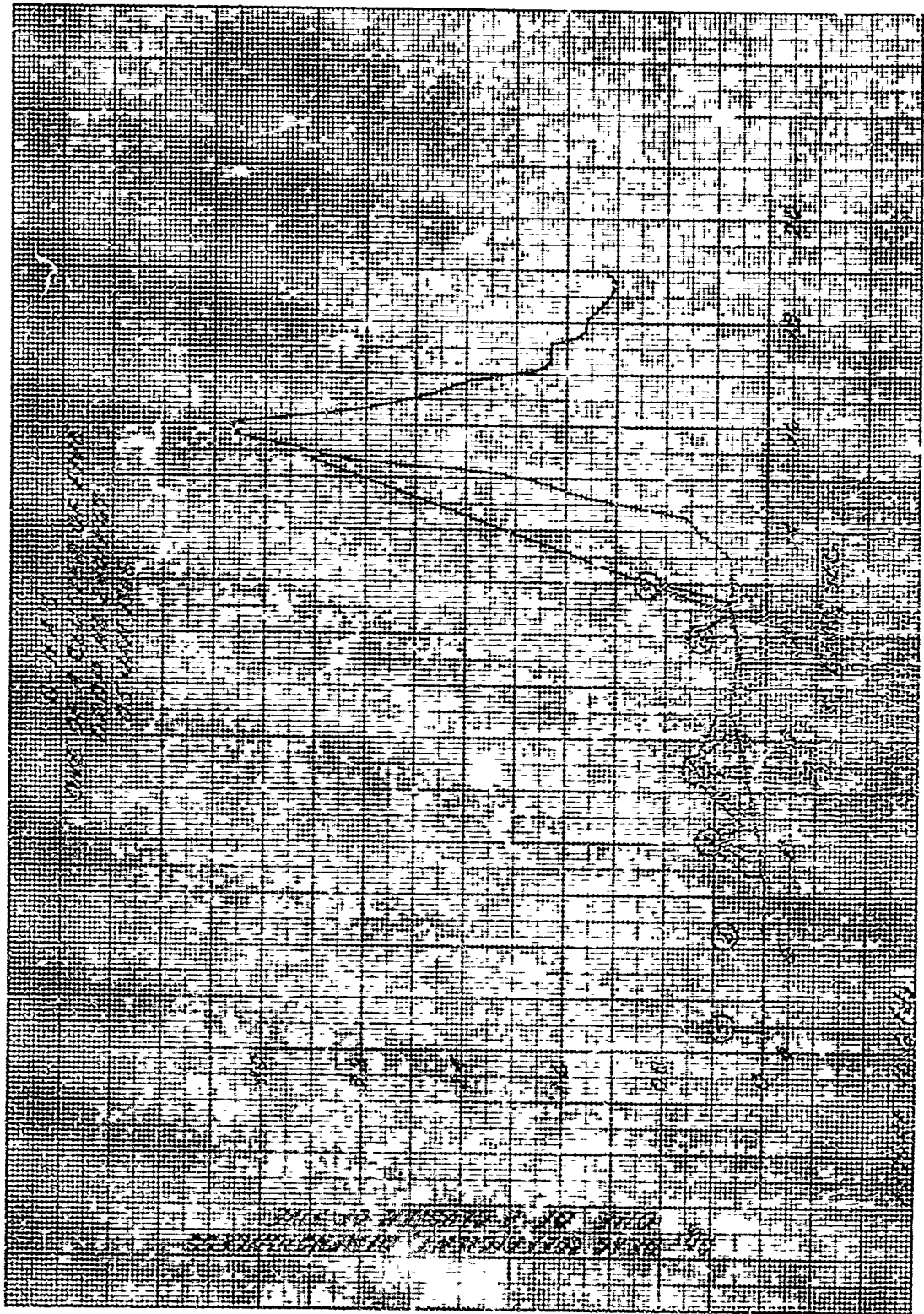


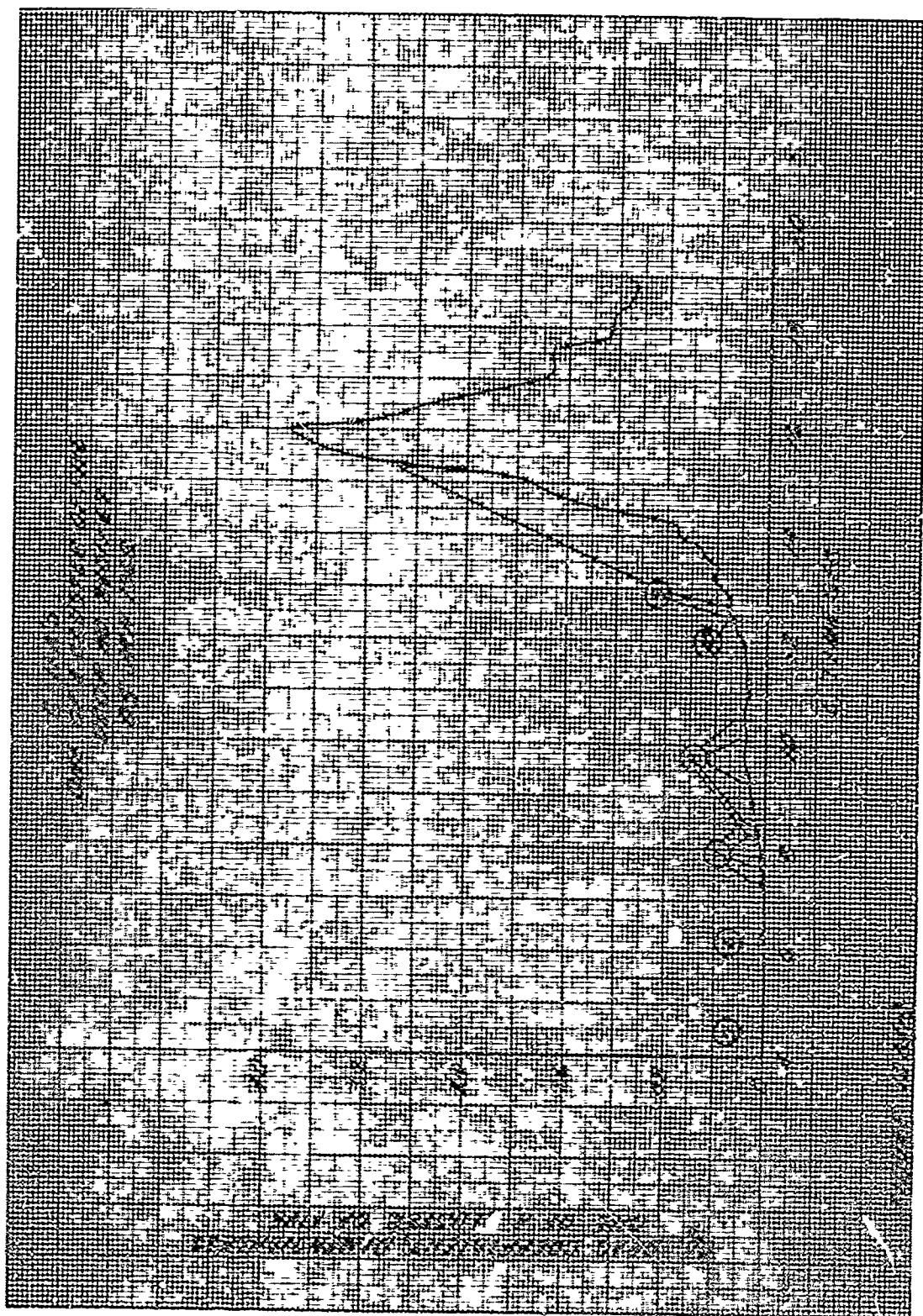


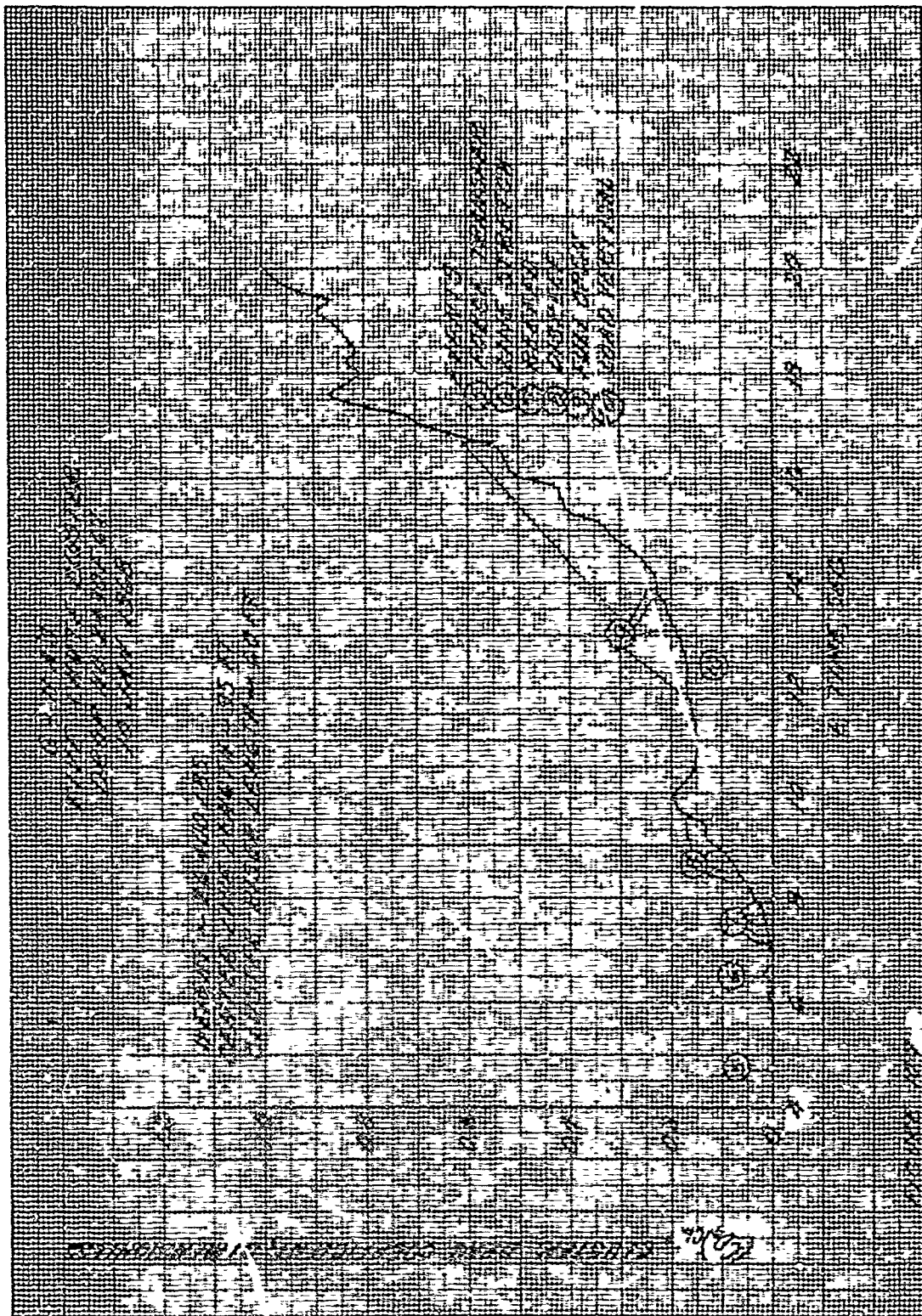


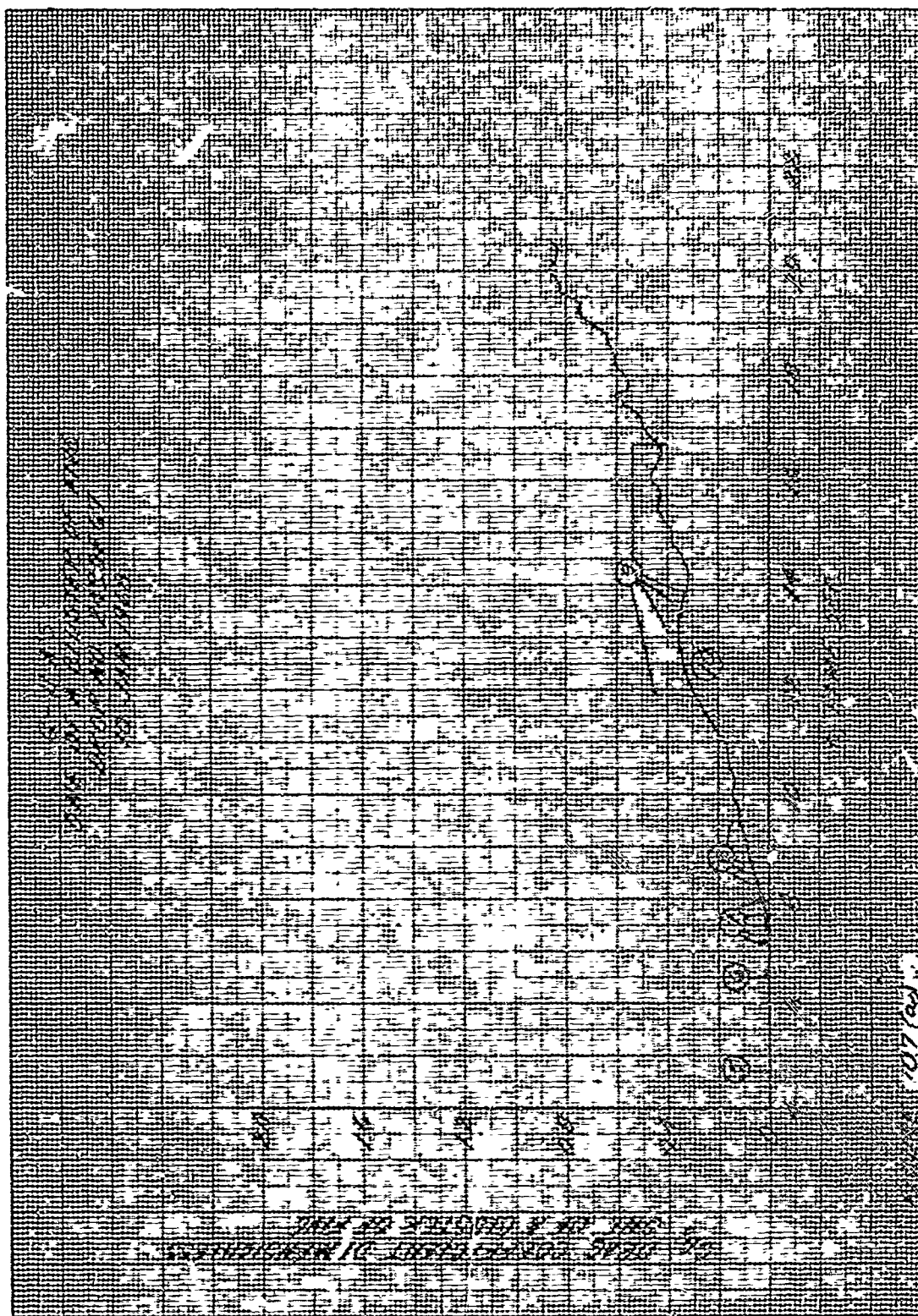




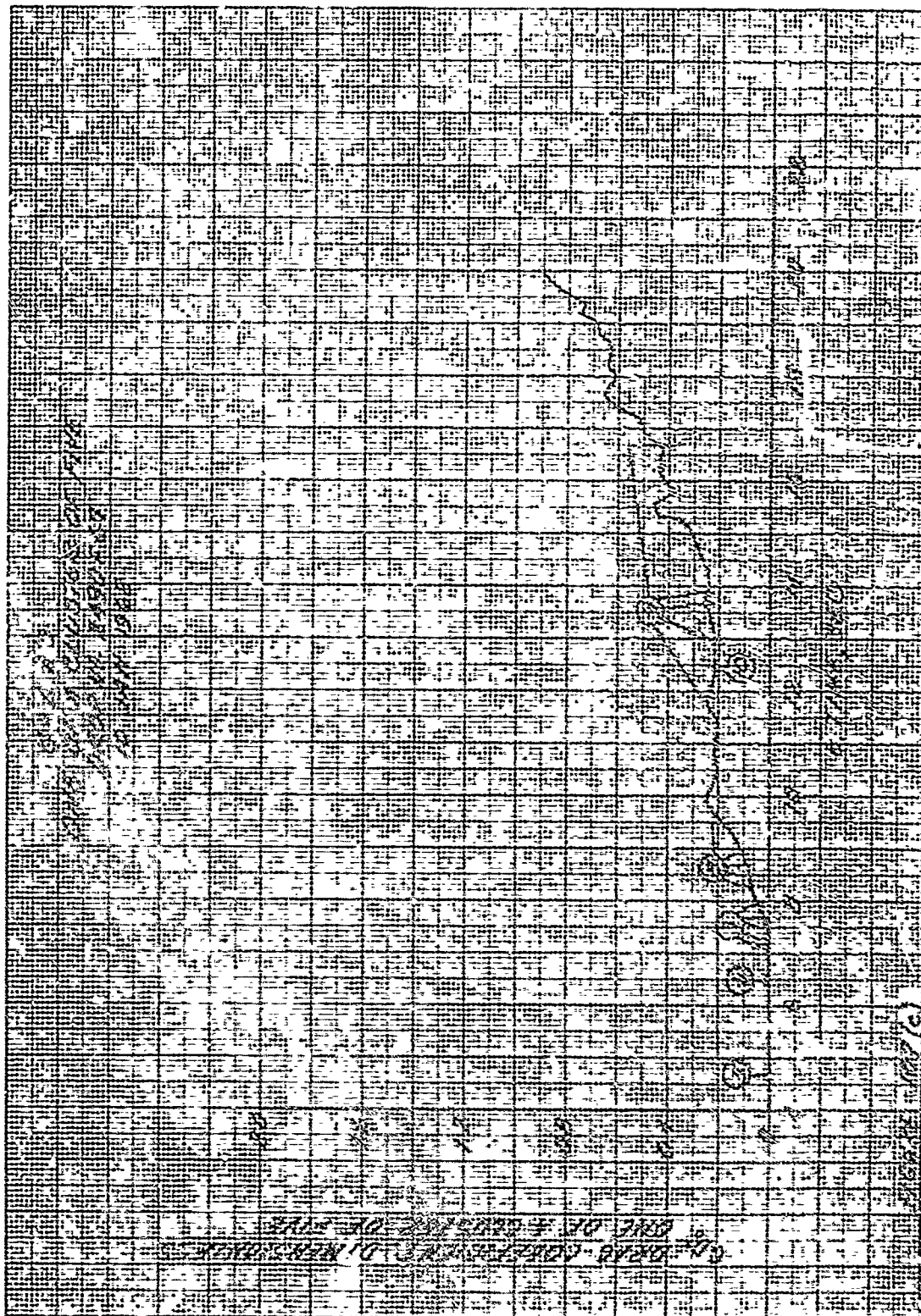


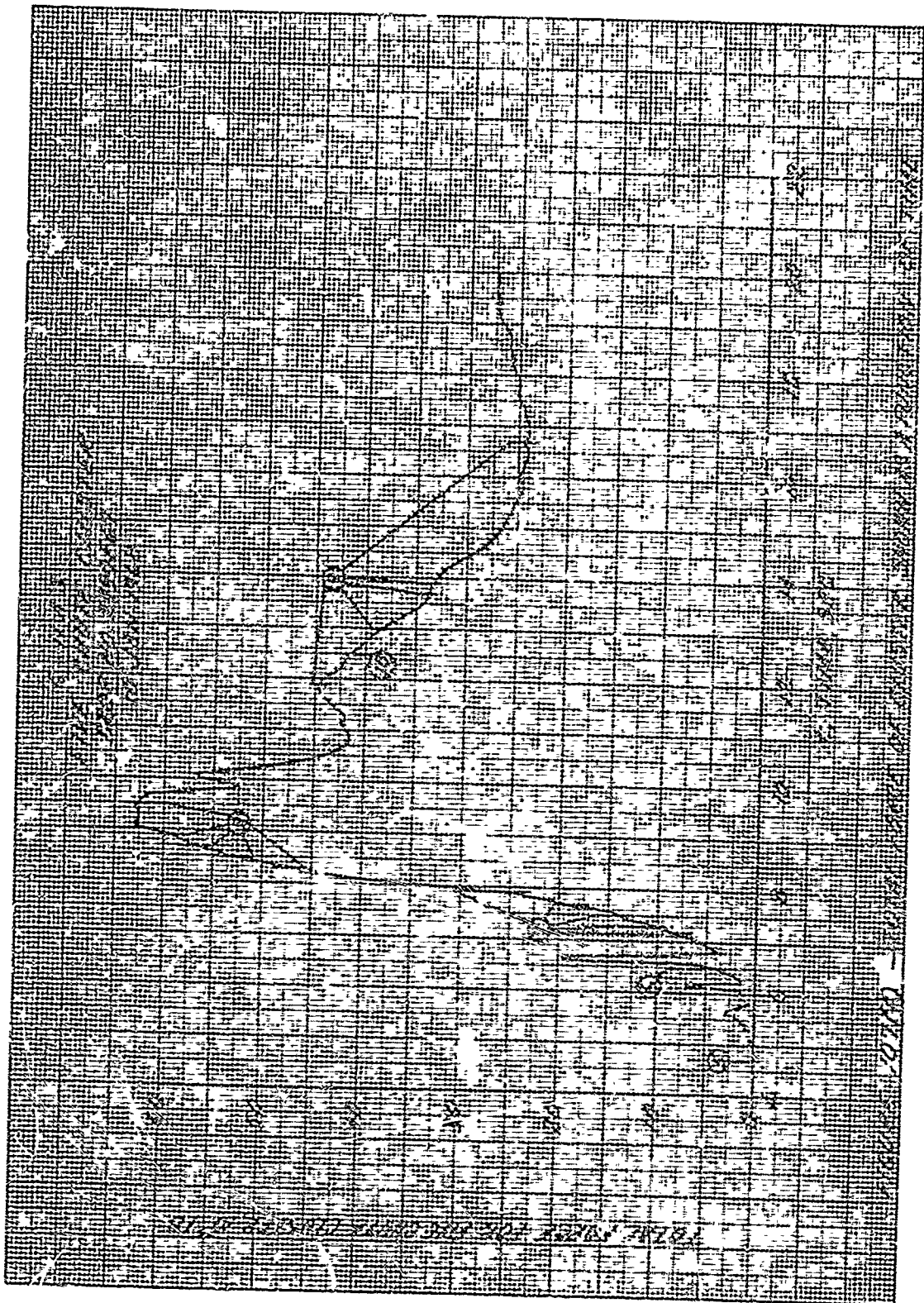


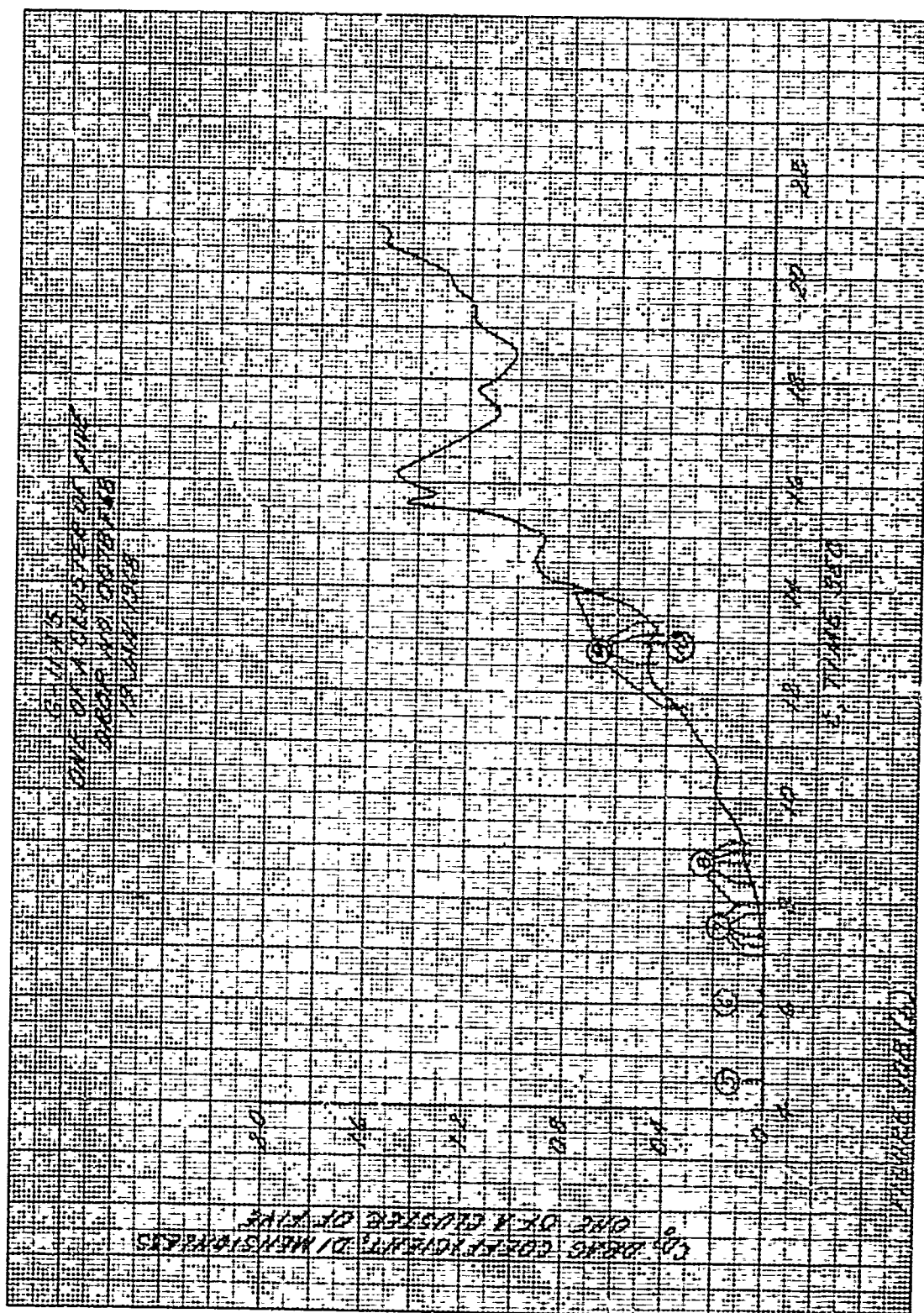


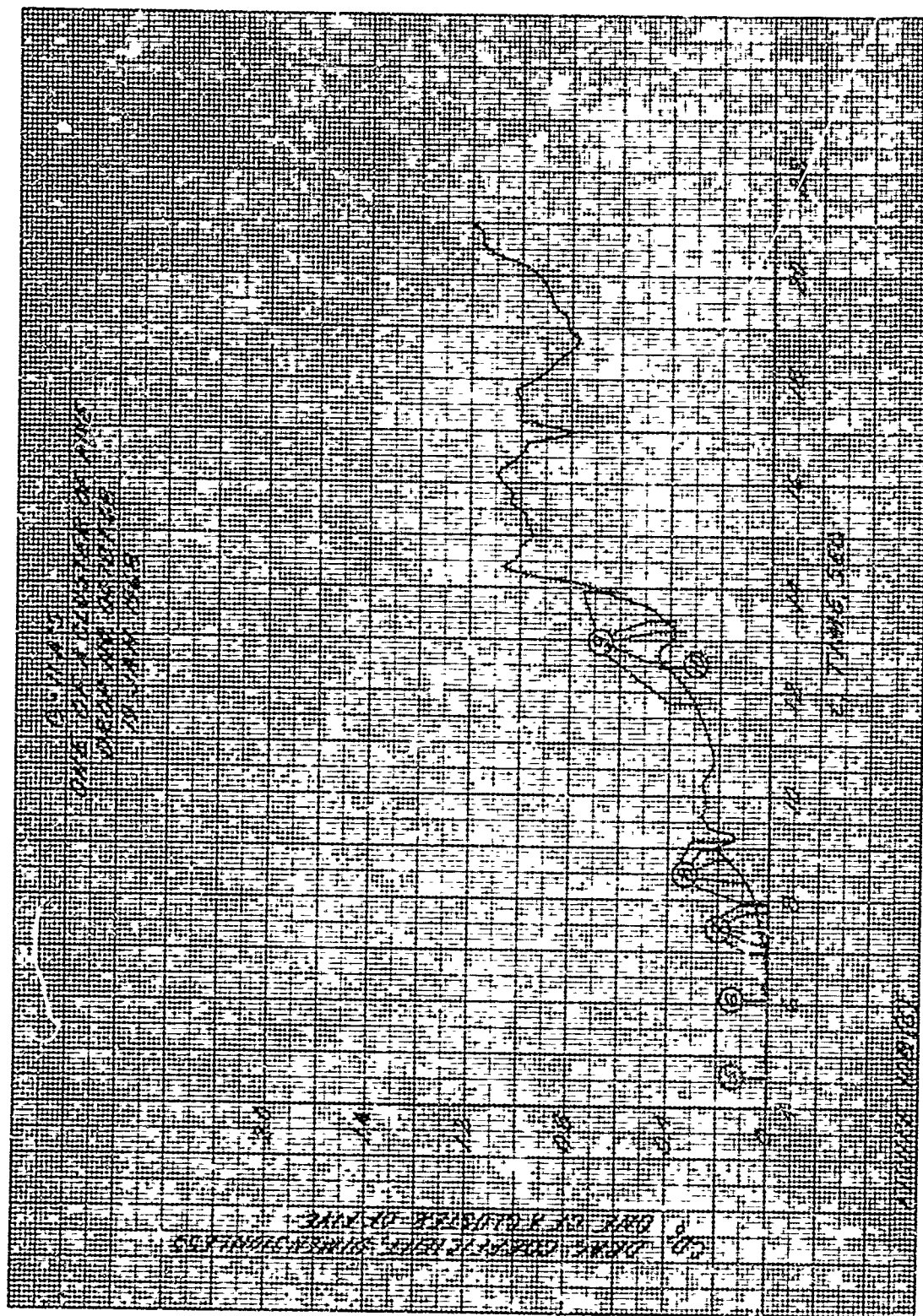


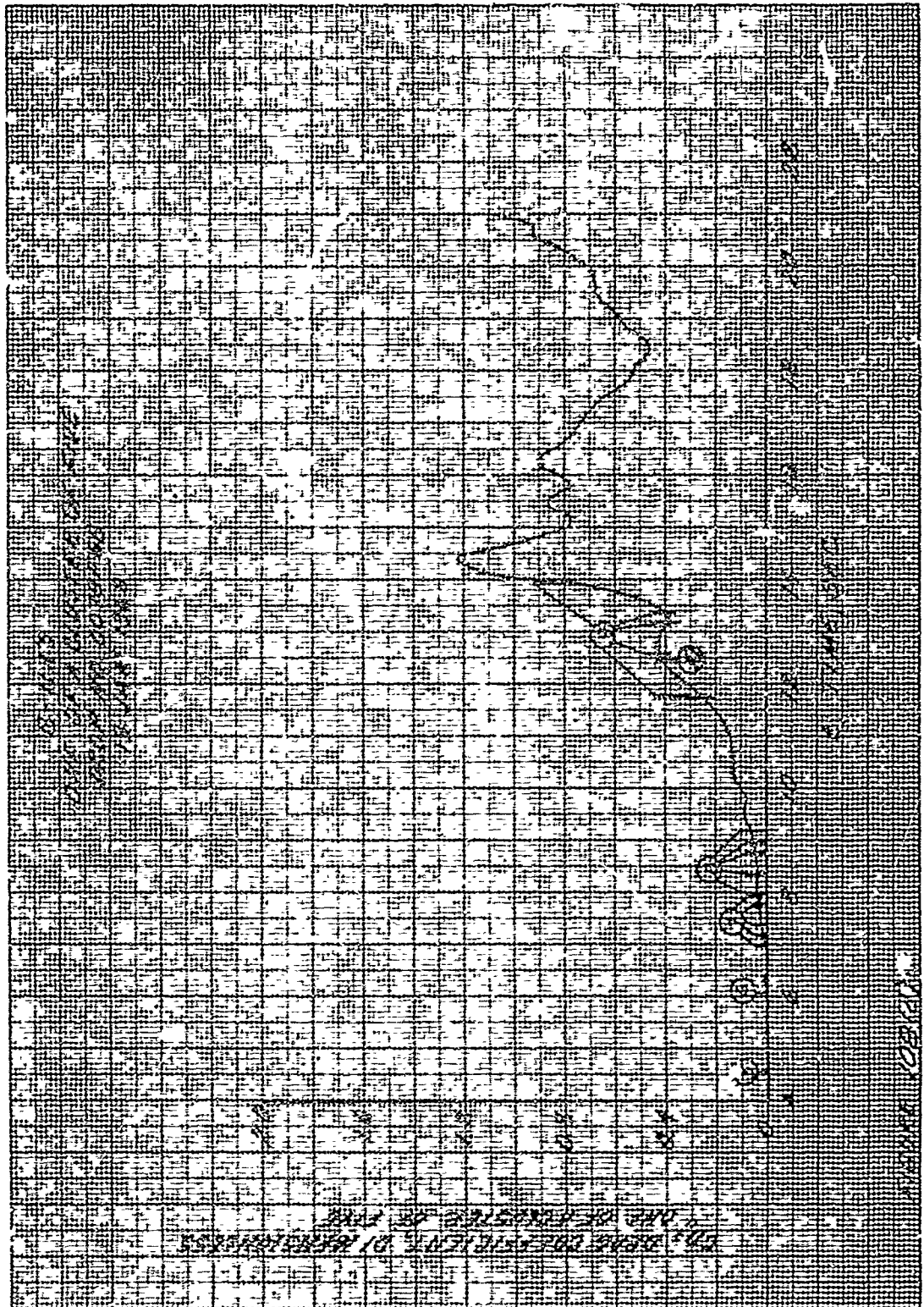


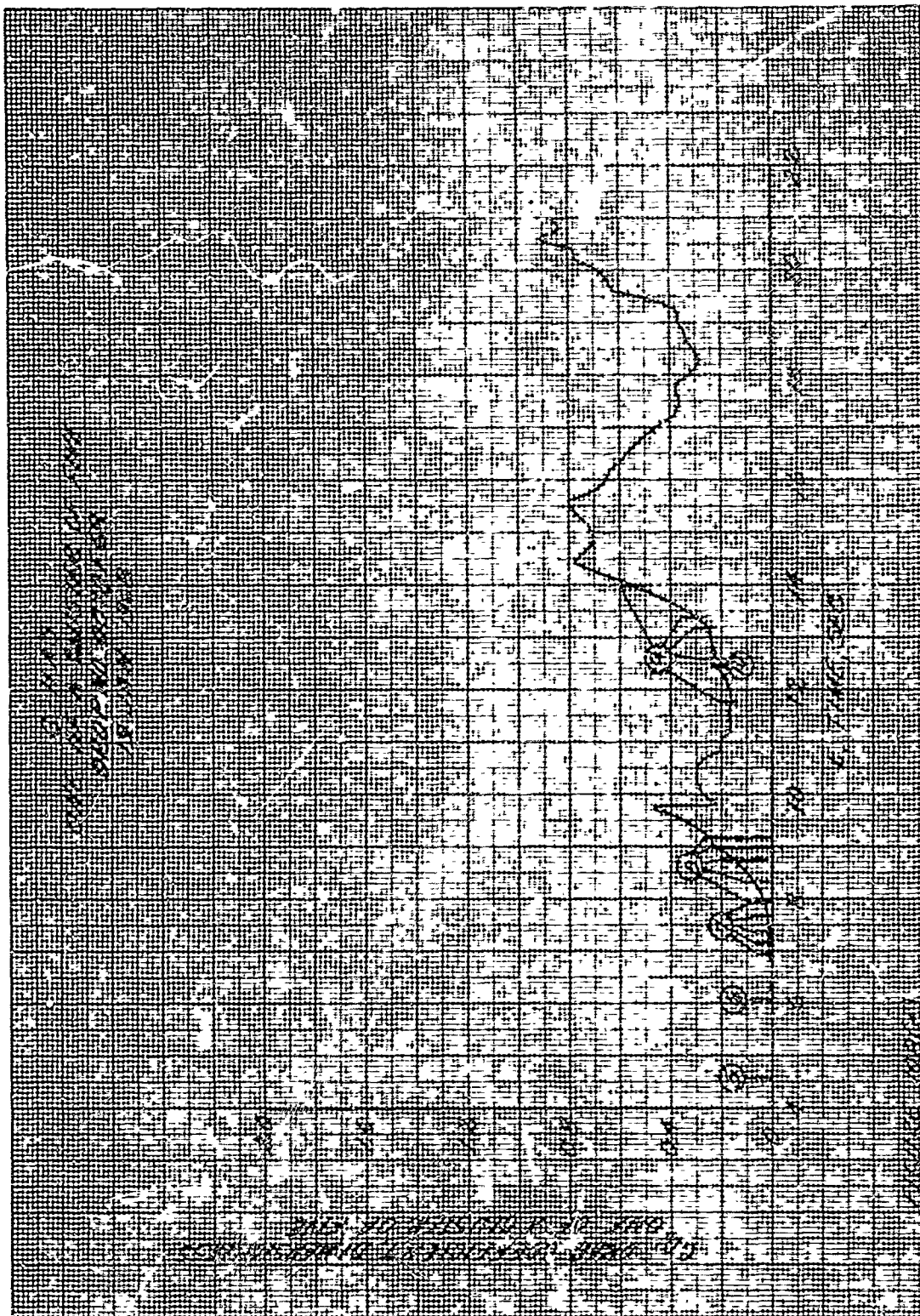














$$(C_{D_o})_{CL} = \frac{\sum_{i=1}^n (F/S_c)}{q}, \quad (10-2)$$

where the force F and the aerodynamic pressure q are known for any t .

Shown in Figs. 107 and 108 are the drag histories for two drops, each of a five-parachute cluster deployed at 130 KEAS. A comparison of these histories reveals them to be fairly consistent. Since the drop associated with Fig. 108 had the highest cluster load (Fig. 108f) its drag history was selected for use in determining the maximum loads imposed on the six-chute 135-ft-diam. cluster. Because there was no way to differentiate the drag histories of the five chutes, the drag of the cluster had to be used.

Figure 109 illustrates how this cluster drag was simplified by linearizing. The necessary zero reference time is chosen as the time at which the payload leaves the aircraft and is concurrent with event 5 as shown in Fig. 108. In this figure, the time difference between event 5 (force transfer) and line stretch is 1.5 sec. Hence, the cluster drag history can be replotted as that shown in Fig. 110.

b. Maximum Cluster Loads

With a drag history for the six-chute 135-ft-diam. cluster, it is now possible to determine the total force that this system experiences in its operational mode. The operational mode is defined by a deployment speed of 150 KEAS and a release altitude of 1500 ft above the terrain. The payload is defined by a gross rigged weight of 50,000 lb.

Five computer trajectory runs were made, one each for cutter delays of 2 through 6 sec. From studies of the El Centro drops contained within this report and from the results of Section 6, it is permissible to assume that the skirt exits the bag at about 1.4 sec after the payload leaves the aircraft. It is at this time that the cutter is actuated. In addition, it is permissible to assume that line stretch occurs at about 1.5 sec after the payload leaves the aircraft and that it takes approximately 1.8 sec after line stretch to reach the reefed state. Table 2 lists the cluster's drag history for the different cutter delays.

TABLE 2
CLUSTER DRAG COEFFICIENT AND RELATED DRAG AREA
USED IN COMPUTER TRAJECTORY RUNS FOR CLUSTER
COMPRISED OF SIX 135-ft-diam. PARACHUTES

Time, sec, from exit, for cutter delay of						$(C_{D_0})_{CL}$	$(C_{D_0} S_0)_{CL}$, ft ²	Event
2 sec	3 sec	4 sec	5 sec	6 sec				
1.5	1.5	1.5	1.5	1.5	1.5	0	0	Line stretch
3.3	3.3	3.3	3.3	3.3	3.3	0.03	2,675	Reef
3.4	4.4	5.4	6.4	7.4	7.4	0.03	2,675	Disreef
5.4	6.4	7.4	8.4	9.4	9.4	0.20	17,150	
7.3	8.3	9.3	10.3	11.3	11.3	0.20	17,150	
10.0	9.0	10.0	11.0	12.0	12.0	0.35	30,000	
11.1	10.1	11.1	12.1	13.1	13.1	0.35	30,000	
12.0	11.0	12.0	13.0	14.0	14.0	0.68	75,500	
12.6	11.6	12.6	13.6	14.6	14.6	0.76	65,200	
13.8	12.8	13.8	14.8	15.8	15.8	1.07	91,900	
14.2	13.2	14.2	15.2	16.2	16.2	0.75	64,400	
18.6	17.6	18.6	19.6	20.6	20.6	1.27	109,000	
30.3	29.3	30.1	31.3	32.3	32.3	0.85	74,000	
100.0	100.0	100.0	100.0	100.0	100.0	0.85	74,000	

*At 1.4 sec after exit, it is assumed that the canopy skirts leave the containing bags, initiating the cutters. At 1.8 sec after line stretch, or 3.3 sec after exit, it is assumed that the cluster has attained its reefed configuration.



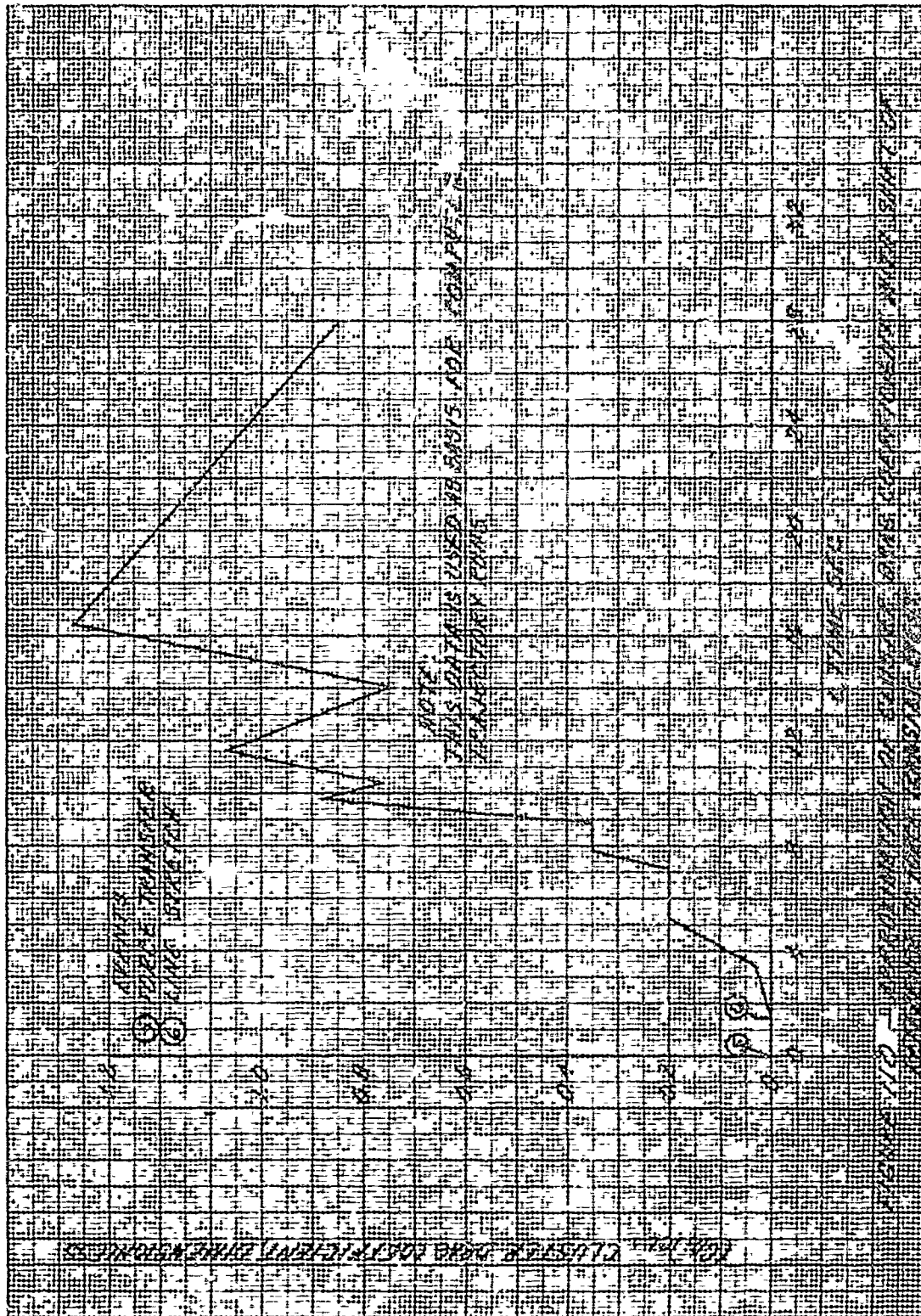


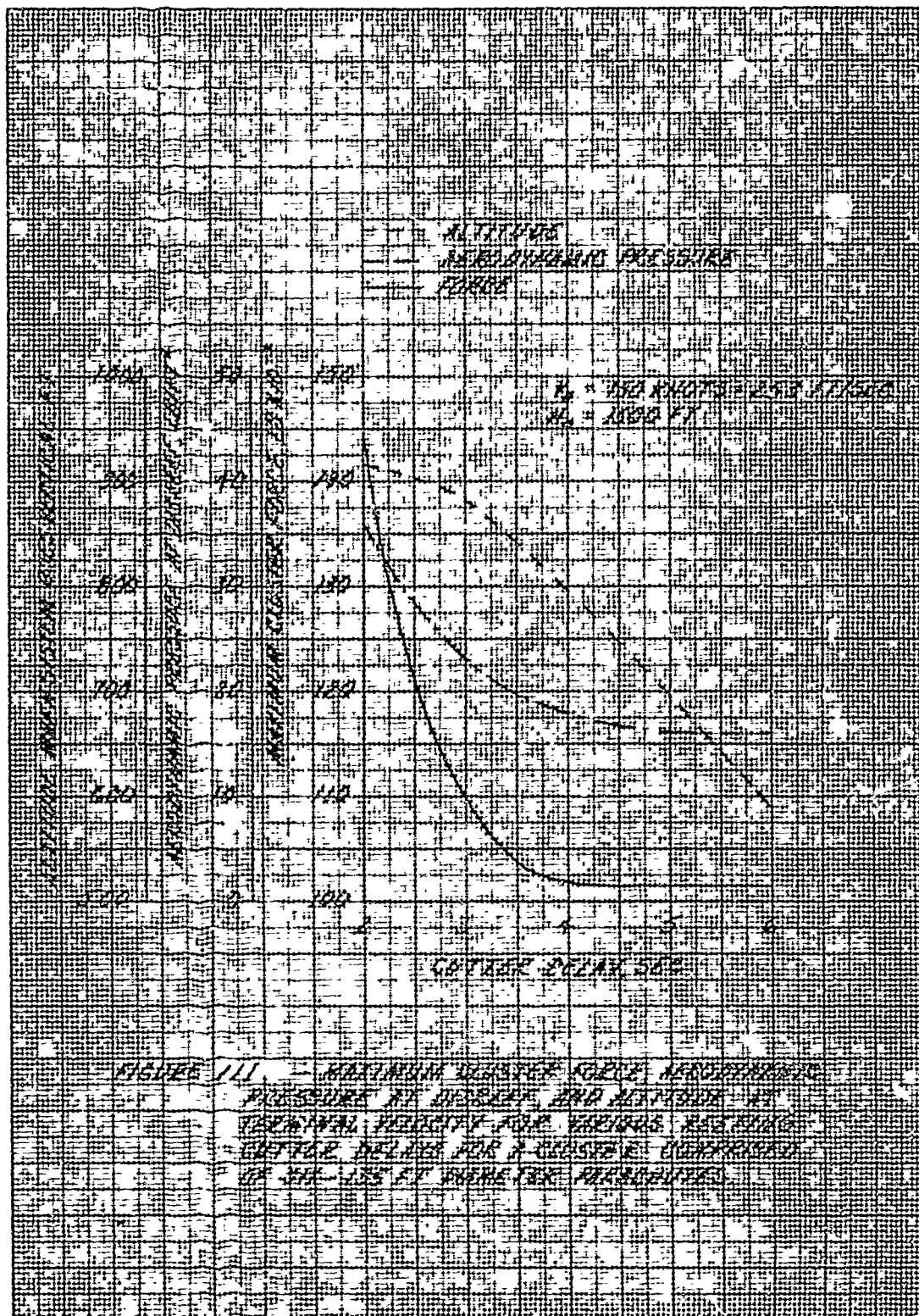
Figure 111 depicts the maximum forces experienced by the cluster for the various cutter delays. As can be seen, the maximum cluster load is associated with the 2-sec-delay cutter. This 144,000 lb exceeds the maximum allowable 2.5-g requirement, that is the maximum allowable 125,000 lb. For this reason, it is necessary to consider the 3-sec-delay cutter. The maximum force is reduced by 31%; and the altitude at which the cluster attains a perpendicular attitude to the horizon is very near that for the 2-sec cutter. Hence, for reasons both of force and of altitude, the 3-sec cutter appears desirable. It becomes necessary, however, to consider the selection of a cutter on the basis of how it can contribute to uniform inflation of the individual chutes comprising the cluster.

Classically, the cutter is used to reduce the loads imposed on a parachute during its opening. For large-diameter parachutes dropped singly, a brief cutter delay, such as 2 sec, contributes very little in this respect; however, it does tend to assist in making the opening more uniform. But for a cluster of large parachutes, the proper cutter delay can reduce the maximum cluster load, both for reef and disreef. During reefed inflation, the cutter enables the individual parachutes to catch up to one another and disreef at nearly the same time. This reduces the peak disreef force experienced by any one parachute. For this reason, it appears that a 4-sec cutter delay is the most desirable. Although the altitude at which the -90° path angle (first vertical) is attained is some 100 ft lower than that for either the 2- or 3-sec delay, the lower reefed force in the cluster and the potential for a lower maximum disreef force in the individual parachute are significant reasons to incur the altitude loss.

With regard to reefing ratio, available data are insufficient to incorporate the effects of reefing ratios into the computer trajectory runs. Since the drag-history data are based on full-scale drops utilizing reefing-line lengths of 19.1% of the G-11A reference circumference, it is logical to apply this ratio to the 135-ft-diam. parachute. Hence, all computer runs for the 135-ft-diam. parachute cluster were premised on use of an 80-ft reefing line.

c. Maximum Load Experienced by Any Single Parachute

Section b (of Section 10) dealt with arriving at the maximum cluster load. This section attempts to arrive at some idea as to the magnitude of the maximum load



experienced by any one chute comprising the cluster. This load will then provide the basis for the design of the six 135-ft-diam. parachutes so far as material strength is concerned.

Reference to Fig. 108(f) reveals that, for this particular full-scale drop, the maximum cluster load of 73,000 lb occurred at approximately 2.9 sec after line stretch (event 5). The force traces for this drop show the load to be distributed among the five parachutes as follows.

$$\begin{aligned}F_{1-5} &= 24,500 \text{ lb,} \\F_{2-5} &= 23,900 \text{ lb,} \\F_{3-5} &= 10,200 \text{ lb,} \\F_{4-5} &= 9,000 \text{ lb,} \\F_{5-5} &= 5,500 \text{ lb.}\end{aligned}\tag{10-3}$$

From the pattern of the load magnitudes, it appeared that two chutes led the opening process, two chutes lagged somewhat, and the fifth chute lagged even more.

The question now arises as to whether the maximum individual parachute load would be higher if only one chute led the inflation process. Reference to Fig. 107(f) reveals that, for this particular drop, the maximum cluster load experienced was 62,900 lb and occurred 2.5 sec after line stretch. This load was distributed among the five chutes as follows.

$$\begin{aligned}F_{1-5} &= 22,000 \text{ lb,} \\F_{2-5} &= 13,100 \text{ lb,} \\F_{3-5} &= 12,500 \text{ lb,} \\F_{4-5} &= 9,600 \text{ lb,} \\F_{5-5} &= 5,700 \text{ lb.}\end{aligned}\tag{10-4a} \tag{10-4b} \tag{10-4c} \tag{10-4d} \tag{10-4e}$$

From this pattern, it can be seen that one chute led the inflation process, two chutes lagged somewhat, and the remaining two lagged even more.

A comparison between the distributions of the maximum cluster loads in these two drops among their respective parachutes indicates that, regardless of whether one chute or two lead the inflation process, the maximum load experienced by any one chute will be of the order of 24,000 lb. This reasoning implies that, for any drop, it appears that at least two chutes will be opening approximately together. If these two chutes lead the inflation process, they share the major portion of the cluster load; if they are behind the lead chute, then together they share a portion of the cluster load approximating the load of the lead chute; finally, if the two chutes lag, then the major portion of the cluster load is distributed among the remaining three chutes, and in no way can it be expected that the load of any one of these three chutes will be greater than the above 24,500 lb.

If, for the drop that experienced a cluster load of 73,100 lb, it was assumed that the inflation of the five chutes was completely uniform, then the maximum load seen by any one chute would have been

$$F_{1-5} = \frac{73,100}{5} = 14,600 \text{ lb.} \quad (10-5)$$

This means then that, because of nonuniformity of inflation of the five chutes, the lead opening chute experienced a load 68% greater than if the opening had been completely uniform. It must be realized that this drop, utilizing only a 2-second-delay cutter, was for all practical purposes a no-cutter recovery system. Hence, nonuniformity in the inflation of the five chutes was at its worst.

In the system arrived at, that is the 135-ft-diam. six-chute cluster, a 4-sec-delay cutter was judiciously chosen on the basis of its effect in reducing the maximum cluster load. Reference to Fig. 112 reveals that the maximum cluster load is predicted to occur at or near the initial stages of the reefed configuration. Assuming that, prior to reef, the nonuniformity factor for cluster inflation is 1.68, then the maximum load felt by the lead opening chute during this stage of inflation is

$$F_{1-5} = \frac{1.68 \times 101,335}{6} = 28,300 \text{ lb.} \quad (10-6)$$

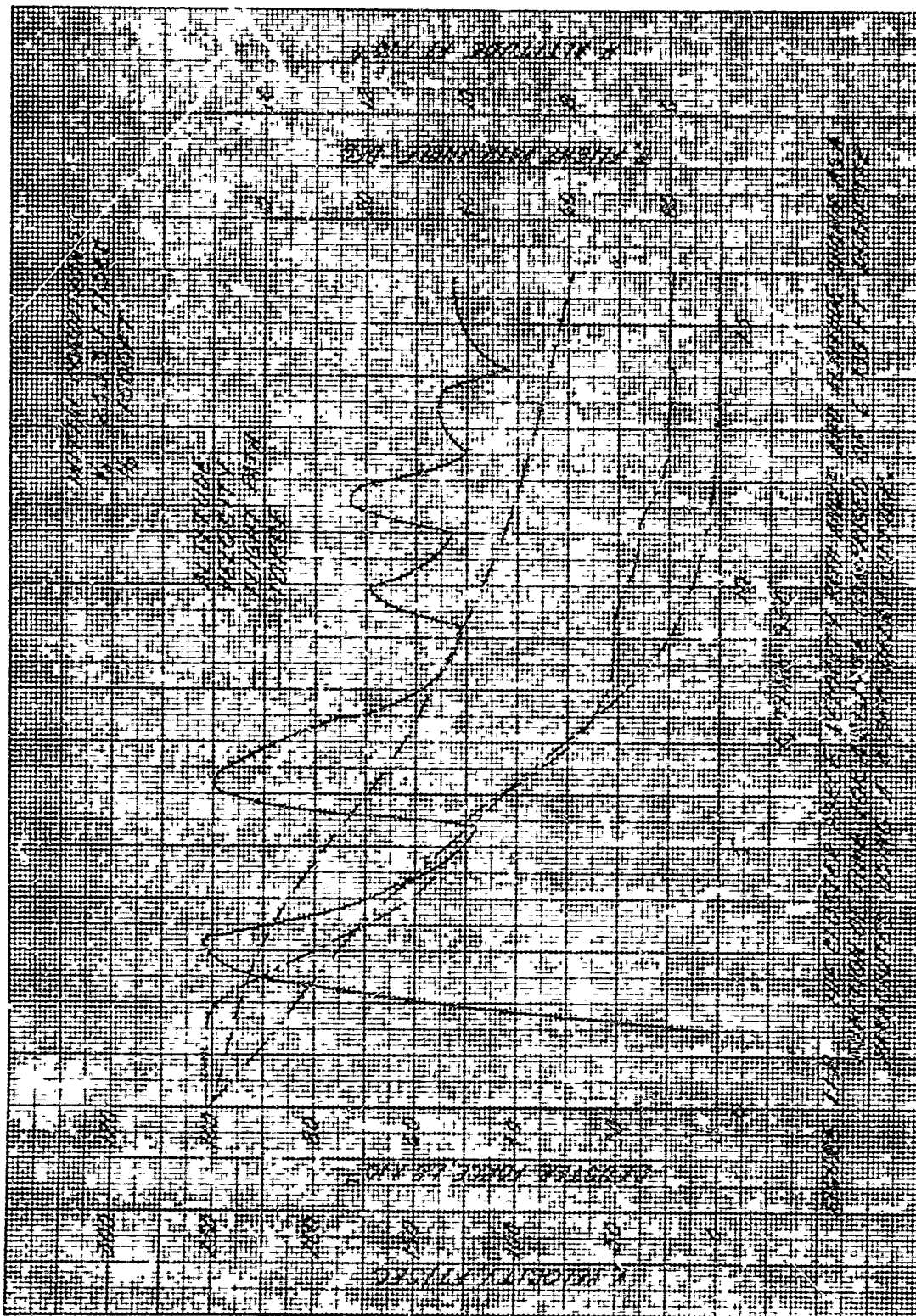


Figure 112 also reveals that the maximum disreef load is approximately the same as the reefed load. However, owing to the 4-sec cutter delay, it is felt that the nonuniformity of inflation after disreef will not be so severe as prior to reef.

d. Reliability with Regard to Maximum Rate of Descent

As was seen in Section 9, the requirement that the rate of descent not exceed 28.5 ft/sec under various conditions of altitude and temperature determined the effective drag area required of the cluster. The parachutes were sized on the basis of careful analysis of existing full-scale drop-test data concerning large-diameter, vent-pulldown, clustered parachutes and on the basis of a nominal descent rate of 24 ft/sec STP; this corresponds to a descent rate of 27.3 ft/sec at the worst-case condition of 5000 ft altitude and +100°F, which is still 1.2 ft/sec under the maximum allowable.

Extensive analysis of clustered parachute drops on the Project Apollo program indicated the standard deviation (σ) for the rate of descent during a given drop and over a series of drops at about 30 ft/sec is about 0.8 ft/sec (ref. 6). Analysis of the drops listed in Table 1 shows that, for these drops, the standard deviation of the average rates of descent varied from more than 1.0 ft/sec for drops of single chutes to about 0.63 ft/sec for clusters of five. This latter information is illustrated in Fig. 28, where it can be seen that, for a six-chute cluster, the deviation in rate of descent is projected to 0.63 ft/sec. Hence, the 1.2-ft/sec design margin indicated in the previous paragraph corresponds to the 1.9σ -value; this means that the impact velocity would be expected to exceed maximum in only one drop out of 19 under worst-case conditions. Therefore, the reliability for worst-case operations (such operations are rarely likely to occur) is approximately 95%.

11. PRELIMINARY DESIGN

The purpose of the preliminary design is to establish an order-of-magnitude strength requirement for the material that is to be selected for use in the parachute assembly. It must be pointed out that the establishment of parachute theory is extremely difficult owing to the very nature of the structure. It is a flexible device, constructed from a fabric, and operates in a highly dynamic mode. So far as stress analysis is concerned, it is not necessary for Pioneer to attempt to conduct a high-order analytical study. Rather,

some basic assumptions are used that, when coupled with experience and intuition, lead to "ball-park" results.

a. Maximum Canopy Stress for a Vent-pulldown Parachute

Use of the vent pulldown leads to opening-shape characteristics somewhat deviate from those normally associated with the standard parachute. This is indicated in a study of movie film depicting deployments of single and clustered G-11A vent pulldowns from an above-terrain altitude of 1500 ft and a release velocity of 150 knots. The general opening shape for all the canopies in these drops is depicted in Fig. 113. This shape is most definitive at or just following full reef, the point at which the parachute loads are at a maximum.

Figure 113 shows that, at full reef, the canopy exhibits prominent domes ("false vents"). The true vent is, of course, pulled down to the skirt area. Hence there is no physical means for the canopy to bleed off pressure. This accounts for the relatively quick opening and resulting high loads associated with the vent-pulldown parachute.

(1) G-11A Cargo Parachute

The G-11A cargo parachute under study herein has a reefing ratio of 20%; that is $D_R = 0.2D_0$. This then implies that, at reefed state, the parachute diameter is 20 ft. Figure 114 shows the results of scaling from the frames of the previously mentioned movie film. As can be observed, the scaling was reasonably accurate. Hence, from this figure it can be established that the high-pressure area of the canopy is located approximately 40 ft from the skirt of the canopy. Figure 115(a) shows that the width of any individual gore at this location is simply

$$2 \times \frac{10}{50} \times \frac{32.5}{2} = 6.5 \text{ in.} \quad (11-1)$$

Since the canopy has 120 gores, this means that, at the location of the high-pressure areas, the circumference can be calculated to be

$$120 \times 6.5 = 780 \text{ in.} = 65 \text{ ft.} \quad (11-2)$$

From scaling the film, it was determined that the false vents lie on a circumference of a circle whose diameter is approximately 18 ft [see Fig. 115(b)]. Hence, the circumference is

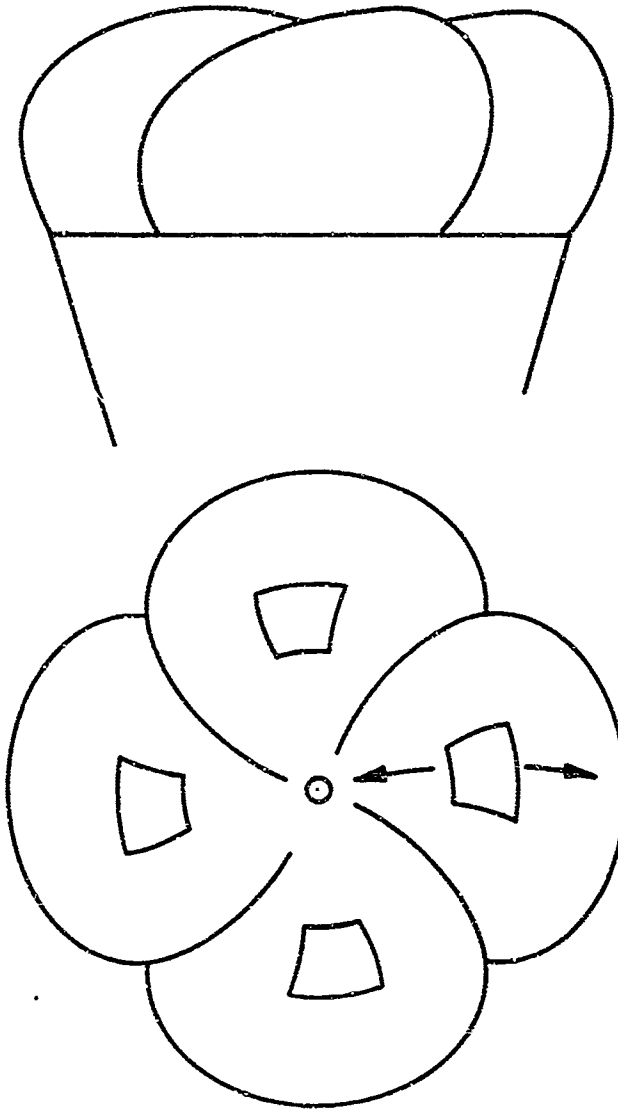


FIGURE 113 - GENERAL SHAPE CHARACTERISTICS ASSOCIATED WITH THE OPENING OF THE G-11A VENT-PULLDOWN PARACHUTE.

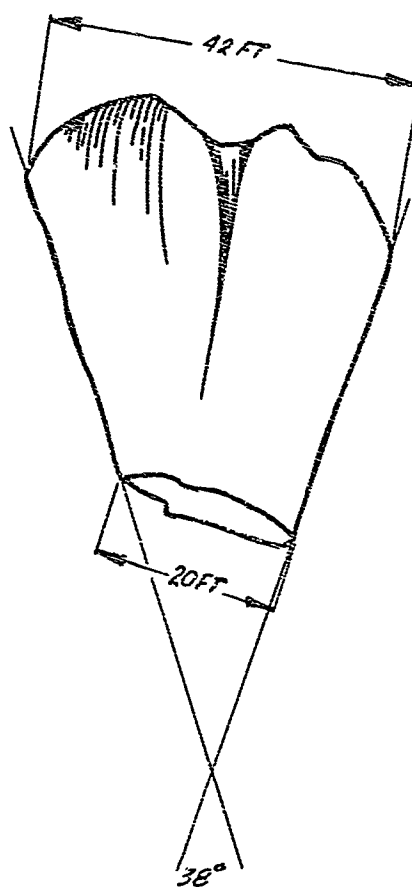
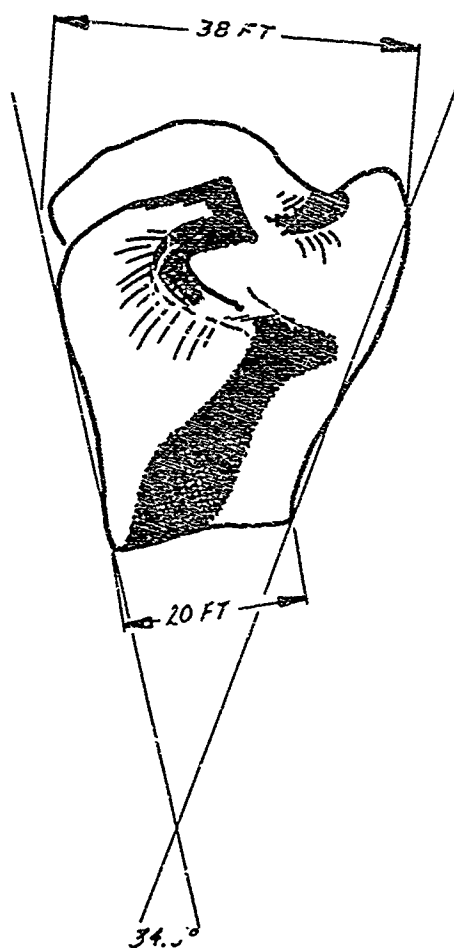


FIGURE 114 - DIMENSIONS SCALED FROM MOVIE FILM
DEPICTING OPENING OF THE G-11A
VENT-PULLDOWN PARACHUTE

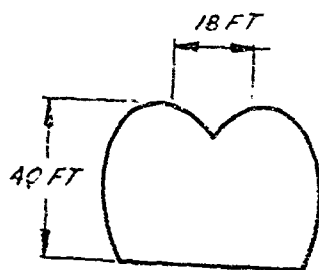
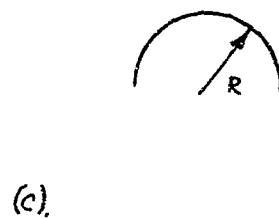
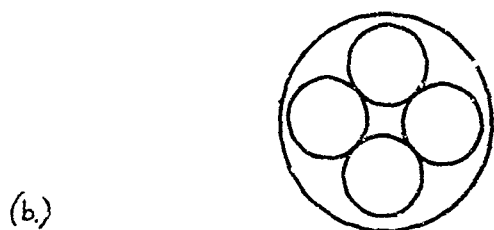
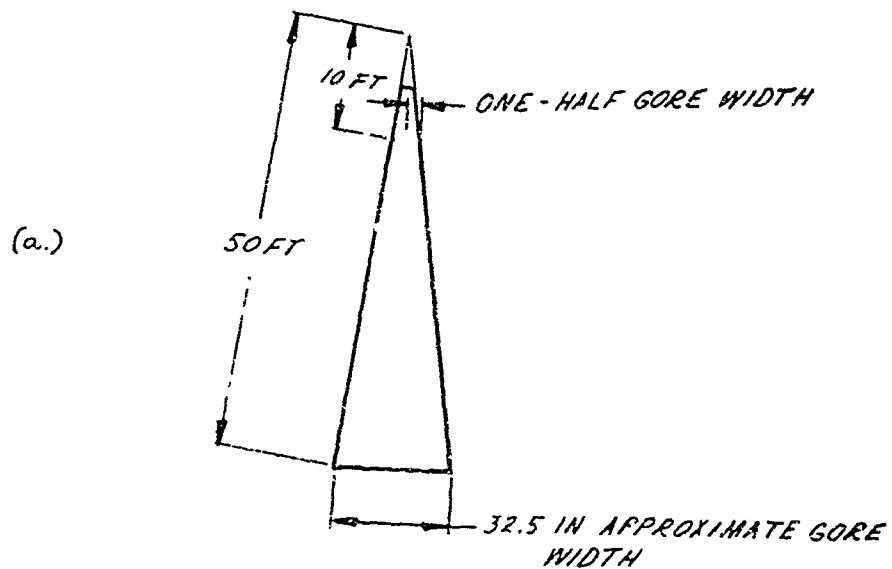


FIGURE 115 - APPROXIMATE DIMENSIONS OF SHAPE ASSOCIATED WITH THE OPENING OF A G-11A VENT-PULLDOWN PARACHUTE.

$$18\pi \approx 56 \text{ ft.}$$

(11-3)

The difference between the above two circumferences is 9 ft. This means that, at the reefed state, there is some 9 ft of fullness, or, for the case of four "false vents," 2.25 ft per false vent. This amounts to some four gores per high-pressure area that have not yet unfolded.

The stress in the canopy is now determined by assuming that each of the high-pressure areas lies on the dome of a hemisphere of 18 ft diameter. Viewed this way, the maximum stress simply becomes the hoop stress; hence,

$$qR = 30 \times 9 = 270 \text{ lb/ft} = 22.4 \text{ lb/in.}, \quad (11-4)$$

where q is the aerodynamic pressure, which El Centro drop-test data reveal to be approximately 30 lb/ft^2 at attainment of full reef.

Figure 81 shows that the strength of 1.6-oz cloth (used for the G-11A canopy) is approximately 70 lb/in. ; however, use of a 1-in. main seam with the canopy gores sewn on the bias increases this strength to approximately 106 lb/in. [refer to P-3171 (revised Feb. 1968), Appendix A, p. 3--Pioneer's response to Natick's RFQ DAA G17-68-Q-0113-011]. The ultimate margin of safety for the maximum canopy stress (accounting for a safety factor of 2.0 and a design factor of 1.5) is

$$\frac{106}{22.5 \times 2.0 \times 1.5} - 1 = +0.57. \quad (11-5)$$

It can be concluded that the above approach to the maximum canopy stress present in the deployment of a vent-pulldown parachute is conservative because, in practice, the main seams carry a significant portion of the parachute load and consequently cut into the smooth hemisphere. From Fig. 115(c) it becomes obvious that, since $R_g < R$, the product of q and R is reduced.

(2) Prototype Parachute Assembly ($D_0 = 135 \text{ ft}$)

For a cluster of six 135-ft-diam. vent-pulldown parachutes, it must be assumed that the high-pressure areas each lie on the dome of a hemisphere of diameter equal to

$$0.18 \times 135 = 24.3 \text{ ft.} \quad (11-6)$$

The aerodynamic pressure at the time of maximum cluster load (at or following attainment of full reef) is approximately 35 lb/ft² (arrived at through trajectory study). Hence the maximum canopy stress is

$$qR = 35 \times 12.15 = 425 \text{ lb/ft} = 35.4 \text{ lb/in.} \quad (11-7)$$

To apply the safety factor of 2.0 and the design factor of 1.5 means that the required strength of the canopy is

$$35.4 \times 2.0 \times 1.5 = 106 \text{ lb/in.} \quad (11-8)$$

b. Selection of Material for the Prototype Parachute Assembly ($D_0 = 135 \text{ ft}$)

(1) Canopy

The canopy material, on the basis of the above calculations, must be 1.6-oz cloth. Use of a 1-in. main seam with the canopy gores sewn on the bias is necessary. Hence, the ultimate margin of safety for the maximum canopy stress (accounting for a safety factor of 2.0 and a design factor of 1.5) becomes

$$\frac{106}{106} - 1 = 0.0. \quad (11-9)$$

Figure 80 shows that, for a 1.6-oz cloth using a 1-in. main seam, the weight of the canopy of a 135-ft-diam. parachute can vary from 165 to 180 lb, depending on the number of gores used in the canopy. The G-11A, a 100-ft-diam. parachute, uses 120 gores, therefore its D_0/N is 0.83. Applying this ratio to the 135-ft-diam. parachute results in a maximum canopy weight. On the other hand, a minimum canopy weight is associated with a D_0/N of 1.18; however, this means that the suspension-line strength requirement will be increased considerably. Hence, for the 135-ft-diam. parachute, it appears that a ratio of $D_0/N = 1.0$ is the most efficient from the point of view of canopy weight and suspension-line strength. This means that the 135-ft-diam. prototype parachute will have 136 gores.

(2) Suspension Lines

Equation (10-6) yields 28,300 lb as the maximum load expected to be experienced by any one parachute assembly in a cluster of six. Reference 8, p. 378,

expresses the strength requirement for each suspension line in a parachute as

$$\text{strength} = \frac{Fjc}{Zueok}, \quad (11-10)$$

where F and Z are the maximum force and number of suspension lines, respectively. The terms j, c, u, o, e, and k are all factors to account for safety and design. They are defined in Section 2.

From Eq. (11-10) the suspension-line strength requirement is found to be

$$\frac{28,300 \times 2.0 \times 1.055}{136 \times 0.8 \times 0.95 \times 0.35 \times 0.95} = 640 \text{ lb.} \quad (11-11)$$

Figures 82 through 84 show that Pioneer Spec. EI-4137 is the most efficient suspension-line material. Figure 84 shows its cost to be about 80% that of MIL-C-5040, Ty. III. Hence, the ultimate margin of safety, accounting for the above safety and design factors, becomes

$$\frac{650}{640} - 1 = +0.02. \quad (11-12)$$

Using 136 suspension lines means that the 135-ft-diam. prototype parachute assembly will have to have 14 groups of suspension lines. There will be 10 suspension lines in each of all but four groups, spaced 90° apart, which will have nine suspension lines.

(3) Riser, Riser Extension, and Center Line

Since there are, at most, 10 suspension lines per group, the strength requirement for the riser becomes

$$640 \times 10 = 6400 \text{ lb.} \quad (11-13)$$

Figures 85 and 86 show that MIL-W-27657, Ty. III, is the most efficient selection. The ultimate margin of safety, accounting for a safety factor of 2.0 and a design factor of 1.5, is calculated to be

$$\frac{6500}{6400} - 1 = +0.02. \quad (11-14)$$

Since there are 136 suspension lines and the strength requirement for each is 640 lb, the strength requirement for the riser extension becomes

$$640 \times 136 = 87,000 \text{ lb.} \quad (11-15)$$

Figure 91 shows 4-ply webbing of Phoenix WN 1811 to be sufficient. The ultimate margin of safety, accounting for the usual safety and design factors, becomes

$$\frac{87,000}{87,000} - 1 = 0.0. \quad (11-16)$$

From the results of El Centro drop tests, it has been ascertained that the center line experiences a maximum load approximately 40% of that of the parachute maximum load. On this basis, the center-line strength requirement, accounting for a safety factor of 2.0 and a design factor of 1.5, becomes

$$28,300 \times 0.40 \times 2.0 \times 1.5 = 31,600 \text{ lb.} \quad (11-17)$$

Figures 88 and 89 show Pioneer Spec. EI-4148 webbing, when used in the double ply, to be the most efficient. The ultimate margin of safety, accounting for safety and design factors, is

$$\frac{31,600}{31,600} - 1 = 0.0. \quad (11-18)$$

c. Consideration of Center Line as Primary Load-carrying Member

There is one point in the preliminary design that has not been made; that is, if the center line experiences 40% of the maximum individual parachute load, then the suspension lines experience only 60% of this load. Equation (11-11), when the maximum force is now 17,000 lb, shows the suspension-line strength requirement to be 384 lb. Figures 82 through 85 show Pioneer Spec. EI-4151 to be the most efficient selection for the suspension line. The ultimate margin of safety for this selection is

$$\frac{460}{384} - 1 = +0.20. \quad (11-19)$$

This margin accounts for a safety factor of 2.0 and a design factor of approximately 1.5.

To continue the above reasoning, the required strength for the riser becomes

$$384 \times 10 = 3840 \text{ lb.} \quad (11-20)$$

Figures 85 through 87 show MIL-W-27657, Ty. II, to be the most efficient selection of webbing for the riser. The ultimate margin of safety, accounting for a safety factor of 2.0 and a design factor of 1.5, becomes

$$\frac{4100}{3840} - 1 = +0.07. \quad (11-21)$$

With regard to the riser extension, its strength requirement remains that indicated in Section 11.b.(3) since it must withstand approximately the total load experienced by the individual parachute.

12. CONCLUSIONS AND RECOMMENDATIONS

On the basis of this study to determine the most suitable design for a prototype cluster-parachute recovery system for a 50,000-lb unit load, it can be concluded that with respect to:

Steady-state Drag

(a) the vent-pulldown technique improves drag characteristics by at least some 20% over the same parachute with no vent pulldown,

(b) the increase in drag owing to the vent pulldown cancels the loss of drag owing to clustering when comparing the drag of a cluster of six vent-pulldown parachutes to the drag of the same single parachute with no vent-pulldown,

(c) the maximum drag efficiency occurs for a vent-pulldown parachute system when the ratio of suspension-line length to parachute diameter (L_S/D_0) is between 1.15 and 1.5 and when the vent is located above the skirt so that the ratio of the center-line length to the parachute diameter (L_C/D_0) is approximately equal to $L_S/D_0 + 0.10$, and

(d) the minimum steady-state drag coefficient for a cluster of six vent-pulldown parachutes is approximately 0.85;

Design

(a) six parachutes represents the most efficient number to comprise the cluster,

(b) the vent-pulldown technique is currently the only practical means available for touching down a 50,000-lb payload using a reasonable-size cluster and reasonable-size parachutes,

(c) a cutter delay of 4 sec is necessary to keep the maximum force experienced by the cluster within reasonable tolerances without incurring severe altitude losses,

(d) each chute requires four cutters,

(e) the maximum force experienced by any one chute in the six-chute cluster is approximately 28,300 lb,

(f) the aerodynamic pressure at the time of maximum force is approximately 35 lb/ft²,

(g) the time required for the parachute canopy skirt to leave the bag is 1.4 to 1.6 sec following payload separation from the aircraft, and

(h) the time required for the parachute assembly to become completely stripped from the bag is 1.5 to 1.8 sec following payload separation from the aircraft.

On the basis of these conclusions, the following is recommended:

(a) six 135-ft-diam. vent-pulldown parachutes,

(b) 1.6-oz/yd² cloth for the canopy,

(c) 1-in. main seams with gores sewn on the bias,

(d) a suspension-line-to-parachute-diameter ratio of 1.25, and a centerline-to-parachute-diameter ratio of 1.35,

(e) a riser-length-to-parachute-diameter ratio of approximately 1.0,

(f) 4-ply webbing of Phoenix WN 1811 for the riser,

(g) 2-ply Pioneer Spec. EI-4148 webbing for the center line,

and

(h) one of the four systems shown in Table 3.

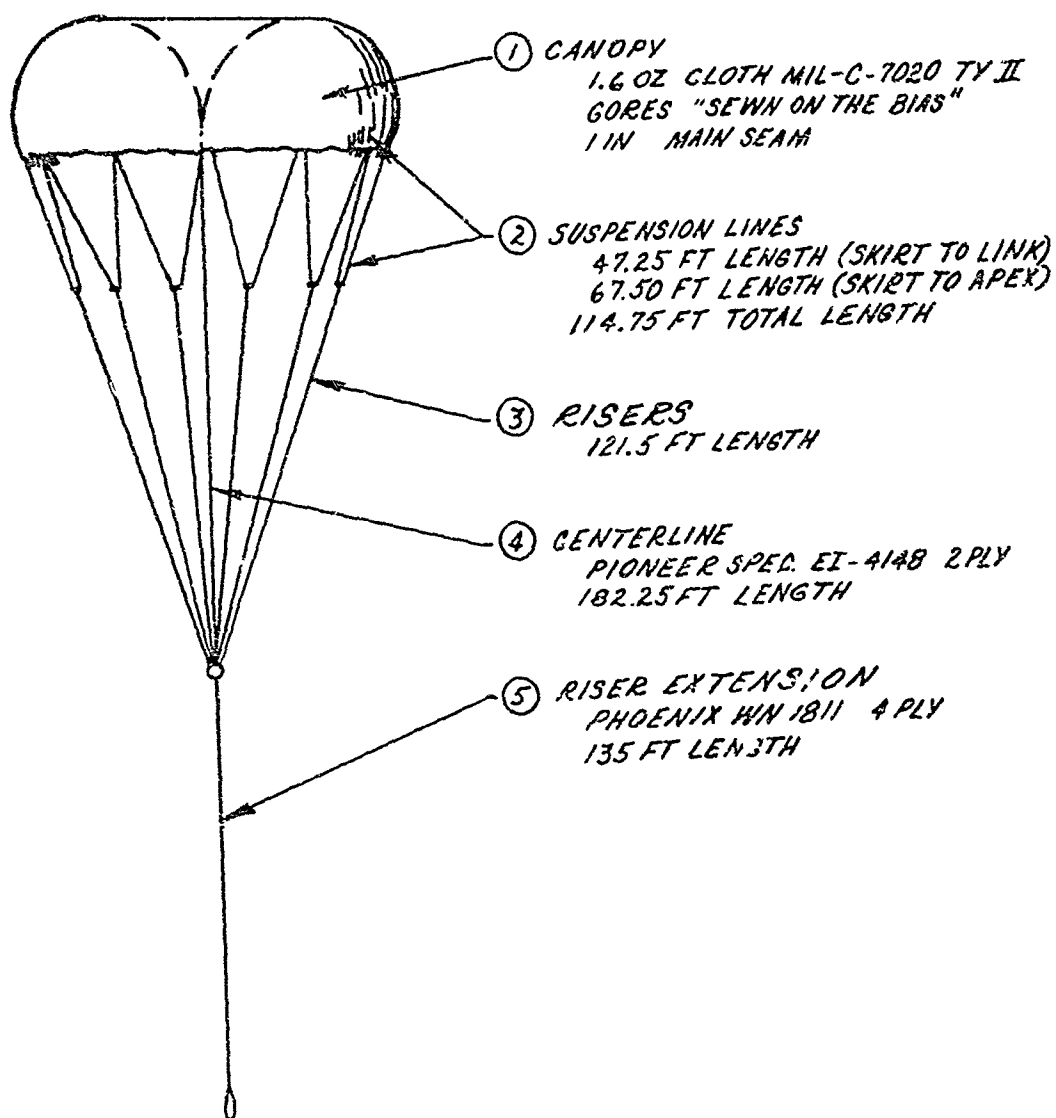


FIGURE 116 - PRELIMINARY ASSEMBLY

TABLE 3 - FOUR PARACHUTE ASSEMBLIES

	IGNORING CENTERLINE AS PRIMARY STRUCTURAL MEMBER		CONSIDERATION OF CENTERLINE AS PRIMARY STRUCTURAL MEMBER	
	MODS TO 3-1A	"BIG BROTHER" TO 6-11A	MODS TO 3-11A	"BIG BROTHER" TO 6-11A
CANOPY 1.602 MIL-C-7020 TYII GORES SEWN ON BIAS WEIGHT = 175 LB MS = 0.0	✓	✓	✓	✓
SUSPENSION LINES PIONEER SPEC EI-437 136 LINES, WEIGHT = 54 LB 14 GROUPS 10 GROUPS - 10 LINES/GROUP 4 GROUPS - 9 LINES/GROUP MS = 0.02	✓			
MIL-C-5040 TYII 160 LINES, WEIGHT = 68 LB 16 GROUPS 10 LINES/GROUP MS = 0.09		✓		
PIONEER SPEC EI-4151 136 LINES, WEIGHT = 34 LB MS = 0.20			✓	
MIL-C-5040 TYII 160 LINES, WEIGHT = 51 LB MS = 0.11				✓
RISERS MIL-W-27657 TY 3 14 LEGS, WEIGHT = 50 LB MS = 0.02	✓			
MIL-W-27657 TY 3 16 LEGS, WEIGHT = 58 LB MS = 0.19		✓		
MIL-W-27657 TY 2 14 LEGS, WEIGHT = 39 LB MS = 0.07			✓	
MIL-W-27657 TY 2 16 LEGS, WEIGHT = 45 LB MS = 0.26				✓
RISER PHOENIX WNBII, 4-PLY 1 ITEM, WEIGHT = 75 LB MS = 0.0	✓	✓	✓	✓
CENTERLINE PIONEER SPEC EI-4148, 2-PLY 1 ITEM, WEIGHT = 31 LB MS = 0.0	✓	✓	✓	✓
TOTAL WEIGHT	387	407	354	377

13. ACKNOWLEDGMENTS

The authors wish to acknowledge the support contributed through reviews and suggestions by Messrs. Arthur W. Claridge, Roman W. Maire, and Stanley Shute, all of the U.S. Army Natick Laboratories, Mr. Claridge being the project officer.

The authors also wish to acknowledge the contribution of Professor H. G. Heinrich and Messrs. Eugene Haak and Robert Noreen, all of the Department of Aeronautics and Engineering Mechanics of the University of Minnesota.

Finally, the authors extend their gratitude to Messrs. James D. Reuter and William J. Everett of Pioneer Parachute Company, Inc., for their guidance, assistance, and cooperation; to Mr. George Kern of Pioneer for his technical editing consultation; to Mr. Samuel Zwick for his drafting assistance; and, finally, to Misses Karen Burke and Sharon Quinn for their typing.

14. REFERENCES

1. U.S. Army, Natick Labs., Request for Quotation DAAG17-68-Q-0113, 31 Oct. 1967, as amended by Amendment No. DAAG17-68-Q-0113-001, 22 Jan. 1968.

2. Stone, J. W., "The Performance of Large Cluster Parachutes." Paper presented at Univ. of Minn. Course in Aerodynamic Deceleration, Jul. 1965.

3. ---, J. H. Wilder, and C. J. Silcott, "Analysis of the Free-Flight Tests of Clustered Large Parachute." Vol. II of Investigation of the Controlled Opening of Single and Clustered Large Parachutes, SEG-TR-66-, Technology Inc., Oct. 1967 (unpubl.).

4. ---, and J. J. Schauer, "Wind Tunnel Tests of Theoretically Suggested Model Chute Modifications." Vol. III, ibid.

5. Knacke, T. W., and L. I. Dimmick, Analysis of Final Recovery Parachutes B-70 Encapsulated Seat and the USD-5 Drone. Final rpt., Contract AF33(616)-8371, Space Recovery Systems, Inc., Apr. 1962.

6. Stone, J. W., Terminal Rate of Descent Analysis - Apollo, Gemini and Mercury Projects. Northrop Ventura rpt., Mar. 1964. (unpubl.).

7. Myers, J.R., Col., USAF, "Load Recovery," in "Letters to the Editor," Aviation Wk. & Space Technol. 88:2, p. 106, Jan. 8, 1968.

8. USAF Flight Dynamics Lab. Research and Technol. Div., Performance of and Design Criteria for Deployable Aerodynamic Decelerators, ASD-TR-61-579, Dec. 1963.

9. Toni, Royce A., The Dynamics of the Unfurling Process of a Parachute System Mortared from a Conveying Body with Application to High Altitude Systems. Langley working paper 439, Jul. 1967.

10. ---, The Dynamics of the Unfurling Process of a Parachute System Mortared from a Body with Application to Systems Tested at Ground Level. Langley working paper 464, Aug. 1967.

11. ---, "Theory on the Dynamics of Bag Strip for a Parachute Deployment Aided by a Pilot Chute." Paper presented at AIAA 2nd Aerodynam. Deceleration Systems Conf., Sep. 23-25, 1968.

APPENDIX

DRAG COEFFICIENT, INFLATION CHARACTERISTICS
AND CLUSTER PERFORMANCE OF MODIFIED
G-11A PARACHUTE MODELS

by

H. G. HEINRICH, R. A. NOREEN,
and D. J. HORN

University of Minnesota
Minneapolis, Minnesota
for
Pioneer Parachute Company

ABSTRACT

Wind tunnel experiments at subsonic speeds were performed to measure the drag coefficient of solid flat parachutes of the type of the G-11A cargo parachute with vent sections pulled down by means of a so-called centerline. This investigation covered also parachute configuration with varying suspension line length with various ratios of suspension to centerline length. A configuration with centerline was identified which is considered to be a nearly optimum solution in view of drag, canopy bulk, weight and simplicity. The drag coefficient of this configuration is $C_{D_0} = 0.78$.

The inflation characteristic from reefed to fully opened stage of the optimum configuration was studied without and with two different internal canopies. These experiments did not yield conclusive results, because the reefed stage was somewhat artificially reproduced by means of a rigid ring holding the canopy inlet open. This is usually the effect caused by an internal canopy, which beneficial action in other studies has been shown to exist during the very early phase of inflation. A further examination of this phenomena was beyond the scope of this study.

Optimum configuration parachutes were assembled to clusters of three and five canopies with varying total distances from canopy skirt to the confluence point at the load. Contrary to common experience, the drag coefficients of these clusters decreased with increasing characteristic distance. It was furthermore observed that clusters with longer characteristic distances performed random motion with a lower frequency than the same arrangement with shorter distances. Therefore, one may speculate that the fast moving clusters experienced an increase of drag due to interference of mass effects as they occur on rotating blade aerodynamic decelerators. The reason for this uncommon behavior may be a so far unknown effect of the centerline. It was also observed that the decrease of drag efficiency with these clusters was less than previously recorded. This fact may also stem from the postulated rotating blade effect. A further investigation of this observation was beyond the scope of this study.

LIST OF SYMBOLS

C_{D_0}	drag coefficient based on canopy surface area S_o
$C_{D_{Std}}$	drag coefficient of the standard configuration G-11A
D_o	nominal canopy diameter
D_{Std}	drag of the standard configuration, G-11A
L_c	length of parachute centerline
L_s	length of parachute suspension lines
σ	statistical deviation from an average

DRAG COEFFICIENT, INFLATION CHARACTERISTIC
AND CLUSTER PERFORMANCE OF MODIFIED
G-11A PARACHUTE MODELS

I. INTRODUCTION

The subject of this project is to study the drag and the opening characteristics of the G-11A parachute with various length centerlines and varying suspension line length with the objective to find the maximum drag under consideration of practically possible line configurations. In inflation studies the effect of internal canopies was also studied.

Parachutes representing the optimum configuration found in this phase were then combined to clusters of three and five canopies and the cluster riser length was varied from 0.5 to 1.5 and 2.5 D_0 . The objective of this study was again determination of an optimum solution in view of drag and simplicity of the configuration.

II. PARACHUTE DRAG AND VARYING SUSPENSION AND CENTERLINE LENGTHS

A. Approach

Exploratory tests for the determination of the optimum drag configuration of the G-11A were made on a model parachute in the open section of the horizontal return wind tunnel at the University of Minnesota (Fig. 1). Since the dynamic pressure in this section varies slightly, the drag coefficients were not calculated directly from the measured drag, but a ratio of drag obtained for each configuration to the drag of the standard G-11A configuration was determined. In order to convert this into realistic drag information, the drag coefficient of the standard G-11A was obtained by means of a smaller model placed in the more precise closed section of the wind tunnel. Introducing this drag coefficient into the previously obtained ratio should provide results with acceptable accuracy.

B. Models

For the exploratory tests in the open section of the wind tunnel, models with 120 gores and a nominal diameter of 40 inches were used. The suspension lines from the canopy were gathered into twelve groups of ten lines. Each of these suspension lines was 14 inches long or 35% of the nominal diameter (Fig. 2). From the group confluence point, a single line leads to the main confluence point of the parachute. The length of the twelve single lines was varied to form the different suspension line lengths required in this study; in the following, the sum of a single line length and the length of the individual suspension lines are simply called the suspension line length.

The small model of the G-11A was a 64 gore parachute with a nominal diameter of 12.75 inches. To form the standard configuration of the G-11A, the suspension line lengths were 12.11 inches or 95% of the nominal diameter. These suspension lines were not grouped, but ran directly from the canopy skirt to the main confluence point.

C. Test Apparatus and Experimental Procedure

The 120 gore model of the G-11A was supported in the open test section of the wind tunnel by a guide wire suspended between two struts in the wind tunnel. The confluence point of the G-11A suspension lines was fastened to a force measuring cantilever beam attached to the upstream strut. The cantilever beam and the support wire were positioned so

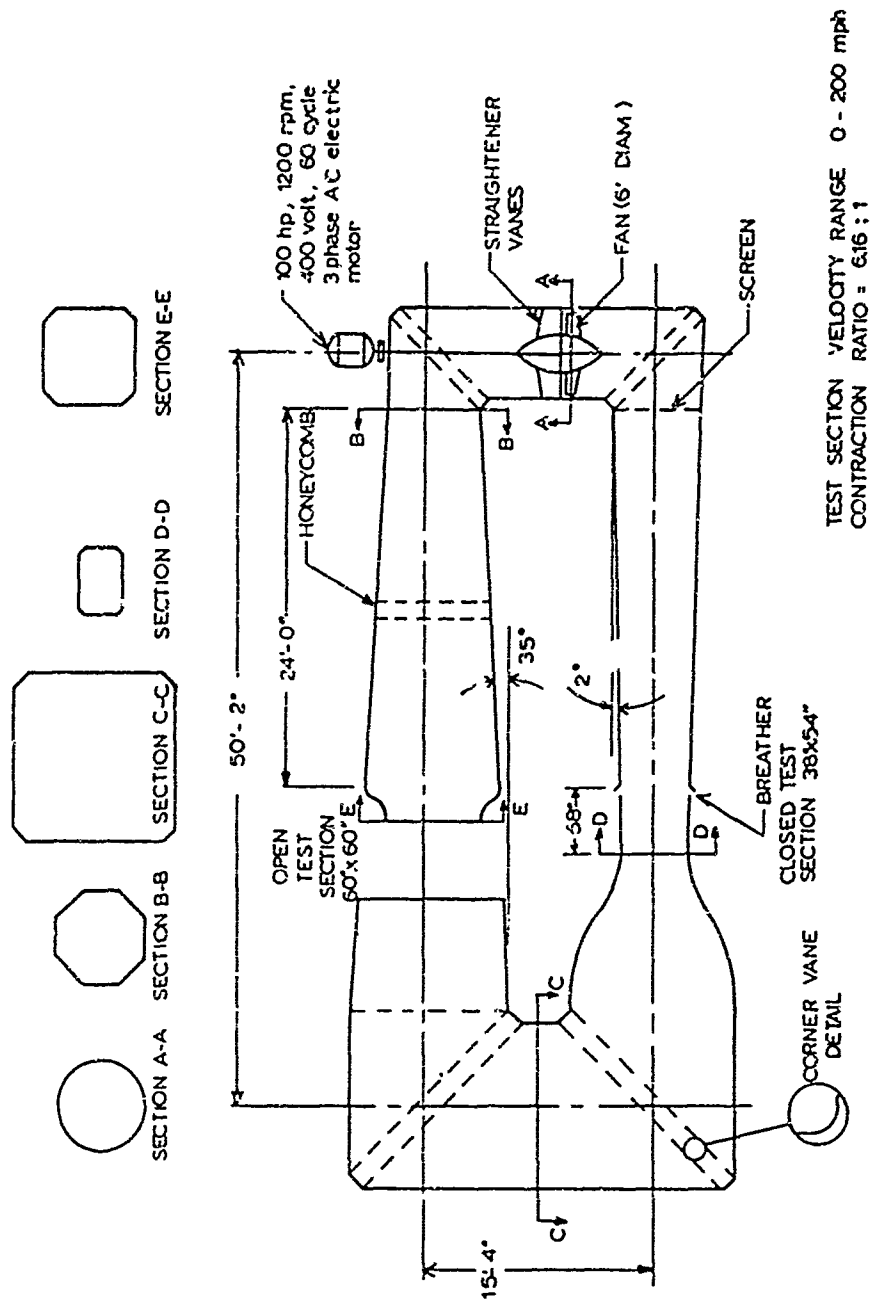


FIG 1 UNIVERSITY OF MINNESOTA HORIZONTAL RETURN WIND
TUNNEL SCHEMATIC LAYOUT

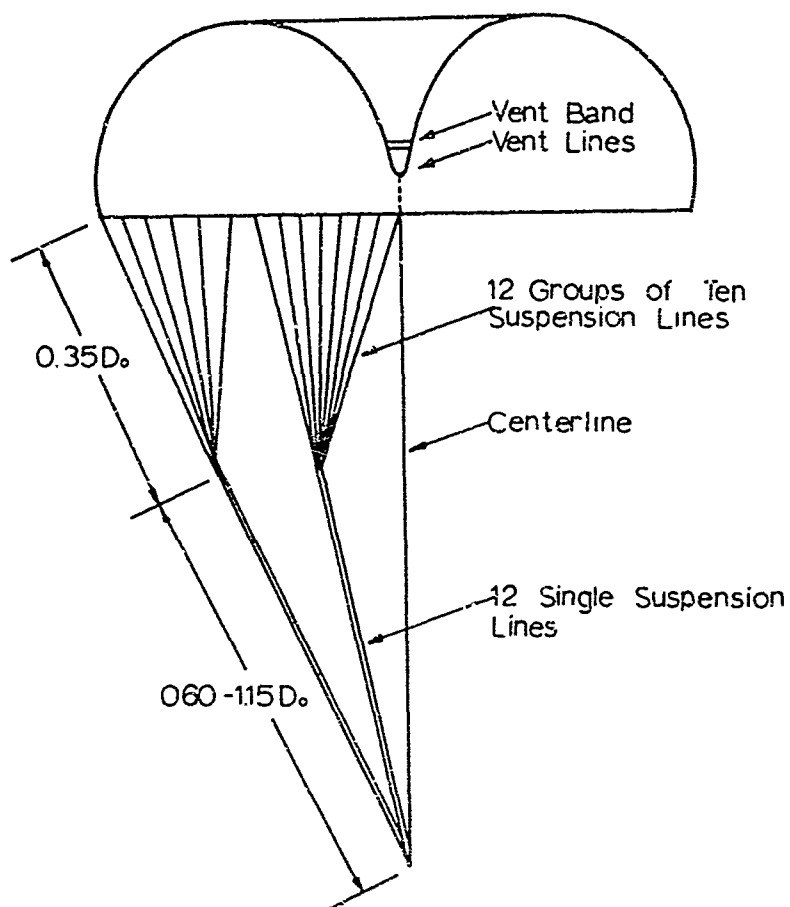


FIG 2 Suspension Line Arrangement for the
120 Gore Model of the G-11A

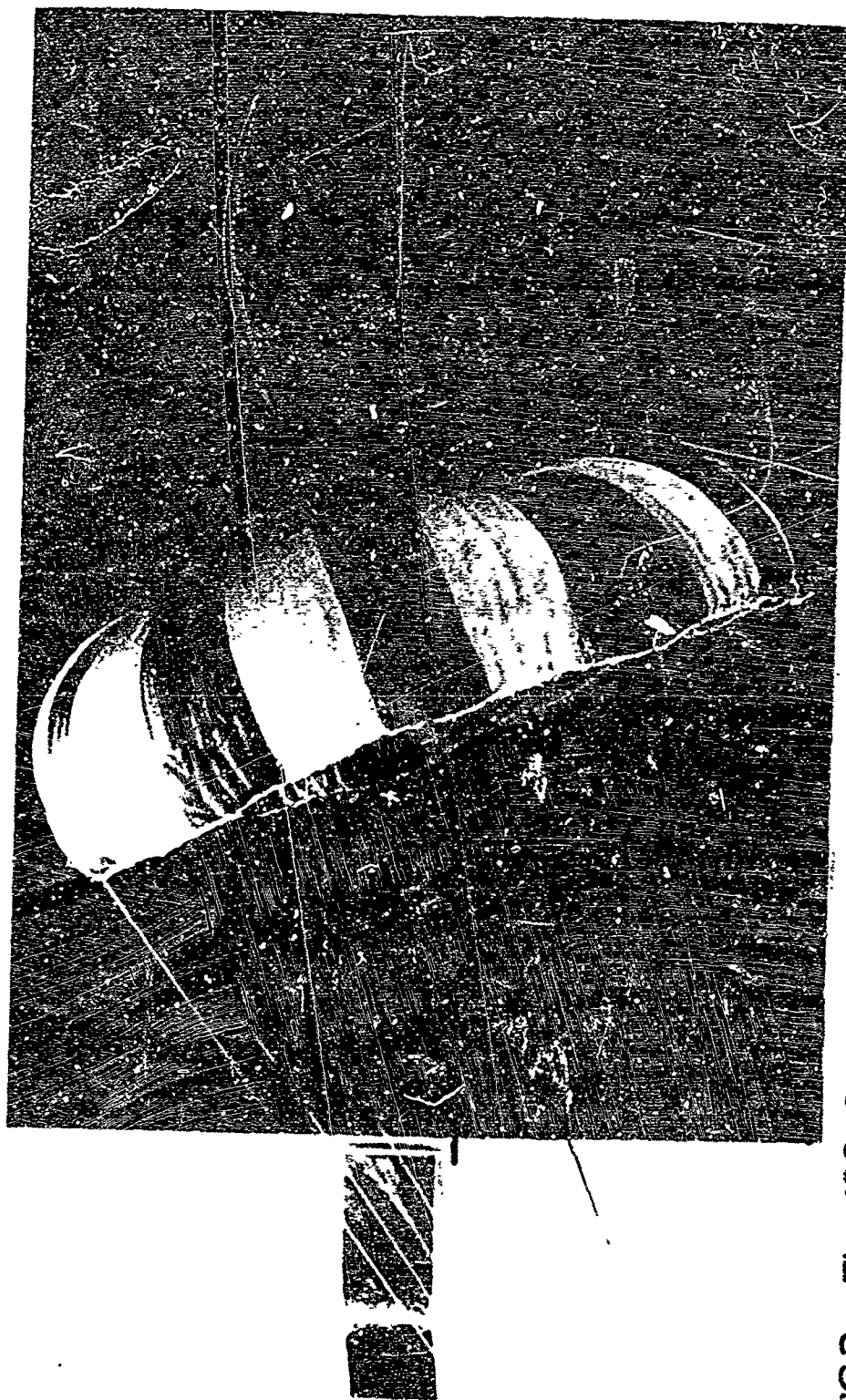


FIG3 The 120 Gore Model of the G-11A Positioned in the Wind Tunnel at its Stable Angle of Attack

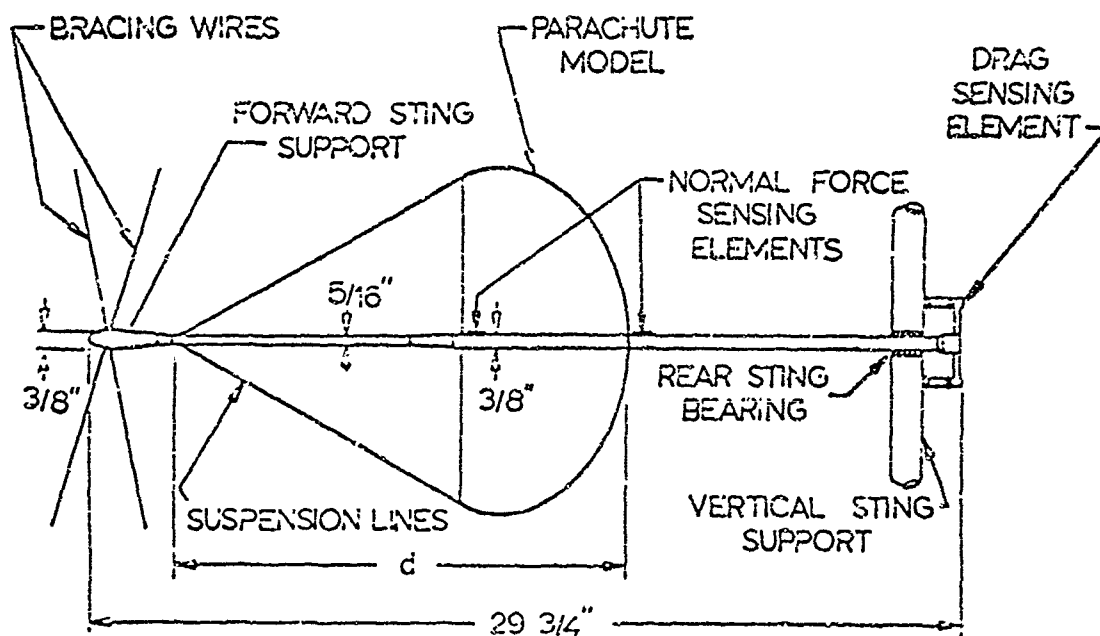
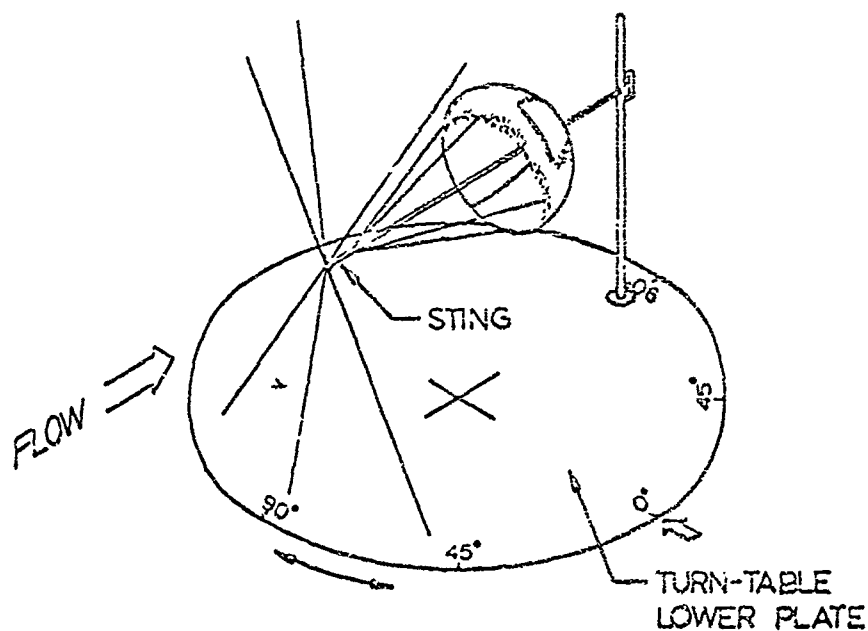


FIG 4 Three Component Sting used to Measure the Drag on the 64 Gore Model of the Standard Configuration, G-11A



FIG 5 The 64 Core Model of the Standard Configuration of the G-11A in the Closed Section of the Wind Tunnel

that the G-11A was allowed to stay at its stable angle of attack, trim angle, while the canopy still remained in the test section (Fig. 3). The centerline, which varies the position of the vent, was attached to the vent and the main confluence point. The lengths of the centerline and the suspension lines were changed, and the drag measured to find the optimum combination which would produce maximum drag.

The small 64 gore model of the standard G-11A configuration was supported in the closed section of the wind tunnel by a three component electric balance (Fig. 4). The angle of attack of the parachute was changed until the normal force vanished, at which point the drag was measured. This represents the drag at the trim angle. Figure 5 shows the 64 gore model in the closed section of the wind tunnel during testing.

D. Results

1. Drag Coefficient of the Standard G-11A Configuration

The standard configuration of the G-11A has a suspension line length of $L_s/D_o = 0.95$. The drag coefficient, C_D , for the standard G-11A was measured at three different dynamic pressures. Table 1 shows the C_D values obtained at each dynamic pressure. The standard value of C_D obtained and to be used in the determination of all other drag coefficients was $C_{D_{Standard}} = 0.64$. The drag on the

standard configuration of the G-11A parachute was also measured on the 120 gore model in the open section of the wind tunnel. This drag was measured three times as a check at a dynamic pressure of 0.5 inches of water, and the average value, determined in this manner, is shown in Table 1. The drag of the standard parachute, used in all further calculations, is $D_{Standard} = 15.32$ lbs.

2. Drag coefficient of the G-11A parachute with $L_s/D_o = L_c/D_o = 0.95$ was found, in three independent tests with $q = 0.5$ in H_2O , to be $C_{D_o} = 0.71$ (Table 2).

3. Different line lengths, but $L_s = L_c$, caused a significant variation of the drag coefficient. Table 3 lists the results of tests with five different lengths while Fig. 6 is a graphical presentation of the drag coefficient as a function of suspension line and centerline length. It

Table I

Drag Coefficient of the 64 Gore Model of the G-11A,
Standard Configuration, and the Drag of the 120 Gore
Model of the G-11A, Standard Configuration ($L_s/D_o = 0.95$)

Configuration Drag Coefficient	Dynamic Pressure, Inch H ₂ O			Average Drag Coefficient
	0.5	1.0	2.0	
Standard Configuration of the 64 Gore Model of the G-11A $L_s/D_o = 0.95$	0.64	0.64	0.63	0.64
Configuration Drag (lbs)	Dynamic Pressure, Inch H ₂ O			Average Drag (lbs)
	0.5			
Standard Configuration of the 120 Gore Model of the G-11A $L_s/D_o = 0.95$	15.32 15.41 15.23	-----	-----	15.32

Table II

Drag Coefficient of G-11A Parachute
with Centerline and Suspension Line
Length Equal

$L_s/D_o = L_c/D_o$	Dia; (lbs)	D/D_{std}^*	$C_{D_o}^{**}$
0.95	17.0	1.11	0.71
0.9	17.07	1.11	0.71
0.95	17.8	1.10	0.70

$$* D_{Standard} = 15.32 \text{ lbs}$$

$$C_{D_{Standard}} = 0.64$$

$$** C_{D_o} = \left(\frac{D}{D_{std}} \times C_{D_{std}} \right)$$

Table III

Drag Coefficient of G-11A Parachute
with Varying Suspension Line Lengths
but Centerline Equal to Suspension
Line Length ($L_s = L_c$)

$L_s/D_o = L_c/D_o$	Drag (lbs)	D/D_{Std}^*	$C_{D_o}^{**}$
0.75	16.3	1.06	0.68
0.95	17.0	1.11	0.71
1.15	17.9	1.17	0.75
1.35	17.98	1.17	0.75
1.50	18.40	1.20	0.77

$$* D_{Standard} = 15.32 \text{ lbs}$$

$$C_{D_{Standard}} = 0.64$$

$$** C_{D_o} = \left(\frac{D}{D_{Std.}} \times C_{D_{Std.}} \right)$$

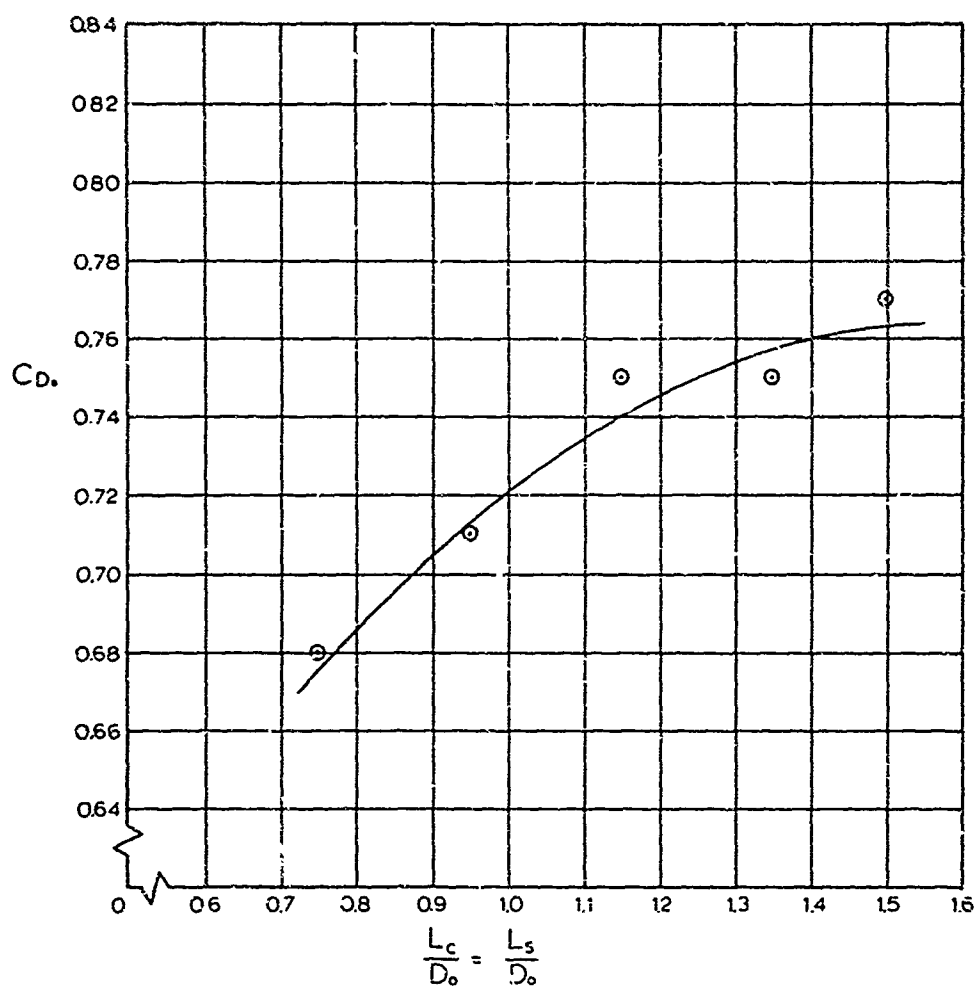


Fig 6 Drag Coefficient of the G-11A Parachute with Varying Suspension Line Length, the Centerline Being Equal to the Suspension Line

Table IV
Drag Coefficient of G-11A Parachute
with Varying Centerline Length but with
Suspension Line Length Constant ($L_c/D_o=1.5$)

L_c/D_o	Drag (lbs)	D/D_{Std}^*	$C_{D_o}^{**}$
1.40	16.80	1.097	0.70
1.40	16.61	1.080	0.69
1.45	18.00	1.170	0.75
1.45	18.18	1.190	0.76
1.45	18.03	1.177	0.75
1.50	18.90	1.23	0.79
1.50	18.44	1.20	0.77
1.50	18.51	1.21	0.77
1.55	18.50	1.21	0.77
1.55	18.70	1.22	0.78
1.55	18.90	1.23	0.79
1.55	18.70	1.22	0.78
1.60	18.60	1.21	0.77
1.60	18.90	1.23	0.79
1.60	18.70	1.22	0.78
1.60	18.86	1.225	0.78
1.65	18.95	1.24	0.79
1.65	18.72	1.22	0.78
1.65	18.90	1.23	0.79
1.65	18.42	1.20	0.77
1.70	17.90	1.17	0.75
1.70	17.70	1.16	0.74
1.75	16.95	1.11	0.71
1.75	17.35	1.13	0.72

* $D_{Standard} = 15.32 \text{ lbs.}$

$C_{D_{Standard}} = 0.64$

** $C_{D_o} = \left(\frac{D}{D_{Std}} \times C_{D_{Std.}} \right)$

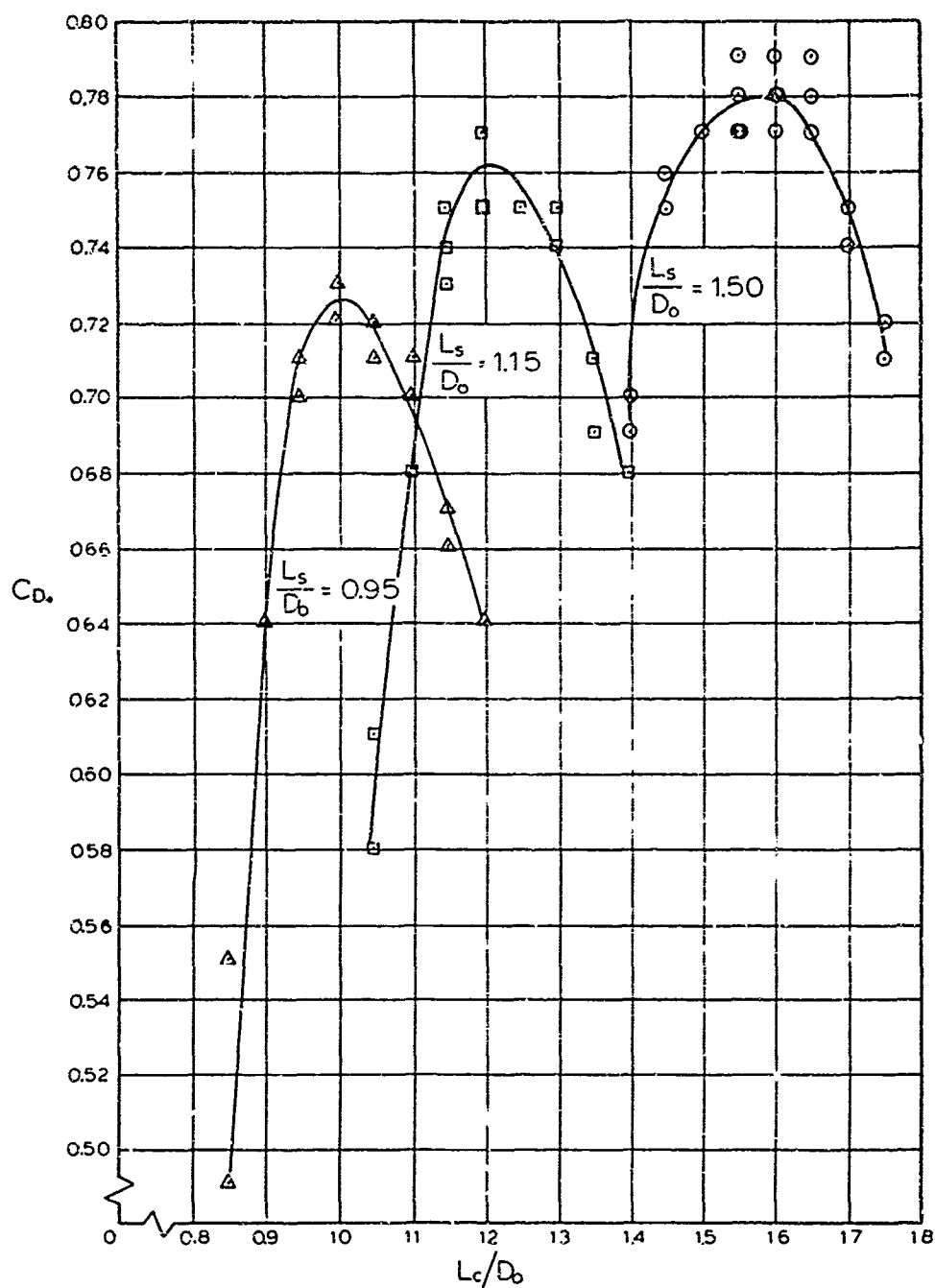


Fig 7 Drag Coefficient of the G-11A Parachute with Varying Center-Line and Different Suspension Line Length ($L_s/D_0 = 0.95, 1.15, 1.50$)

Table V
Drag Coefficient of G-11A Parachute
with Varying Centerline Length but with
Suspension Line Length Constant ($L_s/D_o=1.15$)

L_c/D_o	Drag (lbs)	D/D_{Std}^*	$C_{D_o}^{**}$
1.00	10.60	0.692	0.44
1.05	13.90	0.907	0.56
1.05	14.32	0.950	0.61
1.10	16.35	1.068	0.68
1.10	16.35	1.068	0.68
1.15	17.05	1.152	0.74
1.15	17.52	1.144	0.73
1.20	18.55	1.211	0.77
1.20	17.80	1.162	0.75
1.25	17.90	1.170	0.75
1.25	17.95	1.172	0.75
1.30	17.95	1.171	0.75
1.30	17.76	1.159	0.74
1.35	17.05	1.113	0.71
1.35	16.60	1.083	0.69
1.40	16.35	1.059	0.68
1.40	16.35	1.067	0.68

* $D_{Standard} = 15.32 \text{ lbs}$

$C_{D_{Standard}} = 0.64$

** $C_{D_o} = \left(\frac{D}{D_{Std}} \times C_{D_{Std}} \right)$

Table VI
Drag Coefficient of G-11A Parachute
with Varying Centerline Length but with
Suspension Line Length Constant ($L_s/D_o=0.95$)

L_c/D_o	Drag (lbs)	D/D_{Std}^*	$C_{D_o}^{**}$
0.85	11.77	0.76	0.49
0.87	13.20	0.86	0.55
0.90	12.51	0.82	0.52
0.90	13.40	1.00	0.64
0.91	17.07	1.11	0.71
0.92	15.35	1.10	0.70
1.00	17.43	1.14	0.73
1.00	17.28	1.13	0.72
1.05	17.06	1.11	0.71
1.05	17.20	1.12	0.72
1.10	16.94	1.11	0.71
1.10	16.80	1.10	0.70
1.15	15.10	1.00	0.67
1.15	15.90	1.04	0.66
1.20	15.32	1.00	0.64
1.20	15.41	1.006	0.64

* $D_{Standard} = 15.32 \text{ lbs}$

$C_{D_{Standard}} = 0.64$

** $C_{D_o} = \left(\frac{D}{D_{Std.}} \times C_{D_{Std.}} \right)$

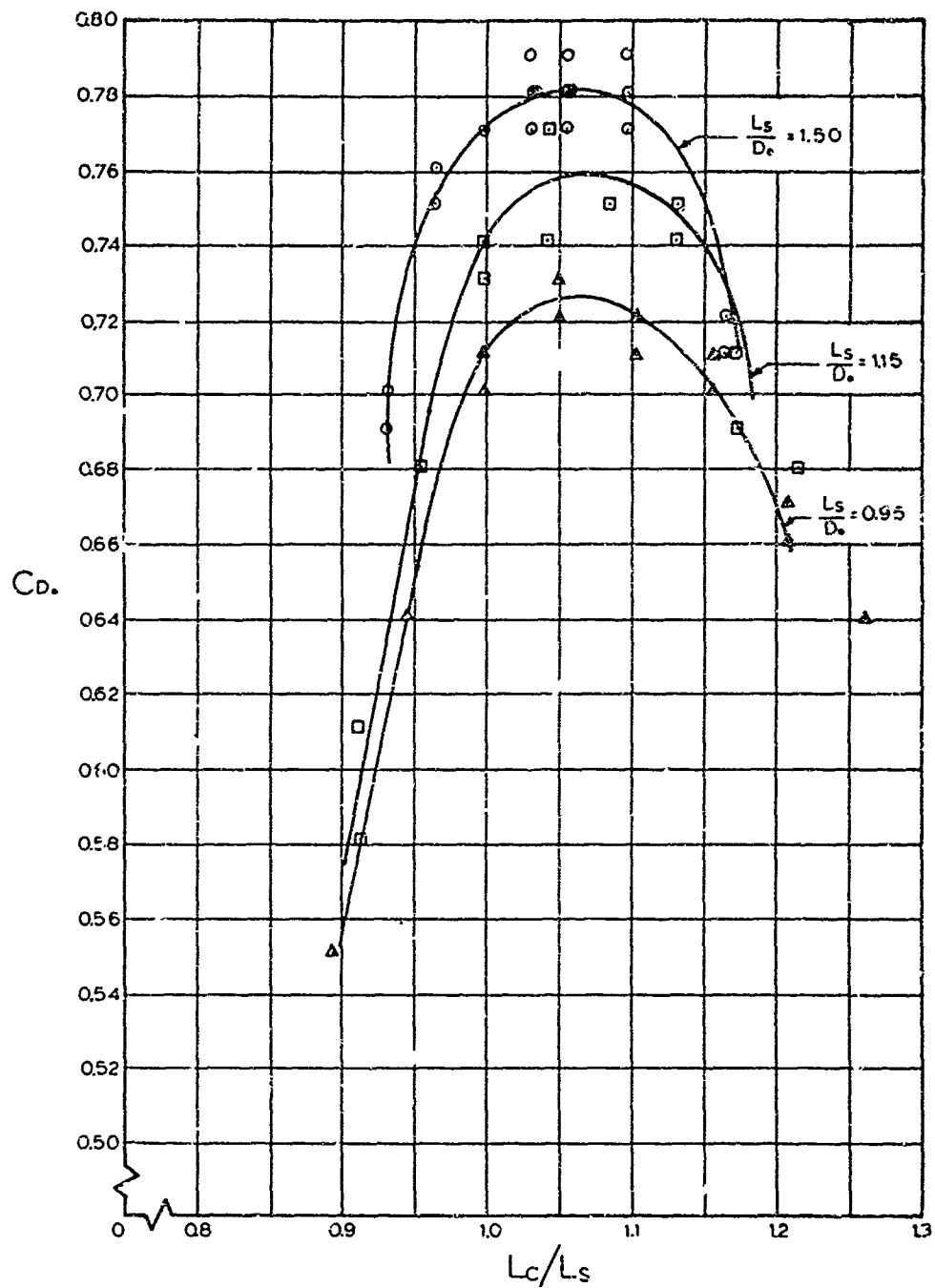


Fig 8 Drag Coefficient of G-11A Parachute
with Different Suspension Line Lengths
($L_S/D_0 = 0.95, 1.15, 1.50$) and Varying
Centerline to Suspension Line Ratios

can be seen that an optimum drag coefficient for this configuration occurs when $L_c/D_o = L_s/D_o = 1.5$.

4. The maximum drag coefficient with varying centerline lengths but constant length of the suspension lines, namely, $L_s/D_o = 1.5$, was found through respective measurements. The results are listed in Table 4 and presented in Fig. 7. It can be seen that the maximum coefficient for $L/D_o = 1.5$ occurs when the centerline is slightly longer, namely, $L/D_o = 1.6$. With this configuration, the average drag coefficient amounts to $C_D = 0.78$.

5. Additional tests with varying centerline length but constant $L/D_o = 0.95$ and 1.15 were performed because the long suspension lines with $L/D_o = 1.5$ are practically not acceptable. The results of these measurements are shown in Tables 5 and 6 and in Fig. 7.

In conclusion it can be stated that a configuration of the G-11A parachute with suspension lines somewhat longer than the standard length, and the centerline from 6 - 10% again longer than the suspension lines may be considered to be an optimum solution in view of drag, bulk, and simplicity of construction. Figure 8, which shows drag coefficients as a function of L_c/L_s with suspension line lengths as parameters, indicates this fact quite clearly.

III. INFLATION CHARACTERISTICS

A. Approach

The phase of inflation from reefed to fully inflated had been identified as the most important one, and an attempt was made to investigate this phase in detail. A parachute configuration was selected which appeared to be the optimum solution in view of the preceding studies, namely $L/D = 1.5$ and $L/D = 1.6$. The inflation characteristics were studied with the centerline alone as well as with a centerline and an internal parachute. Two sizes of internal parachutes were used. Both internal parachutes were positioned such that the distance between planes of the inflated parachute skirts was $0.05 D$ of the main parachute. This position was selected in view of previous work as being the position at which the strongest effect of the internal canopy was observed (Ref. 1).

B. Models

The parachute used was the 120 gore 40 inch parachute used in the drag tests. The two internal canopies were solid flat parachutes with suspension line lengths equal to their nominal diameters. The diameter of the internal parachutes was 22.5% and 15.0% of the nominal diameter of the main parachute.

C. Apparatus and Experimental Procedure

The parachute was supported in the wind tunnel in the same manner as in the exploratory drag tests. However, in order to hold the parachute in the reefed open position, a ring was constructed of a $1/4"$ x $1/8"$ steel band with a diameter equal to 15% of the projected diameter of the G-11A parachute model. The ring was mounted on a strut so that it could be positioned in front of the skirt of the parachute. To hold the parachute in the reefed position, the skirt was laid on the ring and held in place with two spring steel straps (Fig. 9). The straps were removed by an electrical impulse, allowing the parachute to inflate. Figure 10 shows the parachute fully inflated with the mounting ring visible. The opening time of the parachute was defined as the time from disreefing to the maximum force. At this time, the internal canopy is collapsed which is also shown in Fig. 10. Figure 11 is a copy of a typical recording taken by means of an oscillograph. The disreef point is indicated by the electrical impulse sent to the reefing ring straps while a force versus time trace is plotted by the oscillograph.

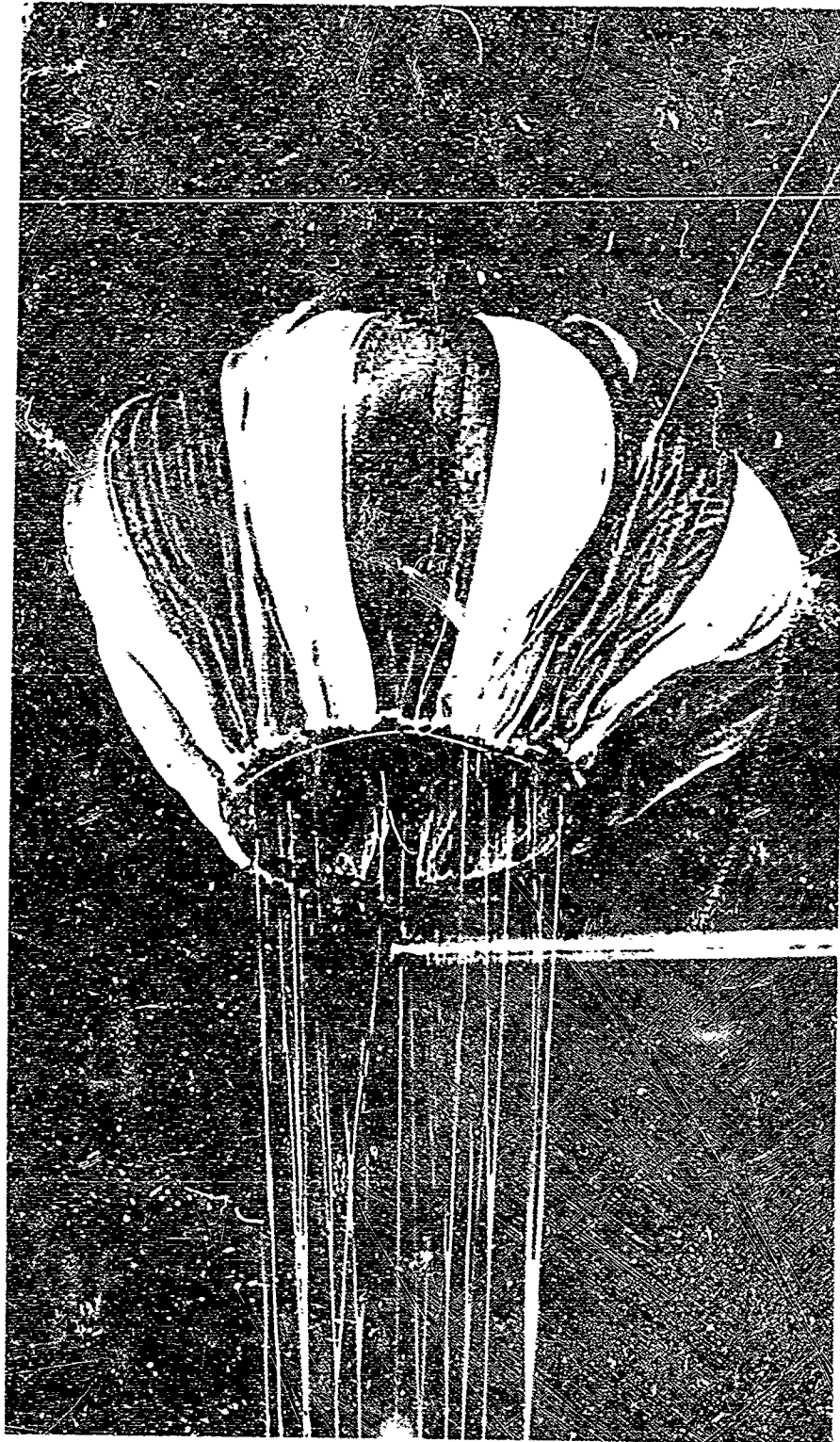


FIG 9 120 Gore Model of the G-11A held in a Reefed Open Position by the Reefing Ring

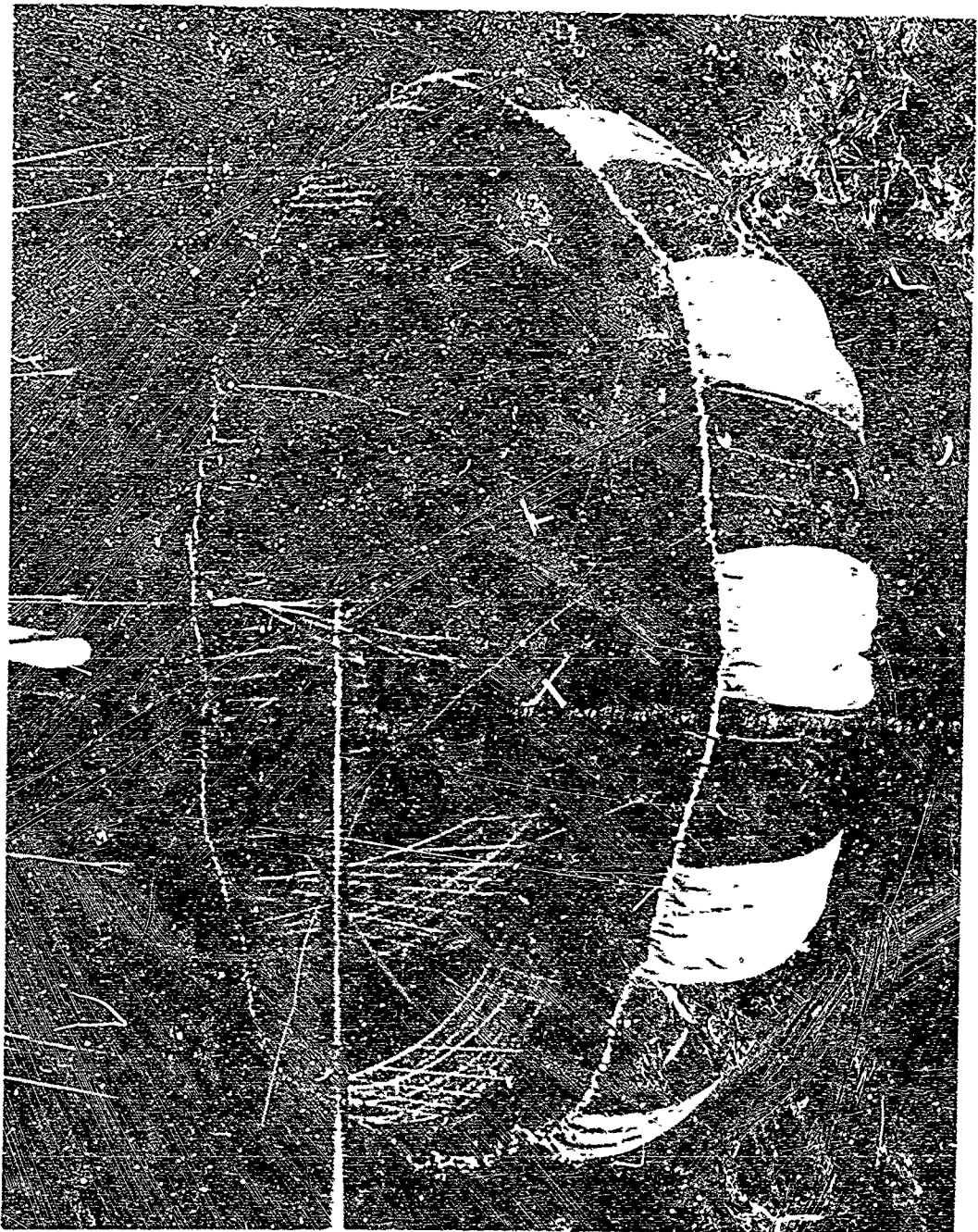


FIG 10 Fully Inflated Model of the G-11A
during Reefed Open to Full Open Studies
with a 0.225 D₀ Internal Parachute

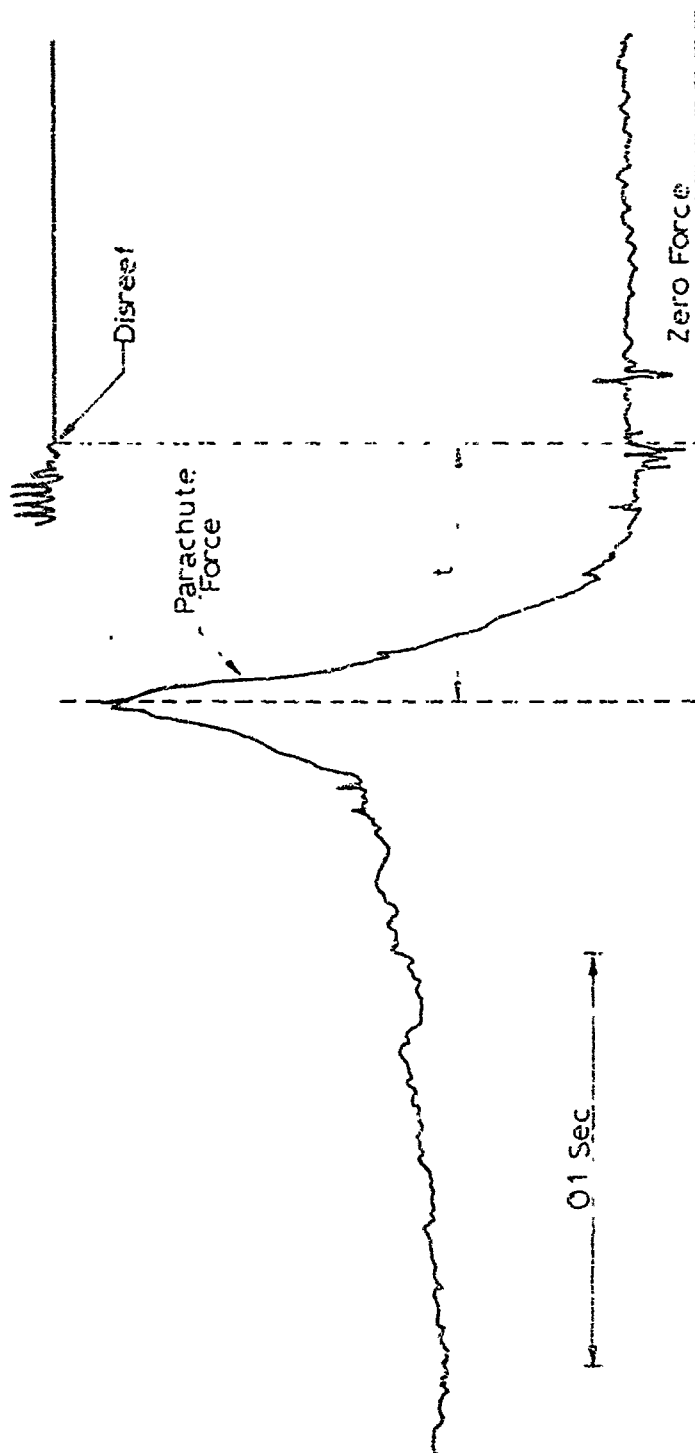


FIG 11 Force-Time Diagram of G-11A Parachute Model from Condition of Reefed-Open to Fully Inflated

Table VII
Opening Times of G-11A Parachute with
Suspension Lines of $1.5D_0$, Centerline of
 $1.6D_0$ and no Internal Parachute

Configuration	Time (sec)
G-11A with $L_c/D_0 = 1.6$ $L_g/D_0 = 1.5$ and no internal parachute	0.058
	0.058
	0.060
	0.057
	0.061
	0.057
	0.058
	0.057
	0.057
	0.061
	0.052
	0.055
	0.053
	0.057
	$t_{ave} = 0.057$
	$\sigma = 0.002$

Table VIII
Opening Times of the G-11A Parachute
with Suspension Lines of 1.5 D, Centerline
Length of 1.6 D, and a 0.15 D, and 0.225 D,
Diameter Internal Parachutes

Configuration	Time (sec)
G-11A with $L_c/D_o = 1.6$ $L_s/D_o = 1.5$ and a 0.15 D _o internal para- chute	0.066
	0.067
	0.066
	0.062
	0.061
	$t_{ave} = 0.064$
	$\sigma = 0.003$
G-11A with $L_c/D_o = 1.6$ $L_s/D_o = 1.5$ and a 0.225 D _o internal para- chute	0.061
	0.060
	0.060
	0.060
	0.053
	0.060
	0.062
	0.059
	0.060
	0.055
	0.055
	$t_{ave} = 0.059$
	$\sigma = 0.002$

D. Results

1. Without internal parachute, the opening time of the parachute from the reefed stage to maximum force was measured several times to obtain a good average value. The average opening time obtained in this manner amounted to $t_{ave} = 0.057$ sec and $\sigma = \pm 0.002$ sec with σ being the statistical deviation.

2. Opening time with centerline and a $0.15 D_0$ and a $0.225 D_0$ internal parachute was measured in the same manner. The internal parachutes were positioned as mentioned before, $0.05 D_0$ behind the skirt of the main parachute and held in place by attaching its confluence point to the centerline. The opening time of the G-11A parachute model with centerline and $0.15 D_0$ internal parachute was $t_{ave} = 0.643$ sec and $\sigma = \pm 0.003$ sec; while the opening time with the $0.225 D_0$ internal parachute was $t_{ave} = 0.059$ sec and $\sigma = \pm 0.002$ sec. The values of opening times without and with an internal parachute are listed in Tables 7 and 8 respectively.

These tests indicate that an internal parachute would not aid in the opening time of the G-11A parachute from the reefed position to the fully opened position. These results are not conclusive however, since the reefing ring probably acts like an internal parachute in the early stages of opening. The advantageous effect of the internal parachute as observed in other studies, occurs during the opening phase from the snatch to the reefed position. In these studies the internal canopy may have choked the air inflow while the ring held the canopy open. Time and fund limitations prevented further study of this condition.

IV. CLUSTER PERFORMANCE

A. Approach

The drag coefficient of three and five clustered parachutes was calculated and compared with actual measurements. In these studies each parachute was adjusted to the optimum configuration as established above, namely $L_s/D_o = 1.5$, $L_c/D_o = 1.6$.

B. Models

Each parachute had 64 gores and a diameter of 12.75 inches as used for the determination of the drag coefficient of the standard G-11A parachute. Each parachute was attached to a riser and the confluence point of the risers was attached to the force measurement beam (Fig. 12). Three different riser lengths of $0.5 D_o$, $1.5 D_o$ and $2.5 D_o$ were used.

C. Test Apparatus and Experimental Procedure

The cluster riser was attached to the force measuring device on the upstream strut. As before, the canopies assume their stable angle of attack and still remain in the test section. Figure 13 shows the three and five canopy clusters in the wind tunnel during testing. The riser length was set at the three positions mentioned, and the drag coefficient of the three and five canopy clusters determined at each riser length.

D. Results

When exposed to the air flow, it was observed that the canopies do not stay at any particular location, but move at random and sometimes very rapidly back and forth across the test section. Clusters with shorter risers move faster than those with longer risers. The measured drag of the various configurations is indicated in Table 9 and Fig. 14. As can be seen, the drag of cluster combinations decreases slightly with cluster riser length and is in general higher than usually reported from full size tests. The drag coefficient of the clusters is expressed as ratio of $C_{D_{cluster}}/nC_{D_o}$, where n is the number of the individual canopies.

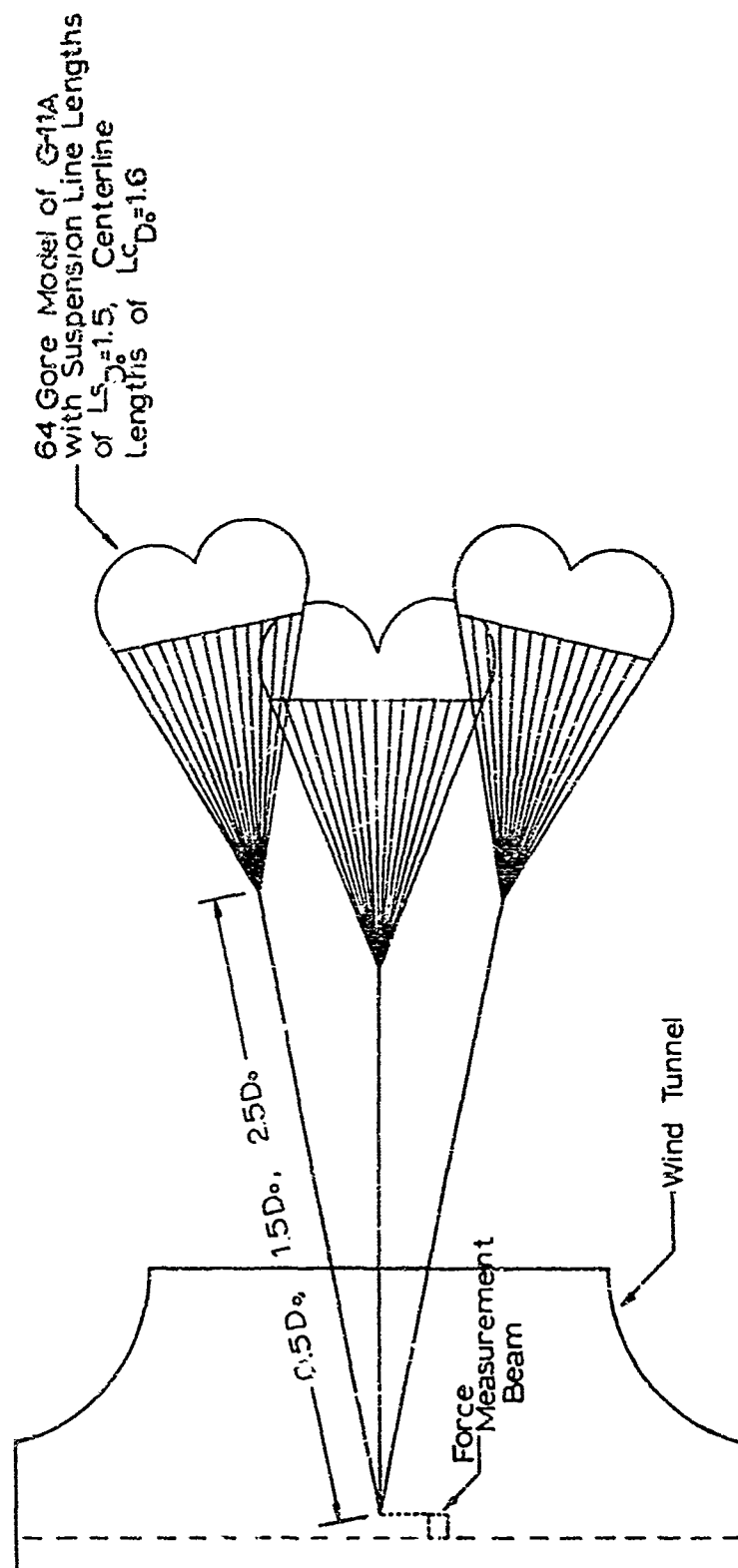
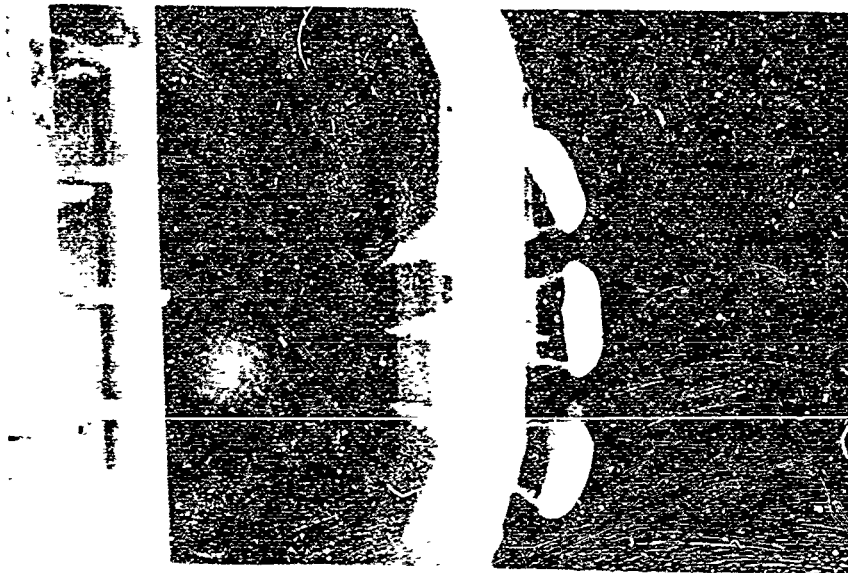
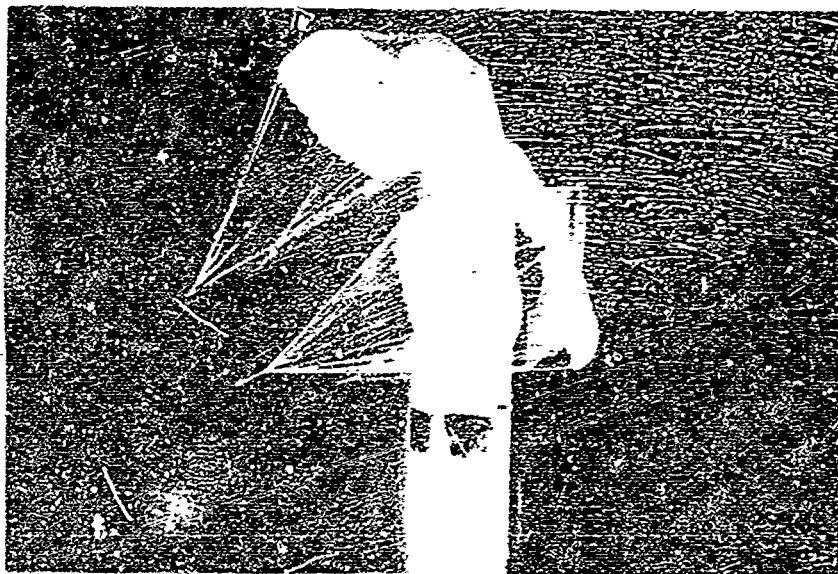


FIG 12 Riser Line Arrangement for the Three and Five Canopy Cluster Studies



a) Cluster of Three 64 Gore Model of the G-11A



b) Cluster of Five 64 Gore Model of the G-11A

FIG 13 Cluster Studies of 3 & 5 Canopy Clusters of G-11A with Suspension Lines of $1.5 D_0$ and Centerline of $1.6 D_0$

Table IX
Drag Coefficient of 3 and 5 Clustered
Parachute Canopies with Varying Cluster
Riser Lengths

Riser Length	Number of Canopies, n	$C_{D_o}^*$	C_{D_o} Average
0.5 D_o	3	0.83	0.86
		0.96	
		0.78	
	5	0.74 0.74 0.83 0.82	0.78
1.5 D_o	3	0.74 0.75 0.82 0.86	0.79
	5	0.73 0.76 0.72	0.74
2.5 D_o	3	0.67 0.78 0.89 0.86	0.80
	5	0.53 0.62	0.58

* $C_{D_o} = \frac{D_{Total}}{q \cdot n \cdot S}$

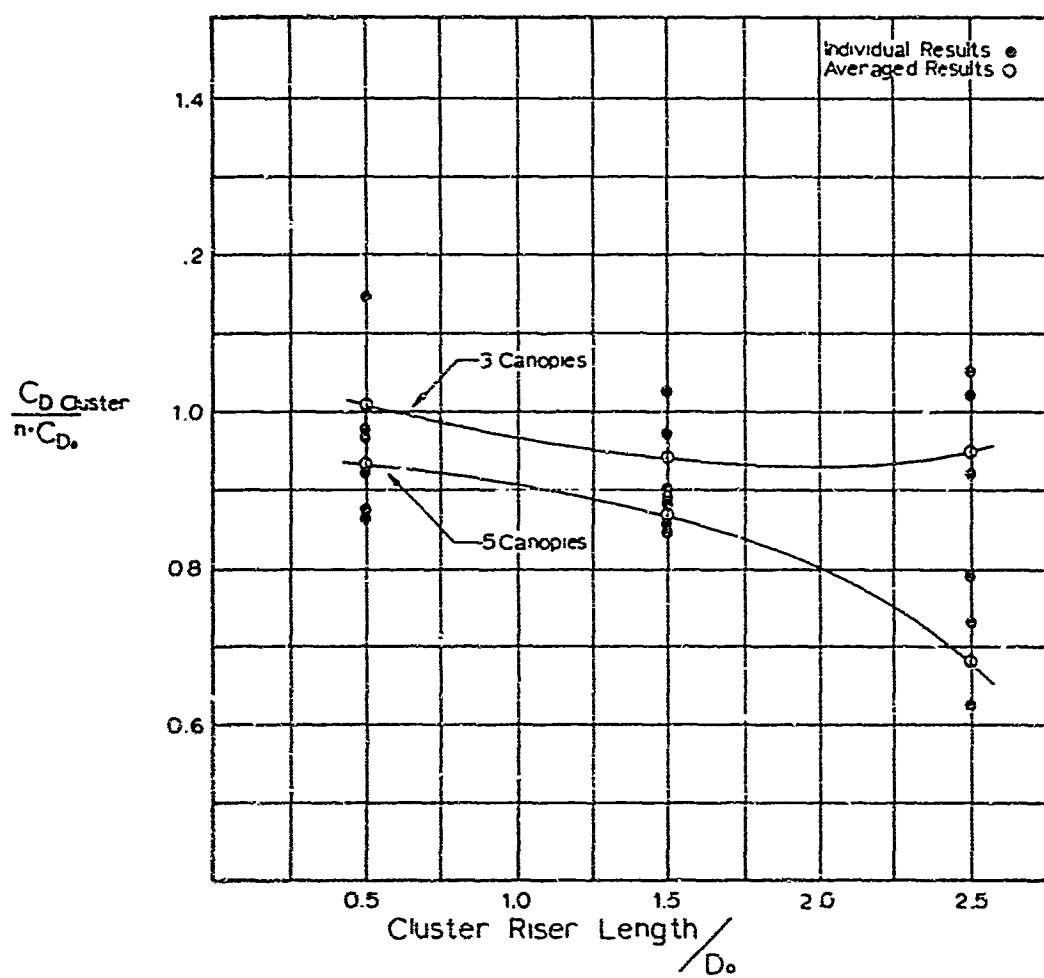


FIG 14 Drag Coefficient of Clustered Parachutes

Reviewing the results, it is surprising that longer risers cause lower drag coefficients. A possible explanation of this observation may be that clusters with shorter risers, which move faster, cause more interference drag than slower moving configuration with longer risers. In this respect, fast moving clusters may reproduce to a certain extent the conditions of rotating blade decelerators.

The drag coefficient of a cluster of five parachutes is generally lower as the one of a cluster of three canopies. This observation has also been made in full size tests. The fact that the model clusters have shown higher drag coefficients than full size configurations may be caused by the relatively faster motion of the models. Larger parachutes are better damped probably because of their larger included and apparent masses. However, the modified form of the canopies involved, due to the action of the centerline, may also cause so far unknown effects. From the standpoint of general knowledge, it would be very interesting to compare the results of these model tests with those of related full size experiments, whereby the motion of the entire cluster with respect to the load and the relative motion of the individual canopies may be a prime point of interest in the observation and recording of the test results.

V. REFERENCES

1. Heinrich, Helmut G. and Niccum, Ronald J.: A Method to Reduce Parachute Inflation Time With a Minor Increase of Opening Force, WADD-TR-60-761, August 1960, ACTIA Document No. AC 268 680.

Unclassified

Security Classification

DOCUMENT CONTROL DATA - R & D

(Security classification of title, body of abstract and indexing annotation must be entered when the overall report is classified)

1. ORIGINATING ACTIVITY (Corporate author)		2a. REPORT SECURITY CLASSIFICATION	
Pioneer Parachute Company, Inc. Manchester, Connecticut		Unclassified	
3. REPORT TITLE		3b. GROUP	
Prototype Cluster-Parachute Recovery System for a 50,000-lb. Unit Load Volume I - Design Study			
4. DESCRIPTIVE NOTES (Type of report and inclusive dates)			
Final Report. May 1968-January 1969			
5. AUTHOR(S) (First name, middle initial, last name)			
Royce A. Toni Marcia G. Wood Wolfgang R. Mueller Milan M. Knor			
6. REPORT DATE	7a. TOTAL NO. OF PAGES	7b. NO. OF REFS	
January 1969	203	11	
8a. CONTRACT OR GRANT NO.	8b. ORIGINATOR'S REPORT NUMBER(S)		
DAAG17-68-0142			
9. PROJECT NO.	9b. OTHER REPORT NO(S) (Any other numbers that may be assigned this report)		
1F162203D195	69-82-AD		
10. DISTRIBUTION STATEMENT			
This document has been approved for public release and sale; its distribution is unlimited.			
11. SUPPLEMENTARY NOTES		12. SPONSORING MILITARY ACTIVITY	
Volume I of study		U.S. Army Natick Laboratories Natick, Massachusetts 01760	
13. ABSTRACT			
<p>This report covers a two-phase, 7-month research and development program to design and fabricate a prototype cargo-recovery parachute assembly for airdropping heavy unit loads in the order of 50,000 lb. The design study covers the trade-off analysis and cost effectiveness aspects for a complete parachute assembly. From these studies, a design analysis and a complete detailed design were made based on the specified performance and design requirements.</p> <p>Use of data reduction on full-scale cargo drops with C-11A parachutes with vent-pull down configuration, scale model wind tunnel tests and parametric studies determined that it is feasible to use a cargo parachute of 135 ft. diam. with a vent-pull down in a cluster of six to recover a load unit of 50,000 lb.</p>			

DD FORM 1473

REPLACES DD FORM 1473, 1 JAN 64, WHICH IS OBSOLETE FOR ARMY USE.

Unclassified

Security Classification

Unclassified

Security Classification

14. KEY WORDS	LINK A		LINK B		LINK C	
	ROLE	WT	ROLE	WT	ROLE	WT
Design	8					
Fabrication	8					
Cluster parachutes	9					
Aerial delivery	4		4			
Airdrop operations	4		4			
Clustering			8			
Parachutes			9			

Unclassified

Security Classification